Czech University of Life Sciences Prague

Faculty of Forestry and Wood Sciences

Disentangling pheromone biosynthesis in European spruce bark beetle, *Ips typographus*.

Ph.D., Dissertation Thesis (DissT).

Author : **Rajarajan Ramakrishnan, M.Sc.**

Field of study : **Forest biology**

Supervisor : **Ing. Anna Jirošová, Ph.D.**

Place & Year : **Prague, 2024.**

CZECH UNIVERSITY OF LIFE SCIENCES PRAGUE

Faculty of Forestry and Wood Sciences

Ph.D. THESIS ASSIGNMENT

Rajarajan Ramakrishnan

Forestry Engineering
Forest Biology

Thesis title

Disentangling pheromone biosynthesis in European spruce bark beetle (Ips typographus; Coleoptera; Scolytinae)

Objectives of thesis

European Spruce Bark Beetle (Ips typographus, Coleoptera, Scolytinae) is a devastating pest of spruce trees present in forests across Europe. This bark beetle uses pheromone-mediated aggregation to effectively overcome host defence. Considering pheromone communication, as an obvious key factor in mass attacks, intervention in pheromone biosynthesis of the beetle is a promising approach to curbing spruce killing behaviour.
Main goal of this dissertation thesis is to study Ips typographus aggregation pheromone biosynthetic pathways, related metabolism and underlying molecular mechanisms. The aim is to verify suggested reaction mechanisms of the aggregation pheromone components mainly 2-methyl-3-buten-2-ol and cis-verbenol as well as creation of monoterpenyl-esters as putative pheromone precursor. Furthermore, the candidates for involved genes and enzyme families will be targeted by differential genome expression approach and the functionality of these genes will be proved by functionally characterization techniques.

Methodology

This work will cover the broad range of "omic" approaches. The metabolomics will be used to determine the production profile of the pheromone compounds and related metabolites in the different beetle life stages and treatments (JHIII treatment). The beetle guts and corpuses will be dissected, extracted and measured by spectrometric methods to compare metabolom and quantify target compounds. The transcriptomic approach will cover the RNA sequencing of beetles tissues from various life stages and JHIII treatment and transcriptoms will be compared by Differential gene expression analysis with using sophisticated software tool such as CLC work bench. The highly upregulated genes with respect to pheromone biosynthesis will be selected and its production profile over the life stages will be supported with realtime quantitative polymerase chain reaction (RT-qPCR). The best candidate genes will be functionally characterized using specific expression among cell lines (bacterial, insect) and in vitro respected enzyme assays for achieving end products.

The proposed extent of the thesis

100-120

Keywords

Ips typographus, Pheromone biosyntheses, Gene characterization, Transcriptomics

---

Recommended information sources

Birgersson, G. & Bergstrom, G. Volatiles released from individual spruce bark beetle entrance holes – quantitative variations during the 1st week of attack. J. Chem. Ecol. 15, 2465-2483, doi:10.1007/bf01020377 (1989).

Gilg, A.B., Bearfield, J.C., Tittiger, C., Welch, W.H., Blomquist, G.J., 2005. Isolation and functional expression of an animal geranyl diphosphate synthase and its role in bark beetle pheromone biosynthesis. Proc. Natl. Acad. Sci. U. S. A. 102, 9760–9765. https://doi.org/10.1073/pnas.0503277102

He, P., Mang, D.Z., Wang, H., Wang, M.M., Ma, Y.F., Wang, J., Chen, G.L., Zhang, F., He, M., 2020. Molecular characterization and functional analysis of a novel candidate of cuticle carboxylesterase in Spodoptera exigua degradating sex pheromones and plant volatile esters. Pestic. Biochem. Physiol. 163, 227–234. https://doi.org/10.1016/j.pestbp.2019.11.022

Chiu, C.C., Keeling, C.I., Bohlmann, J., 2018. Monoterpenyl esters in juvenile mountain pine beetle and sex-specific release of the aggregation pheromone trans -verbenol. PNAS 2–7. https://doi.org/10.1073/pnas.1722380115

Keeling, C.I., Blomquist, G.J., Tittiger, C., 2004. Coordinated gene expression for pheromone biosynthesis in the pine engraver beetle, Ips pini (Coleoptera: Scolytidae). Naturwissenschaften 91, 324–328. https://doi.org/10.1007/s00114-004-0523-y

Keeling, C.I., Li, M., Sandhu, H.K., Henderson, H., Man, M., Yuen, S., 2016. Quantitative metabolome , proteome and transcriptome analysis of midgut and fat body tissues in the mountain pine beetle , Dendroctonus ponderosae Hopkins , and insights into pheromone biosynthesis. Insect Biochem. Mol. Biol. 70, 170–183. https://doi.org/10.1016/j.ibmb.2016.01.002

Li, Z., Dai, L., Chu, H., Fu, D., Sun, Y., Chen, H., 2018. Identification, expression patterns, and functional characterization of chemosensory proteins in Dendroctonus armandi (Coleoptera: Curculionidae: Scolytinae). Front. Physiol. 9, 1–14. https://doi.org/10.3389/fphys.2018.00291

Roy, A., George, S., Palli, S.R., 2017. Multiple functions of CREB-binding protein during postembryonic development : identification of target genes. BMC Genomics 1–14. https://doi.org/10.1186/s12864-017-4373-3

Roy, A., Palli, S.R., 2018. Epigenetic modifications acetylation and deacetylation play important roles in juvenile hormone action. BMC Genomics 1–15. https://doi.org/10.1186/s12864-018-5323-4

Schlyter, F., Birgersson, G., Byers, J.A., Löfqvist, J., Bergström, G., 1987. Field response of spruce bark beetle, Ips typographus, to aggregation pheromone candidates. J. Chem. Ecol. 13, 701–716. https://doi.org/10.1007/BF01020153

Expected date
2023/24 WS – FFWS – State Doctoral Examinations

The Dissertation Thesis Supervisor
Ing. Anna Jirošová, Ph.D.

Supervising department
Department of Forest Protection and Entomology

Advisor of thesis
Dr. Amit Roy

Electronic approval: 11. 1. 2024
prof. Ing. Jaroslav Holuša, Ph.D.
Head of department

Electronic approval: 11. 1. 2024
prof. Ing. Milan Lstibůrek, MSc, Ph.D.
Chairperson of Field of Study Board

Electronic approval: 11. 1. 2024
prof. Ing. Róbert Marušák, PhD.
Dean

Prague on 17. 01. 2024

ANNOTATION:

The European spruce bark beetle, ***Ips typographus*** is a key pest among spruce forests across the many Eurasian regions including the Czech Republic. Host tree colonization by *I. typographus* is mediated by aggregation pheromone blend, consisting of 2-methyl-3-buten-2-ol and *cis*-verbenol synthesized from the beetle gut. The molecular trait of **pheromone biosynthesis** research in *I. typographus* has not been conducted yet in detail. In this research, our primary focus is to reveal the molecular level changes relevant to pheromone biosynthesis across the **bark beetle life stages**. Followed by an artificial hormonal treatment, by applying **juvenile hormone III** (JH III), highlighting the key pathway mechanism using sophisticated **multi-*omics*** approaches. we performed a comparative analysis of metabolites (metabolomics), gene transcripts (transcriptomics), and proteins (proteomics) from gut tissue and fat bodies of *I. typographus* in both sexes.

From a detailed Metabolomic analysis, both the various life stages study and JH III treated study have revealed higher amounts of **2-methyl-3-buten-2-ol** in the gut of the fed male (colonization stage), and JH III treated male beetles. Interestingly, the content of ***cis*-verbenol was higher in the immature male gut** (early stage) along with the fed males, which is an interesting finding in this research. We also **identified** a certain compound, **verbenyl oleate** (the possible storage form of *cis*-verbenol), in the beetle body of the immature stage. A further differential gene expression (DGE) and differential protein expression (DPE) analysis revealed possible candidate genes involved in the biosynthesis of the quantified pheromones and related compounds. A novel hemiterpene-synthesizing candidate isoprenoid-di-phosphate synthase (IPDS) from the **mevalonate pathway**, proposed for 2-methyl-3-buten-2-ol synthesis was significantly expressed in the pheromone-producing beetles. Other putative gene families such as **cytochrome P450** (CYP450) for *cis/trans*-verbenol synthesis, an **esterase** gene family and **glycosyl hydrolase** gene family for concept of *cis*-verbenol storage/release were covered in this research.

Findings from the pheromone biosynthesis research on *I. typographus* are the first such reported results with related gene families. With the further characterization of the identified genes, we can develop novel strategies to disrupt the aggregation behavior of *I. typographus* and thereby prevent vegetation loss. This study also provides insightful evidence of JH III's regulatory role in fundamental beetle metabolism, pheromone biosynthesis, and detoxification in *I. typographus* bark beetles.

Keywords: *Ips typographus*, bark beetle, pheromone biosynthesis, multi-*omics*.

DECLARATION:

I declare that I have independently written the dissertation on the topic “Disentangling pheromone biosynthesis in European spruce bark beetle, *Ips typographus*”, with the use of literature and based on consultations and supervisor’s recommendations. I agree to publishing of the dissertation according to Act no. 111/1998 Coll., on schools, as amended, regardless of the outcome of its defense.

Prague, 2024. Rajarajan Ramakrishnan, M.Sc.,

ACKNOWLEDGEMENT:

For guidance and the opportunity to participate in the research project “Bark beetle, *Ips typographus* pheromone biosynthesis”, first I thank my Ph.D. supervisor, Ing. Anna Jirošová, Ph.D. I also want to thank my project consultant Dr. Amit Roy. I am very grateful for the continuous support of Prof. Ing. Marek Turčáni, Ph.D., throughout the study. Furthermore, I appreciate the support of my friends and co-workers, and the rest of the staff and students from the Department of Excellent Mitigation Team and Faculty of Forestry and Wood Sciences at the Czech University of Life Sciences, Prague, Czech Republic.

I would like to thank Prof. Emeritus Fredrik Schlyter at the Department of Plant Protection Biology, Swedish University of Agricultural Sciences, Alnarp, Sweden for sharing his wide knowledge on the bark beetle research topic under the EU project EXTEMIT-K. I also want to thank Prof. Dr. Jonathan Gershenzon, Department of Biochemistry, Max Planck Institute for Chemical Ecology, Jena, Germany for providing me the opportunity to complete abroad training in his group.

Finally, I would like to express my gratitude to my parents and family members in India for their constant motivation, love, and support. I want to dedicate my Ph.D. thesis work in memory of my father, Mr. Ramakrishnan Kasi.

The dissertation was funded by an EU project: "EXTEMIT-K," No. CZ.02.1.01/0.0/0.0/15_003/0000433, Internal Grant Agency (IGA A_20_02 and IGA A_20_22, RAJARAJAN RAMAKRISHNAN) and the KORF scholarship from Faculty of Forestry and Wood Sciences at the Czech University of Life sciences, Prague, Czech Republic.

Motto

“DREAM is not what you see in sleep,
it is something that DOES NOT LET YOU SLEEP”.

- Dr. A.P.J. Abdul Kalam (scientist, 11th Indian President)

TABLE OF CONTENTS:

LIST OF FIGURES:

LIST OF ABBREVIATIONS:

- CYP450 - Cytochrome P450.
- DGE - Differential gene expression.
- DPE - Differential protein expression.
- GC-MS - Gas chromatograph coupled to mass spectrometer.
- GPPS - Geranyl-di-phosphate synthase.
- HMG-S - 3-hydroxy-3methyl glutaryl Co-A synthase.
- HMG-R - 3-hydroxy-3methyl glutaryl Co-A reductase.
- IPDS - Isoprenoid-di-phosphate synthase.
- IPM - Integrated pest management.
- IPPI - Isopentenyl-di-phosphate isomerase.
- JH III - Juvenile Hormone III
- LC-MS - Liquid Chromatography coupled to the mass spectrometer
- nLC-MS/MS - NanoLiquid Chromatography coupled to two-dimensional mass spectrometer.
- PMK - Phosphomevalonate kinase.
- PCA - Principal Component Analysis.
- PLS-DA - Partial Least Square-Discriminant Analysis.
- qRT-PCR - Quantitative real-time polymerase chain reaction
- UHPLC-ESI-HRMS/MS - Ultra-high-performance liquid chromatography-electrospray ionization -high-resolution tandem mass spectrometry.

LIST OF PUBLISHED ARTICLES:

- **Ramakrishnan R**., Hradecký J., Roy A., Kalinová B., Mendezes C. R., Synek J., Bláha J., Svatoš A., Jirošová A*. 2022a. Metabolomics and transcriptomics of pheromone biosynthesis in an aggressive forest pest *Ips typographus*, Insect Biochemistry and Molecular Biology. https://doi.org/10.1016/j.ibmb.2021.103680

- **Ramakrishnan R**., Roy A., Kai M., Svatoš A., Jirošova A*. 2022b. Metabolome and transcriptome related dataset for pheromone biosynthesis in an aggressive forest pest *Ips typographus*. Data in Brief. https://doi.org/10.1016/j.dib.2022.107912

- **Ramakrishnan R**., Roy A., Hradecký J., Kai M., Harant K., Svatoš A., Jirošová A*. 2024. Juvenile Hormone III Induction Reveals Key Genes in General Metabolism, Pheromone Biosynthesis, and Detoxification in Eurasian Spruce Bark Beetle. Frontiers in Forests and Global change. http://doi.org/10.3389/ffgc.2023.1215813

Articles not included in this thesis:

- Jirošová A., Modlinger R., Hradecký J., **Ramakrishnan R**., Berankova K., Kandasamy D*. 2022. Ophiostomatoid fungi synergize attraction of the Eurasian spruce bark beetle, *Ips typographus* to its aggregation pheromone in field traps. Frontiers In Microbiology. https://doi.org/10.3389/fmicb.2022.980251

1. HYPOTHESES AND OBJECTIVES OF THE STUDY:

Hypothesis 1: Key life stages of *Ips typographus* facilitate information targeting changes in molecular and metabolite levels to identify the aggregation pheromone biosynthesis in the beetle.

In detailed objectives:

I. To identify the key enzymes involved in *de novo* biosynthesis of 2-methyl-3-buten-2-ol.

II. To identify the key enzymes involved in the biosynthesis of *cis*-verbenol synthesis from *α*-pinene sequestered from the host.

III. To identify the key enzymes involved in the *cis*-verbenol conjugate storage mechanism.

Hypothesis 2: The Juvenile Hormone III on *Ips typographus* induces correlated changes in genes, proteins, and metabolites that reflect the requirements of adult beetles with aggregation pheromone biosynthesis.

In detailed objectives:

I. To analyze the impact of Juvenile Hormone III on the expression pattern of key enzymes from the mevalonate pathway (in the context of 2-methyl-3-buten-2-ol/ipsdienol biosynthesis).

II. To analyze the regulation of *cis*-verbenol (related to detoxification) after JH III application.

III. To select the key enzymes involved in *cis*-verbenol conjugates (fatty acyl ester and glycosyl conversion) in the storage and release of *cis*-verbenol.

2. INTRODUCTION & LITERARY ANALYSIS:

2.1 Bark beetle outbreak scenario:

Bark beetle attacks among spruce vegetation in Eurasian forests became a critical issue to be addressed in the context of forest protection and ecological conservation (Hlásny et al., 2019). European spruce bark beetle, ***Ips typographus*** **(Coleoptera; Curculionidae)**, in recent days, is also addressed as Eurasian spruce bark beetle, is a key pest in the destruction of spruce vegetation in many European and Asian countries (Marini et al., 2017). The crisis caused by the biotic activity involving bark beetles in the conifer forest has caused huge wood loss, especially in the Czech Republic (Knížek et al., 2020, Figure 1). The wood loss has recorded a peak of ~14.5 million m^3 of forest area (Lorenc et al., 2020; Hlásny et al., 2021).

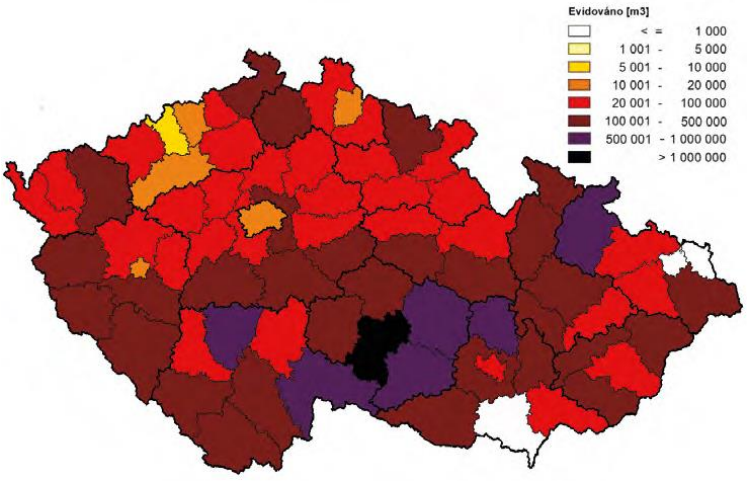

Figure 1:Recorded volume of spruce bark wood loss in the Czech Republic (Knížek et al., 2020)

Many abiotic factors such as regional climatic conditions and landscapes were known to drive the bark beetle attack on the host trees (Seidl et al., 2016; Hartmann et al., 2022). Though insects are known highly viable to climatic changes (Jönsson et al., 2009; Biedermann et al., 2019), the beetle's attack dynamic plays a crucial role in dominating the host tree defense mechanism (Byers, 1989). Bark beetle uses chemical cues to establish social communication in the attack dynamics. An aggregation pheromone blend consisting of 2-methyl-3-buten-2-ol and *cis*-verbenol was identified specific to *Ips*

typographus (Bakke, 1976). Knowing the aggregation phenomenon of a beetle was idolized to control the organism's behavior over the host, thus many monitoring and control measures derived from the known pheromone compounds. Monitoring beetle population methods such as pheromone trap catches, and tree traps by applying the pheromone compounds on certain weak hosts and reducing the attack on many healthier trees (Galko et al., 2016). Added to that, many control methods such as early detection of the attacked trees, sanitation with insecticides, and removal of the attacked trees are also in practice (Wermelinger, 2004; Hlásny et al., 2019). Irrespective of many control measures, the pest outbreak was in exponential increase over the years 2015-2020 in the Czech Republic (Knížek, 2020; Lubojácký et al., 2022). This led to many research questions for effective mitigation of the pest outbreak.

2.2 Spruce vegetation & host selection of bark beetles:

Over the last few centuries, European forests have undergone changes in fundamental tree population variability, greatly influenced by human activities (EEA, 2014, Jansen et al., 2017). Especially, Norway spruce, ***Picea abies*** [L.] Karst., has been widely implanted due to its high ecological plasticity and economic versatility (Schmidt Vogt, 1977). Existence of the spruce vegetation was recorded way back in the 18th century (Andrle, 2017). Irrespective many governments provide policy (EU commission, 2016) to introduce many broad leaf vegetation, spruce vegetation's importance is irreplaceable for the mentioned reasons. Numerous research studies are trending for preserving and proving the importance of the European spruce vegetation *P. abies* in central Europe including the Czech Republic (Szabó et al., 2017). Though forest restructuring involves abiotic factors such as climate change (Hartmann et al., 2018, 2022), altitude, density exposure (Plesa et al., 2017), many biotic factors such as bark beetle activity affect the spruce vegetation (Przepióra et al., 2020; Hlásny et al., 2021). Addressing the bark beetle activity in the spruce vegetation is challenging, as the beetle niche dynamically changes with forest physiological conditions such as temperature and drought (Biedermann et al., 2019).

The success of the bark beetle population depends on selecting appropriate host trees, implying the energy trade-off for the beetle over the years (Raffa et al., 2016, Figure 2). This host selection process varies for different bark beetle species and includes two main theories, active primary attraction to weakened tress (Lehmanski et al., 2023) and random landing of emerged spreading beetles with the decision step based on close encounter with tree smell and taste (Byers, 1989). For example, the Mountain Pine Beetle, *Dendroctonus ponderosae* uses female beetles as a pioneer in the host section, whereas, the Pine engraver, *Ips pini* uses male pioneers in host selection (Schmitz, 1972; Sickle, 1989). In general, the pioneer sex in finding appropriate hosts for colonization are male beetles for most *Ips* species. European spruce bark beetle, *I. typographus* is a primary tree-killing pest for the spruce vegetation and has the male pioneer sex in host selection, whereas a female is the pioneer sex for *Dendroctonous* species (Stadelmann et al., 2014; Seidl et al., 2016; Lehmanski et al., 2023). Added to that, random landing on host trees and selection based on the host tree compounds also influence the selection (Netherer et al., 2021). Hence, host selection by respective pioneer beetles and appropriate chemical cues play a crucial role in the successful next generation with optimum resource and physiological conditions for the beetle (Raffa, 1983; Bohlmann and Gershenzon, 2009).

After host selection, the pioneer beetle uses chemical cues, known as **pheromones,** and recruits further conspecific beetles for colony establishment against the host defense mechanism. The influence of appropriate pheromone blends with species-specific behavior in the field was studied in the early 1970s and 1980s (Bakke et al., 1977; Schlyter et al., 1987). Even though pheromones act as short-distance emissions in intra and inter-species communication and for long-distance host search. The pheromone storage and release should be involved for the beetle survival ability. The success rate of the beetle is not only determined by finding an appropriate host but also by reproducing next-generation beetles with epigenetic inheritance (Netherer et al., 2021, Figure 2). Nevertheless, the bark beetles are also an essential component of every

spruce forest by decomposing the dead and wind-fallen trees, proving the ecological importance of the forest (Peltonen, 1999).

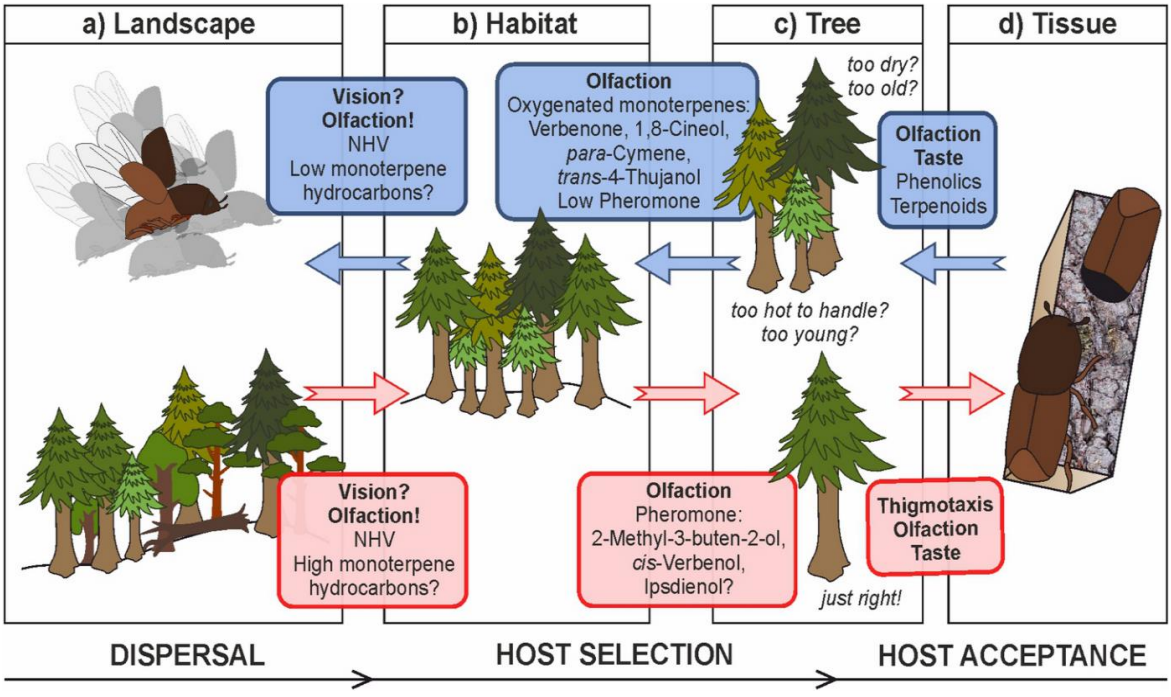

Figure 2: Bark beetle host selection overview.

Behavioral sequence for *Ips typographus* in a) landscape (dispersal), b) habitat, and c) tree (both host selection), and d) tissue (host acceptance) by positive (fair blue arrows and boxes) and negative cues (red arrows and boxes). Focus is set on the pioneering male beetles, whose rapidly produced pheromone signals guide the vast majority of both males and females to aggregate. The individual beetle follows a sequence of steps, guided by visual, chemo-sensory, and thigmotactic cues. Source: (Netherer et al., 2021)

2.3 Bark beetle life stages in biosynthesis studies:

From past research, the bark beetle developmental stages such as freshly emerged adult beetles (as pioneers in finding appropriate hosts) and beetles from mating chambers were considered (Byers et al., 1989, Figure 3). However, recent studies showed the importance of juvenile life stages including larvae and pupae for studying host defense detoxification and winter hibernation mechanisms (Aw et al., 2010; Chiu et al., 2017). Post-winter emerging beetles such as flying beetles, use flight muscle activation for certain pheromone mechanisms (Ivarsson et al., 1995).

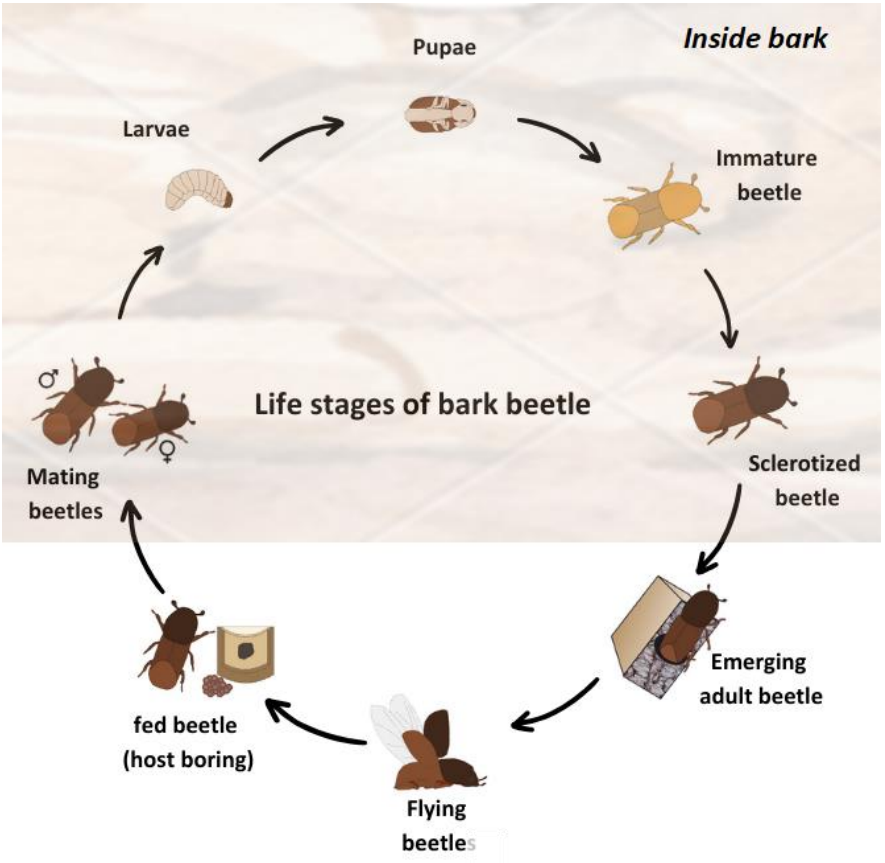

Figure 3**:** Life stages of Bark beetle *Ips typographus*
The life stages inside the tree bark are shown in the shaded region. Source: Recreated from Ramakrishnan et al., 2022a.

Nevertheless, considering all developmental stages of *Ips typographus* as shown in Figure 3 enlists critical interlink between different life stages and the pheromone biosynthesis mechanisms. The juvenile life stages (larvae & pupae) and immature (teneral) beetles were least expected to be involved in *de novo* pheromone biosynthesis. Actual pheromone components start appearing from the life stages such as flying beetles, host boring fed beetles, and beetles from mating chambers were demonstrated in the past research (Birgersson et al., 1984). In the later development stages, the beetles convert the pheromone compound, verbenol into verbenone, for an anti-aggregation compound revealing the food depletion in the attacked tree (Leufvi and Bergström, 1984).

Pheromone production varies across different life stages of the bark beetle lifetime (Birgersson et al., 1984; Aw et al., 2010). The beetle ability to produce certain pheromone components at the required development stage ensures the fitness and success of the beetle. Thus, the importance of various life stages study from the bark beetle, *D. ponderosae* for pheromone switches off and on mechanism was investigated (Pureswaren et al., 2000).

The species-specific physiological recognition for beetle behavior at a certain life stage with aggregation pheromones and repellent involving over 15 different compounds have ensured the commercial aspect such as pheromone-mediated mitigation to the situation with partial success in *I. typographus* management (Galko et al., 2016). Though many pheromone research findings are used in the field of bark beetle management, commercially available pheromone baits are used only for monitoring of seasonal and spatial density of beetle population (Galko et al., 2016).

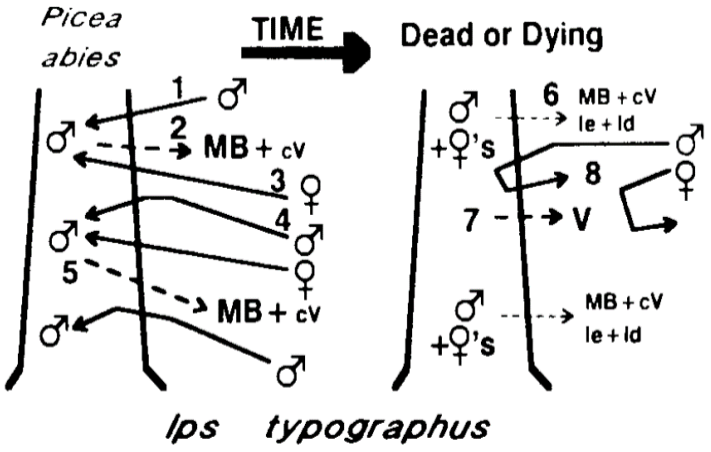

Figure 4. *Ips typographus* attack dynamics upon its natural host *Picea abies* explained in 8 steps Step1: Pioneer Male finding host, Step2: Release of aggregation pheromone blend, MB (2-Methyl-3-buten-2-ol), cV(*cis*-Verbenol), Step 3&4: Attracting more conspecific beetles Step 5: Release of more aggregation pheromone from conspecific beetles, Step 6: Release of pheromonal compounds Ie (ipsenol) and Id (ipsdienol) along with MB & cV, Step 7&8: Repelling the conspecific beetles due to host depletion. Source: Byers, 1989.

2.4 Pheromones biosynthesis in bark beetle:

The first bark beetle pheromone component mixture (ipsdienol, ipsenol, and verbenol) was reported in 1966 from *Ips paraconfusus* (Silverstein et al., 1966). Notably, Bark beetle pheromone compounds such as ipsdienol, *cis/trans*-verbenol, and exo-brevicomin show structural similarity to host tree compounds of some monoterpenes, myrcene, and *α*-pinene (Hughes 1974; Blomquist et al., 2010). Later, it was proven that these compounds were produced by a conversion step such as oxidation of these host compounds or derived from likely fatty acid- derivatives (Byers, 1990; Vanderwel et al 1992). Interestingly, the host compound myrcene can also be identified in the beetle by self-synthesis, whereas the compound *α*-pinene cannot be synthesized in the beetle independently (Hughes 1973; Byers 1990). These findings initiated the concept of ***de novo*** pheromone biosynthesis from the beetle body when required, rather than converting the host monoterpene immediately (Ivarsson et al., 1993; Syebold et al., 1995). Several studies have justified this phenomenon of *de novo* by using isotope-labeled components, ^{14}C-mevalonolactone into 2-methyl-3-buten-2-ol and ^{2}H-myrcene ended up in ^{2}H-ipsenol and ^{2}H-ipsdienol pheromone components (Lanne et al 1989;

Vanderwel, 1994; Tillman et al., 1998). Further pheromones biosynthesis research in *I. pini*, using a molecular platform has revealed key **genes from** the **mevalonate pathway** family in direct connection to the mentioned *de novo* biosynthesis (Nakamura and Abeles, 1985).

Nevertheless, studies from bark beetle, *Dendroctonous sp*., such as *D. ponderosae* have proven several key aggregation pheromone biosynthesis steps (Aw et al., 2010). This involves a synergistic aggregation pheromone, exo-brevicomin (from male) was synthesized from a precursor, 6-(*Z*)-nonen-2-one in fatty acid synthesis from fat bodies (Nadeau et al., 2017), along with the pioneer female aggregation pheromone, *trans*-verbenol (Vanderwel et al., 1992). Another compound for population regulation from *D. ponderosae* male, frontalin (by repelling), was also clarified using another labeled study of ^{14}C-labelled frontalin and it originates via the mevalonate pathway (Tittiger et al., 2016).

The key aggregation pheromones from *I. typographus* male pioneer beetles are **2-methyl-3-buten-2-ol and *cis*-verbenol,** reported in earlier studies of the 1970s and 1980s with quantification of these compounds in attack stages of the beetle (Bakke, 1976; Birgersson et al., 1984). In *I. typographus,* the hemiterpene aggregation pheromone, **2-methyl-3-buten-2-ol** with *de novo* origin was identified with a labeled mevalonate as mentioned above (Lanne et al., 1989; Byers and Birgersson, 1990). These studies clarified the sex-specific and localized aggregation of **pheromone biosynthesis from the midgut** (Hall et al., 2002). Also, the bark beetle aggregation pheromone biosynthesis takes place especially in their hindguts as soon as they start boring into the bark. Later, the components reach the maximum amount during excavation of the nuptial chamber.

***cis*-Verbenol**, another aggregation pheromone of the bark beetle, *I. typographus*, derived from host tree precursor *α*-pinene after hydroxylation (Renwick et al*.,* 1976; Tittiger and Blomquist, 2016). Nevertheless, a similar conversion into *trans*-verbenol was also identified earlier in another bark beetle, *D. ponderosae* by a certain gene of the **cytochrome P450 family (CYP450)** (Wermelinger, 2019). A certain multifunctional

CYP450 was functionally identified for the above-mentioned conversions of host precursor to pheromone *trans*-verbenol in *D. ponderosae* (Chiu et al., 2019).

Also, the aggregation pheromone *cis/trans* verbenol role changes as converted into a derivative **verbenone**. Various microbial roles in the context of pheromone conversion of bark beetle, especially in species *Dendroctonus frontalis*, with a mycangial fungus involvement (Brand et al., 1976; Hunt and Borden, 1990). Many research questions related to bark beetle gut microbes are explored currently with the mentioned interests (Adams et al., 2011; Chakraborty et al., 2020). Other male-specific components of *I. typographus* are **phenyl ethanol, myrtenol, myrtanol** has been reported and the functional clarity of these compounds is yet to be obtained (Birgersson et al., 1984). Phenylalanine, an important precursor for nutrients & cuticle structural proteins in insect physiology also acts as a precursor for phenyl ethanol production in the beetle (Gries, 1990).

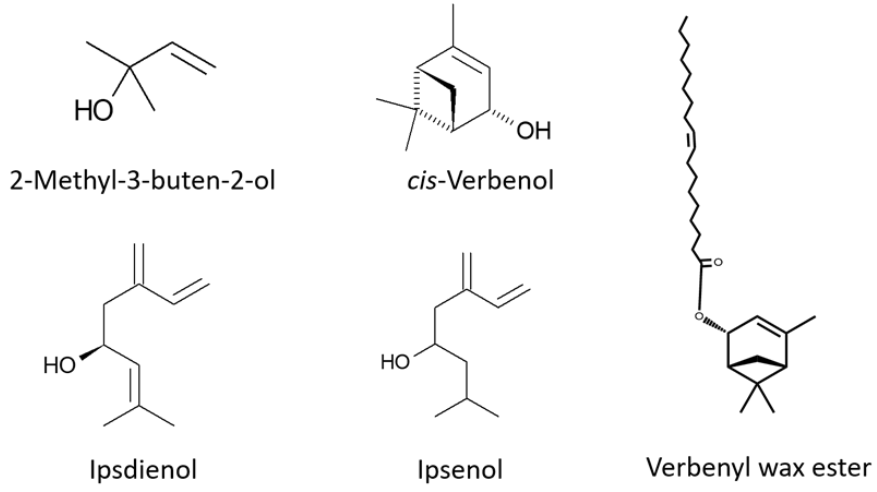

Figure 5A: Structure of pheromone components and relative precursors in *Ips typographus*. Source: Birgersson et al., 1984.

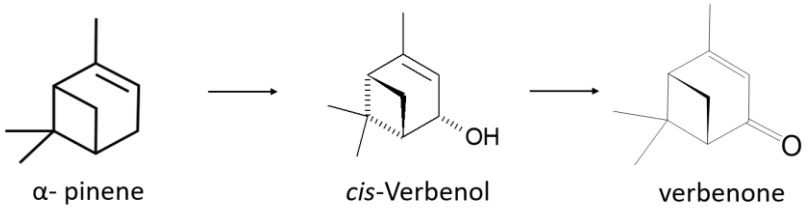

Figure 5B: Conversion of the tree precursor- *α*-pinene into respective pheromone derivatives in bark beetle. Source: Renwick et al., 1976.

An extended concept of the tree precursors-based verbenol storage in fat bodies of the beetle as wax esters became a recent hypothesis to explore (Chiu et al., 2018). Wax esters such as **fatty acids derivatives** of the pheromone (e.g. verbenol oleate) were proposed in crucial pheromone storage reservoirs from the fat bodies of young beetles with abundant food resources. Later, in the matured beetles, the stored wax esters in certain sex (preferably the pioneer beetle) opt for *cis/trans* verbenol release for the required function (Chiu et al., 2018). Nevertheless, the storing wax esters also contain detoxification mechanism molecules (myrtenol-fatty acid esters), observed in both sexes of the bark beetles and yet to be described with clarity in *Ips* species.

2.5 Pathways related to bark beetle pheromone biosynthesis:

The molecular-level effects of JH III on pheromone biosynthesis have been subsequently investigated in various species, including *I. paraconfusus* (Ivarsson and Birgersson, 1995), *I. pini* (Tillman et al., 1998; Blomquist et al., 2010), and *D. ponderosae* (Keeling et al., 2016). JH III induction has been reported for many activated multiple gene families responsible for ***de novo*** pheromone biosynthesis, especially in the mevalonate pathway from the gut tissue (Sarabia et al., 2019).

In *Ips* species, the involvement of **mevalonate pathway** genes in pheromone production was documented (Bearfield et al., 2009). The pathway involves the condensation of acetoacetyl-CoA with acetyl-CoA catalyzed by *3-hydroxy-3-methyl glutaryl-CoA synthase* (HMGS) followed by a reduction of hydroxymethyl glutaryl-CoA to mevalonate, catalyzed by *3-hydroxy-3-methyl glutaryl coenzyme-A reductase* (HMG-R). Later, the mevalonate is phosphorylated by *phosphomevalonate kinase* (PMK), followed by several steps of modification to form the isoprenoid biosynthetic units, isopentenyl diphosphate, and dimethyl allyl diphosphate. Condensation of two isoprenoid units catalyzed by *geranyl-di-phosphate synthase* (GPPS) synthesizes geranyl-di-phosphate, the precursor of bark beetle monoterpenoid pheromones, such as myrcene and ipsdienol (Keeling et al., 2004; Gilg et al., 2005; Bearfield et al., 2009) (Figure 6) Additionally, an *ipsdienol dehydrogenase* was reported for converting the ipsdienol into

ipsenol in *I. pini* (Teran et al., 2012). Nevertheless, identified genes were reported for significant expression in respective pheromone producing *Ips* beetles (Keeling et al., 2004).

The pheromone production across various life stages of the beetle varies according to the beetle requirement and certain gene families were reported with a switch on/off mechanism for the beetle's development and fitness (Birgersson et al., 1984). The pheromone, Verbenol, is not synthesized *de novo*, instead produced by a gene family, **cytochrome P450 (CYP450)** by oxidation of (-) *α*-pinene that adult beetles sequester from the tree (Renwick et al., 1976; Chiu et al., 2019). As part of this detoxification process, *cis*-verbenol (along with myrtenol as another detox product) is deposited in the form of monoterpenyl fatty acid esters in the fat body (Chiu et al., 2018).

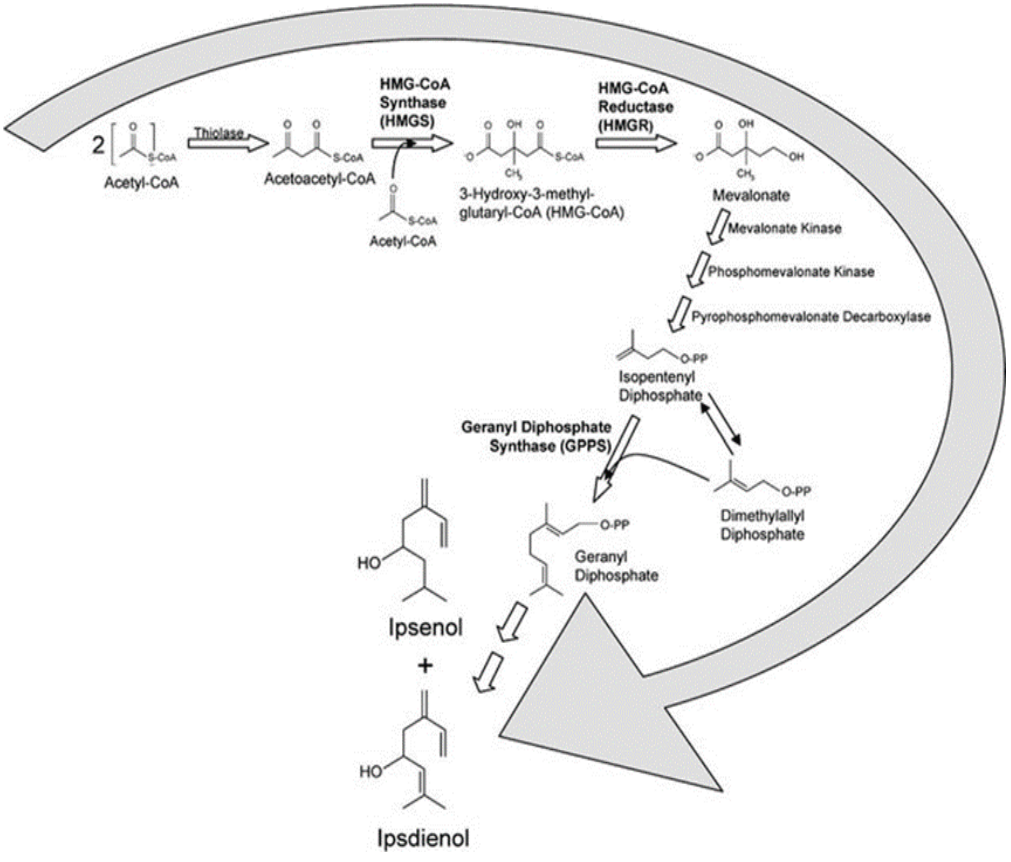

Figure 6: *De novo* pheromone biosynthesis via mevalonate pathway in gut tissue
Source: Bearfield et al., 2009.

The identified conjugates (verbenyl fatty acid esters) supply of the pheromonal component, free *cis*-verbenol by hydrolyzing in adult males when needed. The gene encoding for the formation of a verbenyl fatty acid ester and cleaving function was presumed as a **carboxylesterase or transferases,** which acts on ester bond (Figure 7, Chiu et al., 2018; Blomquist et al., 2021). In *D. ponderosae*, verbenyl conjugates are proposed as a potential pheromone reservoir in adult males (Hughes, 1974; White et al., 1980).

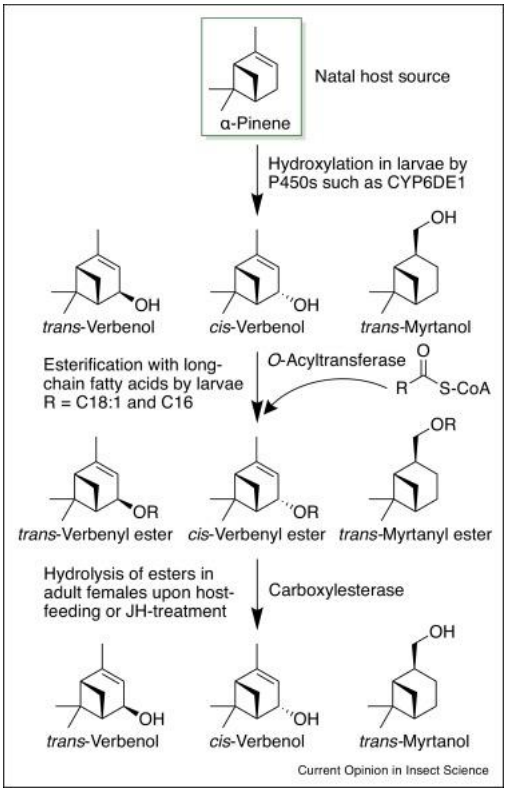

Figure 7: The hypothesized biosynthetic origin of verbenol storage in bark beetles.
Biosynthesis of *trans*-verbenol, *cis*-verbenol, and myrtanol in *D. ponderosae*. Larvae in their natal host hydroxylate *α*-pinene to these alcohols, esterify them with oleic or palmitic acid, and then store them in the fat bodies. Source: Blomquist et al., 2021.

Nevertheless, existing knowledge in the pheromone biosynthesis of *Ips typographus* is limited and yet to be addressed from a molecular perspective. Particularly, biosynthesis of the crucial pheromone components such as 2-methyl-3-buten-2-ol, *cis*-verbenol, phenylethanol, myrcene, verbenone (Bakke, 1976), and pheromone precursors such as

fatty acid esters (Chiu et al., 2018). Thus, the concept of gene regulation with a switch on/off mechanism for certain pheromone production should be analyzed in the relevant life stage of the beetle. Specific enzyme regulation after JHIII and relative life stages of *I. typographus* should be investigated at the molecular platform level using RNA biology, such as gene and protein expression analysis, which is conducted in this research.

2.6 Juvenile hormone regulation on insects:

Hormone regulations play an important role in many morphological and behavioral changes of the class Insecta (Smykal et al., 2014). Especially morphological changes such as body development, reproduction, parental care, mating behavior, molt and growth, diapause, and many other functions are hormonally regulated (Jindra et al., 2013). The two most important classes of insect hormones are **ecdysteroids** and **juvenile hormones** (Miyakawa et al., 2018, Figure 8). In Coleoptera pheromone biosynthesis concepts, juvenile hormone III (JH III) is the most studied (Tillman et al., 1998; Keeling et al., 2016). The primary function of these hormones is to maintain juvenile characteristics and prevent premature metamorphosis. (Goodman and Cusson, 2012). JH III is synthesized in the exocrine gland corpus allatum and transported through the hemolymph by binding proteins to its target receptors (Jindra and Bittova, 2020). JH III has been extensively used to study many gene families involved in insect growth and metamorphosis, along with social behavior (Riddiford et al., 2010; Trumbo, 2018).

Insect larvae initially contain a high amount of JH III, which is subsequently reduced as the larvae undergo metamorphosis into pupae (Treiblmayr et al., 2006). In the pre-metamorphic stages, **JH III has been studied for its influence on the development of larval muscles and the prothoracic glands** producing ecdysteroids, as well as its role in restructuring gut development, fat body, and epidermis in various insect species (Riddiford, 2012; Jindra et al., 2013). In adult insects, JH III influences various aspects, including pheromone production (Tillman et al., 2004) and social behavior (Trumbo, 2018), caste determination (Cristino et al., 2006) aggression and display (Emlen et al.,

2006), migration (Zhu et al., 2009), and neuronal remodeling (Leinwand and Scott, 2021).

In bark beetles, **JH III effects have primarily been studied concerning pheromone biosynthesis induction**. Many pheromone compounds such as Ipsenol and Ipsdienol, known exclusively from *Ips* species been regulated by JH III (Hall et al., 2002). When the beetles bore into the host tree, JH III is released from the endocrine gland, initiating a series of hormonal signaling processes that lead to the production of aggregation pheromone components in male beetles. In nature, this potent blend attracts conspecifics, both males and females, to mass attack to help overcome tree defense. In controlled laboratory conditions, pheromone biosynthesis induction can be achieved by topically applying JH III on the beetle abdomen (Byers and Birgersson, 1990; Ivarsson et al., 1993; Seybold et al., 1995; Tillman et al., 1998). This method triggers the *de novo* synthesis of pheromone compounds while avoiding potential interference with the metabolic pathways involved in the digestion of ingested phloem tissues. Pheromone induction using JH III has been demonstrated in bark beetles such as *Ips pini, Dendroctonus ponderosae*, and *Ips typographus* (Nardi et al. 2002; Tillman et al. 2004; Fang et al., 2021; Ramakrishnan et al. 2022a). However, certain *Ips* species such as *Ips confusus* and *Ips grandicollis*, have been reported to be unresponsive to JH III-induced pheromone induction (Tillman et al., 2004; Bearfield et al., 2009).

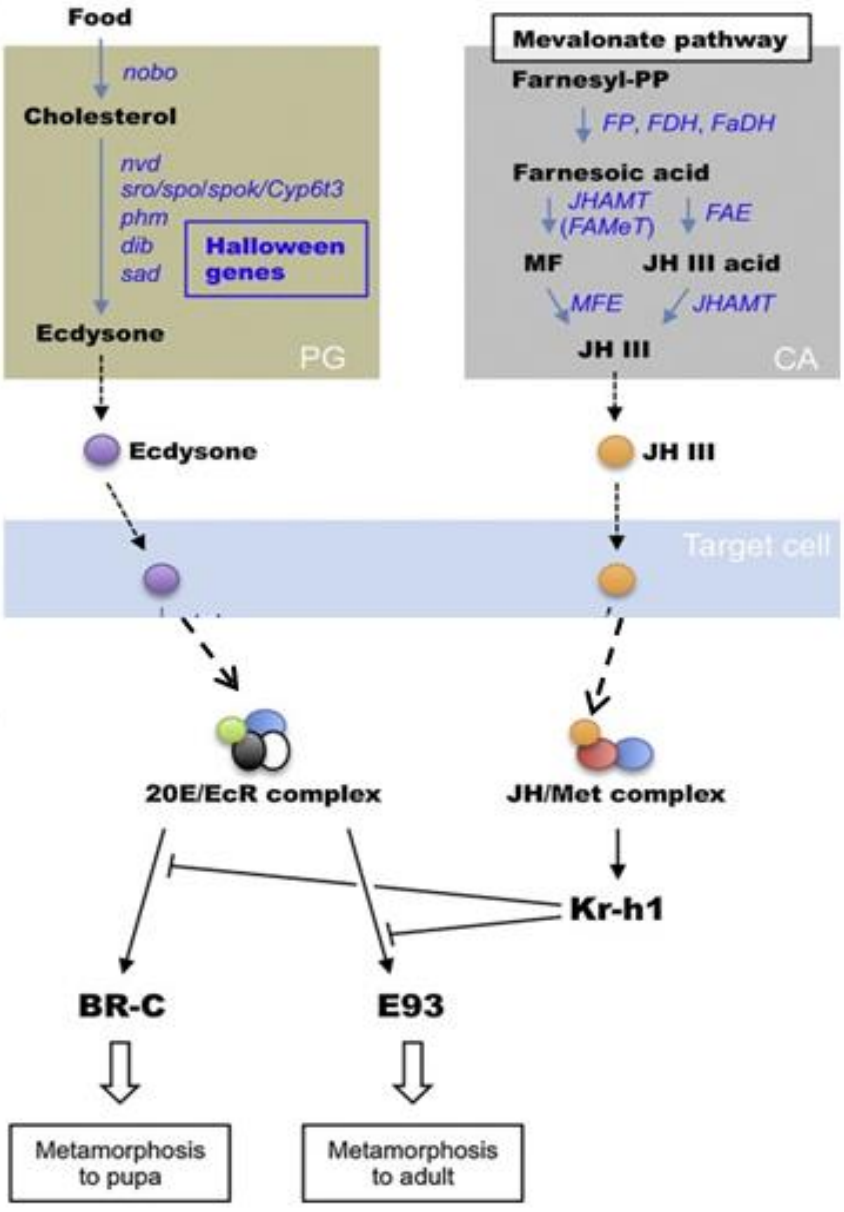

Figure 8*:* Regulation of Ecdysone and JHIII via respective complex in pathways.
Biosynthesis of the hormones in the specific organs to reception at peripheral target cells: Abbreviations: PG, prothoracic grand; CA, corpora allata; Farnesyl-PP, farnesyl pyrophosphate; MF, methyl farnesoate; JH III, juvenile hormone III; 20E, 20-hydroxyecdysone; EcR, ecdysone receptor; Met, Methoprene-tolerant; nobo, noppera-bo; nvd, neverland; sro, shroud; spo, spook; spok, spookier; phm, phantom; dib, disembodied; sad, shadow; shd, shade; FP, farnesyl phosphatase; FDH, farnesol dehy- drogenase; FaDH, farnesal dehydrogenase; FAMeT, farnesoic acid O- methyltransferase; MFE, methyl farnesoate epoxidase; FAE, farnesoic acid epoxidase; JHAMT, juvenile hormone acid O-methyltransferase; BR-C, Broad-Complex; Kr-h1, Krüppel homolog 1. Source: Miyakawa et al., 2018.

2.7 Molecular techniques for the discovery of biosynthetic genes:

Molecular research on many beetle (Coleoptera) organisms has led so far to 12 genome sequencing studies, among which the recently added *Ips typographus* **genome** plays an important role in exploring many basic mechanisms of the organism (Powell et al., 2021). Further high throughput methodologies from RNA-oriented studies with precise analysis were required for molecular pathway research (Stark et al., 2019). Further, genome-annotated RNA and relative enzyme analysis enrich the molecular study with targeted research interests. Many challenging research such as clinical pathology detection, species-specific targeted biopesticides, etc have used the above-mentioned molecular studies for deriving respective solutions (Ernst et al., 2016; Roy et al., 2017). RNA-related methods derived many pest control strategies targeting functional genes (Lancaster et al., 2018). Currently, the technological upgrade has led to achieving the whole transcriptome of a model organism with high-quality data, which was not feasible some years ago (Wang et al., 2009).

Nevertheless, opting for the right method of the above-mentioned RNA sequencing (RNA seq.) methods for analyzing **differential gene expression (DGE)** is a key analysis targeted (Cloonan et al., 2008). For instance, short-read sequencing library preparation involves numerous steps so possibility for bias, whereas long-read or direct RNA sequencing library preparation involves minimum steps, but achieving high-quality RNA is practically impossible. The standard workflow of RNA seq. begins with RNA extraction, followed by mRNA enrichment or ribosomal RNA depletion, cDNA synthesis, and preparation of an adaptor-ligated sequencing library (Stark et al., 2019, Figure 9a).

The library is then sequenced to a read depth of up to a few million reads per sample on high-throughput platforms described below. **In Illumina**, individual cDNA molecules are clustered on a flow cell for sequencing by synthesis 3′ blocked labeled nucleotides. In each round of sequencing, the growing DNA strand is imaged to detect which of the four fluorophores has been incorporated, and reads of **50–500 bp** can be generated. In **Pacific biosciences**, individual molecules are loaded into a sequencing chip to bind a polymerase immobilized at the bottom of a nano well, where reads of up to **50 kb** can

be generated. In **Oxford nanopore**, individual molecules are loaded into motor proteins attached during adaptor ligation. The motor protein controls the translocation of the RNA strand through the nanopore, causing a change in current that is processed to generate sequencing reads of **1–10 kb** (Figure 9b). The final steps are computational by aligning and/or assembling the sequencing reads to a transcriptome, quantifying reads that overlap transcripts, filtering and normalizing between samples, and statistical modeling of significant changes in the expression levels of individual genes and/or transcripts between sample groups (Stark et al., 2019).

Research requirements are determined in choosing the appropriate RNA sequencing methods (Sparks et al., 2017). Many methods are in practice with a key interest in identifying certain functional pathway analyses for bark beetle research (Tillman et al., 1998; Fisher et al., 2021).

Gene characterization:

By completing the analysis of the gene sequencing with the above-mentioned methods, obtained key gene functions certainly need to be validated and confirmed. Molecular methods such as protein engineering the enzymes in living cells (bacteria or insect cells) and followed by checking the activity using **enzyme assays** with specific substrates for confirming the gene functions (Frick et al 2013; Lancaster et al., 2018). Another approach is using **RNA *interference*** (RNA *i*) in silencing the respective gene and checking for protein and targeted products in living organisms (Joga et al., 2016). Both the mentioned methods facilitate knowledge for identifying the responsible function especially biosynthetic genes of the crucial aggregation pheromone components has a promising approach for the mentioned scenario of pest management. The practical application of gene silencing is discussed in the next chapter.

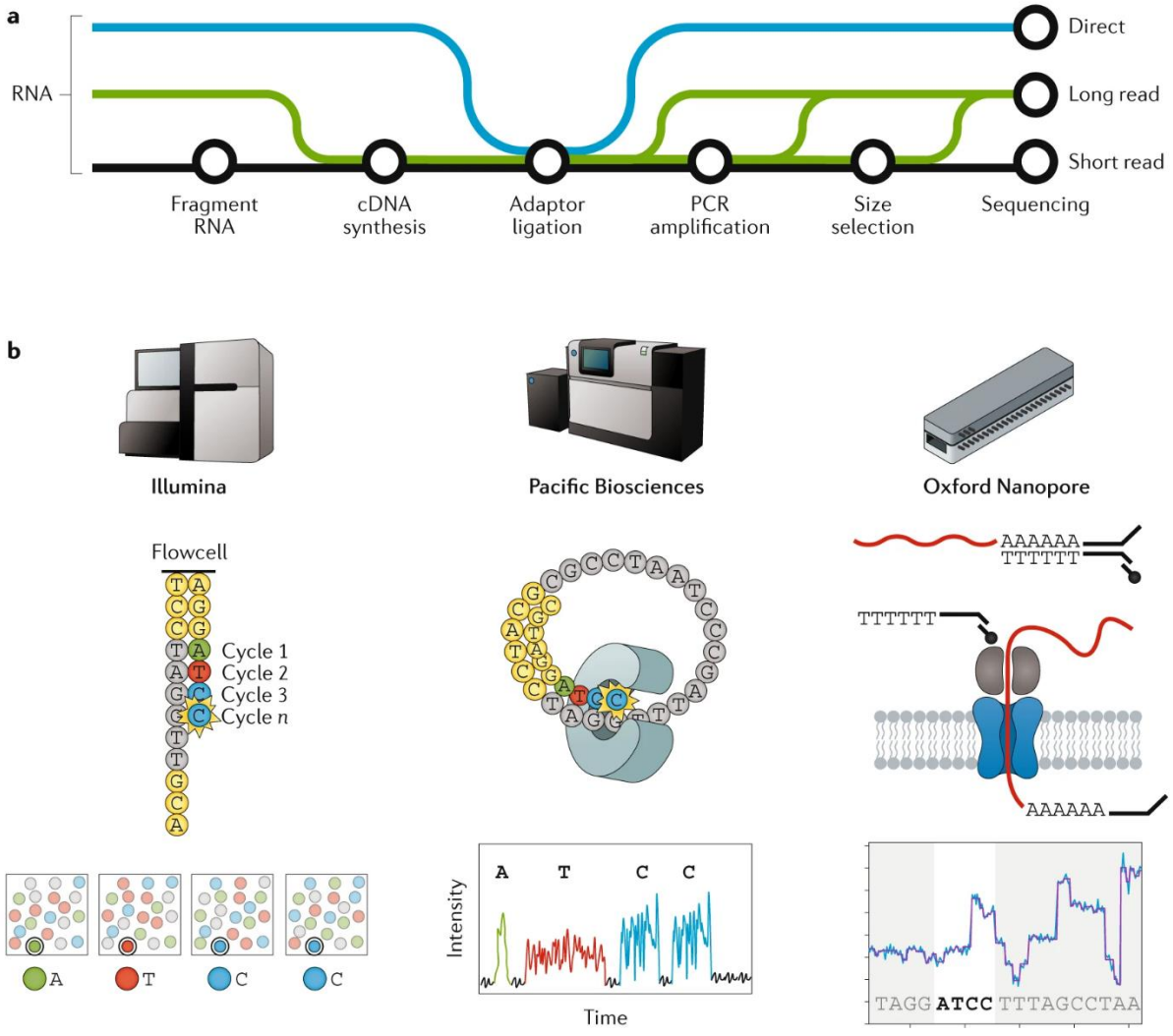

Figure 9: a) Overview of library preparation methods for different RNA-sequencing methods Methods are categorized as short-read sequencing (black), long-read cDNA sequencing (green), or long-read direct RNA-seq. (blue). b: Overview is shown of the three main sequencing technologies for RNA-seq. from left to right, Illumina (Fluorophore labeling), Pacific Biosciences (enzyme immobilization chips), and Oxford nanopore (using motor proteins) for respective methods mentioned. (Source: Stark et al., 2019)

2.8 Integrated Pest Management (IPM) of bark beetle:

The impact of bark beetle attacks over conifer forests in North American, European, and recently also in Asia, led to many ecological and economic crises. The situation forced us to derive control measures against the problem with appropriate solutions through Integrated pest management (IPM) (Lorio et al., 1982). Though IPM for bark beetle calamity was discussed over past decades, pest management has not effective as planned over many years (Schlyter et al., 2001). Actively used methods for bark beetle calamity management include the **early identification** of the infested trees (Kautz et al., 2013). Effective management of the infested regions by **removing the attached trees** and treating the attacked host with **insecticides/repellents** after managing the regions, aiming to prevent further pest spread (Hlásny et al., 2022).

Early studies reported that using an appropriate blend of aggregation pheromones in making **pheromone traps**, reduced over 30% of *I. typographus* infestation (Birgersson, 1984). However, later it was reported that the method is only with limited success (Galko et al., 2016). Another concept of certain **trap trees**, where the attractivity is boosted by applying the aggregation pheromones, is aimed at reducing attacked tree density (Wermelinger, 2004; Hlásny et al., 2019). However, favorable climate impact with rising temperatures increased the beetle population at an exponential rate (Lubojácký et al., 2023). Thus, the **classical methods were not efficient enough** in controlling the beetle infestation (Bentz et al., 2010). Furthermore, in IPM strategies for pest insects, the ecological balance must be maintained with the least or no impact on non-targeted insect populations (Kogan, 1998), which differs from using nonselective insecticides. Hence, species-specific approaches were proposed to overrule the impact on other insects with many new possible approaches with molecular methods (Joga et al., 2016).

Molecular methods such as **RNA *interference*** are a phenomenon of gene silencing on targeted organisms and are widely used in controlling pest management in many agricultural crop protection programs (Gordon et al., 2007; Zotti et al., 2015). By silencing a certain functional gene, a targeted insect can be retained with minimum damage to the crop hence preventing ecological loss of the pest. While this application

has an advantage with certain species specificity, the complex system in the gene silencing of Coleoptera insects is challenging and in bark beetles, almost no evidence of RNA*i* research can be identified till date (Joga et al., 2016). Targeting the **species-specific** non-lethal genes of the beetle along with characterizing them aims to address the pest's aggregation behavior with minimum ecological damage. A similar approach was demonstrated in a moth, *Helicoverpa armigera* when reproduction was modified by silencing genes responsible for sex pheromones production (Dong et al., 2017). However, selecting an appropriate delivery method for specific insect orders is challenging. In wood-feeding insects, the aspect of dsRNA delivery can be achieved by spraying over the tree trunk (Li et al., 2015) or by injecting it into the tree's sap stream (Hunter et al., 2012). The delivery of dsRNA by these methods will be used for effective silencing of the pheromone biosynthetic genes in the beetle upon phloem feeding. However, the appropriate method should be considered when choosing an effective outcome (Joga et al., 2021).

This approach is familiar with existing forest pest management practices (i.e., silvicultural, biological), and can aid a multi-faceted management approach that keeps the tree-killing forest pest populations in the endemic stage while conserving the beneficial species.

3. SUMMARY OF WORK METHODOLOGY:

This chapter contains the methods established to achieve the results mentioned in the following chapter.

3.1 *Ips typographus* rearing conditions in the laboratory:

Spruce logs (*Picea abies*) naturally infested with *I. typographus* (F0 generation) were obtained from plots at the CZU forest, near Kostelec nad Černými lesy. The infested logs were stored in a cold chamber (4°C) until used. Fresh spruce logs (app. 50 cm) were infested with F0 generation beetles (150 beetles per log) and maintained under laboratory conditions (70% humidity, 24°C,16:8 h day/night period, and ventilated plastic containers of 56x39x28 cm/45 l volume) for incubation to establish the F1 generation. With four weeks of incubation time, the F1 generation of the beetle with different life stages was collected. The different life stages are larvae, pupae, immature beetles (golden-colored teneral beetles with soft cuticle), sclerotized beetles (beetles with dark cuticle, still in the breeding log), emerged beetles (beetles emerged from the breeding log), flying beetles (emerged beetles with 24 h of flying), fed beetles (males and females separately excavating nuptial chambers in an uninfested spruce log for 24 h), mated beetles (male introduced first in an uninfested spruce log, followed by the introduction of a female after 24 h and collection of beetles from mating chambers after 48 h). After collecting beetles at appropriate life stages, they were sorted according to sex and external morphological characteristics (Schlyter and Cederholm, 1981) (except larvae and pupae).

The emerged beetles were sorted by sex and used for hormone (JH III) treatment. Acetone (0.5 µl; control) and 10 µg of JH III (0.5 µl of 20 µg/µl acetone) were applied topically on the abdomen of beetles. After application, beetles were kept under the laboratory conditions mentioned above for 8 h. Beetles were frozen in liquid nitrogen and stored at -80°C for further processing. Before analysis, the guts were dissected from beetles of different life stages (except larvae and pupae) for further metabolomic and

DGE analysis. In this study, the beetle body refers to the remaining tissue with the fat after the gut, elytra, and wings have been removed.

3.2 Metabolomic Analysis:

3.2.1 Gas chromatograph coupled to mass spectrometer (GC-MS) analysis:

Guts were dissected from the frozen beetles and immediately submerged in 2 ml analytical vials (10 guts/100 µl) of cold pentane or hexane. The beetle body was placed in another vial with chloroform. (10 beetle bodies /1000 µl chloroform) (Birgersson et al. 1984; Birgersson and Bergstrom, 1989)

GC-MS Agilent 7890B (Agilent Technologies, Palo Alto, CA, USA) employing time of flight mass analyzer Pegasus 4D (LECO, St. Joseph, MI, USA) was used for the separation, identification, and quantification of extracted compounds. One microliter of the extract was injected into a cold PTV injector (20°C) in split 10:1 mode. After injection, the inlet was heated to 275°C at a rate of 8°C/s. Separation was conducted on HP-5MS UI capillary column (30 m, 0.25 mm i.d., 0.25 µm film thickness) from Agilent. The GC oven temperature program was as follows: 40°C for 1 min; then ramped at a rate of 10°C min^{-1} to 210°C; then at 20°C min^{-1} to 320°C and held for 6 min. The total GC run time was 29.5 min. Ions (ionization energy at 70eV) were collected in a mass range of 35-500Da with a frequency of 10Hz.

Two-dimensional comprehensive gas chromatography was employed using the same instrument for the separation and quantification of compounds in beetle body extract. Here, injection in split mode (100:1) was used and secondary GC and modulator were programmed with an offset of 5°C and 15°C to the first dimension GC oven, respectively. Column BPX-50 (SGE, Australia, 1.5 m, 0.1 mm i.d, 0.1 µm film thickness) was used for two-dimensional separation. A modulation period of 5 seconds was maintained for the whole length of the analysis. The temperature program was 40°C (1,7 min); 10°C/ min 210°C; 20°C/ min 320°C (15 mins). The total GC run time was 39.2 min.

Automated spectral deconvolution and peak finding algorithms were carried out using ChromaTOF software (LECO, St. Joseph, MI, USA). In target compound analysis,

peak areas of unique mass from the compound's mass spectrum were used for quantification. Linear calibration curves were constructed using responses of measured calibration mixtures diluted from standards. Extracts from the beetle body were targeted and quantified for verbenyl oleate and myrtenyl oleate based on external calibration standards prepared by organic synthesis (Chiu et al., 2018).

In non-target analysis, a peak alignment tool was used to compare and align all chromatographic signals with a signal-to-noise ratio (S/N) higher than 25 in all samples of gut extract. Non-target search in the beetle body was then performed using a parameter of S/N=50. The data were cleaned, normalized (constant raw sum), and evaluated using principal component analysis (PCA) and partial least square-discriminant analysis (PLS-DA) in SIMCA 15 software (Sartorius Stedim Data Analytics AB, Malmö, Sweden). For the tentative identification of compounds, a comparison with mass spectra at the National Institute of Standards and Technology (NIST 2017) library was performed. For identity confirmation, retention indexes from NIST or retention times of respective standards were used.

3.2.2 Ultra-high-performance liquid chromatography-electrospray ionization -high-resolution tandem mass spectrometry (UHPLC-ESI-HRMS/MS) analysis:

For nonpolar extraction, dissected guts (5 guts /sample) were collected in ethyl acetate (5 µl/gut) and stored at -80°C before analysis. Gut extracts (solvent without gut) were removed for nonpolar fraction. For polar extraction, the rest of the solvent was removed by a gentle stream of nitrogen, and the remaining tissue was extracted (7 ml/gut) with MeOH/water/acetic acid (70/30/0.5 v/v) mixture containing 13C2-myristic acid (1 µg/ml) standard. After sonication on ice (5 min) the tissue was disrupted with a pre-chilled Eppendorf tip and sonicated for an additional 5 min. The samples were then centrifuged at 4000 RPM for 3 min and the supernatant was collected in a new vial with 100 µl glass insert. Gut extracts were analyzed for UHPLC-HRMS/MS using nonpolar and polar fractions.

UHPLC-ESI-HRMS/MS was performed at Ultimate 3000 series RSLC (Dionex) coupled with a Q-Exactive HF-X mass spectrometer (Thermo Fisher Scientific, Waltham, USA).

Water (solvent A) and acetonitrile (solvent B, LiChrosolv hypergrade for LC-MS; Merck, Darmstadt, Germany), both with 0.1% (v/v) formic acid (Eluent for LC-MS, Sigma Aldrich, Steinheim, Germany) were used for the binary solvent system. After injection of 10 µl extract, chromatographic separation was performed with a constant flow rate of 300 µl/min using an Acclaim C18 column (150 × 2.1mm, 2.2 µm; Dionex, Borgenteich, Germany). Solvent gradients (B 0.5–100% v/v for 15 min; 100% B for 5 min; 100–0.5% v/v for 0.1min; 0.5% for 5 min) were used. Ionization in the HESI ion source was achieved by 4.2 kV cone voltage, 35 V capillary voltage, and 300°C capillary temperature in the transfer tube in positive ion mode and 3.3 kV cone voltage, 35 V capillary voltage and 320°C capillary temperature in negative mode. Mass spectra were recorded in the positive and negative ion mode at m/z 80–800 mass range in duplicate. Date-dependent acquisition using the TOP5 routine was used with one survey scan mass resolution 60,000 (HWFM) and 5 CID scans with 7,500 resolution in a 0.3 sec. Colision-induced dissociation (cd) of quadrupole selected precursor (0.8 Da mass window) was done in a collision cell at typical normalized fragmentation energy 30 eV. For identification pairs of the accurate mass of ions and of their collision-induced ionization fragments with the retention time values were interpreted using software XCALIBUR (Thermo Fisher Scientific, Waltham, USA). For the identification of metabolites samples were compared and statistically evaluated using the software MetaboAnalyst 2.0, and determined masses were compared with the database. The high-resolution LC-MS raw spectra were first centroided by converting them to mzXML format using the MS Convert feature of Proteo Wizard 3.0.18324. Data processing was subsequently carried out with R Studio v1.1.463 using the Bioconductor XCMS package v 3.4.2 (Smith et al. 2006; Tautenhahn et al. 2008; Benton et al. 2010), which contains algorithms for peak detection, peak deconvolution, peak alignment, and gap filling. The resulting peak list was uploaded into Metaboanalyst 4.0 (Chong et al., 2018), a web-based tool for metabolomics data processing, statistical analysis, and functional interpretation where statistical analysis and modeling were performed. K-nearest neighbor missing value estimation was used to replacing gaps. Data filtering was implemented by detecting and removing non-informative variables that are characterized by near-constant values throughout the

experimental conditions by comparing their robust estimate interquartile ranges (IQR). Data was auto-scaled. Out of the 3020 mass features originally detected, were used for the Principal Least Square Discriminant Analysis. For the identification of candidate metabolites, the individual mass features that contributed to the separation between the different classes were further characterized by applying a range of univariate and multivariate statistical tests to determine their importance including the Pls-da importance variables, t-test, and Random Forest. Along with retention time, accurate mass and MS/MS spectra, the generated information was probed with existing literature and databases. MS/MS spectra files were also centroided and imported into GNPS (Wang et al., 2016) for spectral matches and classical molecular networking.

3.3 Differential gene expression (DGE) analysis:

Gut tissue was dissected using RNA later solution and 10 guts per biological sample were obtained. Four biological replicate included three technical replicates for each biological replicates were performed. RNA extraction was completed using the preoptimized protocol (Roy et al., 2017; Sellamuthu et al., 2022). The quality and quantity of the extracted RNA were evaluated using agarose gel and Qubit, respectively. Integrity was determined using the 2100 Bioanalyzer system (Agilent Technologies, Inc). Pure RNA samples (RIN>7) were sent for sequencing to NoVo gene sequencing company, China. Sequencing was completed with NOVAseq6000 (PE150, 30 million raw reads). RNA (1 µg) was used for cDNA synthesis using the M-MLV reverse transcriptase kit following the manufacturer's protocol and stored at −80°C for downstream analysis.

3.3.1 RNA sequencing (RNA-seq.) analysis:

Gene expression from the RNA-seq. data was quantified using CLC workbench and standardised via a pre-optimised setting for mapping exon regions exclusively with genome reference (Powell et al., 2020). Later, a TPM algorithm was used to correct the sequence dataset biases and variation in transcript sizes using correct estimates for relative expression levels. Finally, empirical DGE analysis was performed using the recommended parameters (Roy et al., 2017; Roy and Palli, 2018). For DGE, FDR

corrected p-value cut off <0.05 and fold change cut off ± 4 -fold as a threshold value for being significant. Genes that are differentially expressed were annotated using the "cloud blast" with functional features using a "Blasto2GO plug-in" in CLC Genomic Workbench. A nucleotide blast was performed against the arthropod database with an E-value cut off 1.0E-10. Both annex and GO slim were used to improve the GO term identification further by crossing the three GO categories (biological process, molecular function, and cellular component) to search for name similarities, GO term, and enzyme relationships within KEGG (Kyoto Encyclopaedia of Genes and Genomes) pathway database.

3.3.2 Quantitative-RealTime PCR (qRT-PCR) analysis:

Total RNA was extracted from male gut tissue samples to validate the RNA sequencing data. Twenty genes, including eight genes from the mevalonate pathway, nine genes from CYP450, and three gene esterases were selected for qRT-PCR based on the differential expression level and specific functions in supplementary table 1. Primers were designed using IDT`s primer design software (www.idtdna.com). cDNA was synthesized using an M-MLV reverse transcriptase kit following the manufacturer's protocol. qRT-PCR was performed using SYBRTM Green PCR master mix (Applied Biosystems, USA) under the following parameters: 95°C for 3 min, 40 cycles of 95°C for 3 s, 60°C for 34 s (Roy et al., 2017; Cheng et al., 2018). A melting curve was generated to ensure single-product amplification and eliminate the possibility of primer dimers and nonspecific amplicons. The relative expression levels of the target genes were calculated using the 2-ΔΔCt method with two housekeeping genes as a reference for normalization and four biological replications.

3.4 Differential protein expression (DPE) analysis:

Frozen beetles were dissected under dry ice, and four biological replicates of each treatment were used for protein extraction and analysis. Each biological replicate contained tissue of three individual guts. Protein extraction was lysed in a cold buffer containing 50 mm Tris-HCl, pH 7.5, 1 mM EDTA, 150 mM NaCl, 1% N-octylglycoside, and

0.1% sodium deoxycholate. Gut tissue in the buffer with protease inhibitor mixture (Roche) was incubated for 15 min on ice. Lysates were cleared by centrifugation, and after precipitation with chloroform/methanol, proteins were resuspended in 6 m urea, 2 m thiourea, 10 mm HEPES, pH 8.0 and proceeded for digestion (Cox et al., 2014).

The samples were homogenized and lysed by boiling at 95°C for 10 min in 100 mM TEAB (triethylammonium bicarbonate) containing 2% SDC (sodium deoxycholate), 40 mM chloroacetamide, and 10 mM Tris-2-carboxyethyl phosphine. Followed by, samples were put in sonication (Bandelin Sonoplus Mini 20, MS 1.5) and the obtained proteins were measured for concentration using a standard protein assay kit (Thermo Fisher Scientific, USA). About 30 µg of protein per sample was used for MS sample preparation.

SP3 beads were used for sample processing. Five µl of SP3 beads were mixed with 30 µg protein in a lysis buffer and made up to 50 µl with TEAB (100 mM). Protein binding was induced by adding ethanol to a final concentration of 60% (vol/vol). The samples were thoroughly mixed and incubated at 24°C for 5 min. After SP3 was bound to the proteins, the tubes were placed on a magnetic rack, and the remaining unbound supernatant was discarded. Using 180 µl of 80% ethanol, beads were washed twice. After washing, samples were digested with trypsin (trypsin/protein ratio 1/30) and reconstituted in 100 mM TEAB at 37°C overnight. Digested samples were acidified using trifluoro acetic acid for 1% final concentration. Finally, peptides were desalted using in-house stage tips packed with C18 disks (Empore) (Rappsilber et al., 2007).

3.4.1 NanoLiquid Chromatography (nLC)-MS/MS analysis:

nLC-MS/MS analysis was performed with nano-reversed-phase columns (EASY-Spray column, 50 cm × 75 µm ID, PepMap C18, 2 µm particles, 100 µm pore size). In this analysis, mobile phase buffer A (0.1% formic acid in water) and mobile phase buffer B (acetonitrile and 0.1% formic acid) were used. Samples were loaded in a trap column of C18 PepMap100, 5 µm particle size, 300 µm x 5 mm from Thermo Scientific. About 4 min at 18 µl/min loading buffer with water, 2% acetonitrile, and 0.1% trifluoroacetic acid were used for loading. Peptides were eluted with a mobile phase B gradient of 4–35%

over 120 min. The eluted peptide cations were converted into gas-phase ions by electrospray ionization. A Thermo Orbitrap Fusion (Q-OT-qIT, Thermo Scientific) was used for the analysis. Survey scans of peptide precursors from 350–1400 m/z were performed using an Orbitrap at 120 K resolution (200 m/z) with a 5 × 105 ion count target. Tandem MS was isolated at 1,5 using a quadrupole, HCD fragmentation with a normalized collision energy of 30, and rapid scan analysis in the ion trap. The second mass spectral ion count target was set to 104, and the maximum injection time was 35 ms. Precursors with charge states two to six were strictly sampled and the selected precursor and its isotopes were included in the dynamic exclusion duration of 30 s with 10-ppm tolerance. Monoisotopic precursor selection was performed, and the instrument was run in 2 s cycles speed mode (Hebert et al., 2014).

All data were analyzed and quantified using MaxQuant software (version 2.0.2.0) (Cox and Mann, 2008). The FDR was limited to 1% for both full proteins and small peptides. The peptide lengths of the seven amino acids are specified. An MS/MS spectral search was performed using the Andromeda search engine against the *I. typographus* genome database. The C-termini of Arg and Lys were set for enzyme specificity, allowing the cleavage of proline bonds with a maximum of two missed cleavages. Cysteine dithiomethylation was selected as the fixed modification. Various modifications were considered with N- N-terminal protein acetylation and methionine oxidation. Matches between the run features from MaxQuant were used to transfer the identified peaks to other LC-MS/MS systems. Runs based on masses and retention times (with a maximum deviation of 0.7 min) were also considered for quantification. A label-free MaxQuant algorithm was used for quantification (Cox et al., 2014). Data analysis was performed using Perseus 1.6.15.0 (Tyanova et al., 2016).

3.5 Statistics:

Statistical analysis of quantified data was performed using a one-way analysis of variance (ANOVA) and Fisher (LSD) test with a 95% confidence interval in the XLSTAT-Student 2020 licensed version and TIBCO Statistics (USA, 2021). UHPLC-HRMS-MS data

analysis was performed using MetaboAnalyst 4.0. G -MS data were cleaned for residua of analysis, normalized (constant raw sum), and evaluated using principal component analysis (PCA) in the SIMCA 17 software (Sartorius Stedim Data Analytics AB, Malmô, Sweden). The data from transcriptome and proteome was normalized using CLC workbench 21.0.5 (QIAGEN Aarhus, Denmark) and MaxQuant software (version 2.0.2.0) respectively for significant data ($P< 0.05$).

4. RESULT SYNTHESIS:

The result synthesis chapter is segregated with peer-reviewed **three published scientific articles**.

- **Publication 1:** Research findings show results after testing hypothesis 1 for the respective pheromone compounds and expression of relevant gene families from key life stages of *I. typographus* gut tissue using a comparative study of transcriptome and metabolome. **Ramakrishnan et al., 2022a.**
- **Publication 2:** Followed by the previous publication on pheromone biosynthesis across life stages of hypothesis 1, a special data set revealing added information from analytical methods, and the gene families which also related to other functions such as detoxifications from a specific life stage *of I. typographus* male and female gut tissue were highlighted here. **Ramakrishnan et al., 2022b**.
- **Publication 3:** The final publication contains findings after checking hypothesis 2 by an artificial pheromone biosynthesis method of inducing the beetle with juvenile hormone III (JH III) and focuses exclusively on the pheromone-related pathways from *I. typographus* male and female beetles using an elaborated transcriptome, proteome, and metabolomic analyses. **Ramakrishnan et al., 2024**.

4.1 Publication 1:

Metabolomics and transcriptomics of pheromone biosynthesis in an aggressive forest pest *Ips typographus*

Citation: Ramakrishnan, R., Hradecký, J., Roy, A., Kalinová, B., Mendezes C. R., Synek, J., Bláha, J., Svatoš, A., Jirošová, A., 2022a. Metabolomics and transcriptomics of pheromone biosynthesis in an aggressive forest pest *Ips typographus*. Insect Biochem. Mol. Biol 0965-1748. https://doi.org/10.1016/j.ibmb.2021.103680

Summary:

Publication 1 contains essential information after testing hypothesis 1 to identify candidate genes involved in **pheromone biosynthesis and the related compounds across the key life stages of *Ips typographus***. In this study, we performed metabolomic and transcriptomic analyses of the pheromone biosynthesis at important life stages of *I. typographus*. Quantified pheromone metabolites from analytical methods confirmed the specific life stages of the beetle to focus on the targeted objective. Also, the gene expressions from the molecular methods were co-related with the pheromone occurring life stages narrowed down the potential candidates. The candidates from three gene families, **mevalonate pathway** with five genes key including **isoprenoid-di-phosphate synthase (IPDS)**, **Cytochrome P450 genes**, and **esterase genes**. The identified genes from key life stages of male *I. typographus* that involved in pheromone biosynthesis were identified from the respective life stages for significant gene expression patterns. Identified gene candidates were proposed for the biosynthetic functions based on relevant co-relation analysis and literature support from other bark beetle species.

Insect Biochemistry and Molecular Biology 140 (2022) 103680

Contents lists available at ScienceDirect

Insect Biochemistry and Molecular Biology

journal homepage: www.elsevier.com/locate/ibmb

Metabolomics and transcriptomics of pheromone biosynthesis in an aggressive forest pest *Ips typographus*

Rajarajan Ramakrishnan [a], Jaromír Hradecký [a], Amit Roy [a], Blanka Kalinová [a], Rya C. Mendezes [b], Jiri Synek [a], Jaromír Bláha [a], Aleš Svatoš [b,c], Anna Jirošová [a,*]

[a] Faculty of Forestry and Wood Sciences, Czech University of Life Sciences Prague, Czech Republic
[b] Max Planck Institute for Chemical Ecology, Jena, Germany
[c] Institute of Organic Chemistry and Biochemistry, the Czech Academy of Sciences, Prague, Czech Republic

ARTICLE INFO

Keywords:
Pheromone biosynthesis
Bark beetle
Spruce
Gut tissue
de novo
Omics

ABSTRACT

Eurasian spruce bark beetle, *Ips typographus*, is a destructive pest in spruce forests. The ability of *I. typographus* to colonise host trees depends on its massive aggregation behaviour mediated by aggregation pheromones, consisting of 2-methyl-3-buten-2-ol and *cis*-verbenol. Other biologically active compounds such as ipsdienol and verbenone have also been detected in the beetle. Biosynthesis of 2-methyl-3-buten-2-ol and ipsdienol *de novo* from mevalonate and that of *cis*-verbenol from *α*-pinene sequestrated from the host have been reported in preliminary studies. However, knowledge on the molecular mechanisms underlying pheromone biosynthesis in this pest is currently limited. In this study, we performed metabolomic and differential gene expression (DGE) analysis for the pheromone-producing life stages of *I. typographus*. The highest amounts of 2-methyl-3-buten-2-ol (238 ng/gut) and *cis*-verbenol (23 ng/gut) were found in the fed male gut (colonisation stage) and the immature male gut (early stage), respectively. We also determined the amount of verbenyl oleate (the possible storage form of *cis*-verbenol), a monoterpenyl fatty acid ester, to be approximately 1604 ng/mg in the immature stage in the beetle body. DGE analysis revealed possible candidate genes involved in the biosynthesis of the quantified pheromones and related compounds. A novel hemiterpene-synthesising candidate isoprenyl-di-phosphate synthase Ityp09271 gene proposed for 2-methyl-3-buten-2-ol synthesis was found to be highly expressed only in the fed male beetle gut. Putative cytochrome P450 genes involved in *cis/trans*-verbenol synthesis and an esterase gene Ityp11977, which could regulate verbenyl oleate synthesis, were identified in the immature male gut. Our findings from the molecular analysis of pheromone-producing gene families are the first such results reported for *I. typographus*. With further characterisation of the identified genes, we can develop novel strategies to disrupt the aggregation behaviour of *I. typographus* and thereby prevent vegetation loss.

1. Introduction

Bark beetle attacks on spruce vegetation in Eurasian forests are becoming a critical issue that needs to be addressed. *Ips typographus* (Coleoptera, Curculionidae), especially, is a destructive pest for spruce vegetation in European countries (Biedermann et al., 2019). Specifically, in the Czech Republic, vegetation loss was estimated at up to 14.5 million m^3 during recent years (Knížek, 2020). The crisis caused by the beetles in spruce forests in recent years has increased by many folds compared to previous reports (Huang et al., 2020; Thom and Seidl 2016).

I. typographus males are the pioneer sex in finding the suitable host tree during colonisation. After landing, males produce the aggregation pheromones; these males are then joined by conspecific beetles for the mass attack. Once enough beetles are recruited to overcome tree defence, anti-aggregation compounds are produced in beetle galleries to regulate the colonisation density within the tree. The aggregation pheromones of *I. typographus* consist of two essential compounds: 2-methyl-3-buten-2-ol and *cis*-verbenol (Schlyter et al., 1987). During colonisation, the pheromone compounds ipsdienol and ipsenol have been identified in beetles after mating in the gallery mating chambers. In the later colonisation phase, an anti-attractant verbenone is produced with the possible involvement of microorganisms (Hunt and Borden

* Corresponding author. Faculty of Forestry and Wood Sciences, Czech University of Life Sciences Prague , Kamýcká 129, 165 21 Praha 6, Suchdol, Czech Republic.
E-mail address: jirosovaa@fld.czu.cz (A. Jirošová).

https://doi.org/10.1016/j.ibmb.2021.103680
Received 4 August 2021; Received in revised form 8 October 2021; Accepted 5 November 2021
Available online 19 November 2021

Abbreviations

ANOVA	Analysis of variance
DGE	Differential gene expression
FPPS	Farnesyl-di-phosphate synthase
GPPS	Geranyl-di-phosphate synthase
IPDS	Isoprenoid-di-phosphate synthase
IPPI	Isopentyl-di-phosphate isomerase
KEGG	Kyoto Encyclopedia of Genes and Genomes
PCA	Principal component analysis

1990) for redirecting the arriving beetles to the surrounding unoccupied trees (Byers and Birgersson 1990). Furthermore, most pheromones are produced in the beetle's gut tissue (Byers and Wood 1981). The schematic pathway putatively involved in the production of various pheromone compounds in *I. typographus* gut tissue is depicted in Fig. 1.

The process of *de novo* pheromone biosynthesis in bark beetle gut tissue has been described (Hall et al., 2002). 2-Methyl-3-buten-2-ol, the hemiterpene aggregation pheromone of *I. typographus*, was reported to be synthesised *de novo* from mevalonate, based on results obtained from radiolabelling experiments (Lanne et al., 1989). However, the reactions and enzymes involved in the conversion of mevalonate pathway intermediates into 2-methyl-3-buten-2-ol in *I. typographus* have not yet been described. An enzyme, isoprenyl diphosphate synthase (IPDS) is considered to be involved in prenyl transfer and sequential carbo-cation formation from dimethylallyl diphosphate during 2-methyl-3-buten-2-ol synthesis in trees (Fisher et al., 2000). Other IPDS are known for their involvement in the biosynthesis of pheromone compounds such as frontalin in *Dendroctonus ponderosae* (Keeling et al., 2013) and murgantiol in the harlequin bug (Lancaster et al., 2018). To date, studies have shown that the mevalonate pathway genes encoding 3-hydroxy-3--methyl glutaryl coenzyme-A synthase (HMG-S), 3-hydroxy-3-methyl glutaryl coenzyme-A reductase (HMG-R), isopentyl-di-phosphate isomerase (IPPI), farnesyl-di-phosphate synthase (FPPS), and geranyl-di-phosphate synthase (GPPS) were up regulated after feeding in *I. pini* (Keeling et al., 2004). In *I. duplicatus*, HMG-R inhibition reduced pheromone production (Ivarsson et al., 1993). Similar to feeding (attack stage of the beetle in colonisation), another method involving the topical application of juvenile hormone (JH III) is known to stimulate *de novo* pheromone biosynthesis in some, but not all bark beetles (Keeling et al., 2016; Tillman et al. 1998, 2004).

Cis-verbenol is produced from the host tree-derived precursor α-pinene after hydroxylation, which is catalysed by cytochrome P450 (CyP450) (Renwick et al., 1976). A similar process for the synthesis of *trans*-verbenol from α-pinene using CyP6DE1 was described in *D. ponderosae* (Chiu et al., 2019). In *Ips* sp., the CyP450 gene family also has functions in processes such as cuticular hydrocarbon synthesis

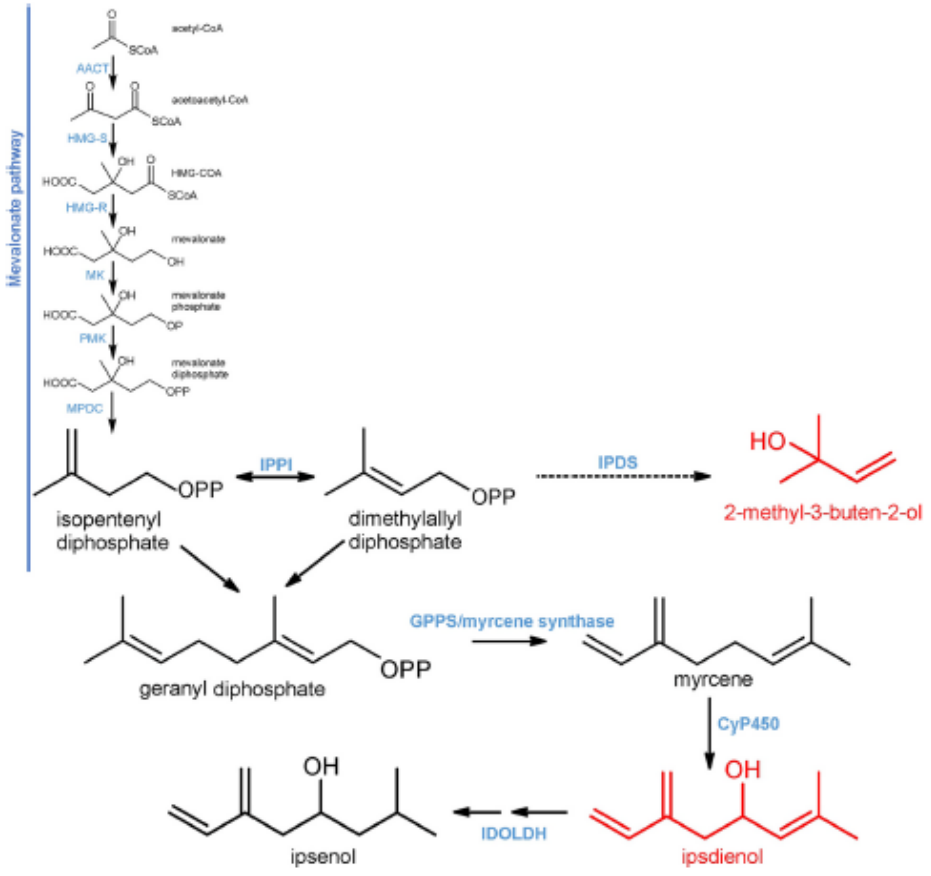

Fig. 1A. Proposed biosynthetic pathways of *Ips typographus* male pheromone biosynthesis. Mevalonate pathway: biosynthesis of pheromone components hemiterpene 2-methyl-3-buten-2-ol and ipdienol. Red: Structures of active pheromone compounds and monoterpenyl ester precursor, Blue: Enzymes suggested to be involved in proposed biosynthetic steps. (For interpretation of the references to colour in this figure legend, the reader is referred to the Web version of this article.)

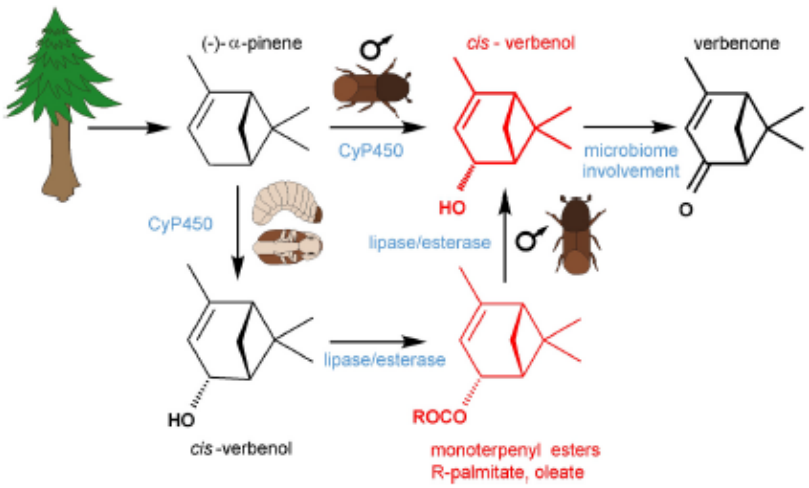

Fig. 1B. Proposed biosynthetic pathways of *Ips typographus* male pheromone biosynthesis. Biosynthetic pathway of *cis*-verbenol via the hydroxylation of sequestered tree α-pinene or through release from precursor monoterpenyl esters. Red: Structures of active pheromone compounds and monoterpenyl ester precursor, Blue: Enzymes suggested to be involved in proposed biosynthetic steps. (For interpretation of the references to colour in this figure legend, the reader is referred to the Web version of this article.)

(CyP4G55//56) (MacLean et al., 2018) and detoxification mechanisms (CyP6DE3) (Nadeau et al., 2017). In addition, at the terminal step of ipsdienol synthesis, the hydroxylation of myrcene is also catalysed by CyP450 (CYP9T1/T2) (Song et al., 2013). Later, ipsdienol is oxidised into ipsdienone by ipsdienol dehydrogenase (Figueroa-Teran et al., 2012). Verbenone, an anti-attractant for many bark beetles, including *I. typographus*, is presumably produced with gut microbes involvement (Hunt and Borden 1990; Xu et al., 2016), even though the possibility of verbenol oxidation by beetles enzyme cannot be entirely excluded. Other than the pheromones mentioned above, compounds such as *trans*-verbenol, myrcene, phenylethanol, and myrtenol have also been detected in the *I. typographus* gut (Birgersson et al., 1984; Schlyter et al., 1987). However, the roles of these compounds on beetle behaviour, if any, are not yet known.

Recently, *cis/trans*-verbenol production from monoterpenyl fatty acid esters of oxygenated monoterpenes has been reported in the fat body of *D. ponderosae* (Chiu et al., 2018). It was hypothesised that the *cis/trans*-verbenol derivative verbenyl oleate and other unknown esters, possibly represent the storage form of the pheromone in earlier life stages (larvae, pupae, & immature) of bark beetle. During colonisation, adult beetles hydrolyse esters and release verbenol as pheromones in the absence of the host-derived precursor (α-pinene). Hydrolysis of monoterpenyl esters requires the occurrence of a catalytic reaction involving esterase/lipase (Chiu et al., 2018).

Disrupting pheromone biosynthesis by targeting genes responsible for the biosynthesis of key aggregation pheromones in gut tissue of *I. typographus* could be a promising approach for managing the activity of this pest species. To achieve this goal, it is essential to identify candidate genes involved in pheromone biosynthesis and the related compounds. In this study, we performed metabolomic and transcriptomic analyses of the pheromone biosynthesis at important life stages of *I. typographus*. The candidate gene families involved in *I. typographus* pheromone compounds biosynthesis was searched in respective life stages of the beetle. The candidate genes involvement in certain life stage was validated using relative expression analysis.

2. Materials and methods

2.1. Rearing conditions for different life stages of I. typographus

Spruce logs (*Picea abies*) naturally infested with *I. typographus* (F0 generation) were obtained from plots at Czech University of Life Sciences, Prague, near Kostelec nad Černými lesy. The infested logs were stored in a cold chamber (4 °C) until used. Fresh spruce logs (app. 50 cm) were infested with F0 generation beetles (150 beetles per log) and maintained under laboratory conditions (70% humidity, 24 °C,16:8 h day/night period, and ventilated plastic containers of 56x39x28 cm/45 l volume) for incubation to establish the F1 generation. After 3–4 weeks of incubation, F1 generation beetles at different life stages were collected: larvae, pupae, immature beetles (golden-coloured teneral beetles with soft cuticle), sclerotised beetles (beetles with dark cuticle, still in the breeding log), emerged beetles (beetles emerged from the breeding log), flying beetles (emerged beetles with 24 h of flying), fed beetles (males and females separately excavating nuptial chambers in an uninfested spruce log for 24 h), mated beetles (male introduced first in an uninfested spruce log, followed by introduction of a female after 24 h and collection of beetles from mating chambers after 48 h). After collecting beetles at appropriate life stages, they were sorted according to sex and external morphological characteristics (Schlyter and Cederholm 1981) (except larvae and pupae).

Furthermore, the beetles that emerged were sorted by sex and used for hormone (JH III) treatment. Acetone (0.5 μl; control) and JH III (20 μg/μl acetone) were applied topically on the abdomen of beetles. After application, beetles were kept under laboratory conditions mentioned above for 8 h. Beetles were frozen in liquid nitrogen and stored at −80°C for further processing. Before analysis, the guts were dissected from beetles of different life stages (except larvae and pupae), and visibly adhered foreign bodies from the gut were cleansed with the help of a stereomicroscope for further metabolomic and DGE analysis. In this study, the beetle body refers to remaining tissue with the fat after gut, elytra, and wings have been removed.

2.2. Metabolomic analysis

2.2.1. Gas chromatograph coupled to mass spectrometer (GC-MS) analysis

Guts were dissected from the frozen beetles, and immediately submerged in 2 ml-analytical vials (10 guts/100 μl) of cold pentane. The beetle body was placed in another vial with chloroform. (10 beetle bodies/1000 μl chloroform) (Birgersson and Bergström, 1989; Birgersson et al., 1984).

GC-MS Agilent 7890B (Agilent Technologies, Palo Alto, CA, USA) employing time of flight mass analyser Pegasus 4D (LECO, St. Joseph, MI, USA) was used for the separation, identification and quantification of extracted compounds. One microliter of the extract was injected into a cold PTV injector (20C) in split 10:1 mode. After injection, the inlet was heated to 275 °C at a rate of 8 °C/s. Separation was conducted on HP-

5MS UI capillary column (30 m, 0.25 mm i.d., 0.25 μm film thickness) from Agilent. The GC oven temperature program was as follows: 40 °C for 1 min; then ramped at a rate of 10 °C min^{-1} to 210 °C; then at 20 °C min^{-1} to 320 °C and held for 6 min. The total GC run time was 29.5 min. Ions (ionisation energy at 70eV) were collected in a mass range of 35–500Da with a frequency of 10Hz.

Two-dimensional comprehensive gas chromatography was employed using the same instrument for the separation and quantification of compounds in beetle body extract. Here, injection in split mode (100:1) was used and secondary GC and modulator were programmed with an offset of 5 °C and 15 °C to first dimension GC oven, respectively. Column BPX-50 (SGE, Australia, 1.5 m, 0.1 mm i.d, 0.1 μm film thickness) was used for two-dimensional separation. A modulation period of 5 s was maintained for the whole length of the analysis. The temperature program was 40 °C (1,7 min); 10 °C/min 210 °C; 20 °C/min 320 °C (15 min). The total GC run time was 39.2 min.

Automated spectral deconvolution and peak finding algorithms were carried out using ChromaTOF software (LECO, St. Joseph, MI, USA). In target compound analysis, peak areas of unique mass from compounds mass spectrum were used for quantification. Linear calibration curves were constructed using responses of measured calibration mixtures diluted from standards. From the beetle body extract, verbenyl oleate and myrtenyl oleate were quantified based on external calibration according to responses of standards prepared by organic synthesis (Chiu et al., 2018).

In non-target analysis, peak alignment tool was used to compare and align all chromatographic signals with a signal to noise ratio (S/N) higher than 25 in all samples of gut extract. Non-target search in the beetle body was then performed using a parameter of S/N = 50. The data were cleaned, normalized (constant raw sum), and evaluated using principal component analysis (PCA) and partial least square-discriminant analysis (PLS-DA) in SIMCA 15 software (Sartorius Stedim Data Analytics AB, Malmö, Sweden). For tentative identification of compounds, comparison with mass spectra at the National Institute of Standards and Technology (NIST 2017) library was performed. For identity confirmation, retention indexes from NIST or retention times of respective standards were used.

2.2.2. Ultra-high-performance liquid chromatography-electrospray ionisation -high resolution tandem mass spectrometry (UHPLC-ESI-HRMS/MS) analysis

For nonpolar extraction, dissected guts (5 guts/sample) were collected in ethyl acetate (5 μl/gut) and stored at −80 °C prior analysis. Gut extracts (solvent without gut) were removed for nonpolar fraction. For polar extraction, rest of solvent was removed by a gentle stream of nitrogen and the remaining tissue was extracted (7 ml/gut) with MeOH/water/acetic acid (70/30/0.5 v/v) mixture contains ^{13}C2-myristic acid (1 μg/ml) standard. After sonication on ice (5 min) the tissue was disrupted with a pre-chilled Eppendorf tip and sonicated an additional 5 min. The samples were then centrifuged at 4000 RPM for 3 min and the supernatant was collected in new vial with 100 μl glass insert. Gut extracts with nonpolar and polar fractions were used for UHPLC-HRMS/MS analysis.

UHPLC-ESI-HRMS/MS was performed at Ultimate 3000 series RSLC (Dionex) coupled with Q-Exactive HF-X mass spectrometer (Thermo Fisher Scientific, Waltham, USA). Water (solvent A) and acetonitrile (solvent B, LiChrosolv hypergrade for LC-MS; Merck, Darmstadt, Germany), both with 0.1% (v/v) formic acid (Eluent for LC-MS, Sigma Aldrich, Steinheim, Germany) were used for the binary solvent system. After injection of 10 μl extract, chromatographic separation was performed with constant flow rate of 300 μl/min using an Acclaim C18 column (150 × 2.1 mm, 2.2 μm; Dionex, Borgenteich, Germany). Solvent gradients (B 0.5–100% v/v for 15 min; 100% B for 5 min; 100–0.5% v/v for 0.1min; 0.5% for 5 min) were used. Ionization in HESI ion source was achieved by 4.2 kV cone voltage, 35 V capillary voltage and 300 °C capillary temperature in the transfer tube in positive ion mode and 3.3 kV cone voltage, 35 V capillary voltage and 320° C capillary temperature in negative mode. Mass spectra were recorded in the positive and negative ion mode at m/z 80–800 mass range in duplicate. Date dependent acquisition using TOP5 routine was used with one survey scan mass resolution 60,000 (HWFM) and 5 CID scans with 7,500 resolution in ca 0.3 s. Collision-induced dissociation (hcd) of quadrupole selected precursor (0.8 Da mass window) was done in a collision cell at typical normalized fragmentation energy 30 eV. For identification pairs of the accurate mass of ions and of their collision-induced ionization fragments with the retention time values were interpreted using software XCALIBUR (Thermo Fisher Scientific, Waltham, USA). For identification of metabolites samples were compared and statistically evaluated using software MetaboAnalyst 2.0, and determined masses compared with database. The high-resolution LC-MS raw spectra were first centroided by converting them to mzXML format using the MS Convert feature of Proteo Wizard 3.0.18324. Data processing was subsequently carried out with R Studio v1.1.463 using the Bioconductor XCMS package v 3.4.2 (Benton et al., 2010); (Smith et al., 2006; Tautenhahn et al., 2008), which contains algorithms for peak detection, peak deconvolution, peak alignment and gap filling. The resulting peak list was uploaded into Metaboanalyst 4.0 (Chong et al., 2018), a web-based tool for metabolomics data processing, statistical analysis, and functional interpretation where statistical analysis and modelling was performed. Missing values were replaced using a (K-nearest neighbour) KNN missing value estimation. Data filtering was implemented by detecting and removing non-informative variables that are characterized by near-constant values throughout the experimental conditions by comparing their robust estimate interquartile ranges (IQR). Data was auto scaled. Out of the 3020 mass features originally detected, were used for the Principal Least Square Discriminant Analysis. For the identification of candidate metabolites, the individual mass features that contributed to the separation between the different classes were further characterized by applying a range of univariate and multivariate statistical tests to determine their importance including the Pls-da importance variables, t-test and Random Forest. This information, along with retention time, accurate mass and MS/MS spectra were used to probe into existing literature and databases. MS/MS spectra files were also centroided and imported into GNPS (Wang et al., 2016) for spectral matches and classical molecular networking. Dataset is available in Dryad link (open access).

2.3. Differential gene expression (DGE) analysis

Gut tissue was dissected using RNA*later* solution (10 μl/gut), and 10 guts per biological sample were obtained. RNA extraction was performed using the preoptimized protocol (Roy et al., 2017). The quality and quantity of the extracted RNA were evaluated using agarose gel and Qubit, respectively. Integrity was determined using the 2100 Bioanalyzer system (Agilent Technologies, Inc). Good quality RNA samples (RIN>7) were sent for sequencing (150bp paired-end reads, minimum 30 mil. reads per sample) to Novo-gene sequencing company, China.

2.3.1. RNA sequencing (RNA-seq.) analysis

Gene expression from the RNA-seq. data was quantified using CLC workbench and standardised via a pre-optimised setting for mapping exon regions exclusively with genome reference (Powell et al., 2020). Furthermore, the biases in the sequences datasets and different transcript sizes were corrected using the TPM algorithm to obtain correct estimates for relative expression levels. Finally, empirical DGE analysis was performed using the recommended parameters (Roy et al., 2017; Roy and Palli 2018). For DGE, FDR corrected p-value cut off < 0.05 and fold change cut off ±4 -fold as a threshold value for being significant. Differentially expressed genes were functionally annotated using the "cloud blast" feature within the "Blast2GO plug-in" in CLC Genomic Workbench. Nucleotide blast was performed against the arthropod database with an E-value cut off 1.0E-10. Both annexe and GO slim was

used to improve the GO term identification further by crossing the three GO categories (biological process, molecular function, and cellular component) to search for name similarities, GO term and enzyme relationships within KEGG (Kyoto Encyclopedia of Genes and Genomes) pathway database.

2.3.2. Quantitative-RealTime PCR (qRT-PCR) analysis

Total RNA was extracted from male gut tissue samples to validate the RNA sequencing data. Twenty genes, including eight genes from the mevalonate pathway, nine genes from CyP450 and three gene esterases were selected for qRT-PCR based on the differential expression level and specific functions in Supplementary Table 1. Primers were designed using IDT's primer design software (www.idtdna.com). cDNA was synthesised using an M-MLV reverse transcriptase kit following the manufacturer protocol. qRT-PCR was performed using SYBR™ Green PCR master mix (Applied Biosystems, USA) under the following parameters: 95 °C for 3 min, 40 cycles of 95 °C for 3 s, 60 °C for 34 s (Cheng et al., 2018; Roy et al., 2017). A melting curve was generated to ensure single product amplification and eliminate the possibility of primer dimers and nonspecific amplicons. The relative expression levels of the target genes were calculated using the $2^{-\Delta\Delta Ct}$ method with two housekeeping genes, ribosomal protein L6 and S18, as a reference for normalisation (Ramakrishnan et al., in prep.). Four biological replications, each with three technical replicates, were performed for each set of samples.

2.4. Statistics

Statistical analysis of quantified data (GC-MS and qRT-PCR) was performed using one-way analysis of variance (ANOVA) and Fisher (LSD) test with 95% confidence interval in XLSTAT-Student 2020 licensed version.

3. Results

3.1. Metabolomic analysis

3.1.1. GC-MS analysis

3.1.1.1. Identification of metabolic compounds in gut extracts obtained from beetles of all life stages. Based on the relative abundances of compounds in pentane gut extract, a principal component analysis (PCA) score plot was obtained. The PCA score plot covers more than 75% of the variability in the dataset and shows good separation between fed male guts and in immature male gut extracts. For the separation of fed males, the 2-methyl-3-buten-2-ol was the vital compound, whereas, for immature males, the most decisive variables were *cis*-verbenol and myrtenol. Other life stages did not separate to clusters. Odd-numbered hydrocarbons such as heptacosane (C27), pentacosane (C25) and their respective unsaturated hydrocarbons heptacosene and pentacosene were found associated with emerged and sclerotised stages (Fig. 2).

Another qualitative analysis of gut extracts from three male life stages (fed, sclerotised and emerged) showed clear separation in a PCA plot. The separation was influenced by the relative abundance of 2-methyl-3-buten-2-ol, as a decisive variable for fed males. Other compounds such as *cis*-verbenol, phenylethanol and tree compounds such as α-pinene, β-pinene had lower influence. Interestingly, fatty acid esters (methyl oleate and methyl palmitate) were identified in the mentioned compounds. For emerged male gut extracts, the most decisive compounds were odd-numbered hydrocarbons heptacosane (C27), pentacosane (C25) and their respective unsaturated forms (heptacosene and pentacosene). In sclerotised male gut extracts, the most decisive compounds were sesquiterpenes longipinene (C15) and curcumene (C15) (Supplementary Fig. 1).

3.1.1.2. Quantification of metabolites in gut extracts of beetles from different life stages. Levels of active pheromone compounds 2-methyl-3-buten-2-ol, *cis*-verbenol, ipsdienol, and verbenone were quantified in the beetle's gut (Fig. 3A). Concentrations ranged from trace amount to a maximum of 250 ng/gut. As expected, aggregation pheromone 2-methyl-3-buten-2-ol was observed only in males; however, trace amounts were found in females after mating. The highest amount of 2-methyl-3-buten-2-ol was 238 ng/beetle gut. However, trace amounts (5 ng–6 ng/beetle gut) were found in male beetles after emerging. Another aggregation pheromone, *cis*-verbenol, was quantified in the guts of immature beetles of both sexes (16–23 ng/gut). After the sclerotised stage, *cis*-verbenol disappeared and reappeared in later stages in male beetles. *Cis*-verbenol shows high levels at later stages in males such as flying, fed, and mated. A similar pattern was also found for an anti-attractant, verbenone. However, levels of verbenone were lower (<5 ng/gut). Ipsdienol, the compound typical in mated *Ips typographus* males, was detected in trace amounts (< 1 ng/gut) in mated male guts (Fig. 3A).

Levels of other compounds present in *I. typographus* gut extract with the less known behavioural functions, such as *trans*-verbenol, myrtenol, phenylethanol and alpha-myrcene were also quantified. *Trans*-verbenol (23 ng/gut) and myrtenol (38 ng/gut on average) were produced in the gut of both immature males and females. Though these two compounds were not found in sclerotised and emerging beetles, *trans*-verbenol and myrtenol started reappearing along with phenylethanol and alpha-myrcene in the later mature male beetle gut (fed and mated stages) (Fig. 3B). Further quantification of two hydrocarbons representatives (unsaturated heptacosene and saturated pentacosane) in the beetle gut across the life stages showed the occurrence of the compounds in the range of 200–600 ng/beetle gut in the emerged stage and 100–200 ng/beetle gut in other mature life stages of male beetles. The immature stage gut has the least amount (less than 50 ng/beetle gut). The amount of unsaturated heptacosene was three times higher than the amount of pentacosane (Supplementary Fig. 2.)

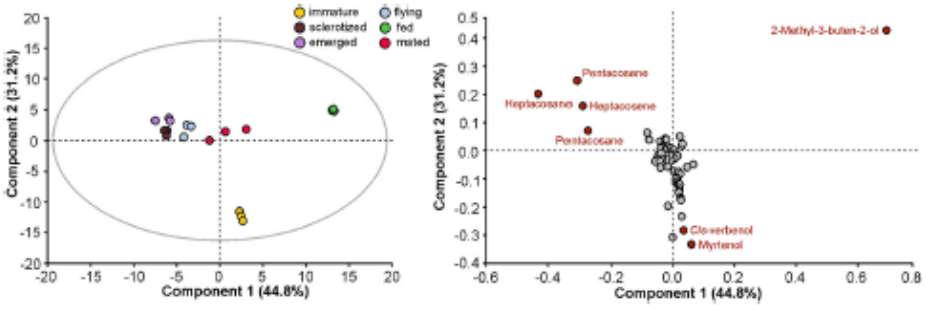

Fig. 2. Principal component analysis (PCA plot) for GC-MS chromatogram. PCA plot on the left shows male gut extract distribution at different life stages based on identified compounds on the right side with respective quadrants from the analysis.

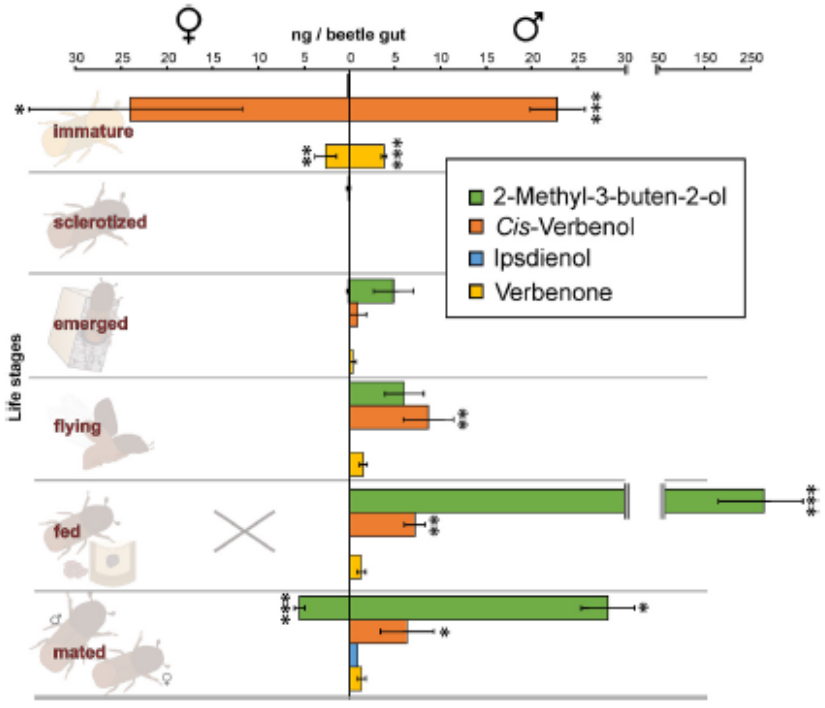

Fig. 3A. GC-MS quantification of behaviourally active pheromone compounds from gut tissue of *I. typographus* males and females at different life stages. Statistics: One-way ANOVA with Fisher (LSD) test with 95% confidence interval with Sclerotized stage as control group. *** represents $P < 0.001$, ** represents $P < 0.01$, * represents $P < 0.05$. X in Fig. indicates that the stage was not analysed. x axis: mean ± SE.

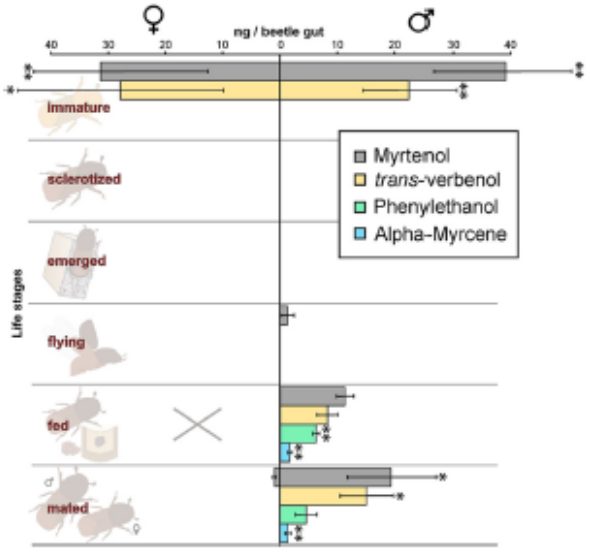

Fig. 3B. GC-MS quantification of compounds (behaviour unknown) obtained from gut tissue of *I. typographus* males and females at different life stages. Statistics: One-way ANOVA with Fisher (LSD) test with 95% confidence interval with Sclerotized stage as control group. ** represents $P < 0.01$, * represents $P < 0.05$. X in Fig. indicates that the stage was not analysed. x axis: mean ± SE.

3.1.1.3. Identification of metabolites in beetle body. The metabolomic profiles of the extracts of the beetle body from different life stages, including larvae and pupae, were compared (Fig. 4A). We aimed to compare semi-polar compounds, present mainly in the fat body, with relevance to pheromone biosynthesis. The PCA plot shows distinct separation of larvae from other life stages (Fig. 4A). This separation was associated with ethyl hexadecanoate (Fig. 4A). The pupae and immature beetles were clustered together. The cluster corresponded with monoterpenyl fatty acid esters, especially verbenyl and myrtenyl oleate (Fig. 4A). Other life stages did not cluster efficiently. (Fig. 4A). Further 2D GC-MS chromatogram from the mentioned samples provided clear distribution of fatty acid esters, including verbenyl palmitate, verbenyl oleate, myrtenyl oleate, and many other unidentified fatty acid esters (Fig. 4B).

3.1.1.4. Quantification of fatty acid esters and hydrocarbons in the beetle body. We quantified verbenyl oleate and myrtenyl-oleate in the beetle body from different life stages, including larvae and pupae. Verbenyl oleate and myrtenyl oleate were quantified in trace amounts (52 ng/mg of the body) for larvae and up to 475 ng/mg of the body in pupae. Though verbenyl oleate was quantified up to 1604 ng/mg of the beetle body and 1424 ng/mg of the beetle body at an immature stage of male and female, respectively, it was identified only in the male body in later mature stages (sclerotised, emerged, flying, fed, and mated), ranging 50–200 ng/mg of body. Further, myrtenyl oleate was also quantified in larvae (17 ng/mg of the body) and pupae (511 ng/mg of the body). In the immature stage, myrtenyl oleate levels were higher in males (519 ng/mg of the body) than in females (221 ng/mg of the body). Later, myrtenyl oleate could not be found in mature stages (sclerotised, emerged and flying). Interestingly, myrtenyl oleate reappeared in a fed and mated beetle body of male with traces amount (25–26 ng/mg of the body), below the quantification limit. (Fig. 5A). Quantification of previously mentioned two hydrocarbon representatives (unsaturated heptacosene and saturated pentacosane) in the beetle body across the life stages showed the compounds occurrence in similar pattern as in the

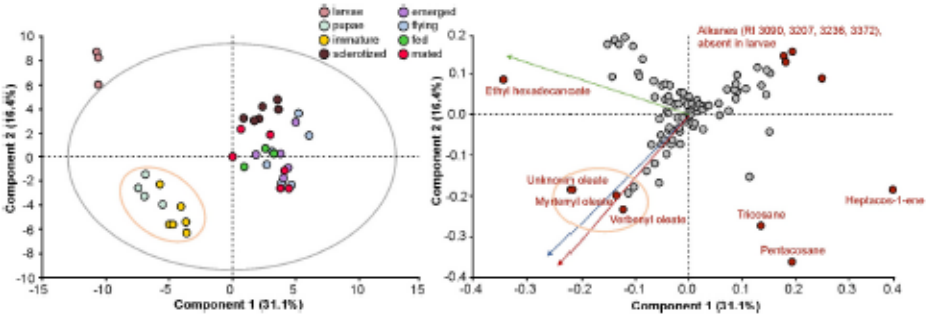

Fig. 4A. Principal component analysis (PCA plot) for GC-MS chromatogram. PCA plot on the left shows the distribution of different life stages and on the right showed respective compounds. Tissue: male beetle body.

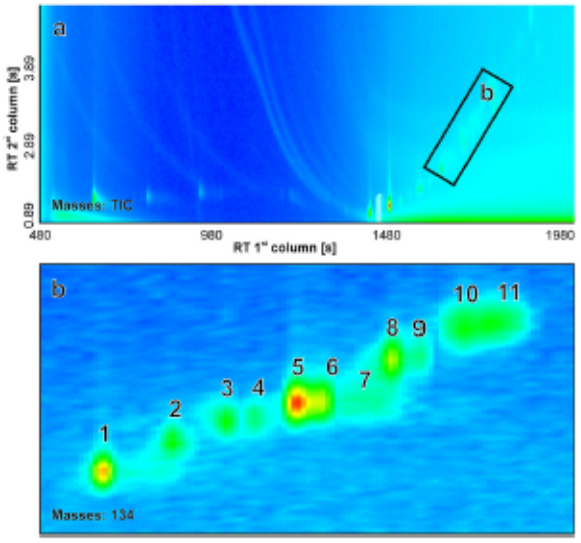

Fig. 4B. Chromatogram (a) from GCxGC-MS of total ion current with the region (b) showing fatty acid esters generated on *m/z* 134: 1-verbenyl palmitate; 5- verbenyl oleate; 8-myrtenyl oleate; 2,3,4,6,7,9,10,11- un-identified fatty acid esters. Tissue: immature male body.

beetle gut but with higher amount reaching 2000–10000 ng/mgof beetle body (Supplementary Fig. 2.)

The relative abundance of verbenyl oleate, methyl oleate (proposed residue from verbenyl oleate), and *cis*-verbenol among different life stages of male beetle extract from gut and body are presented as a percentage (Fig. 5B). The results showed a correlation between the quantity of the three compounds with a change across the life stages. The immature stage showed high levels of verbenyl oleate and *cis*-verbenol, with less than 10% of methyl oleate. Importantly, in the fed males, where *cis*-verbenol is produced, the percentage of vebenyl oleate as a putative precursor decreased (<5% abundance), and the percentage of methyl oleate and *cis*-verbenol as putative products increased. A similar pattern was also found in mated beetle (Fig. 5B).

3.1.1.5. Quantification of metabolites in beetle gut extract after JH III treatment. 2-Methyl-3-buten-2-ol (60 ng/gut) levels were significantly higher in male beetles after JH III treatment compared to those after acetone treatment (control). Additionally, *cis*-verbenol (12–15 ng/gut) levels also increased, albeit with low significance, in male beetles after JH III treatment. Whereas female beetles produced a trace amount of these compounds in both JH III treated and control groups. Traces of verbenone were detected in both treatments of male and female gut extracts (Fig. 6).

3.1.2. UHPLC-ESI-HRMS/MS analysis

In UHPLC-HR MS/MS, metabolomic data were obtained for polar metabolites to complement GC/MS data. We examined compounds related to pheromone biosynthesis. Untargeted analysis was performed in both positive and negative ion mode in the mass range from *m/z* 80 to *m/z* 800. Typically, ca 3000 mass features were detected and automatically selected for CID fragmentation using the TOP5 instrument algorithms setting. Several hundred (500–600) MS/MS spectra were collected in an individual run. These mass data were used for compound identification using the GNPS network engine (Wang et al., 2016), and obtained library hits were manually evaluated and modified wherever needed. One hundred forty-six compounds were identified in positive ion mode and sixty-one compounds in negative mode (Ramakrishnan et al., in prep.). They belonged to diverse structural classes. Amino acid/peptides were abundant in positive mode data. In negative mode, phenyl-propanoids were the most abundant class (Ramakrishnan et al., in prep.). Metabolites in individual life stages were well separated both in positive and negative ion modes (Supplementary Fig. 3). Several compounds responsible for PCA data separations were identified (Ramakrishnan et al., in prep.). However, pheromone biosynthesis-related compounds could not be identified.

While tracing potential precursors of 2-methyl-3-buten-2-ol, we checked for isopentenyl pyrophosphate (IPP) and/or dimethylallyl pyrophosphate (DMAPP). It was detected as a minor peak with Rt 4.73 min at *m/z* 244.99760, and corresponding molecular formulae $C_5H_{11}O_7P_2$ $[M\text{-}H]^-$ and delta −0.704 mmu was calculated. CID spectra and Rt correspond to an authentic standard, and CID spectrum is characterised by intense *m/z* 78.9578 PO_3^- ion. Under the used chromatographic conditions, we could not separate a mixture of authentic IPP and DMAPP standards and the peak is assigned as a mixture of both compounds. However, peak intensity was too low to obtain reliable integration data, and other isobaric compounds were co-eluted in this retention time window contaminating the mass spectra. However, upstream IPP/DMAPP intermediate, mevalonate-5-phosphate (Rt 9.2 min, *m/z* 227.0323 $C_6H_{12}PO_7$ delta −0.312 mmu; with MS/MS fragments at *m/z* 78.9581 (PO_3) and 98.9687 (H_2PO_4) characteristic for monophosphate), was more abundant, providing better data. Mevalonate-5-phosphate abundance peaks were found with interesting patterns in the male beetle gut. The compound appeared with high abundance in the flying stage and its abundance reduced in the fed stage. Later, Mevalonate-5-phosphate reappeared in the mated stage. A similar pattern was observed in the female with a low significance (Fig. 7).

3.1.2.1. Analysis of fatty acid esters and glycosides at different life stages using UHPLC/HRMS-MS. We also detected the verbenyl and myrtenyl

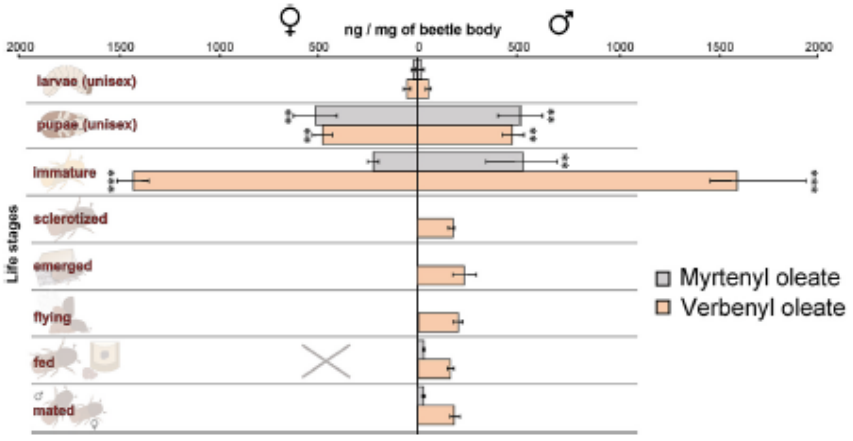

Fig. 5A. Myrtenyl and verbenyl oleate in the body of *I. typographus* male and female beetles at different life stages (GC-MS). Statistics: One-way ANOVA with Fisher (LSD) test with 95% confidence interval with Sclerotized stage as control group. *** represents $P < 0.001$, ** represents $P < 0.01$, * represents $P < 0.05$. X in Fig. indicates that the stage was not analysed. x axis: mean ± SE.

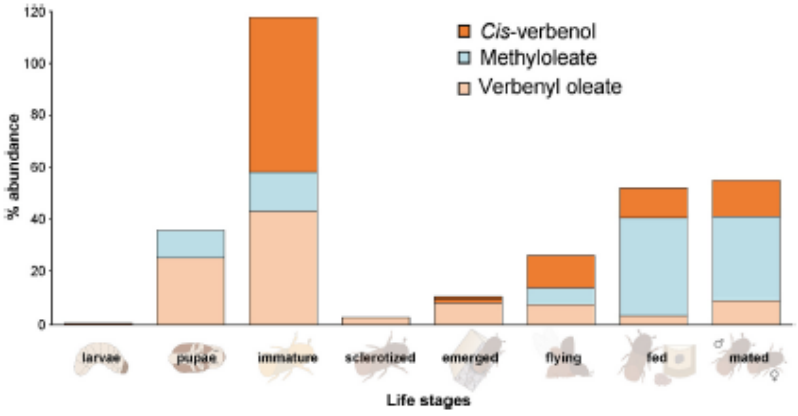

Fig. 5B. Relative abundance of *cis*-verbenol, verbenyl oleate, and methyl oleate in *I. typographus* male gut tissue at various life stages. Percentage abundance was calculated as a ratio of quantified compounds at individual life stages to the sum of quantified compounds at all life stages, obtained from GC-MS quantification data. x axis: mean ± SE.

oleates using UHPLC/HRMS-MS similar to previously described GC/MS identification (see above) as minor peaks at *m/z* 417.37227, $C_{28}H_{49}O_2$ $(M + H)^+$, delta −0.437 mu. The highest intensities were at early life stages, but due to overall low-intensity, data were not suitable for further analyses. In polar extracts analysed in positive mode, potential diglycosides as tree peaks with 9.11, 9.26, and 9.40 min Rt (proportion 53/26/21) at *m/z* 464.24863, $C_{21}H_{38}NO_{10}$ $[M + NH_4]^+$, delta −0.393 were observed. CID after the neutral loss of Gly-Gly-NH_3 adduct yielded an informative ion at *m/z* 135.11696 $C_{10}H_{15}$ indicated a potential terpene with four double bond equivalents. It is accompanied by other carbocations at *m/z* 109.10178 (C_8H_{13}), 107.08591 (C_8H_{11}), 93.07040 (C_7H_9, base peak) and 79.05479 (C_6H_7). In negative mode, corresponding diglycosides were also detected at *m/z* 445.20761, C21H33O10, delta −0.310 mu, $[M\text{-}H]^-$. No authentic standard is available, and the final structure should be further confirmed by chemical synthesis. But the presence of peaks and CID spectra indicate that these compounds are likely diglycosides of oxidative products of α-pinene like myrtenol and *cis/trans* verbenols.

3.2. DGE analysis

To further evaluate the expression profiles of genes associated with the biosynthesis of key pheromone components 2-methyl-3-buten-2-ol and *cis*-verbenol, we chose the gut tissue from two important stages (immature male and fed male) of the beetle for RNA-seq. based transcriptome analysis, followed by validation by qRT-PCR. Among a total of 23937 annotated genes in the *I. typographus* genome, the expression of 11657 genes was found to be upregulated in the fed male gut, and the expression of 7484 genes was upregulated in the immature male gut (heat map, Fig. 8A).

It is known that mevalonate is involved in 2-methyl-3-buten-2-ol synthesis (Lanne et al., 1989); moreover, our UHPLC-HRMS/MS analysis revealed the presence of mevalonate-5-phosphate (a mevalonate pathway intermediate) at different life stages in *I. typographus*. Therefore, we targeted the mevalonate pathway genes. Interestingly, five of the targeted genes showed upregulated expression in the fed stage; these included genes encoding geranyl diphosphate synthase/isoprenoid diphosphate synthase (IPDS) (Ityp09271), isopentyl diphosphate: dimethylallyl diphosphate isomerase (IPPI) (Ityp04875), 3-hydroxy-3--methylglutarylCoenzyme-A reductase (HMG-R) (Ityp17150),

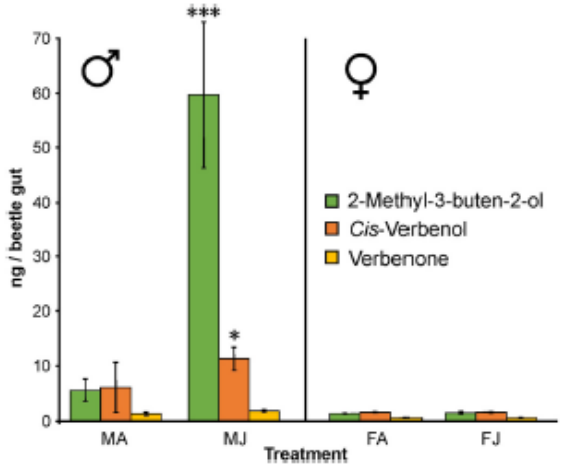

Fig. 6. Production of pheromone compounds after topical application of juvenile hormone III in male and female *I. typographus*. Treatment: MA/FA- male/female acetone treated beetle gut. MJ/FJ- Male/female JH III treated beetle gut. Statistics: One-way ANOVA with Fisher (LSD) test with 95% confidence interval. *** represents $P < 0.001$, * represents $P < 0.05$. $N = 3$. x axis: mean ± SE.

3-hydroxy-3-methylglutarylCoenzyme-A synthase (HMG-S) (Ityp09137), and phosphomevalonate kinase (PMK) (Ityp06045) (Fig. 8B). However, genes involved in sesqui- and monoterpene synthesis, such as those encoding farnesyl diphosphate synthase (FPPS) (Ityp09272) and ipsdienol dehydrogenase (Ityp14703), showed downregulated expression in the fed stage (Fig. 8A and B). Along with the identified IPDS gene family (Ityp09271), two orthologs of GPP/Myrcene synthase genes Ityp17873, Ityp17861 also showed moderately up regulated in the fed stage (Supplementary Fig. 3). qRT-PCR was performed for the abovementioned genes, and the expression levels were consistent with those obtained upon RNA-seq. qRT-PCR validation for the GPPS orthologs Ityp17873 and Ityp17861 were not performed in this study due to low read numbers in the RNA seq. analysis. (Fig. 8B).

Using qRT-PCR, the expression level of the five abovementioned mevalonate pathway genes was validated in the gut tissue of *I. typographus* at different life stages (Fig. 9). We calculated the relative expression of the genes at five mature male stages (sclerotised, emerged, flying, fed, and mated) with the immature stage used as a reference. Four genes, IPPI (Ityp04875), HMG-R (Ityp17150), HMG-S (Ityp09137) and PMK (Ityp06045), showed similar expression patterns in the emerged, flying, and fed male gut. On the other hand, IPDS (Ityp09271) expression showed a significant upregulation ($p \leq 0.05$) in the fed male gut only. This gene was moderately expressed in the sclerotised, emerged, and flying stages and downregulated in the mated male gut (Fig. 9).

Among the cytochrome P450 (CyP450) gene families, 56 CyP450 genes were differentially expressed in the gut tissue at two life stages (fed and immature male). Among the CyP450 genes identified, 24 genes were upregulated, and 32 genes were downregulated in the fed male gut. A neighbour-joining phylogenetic tree was constructed based on sequence similarity with a functionally known gene from *D. ponderosae*. Sequences were obtained from the NCBI database to elucidate the evolutionary relationship of CyP450 using the MEGA X program. The phylogenetic tree showed seven subgroups of identified CyP450 genes (Fig. 10A). These clusters had candidates with names such as CyP450- 6 like, CyP450- 4 like, and CyP450 9e2 like, along with a few uncertain CyP450 genes (Ramakrishnan et al., in prep.). Potential candidates Ityp 0496 (C1) and Ityp03903 (C2) showed high similarity to the *trans*--verbenol synthesising gene CyP6DE1 (a1like), and Contig Ityp03140 (C3) and Ityp03230 (C4) were similar to detoxification CyP6DE3 (a2 like) from *D. ponderosae* (Supplementary Table 1). C1 and C2 were moderately upregulated, and C3 and C4 were downregulated in the fed male gut (Fig. 10B). RNA-seq data showed opposite expression patterns for C1, C2, C3, and C4 when compared with the qRT-PCR results (data not shown).

According to the RNA-seq data, contig sequences of Ityp 03153 (C5), Ityp 03146 (C6), and Ityp 01834 (C7) showed similarity to CyP450-9T1/T2, which is involved in ipsdienol synthesis from other *Ips* sp. Furthermore, contig sequences of Ityp 04142 (C8) and Ityp 04140 (C9) showed similarity to CyP4G55/56, which is involved in hydrocarbon synthesis in bark beetle (Supplementary Table 1). qRT-PCR results of C5 to C9 in the mated male gut, compared with those in the sclerotised beetle, showed upregulated expression of C5 and C7 in the mated male gut. At this life stage, synthesis of ipsdienol pheromone is expected. C8 showed upregulated expression in the sclerotised stage. C9 showed upregulation in mated stages, which corresponds to a higher hydrocarbon production (Fig. 10C, Supplementary Fig. 2).

In addition, we chose three esterase gene sequences from the RNA seq. data. E1 (Ityp_7084), E2 (Ityp_9460), and E3 (Ityp_11977) showed similarity to BT127766.1 in *D. ponderosae*, which is expected to play a role in fatty acid ester storage (Supplementary Table 1). The qRT-PCR results of these genes showed that E1 expression was upregulated in the fed male gut and E3 expression was upregulated in the immature male gut. Although the qRT-PCR result of E2 showed an expression pattern opposite to that of the RNA-seq data, the expression patterns of

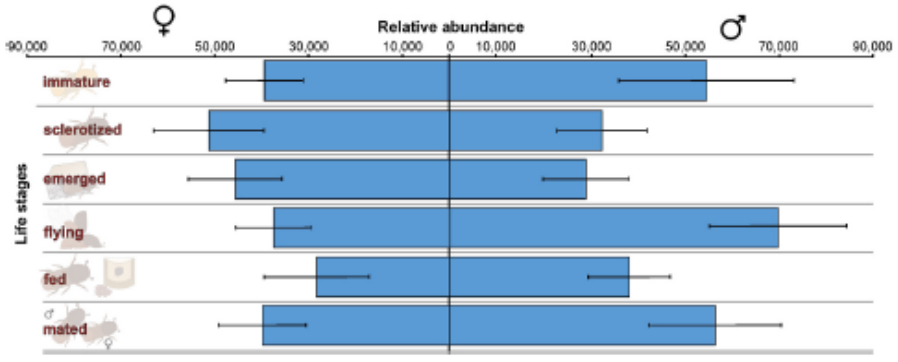

Fig. 7. Intensity of putatively identified mevalonate-5-phoshate, *m/z* 227.0323 plotted for *I. typographus* gut tissues obtained at different life stages. Gut extracts were analysed using an UPLC-ESI-MS/MS instrument in negative ion mode with TOP 5 scanning with one precursor ion scan and 5 MS/MS scans. Bars represent the standard error of the mean, $N = 3$.

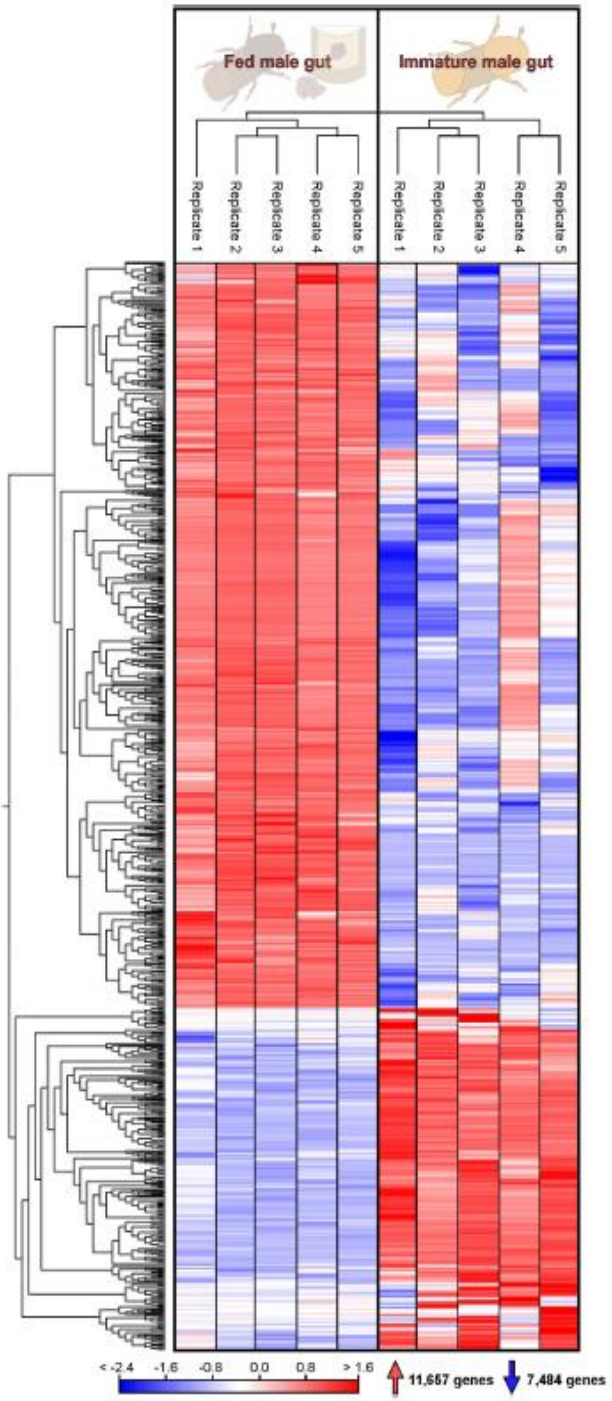

Fig. 8A. RNA-seq. data: Heat map (TPM) of the differentially expressed genes in fed male gut vs immature male gut. The values were chosen after FDR corrected P-value, $P < 0.05$, fold change ± 4. Red colour: high expression. Blue colour: low expression. Number next to arrow shows total number of gene with high and low expression. $N = 5$. (For interpretation of the references to colour in this figure legend, the reader is referred to the Web version of this article.)

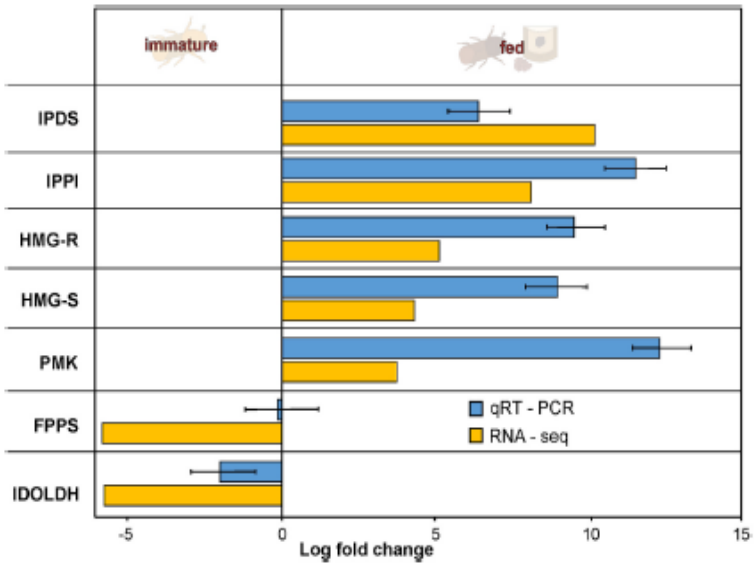

Fig. 8B. Relative expression of mevalonate pathway gene, as determined by RNA-seq. and qRT-PCR. Tissue: fed male gut vs immature male gut. Yellow: log fold change values from RNA-seq. data. Blue: log fold change values from qRT-PCR data. Error bar indicate standard error. (For interpretation of the references to colour in this figure legend, the reader is referred to the Web version of this article.)

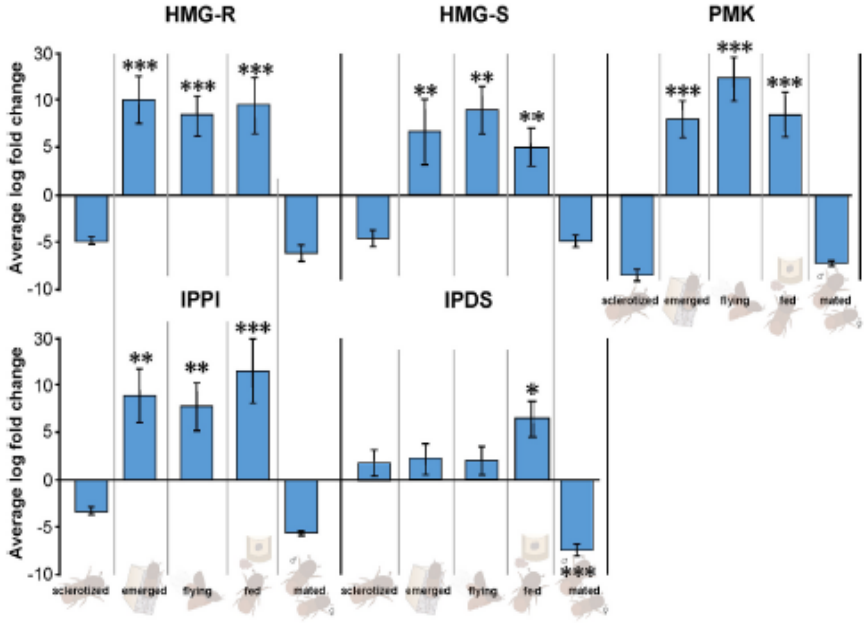

Fig. 9. Relative expression of mevalonate pathway genes in male gut tissue of *I. typographus* at different life stages, as determined by qRT-PCR. Statistics: One-way ANOVA with Fisher (LSD) test with 95% confidence interval with Sclerotized stage as control group. *** represents $P < 0.001$, ** represents $P < 0.01$, * represents $P < 0.05$. $N = 4$.

E1 and E3 were consistent with those from the RNA-seq data (Fig. 11).

4. Discussion

Our study provides a comprehensive metabolomic analysis of pheromone production in *I. typographus*, followed by DGE analysis for genes involved in pheromone biosynthesis. Our metabolomics data agree with the data from previous studies (Birgersson et al., 1984) and extend our knowledge regarding different beetle life stages, specifically focused on the key stages of aggregation pheromone production. As previously known, the aggregation pheromone blend of *I. typographus* consists of 2-methyl-3-buten-2-ol and *cis*-verbenol, and these components were

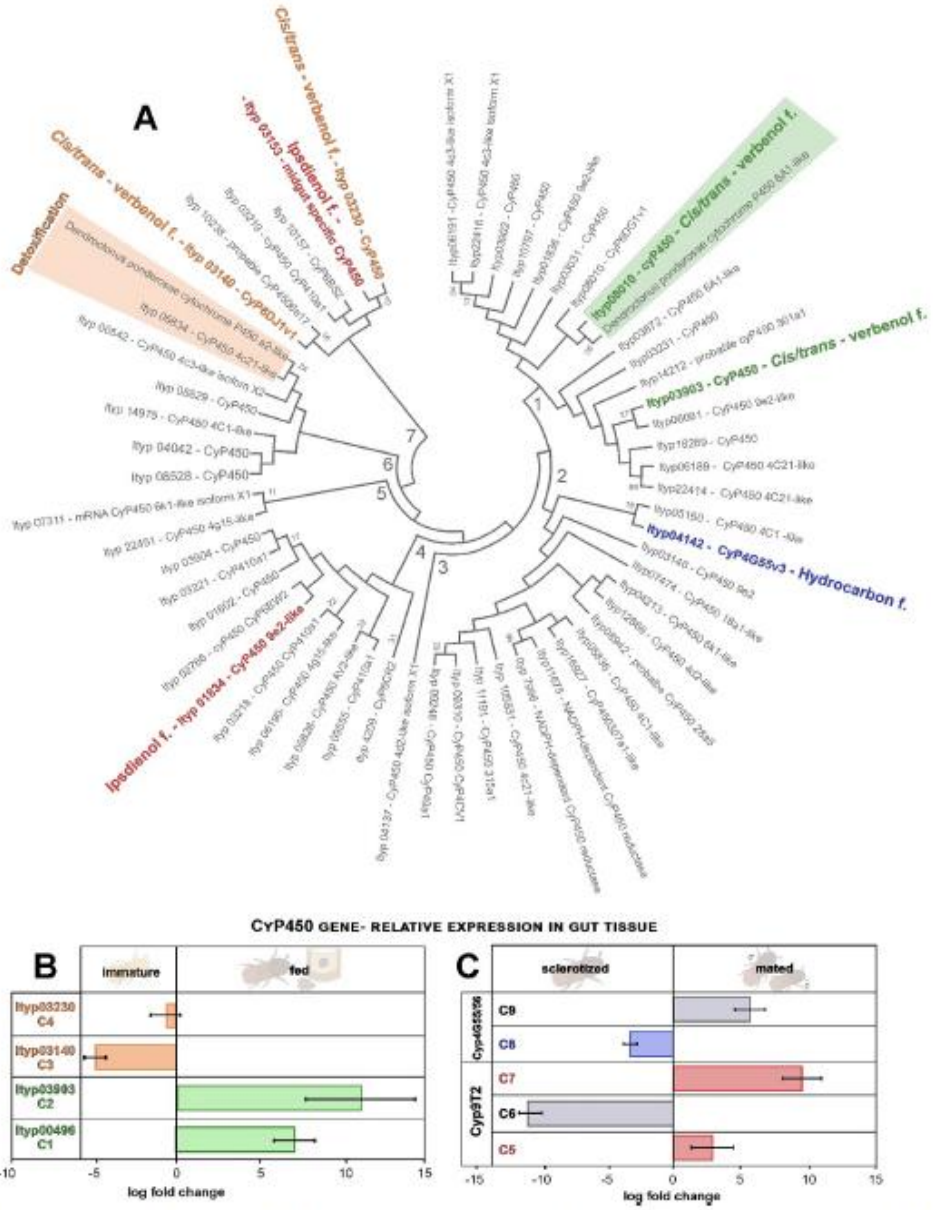

Fig. 10. A: Phylogenetic clustering of CyP450 genes based on sequence similarity identified in RNA-seq. data. Mega X, boot strap 100 times. The highlighted region indicates genes with known functions. B: Relative expression of genes of the CyP450 family, as determined by qRT-PCR. C1–C4 (functionally proposed for *cis/trans* verbenol synthesis): Tissues compared: Immature male gut vs fed male gut. C: C5–C7: A sequence like CyP9T2 (functionally known for ipsdienol synthesis from myrcene). C8 and C9: A sequence like CyP4G55/56 (functionally known for hydrocarbon synthesis). Tissues compared: mated male gut vs sclerotised beetle gut.

highly abundant in the fed male gut (colonisation stage). Surprisingly, the aggregation pheromones started appearing in the beetle gut as soon as they emerged from the host. *Cis*-verbenol, the compound derived from a tree precursor (α-pinene), was found more abundantly in the immature stages of both sexes and disappeared during beetle maturation. However, *cis*-verbenol reappeared in quantifiable amounts in mature male beetles only, the sex at which pheromonal compounds are released. The linking of *cis*-verbenol to monoterpene detoxification among early life stages, such as larvae, pupae, and immature beetles, should also be considered in this scenario. The content of verbenone follows a pattern similar to that of *cis*-verbenol (residue of verbenone synthesis) among the various life stages. Ipsdienol is produced only in mated males. Compounds with unknown biological activity, such as *trans*-verbenol, myrtenol, phenylethanol, and myrcene, were produced in more developed stages of beetles with male sex-specific gut tissues, supporting the previous knowledge on these compounds (Birgersson et al., 1984).

Similar to Chiu et al. (2018), we analysed extracts from the beetle body (focused on the fat body without the gut) and quantified the possible detoxification products (verbenyl oleate and myrtenyl oleate)

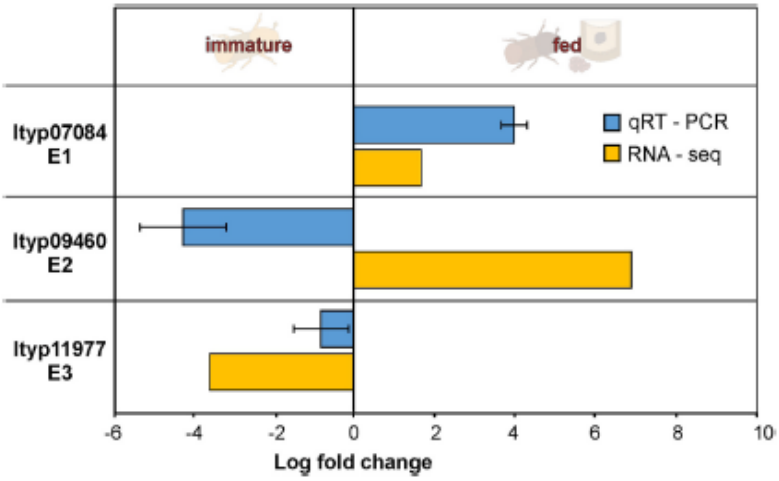

Fig. 11. Relative expression of esterase gene (RNA-seq. and qRT-PCR). Tissue: fed male gut vs immature male gut. Yellow: log fold change values from RNA-seq. Blue: log fold change from qRT-PCR. Error bar indicate standard error. N = 4. (For interpretation of the references to colour in this figure legend, the reader is referred to the Web version of this article.)

from the beetle's body. Verbenyl oleate is a putative pheromone storage fatty acid ester. As *cis*-verbenol biosynthesis patterns were seen among the different life stages of the beetle gut, we proposed that oleates were found initially in the immature beetle of both sexes. Later, only verbenyl oleate synthesis continued with male specificity in the mature beetle body. Since we have also identified the fatty acid esters methyl oleate and methyl palmitate along with the *cis*-verbenol cluster in PCA at three male life stages (sclerotised, emerged, and fed) in the GC-MS analysis, we performed a correlation pattern analysis based on the quantification of the mentioned compounds. The relative abundance of *cis*-verbenol, verbenyl oleate, and methyl oleate showed an interesting pattern between life stages. Moreover, co-relation of the verbenyl oleate reduction and methyl oleate increasing with pheromonal *cis*-verbenol can be seen in fed and mated stages. At the immature stage, the abundance of verbenyl oleate was high, whereas the abundance of methyl oleate was low. From this finding, we propose that α-pinene and myrcene from the host source undergo detoxification into oxygenated monoterpenes *cis*-verbenol and myrtenol, which further bind to lipid molecules, such as methyl oleate, to form verbenyl oleate and myrtenyl oleate and are stored in the fat body of *I. typographus* during the early life stages. Later, when feeding males tend to produce *cis*-verbenol as an aggregation pheromone compound, where α-pinene is a limited resource, the stored esters can be broken down into the required pheromones and residues of lengthy fatty acids. A similar concept was also proposed and studied in *D. ponderosae* (Chiu et al., 2018). Our hypothesis of methyl oleate and *cis*-verbenol synthesis from the monoterpenyl esters is a novel concept proposed yet in beetle pheromone storage mechanism. Though, other detoxification products, such as verbenyl and myrtenyl diglycosides of oxygenated monoterpenes were identified via UHPLC-HR-MS/MS, its involvement as pheromone storage requires further research. The occurrence of long chain hydrocarbons in male beetle gut and body was following a similar pattern across the life stages with a higher amount (10–15 folds) in beetle body than gut. Especially the hydrocarbons were least occurred in immature stage and increased in emerged stage. Later, decreased in flying and fed stages. This pattern corresponds with beetle cuticular development and impregnation in emerged beetles. Though, the hydrocarbon biosynthesis in insects is located in specialized cells - oenocytes, hydrocarbons are transported towards other body parts through haemolymph in the form of liphophorines, which can be hypothesised as a source of hydrocarbons in gut extracts (Bagnères and Blomquist, 2010).

JH III induction for pheromone synthesis among bark beetles is well studied (Bearfield et al., 2009; Chiu et al., 2018; Fang et al., 2021; Tillman et al., 2004). However, not all *Ips* sp. follow the same regulation pattern after hormone treatment (Tillman et al., 2004). Here, we have attempted aggregation pheromone quantification from the *I. typographus* sp. gut after JH III treatment for the first time, and the treatment was shown to induce significant *de novo* synthesis of the aggregation pheromone 2-methyl-3-buten-2-ol. This finding is similar to the findings in *I. pini*, where JH III treatment influences *de novo* pheromone synthesis (Seybold and Tittiger 2003). Trace amounts of *cis*-verbenol, another aggregation pheromone, and its residue verbenone, both of which are thought to be synthesised non-*de novo*, were also found after JH III treatment. Thus, *cis*-verbenol may be synthesised after JH III treatment from the gut, as postulated in our hypothesis of verbenol release from the stored verbenyl oleate. This release could involve certain esterase/lipase/hydrolase gene families expressed in the gut tissue after the treatment (Chiu et al., 2018).

UHPLC/HRMS-MS showed the presence of mevalonate-5-phosphate at all life stages. Interestingly, higher amounts of mevalonate-5-phosphate were produced during the flying male stage, followed by a reduction during the fed male stage and re-expression during the mated male stage (Fig. 7). This finding indicates that mevalonate-5-phosphate could be an active substrate for 2-methyl-3-buten-2-ol synthesis. The higher amount of mevalonate-5-phosphate during the flying stage also supports previous data on flight muscle activation driving *de novo* pheromone biosynthesis in other *Ips* sp., (Ivarsson et al., 1998). Since 2-methyl-3-buten-2-ol is male-specific in *I. typographus*, the abundance of the precursor mevalonate-5-phosphate in both sexes cannot be ignored. The mevalonate pathway involves a variety of isoprenoid metabolic pathways, and pathway intermediates can be expected to be found in both sexes. Thus, a further molecular study of *de novo* synthesis is required.

Finding more on relevant gene families involved in the biosynthesis of vital compounds that have provided clarified developmental knowledge in the class Insecta (Blomquist et al., 2010; Jirosová et al., 2017), we performed DGE analysis of the gut tissues and observed a distinct expression pattern of various gene families after annotation. The gene families, including pheromone synthesis and detoxification genes, were upregulated after feeding. Based on a previous finding from *Ips* sp., (Lanne et al., 1989) and our metabolomic data on mevalonate-5-phosphate intermediates, we narrowed down our study to

focus on mevalonate pathway gene family members, including PMK (Ityp06045), HMG-S (Ityp09137), HMG-R (Ityp17150), IPPI (Ityp04875) and IPDS (Ityp09271). These genes were shown to influence pheromone production in *Ips* sp., especially *HMG*-R, which, when inhibited, completely suppress pheromone production pathways (Ivarsson et al., 1993; Tillman et al., 2004). In particular, the isoprenoid gene family member isoprenyl diphosphate synthase (IPDS) - Ityp09271, was identified in the fed male gut of *I. typographus*, along with 2-methyl-3-buten-2-ol. Hence, we propose that IPDS could play the role of a novel hemiterpenoid prenyl transferase in 2-methyl-3-buten-2-ol *de novo* synthesis. Though IPDS is known to be involved in pheromone synthesis in other insects (Lancaster et al., 2018), such as the bark beetle *D. ponderosae* (frontalin pheromone) (Keeling et al., 2013), we are proposing a function for IPDS in hemiterpene synthesis in the animal family for the first time. The actual known function of IPDS (also known as GPPS) in the extension of myrcene synthesis (Gilg et al. 2005, 2009) should also be considered. Based on the involvement of GPPS in myrcene synthesis, we identified other orthologs of IPDS/GPPS— Ityp17873 and Ityp17861— from RNA seq data (Supplementary Fig. 3). The expression of these orthologs was not as high as the proposed candidate Contig_Ityp09271 in the fed male gut. Thus, the low expression of the GPPS gene orthologs co-relates with the low ipsdienol (myrcene derivative) presence during the fed stage. Even though studies showing the involvement of the mevalonate pathway in other bark beetles (Bearfield et al., 2009; Sarabia et al., 2019) and insects (Zhang et al., 2017) have been published, our study is the first reported detailed molecular analysis of the gene family in *Ips typographus* sp., as per our knowledge.

It is known that the CyP450 gene is involved in verbenol synthesis in bark beetle *sp.*, (Nadeau et al., 2017). Here, we found 56 CyP450 genes expressed in the gut tissue of *I. typographus*, accounting for 66.6% of the total number of CyP450 genes (84) in the beetle genome (Powell et al., 2020). CyP450- C1 (Ityp3903) and C2 (Ityp0496) showed high sequence similarity with CyP450 (A1 like- CYP6DE1) from *D. ponderosae* involved in *trans*-verbenol production (Chiu et al., 2019). In addition, we also identified candidate CyP450- C3 (Ityp3140) and CyP450- C4 (Ityp3230), showing sequence similarity with the CyP450 gene family (A2 like) -CYP6DE3, known to be involved in the detoxification in other bark beetles (Nadeau et al., 2017). Though we selected candidates involved in two different functions, these four CyP450 genes were all expressed in the fed and immature life stages. As reported by Chiu et al. (2019), the gene involved in *trans*-verbenol production is also involved to some extent in *cis*-verbenol synthesis and detoxification mechanism involving α-pinene (Reid and Purcell 2011; Renwick et al., 1976). We propose four identified candidates (C1–C4) as possible *cis/trans*-verbenol synthesising in the bark beetle, involving α-pinene. Functional validation of the gene candidate is required before naming the gene for the proposed function. Furthermore, CyP450 genes, Ityp4140 (C8) and Ityp4142 (C9), similar to CYP4Gs involved in converting long-chain linear aldehydes and alcohols into hydrocarbons, were identified with the help of a known sequence from recent studies (MacLean et al., 2018). The location of oenocytes, cells where hydrocarbons are synthesised, varies among insects. In Coleoptera, the oenocytes were observed in the fat body and tracheal system (Makki et al., 2014). According to that, the CYP4G55 gene putatively responsible for the terminal step of hydrocarbon biosynthesis was previously found in fat and the whole body of *D. ponderosae* and *I. pini* (MacLean et al., 2018; Nadeau et al., 2017; Huber et al., 2007). Hence, unforeseen identification of CYP4Gs (C8 and C9) from our transcriptome analysis of gut tissue, therefore, can be justified with a presumable assumption of oenocytes association from the tracheal system with the external layer of gut tissue. However, comparison of the gene expression in different tissues such as fat body or antennae comparison with gut tissue and histological location of oenocytes is required to confirm the site of hydrocarbon synthesis in *I. typographus*. Also, CyP450 (Ityp1834 and Ityp3153), similar to CyP9T1/T2, known for myrcene hydrolase, were proposed (Song et al., 2013). Though there is recent research on CyP6 involvement in aggregation pheromone production in other *Ips* sp. (Fang et al., 2021), the corresponding CyP450 gene from the 6-like family needs to be identified for further functional clarification in *I. typographus*.

The esterase gene (Esterase FE4-like and venom carboxylesterase – 6 like) identified in this work shows high similarity with the esterase gene BT127766.1 from *D. ponderosa* sp., which is involved in a possible pheromone storage function (Bernier et al., 2020). Respective candidates were selected from the transcriptome data based upon sequence similarity. To verify the proposed functional correlation, the involvement of the esterase gene family identified in this study in *cis*-verbenol storage as a fatty acid ester in the immature stage was evaluated. Further validation of the mentioned sequences in the life stages of *I. typographus* showed that esterase Ityp_11977 (E3) occurs in the immature stage. Since *cis*-verbenol occurs in the immature stage and verbenyl oleate in the immature body, the proposed candidate can be considered a valid gene for functional study, also investigated in other bark beetles (Chiu et al., 2018). Further, we also hypothesise another two-step conversion of verbenyl oleate to *cis*-verbenol and fatty acids. The first step would be the hydrolysis of the oleate catalysed by another esterase/lipase, and consequently, the released fatty acid would be methylated by a putative methyltransferase. However, gene/s responsible for the verbenol release from the stored fatty acid esters and the mentioned methyltransferase is uncertain from our study. Further functional characterisation is required for the validation of the identified putative genes. Our study leads to a deeper, more molecular understanding of pheromone biosynthesis in *I. typographus*.

Availability of data and materials

All the data and resources generated for this study are included in the article and the supplemental materials. The RNA sequences have been submitted in NIH under the accession PRJNA679450. We are willing to share all the data and resources in this study with the public.

Author's contribution

RR: Conceptualization, methodology, formal analysis, resources, writing – original draft; JH: GC-Metabolomic data analysis, review & editing; AR- RNA-seq. data curation, molecular work support, review & editing: BK: GC-Metabolomic analysis review & editing; RM: UHPLC/HRMS-MS data curation; JS: Beetle rearing; JB: GC-Metabolomic analysis, AS: UHPLC/HRMS-MS data analysis, writing, review & editing; AJ: Conceptualization, methodology, formal analysis, editing, supervision.

Declaration of competing interest

All authors declare that they have no competing interests.

Acknowledgements

The research was funded by "EXTEMIT-K," No. CZ.02.1.01/0.0/0.0/15_003/0000433 and Internal Grant commission (IGA A_20_02, RAJARAJAN RAMAKRISHNAN) at the Faculty of Forestry and Wood Sciences, Czech University of Life sciences, Prague, Czech Republic. We thank Ales Machara, Ph.D., from the Institute of Organic Chemistry and Biochemistry, Prague, Czech Republic for synthesis of standards for GC-MS analysis, and Jan Bily, PhD. and Gothandapani Sellamuthu, PhD. for faciliating molecular work support.

Appendix A. Supplementary data

Supplementary data to this article can be found online at https://doi.org/10.1016/j.ibmb.2021.103680.

References

Bearfield, J.C., Henry, A.G., Tittiger, C., Blomquist, G.J., Ginzel, M.D., 2009. Two regulatory mechanisms of monoterpenoid pheromone production in *Ips* spp. of bark beetles. J. Chem. Ecol. 35, 689–697. https://doi.org/10.1007/s10886-009-9652-2.

Benton, H.P., Want, E.J., Ebbels, T.M.D., 2010. Correction of mass calibration gaps in liquid chromatography-mass spectrometry metabolomics data. Bioinformatics 26, 2488–2489. https://doi.org/10.1093/bioinformatics/btq441.

Bernier, K., Sergerie, R., Keeling, C.I.E.S.A., 2020. Functional Characterization of a *Dendroctonus ponderosae* Esterase. Entomology Society of America -ESA conference poster, Université Laval Quebec, Canada- unpublished). https://www.eventscribe.com/2020/entomology2020/searchGlobal.asp.

Biedermann, P.H.W., Müller, J., Grégoire, J.C., Gruppe, A., Hagge, J., Hammerbacher, A., Hofstetter, R.W., Kandasamy, D., Kolarik, M., Kostovcik, M., Krokene, P., Sallé, A., Six, D.L., Turrini, T., Vanderpool, D., Wingfield, M.J., Bässler, C., 2019. Bark beetle population dynamics in the Anthropocene: challenges and solutions. Trends Ecol. Evol. 34, 914–924. https://doi.org/10.1016/j.tree.2019.06.002.

Birgersson, G., Bergström, G., 1989. Volatiles released from individual spruce bark beetle entrance holes Quantitative variations during the first week of attack. J. Chem. Ecol. 15, 2465–2483. https://doi.org/10.1007/BF01020377.

Birgersson, G., Schlyter, F., Löfqvist, J., Bergström, G., 1984. Quantitative variation of pheromone components in the spruce bark beetle *Ips typographus*from different attack phases. J. Chem. Ecol. 10, 1029–1055. https://doi.org/10.1007/BF00987511.

Blomquist, G.J., Figueroa-Teran, R., Aw, M., Song, M.M., Gorzalski, A., Abbott, N.L., Chang, E., Tittiger, C., 2010. Pheromone production in bark beetles. Insect Biochem. Mol. Biol. 40, 699–712. https://doi.org/10.1016/j.ibmb.2010.07.013.

Bagnères, A.G., Blomquist, G.J., 2010. Site of synthesis, mechanism of transport and selective deposition of hydrocarbons. https://doi.org/10.1017/CBO9780511711909.006, 5, 75-99.

Byers, J.A., Wood, D.L., 1981. Antibiotic-induced inhibition of pheromone synthesis in a bark beetle. Science 213, 763–764. https://doi.org/10.1126/science.213.4509.763.

Byers, J.A., Birgersson, G., 1990. Pheromone production in a bark beetle independent of myrcene precursor in host pine species. Naturwissenschaften 77, 385–387. https://doi.org/10.1007/BF01135739.

Cheng, C.H., Wickham, J.D., Chen, L., Xu, D.D., Lu, M., Sun, J.H., 2018. Bacterial microbiota protect an invasive bark beetle from a pine defensive compound. Microbiome 6, 132. https://doi.org/10.1186/s40168-018-0518-0.

Chiu, C.C., Keeling, C.I., Bohlmann, J., 2018. Monoterpenyl esters in juvenile mountain pine beetle and sex-specific release of the aggregation pheromone trans-verbenol. Proc. Natl. Acad. Sci. U. S. A. 115, 3652–3657. https://doi.org/10.1073/pnas.1722380115.

Chiu, C.C., Keeling, C.I., Bohlmann, J., 2019. The cytochrome P450 CYP6DE1 catalyzes the conversion of alpha-pinene into the mountain pine beetle aggregation pheromone *trans*-verbenol. Sci. Rep. 9, 1477. https://doi.org/10.1038/s41598-018-38047-8.

Chong, J., Soufan, O., Li, C., Caraus, I., Li, S.Z., Bourque, G., Wishart, D.S., Xia, J.G., 2018. MetaboAnalyst 4.0: towards more transparent and integrative metabolomics analysis. Nucleic Acids Res. 46, W486–W494. https://doi.org/10.1093/nar/gky310.

Fang, J.X., Zhang, S.F., Liu, F., Cheng, B., Zhang, Z., Zhang, Q.H., Kong, X.B., 2021. Functional investigation of monoterpenes for improved understanding of the relationship between hosts and bark beetles. J. Appl. Entomol. 145, 303–311. https://doi.org/10.1111/jen.12850.

Figueroa-Teran, R., Welch, W.H., Blomquist, G.J., Tittiger, C., 2012. Ipsdienol dehydrogenase (IDOLDH): a novel oxidoreductase important for *Ips pini* pheromone production. Insect Biochem. Mol. Biol. 42, 81–90. https://doi.org/10.1016/j.ibmb.2011.10.009.

Fisher, A.J., Baker, B.M., Greenberg, J.P., Fall, R., 2000. Enzymatic synthesis of methylbutenol from dimethylallyl diphosphate in needles of *Pinus sabiniana*. Arch. Biochem. Biophys. 383, 128–134. https://doi.org/10.1006/abbi.2000.2051.

Gilg, A.B., Bearfield, J.C., Tittiger, C., Welch, W.H., Blomquist, G.J., 2005. Isolation and functional expression of an animal geranyl diphosphate synthase and its role in bark beetle pheromone biosynthesis. Proc. Natl. Acad. Sci. U. S. A. 102, 9760–9765. https://doi.org/10.1073/pnas.0503277102.

Gilg, A.B., Tittiger, C., Blomquist, G.J., 2009. Unique animal prenyltransferase with monoterpene synthase activity. Naturwissenschaften 96, 731–735. https://doi.org/10.1007/s00114-009-0521-1.

Hall, G.M., Tittiger, C., Andrews, G.L., Mastick, G.S., Kuenzli, M., Luo, X., Seybold, S.J., Blomquist, G.J., 2002. Midgut tissue of male pine engraver, Ips pini, synthesizes monoterpenoid pheromone component ipsdienol de novo. Naturwissenschaften 89, 79–83. https://doi.org/10.1007/s00114-001-0290-y.

Huang, J.B., Kautz, M., Trowbridge, A.M., Hammerbacher, A., Raffa, K.F., Adams, H.D., Goodsman, D.W., Xu, C.G., Meddens, A.J.H., Kandasamy, D., Gershenzon, J., Seidl, R., Hartmann, H., 2020. Tree defence and bark beetles in a drying world: carbon partitioning, functioning and modelling. New Phytol. 225, 26–36. https://doi.org/10.1007/s00114-001-0290-y.

Huber, D.P.W., Erickson, M.L., Leutenegger, C.M., Bohlmann, J., Seybold, S.J., 2007. Isolation and extreme sex-specific expression of cytochrome P450 genes in the bark beetle, Ips paraconfusus, following feeding on the phloem of host ponderosa pine, Pinus ponderosa. Insect Mol. Biol. 16, 335–349. https://doi.org/10.1111/j.1365-2583.2007.00731.x.

Hunt, D.W.A., Borden, J.H., 1990. Conversion of verbenols to verbenone by yeasts isolated from *Dendroctonus ponderosae* (Coleoptera, Scolytidae). J. Chem. Ecol. 16, 1385–1397. https://doi.org/10.1007/BF01021034.

Ivarsson, P., Schlyter, F., Birgersson, G., 1993. Demonstration of *de-novo* pheromone biosynthesis in *Ips duplicatus* (Coleoptera, Scolytidae) - inhibition of Ipsdienol and E-myrcenol production by compaction. Insect Biochem. Mol. Biol. 23, 655–662. https://doi.org/10.1016/0965-1748(93)90039-U.

Ivarsson, P., Tittiger, C., Blomquist, C., Borgeson, C.E., Seybold, S.J., Blomquist, G.J., Högberg, H.E., 1998. Pheromone precursor synthesis is localized in the metathorax of *Ips paraconfusus* Lanier (Coleoptera: Scolytidae). Naturwissenschaften 85, 507–511. https://doi.org/10.1007/s001140050541.

Jirosová, A., Jančařík, A., Menezes, R.C., Bazalová, O., Dolejšová, K., Vogel, H., Jedlička, P., Buček, A., Brabcová, J., Majer, P., Hanus, R., Svatoš, A., 2017. Co-option of the sphingolipid metabolism for the production of nitroalkene defensive chemicals in termite soldiers. Insect Biochem. Mol. Biol. 82, 52–61. https://doi.org/10.1016/j.ibmb.2017.01.008.

Keeling, C.I., Blomquist, G.J., Tittiger, C., 2004. Coordinated gene expression for pheromone biosynthesis in the pine engraver beetle, *Ips pini* (Coleoptera: Scolytidae). Naturwissenschaften 91, 324–328. https://doi.org/10.1007/s00114-004-0523-y.

Keeling, C.I., Chiu, C.C., Aw, T., Li, M., Henderson, H., Tittiger, C., Weng, H.B., Blomquist, G.J., Bohlmann, J., 2013. Frontalin pheromone biosynthesis in the mountain pine beetle, *Dendroctonus ponderosae*, and the role of isoprenyl diphosphate synthases. Proc. Natl. Acad. Sci. U. S. A. 110, 18838–18843. https://doi.org/10.1073/pnas.1316498110.

Keeling, C.I., Li, M., Sandhu, H.K., Henderson, H., Saint Yuen, M.M., Bohlmann, J., 2016. Quantitative metabolome, proteome and transcriptome analysis of midgut and fat body tissues in the mountain pine beetle, *Dendroctonus ponderosae* Hopkins, and insights into pheromone biosynthesis. Insect Biochem. Mol. Biol. 70, 170–183. https://doi.org/10.1016/j.ibmb.2016.01.002, 2019.

Knížek, M., 2020. Historie a současnost kůrovcových kalamit ve střední Evropě. Zpravodaj ochrany lesa, Škodliví činitelé v lesích Česka. Svazek 23. https://www.vulhm.cz/files/uploads/2020/10/ZOL_23_2020.pdf.

Lancaster, J., Khrimian, A., Young, S., Lehner, B., Luck, K., Wallingford, A., Ghosh, S.K. B., Zerbe, P., Muchlinski, A., Marek, P.E., Sparks, M.E., Tokuhisa, J.G., Tittiger, C., Köllner, T.G., Weber, D.C., Gundersen-Rindal, D.E., Kuhar, T.P., Tholl, D., 2018. De novo formation of an aggregation pheromone precursor by an isoprenyl diphosphate synthase-related terpene synthase in the harlequin bug. Proc. Natl. Acad. Sci. U. S. A. 115, E8634–E8641. https://doi.org/10.1073/pnas.1800008115.

Lanne, B.S., Ivarsson, P., Johnsson, P., Bergström, G., Wassgren, A.-B., 1989. Biosynthesis of 2-methyl-3-buten-2-ol, a pheromone component of *Ips typographus* (Coleoptera, Scolytidae). Insect Biochem. 19, 163–167. https://doi.org/10.1016/0020-1790(89)90087-5.

MacLean, M., Nadeau, J., Gurnea, T., Tittiger, C., Blomquist, G.J., 2018. Mountain Pine beetle (*Dendroctonus ponderosae*) CYP4Gs convert long and short chain alcohols and aldehydes to hydrocarbons. Insect Biochem. Mol. Biol. 102, 11–20. https://doi.org/10.1016/j.ibmb.2018.09.005.

Makki, R., Cinnamon, E., Gould, A.P., 2014. The development and functions of oenocytes. In: Annual Review of Entomology, vol. 59, pp. 405–425. https://doi.org/10.1146/annurev-ento-011613-162056.

Nadeau, J.A., Petereit, J., Tillett, R.L., Jung, K., Fotoohi, M., MacLean, M., Young, S., Schlauch, K., Blomquist, G.J., Tittiger, C., 2017. Comparative transcriptomics of mountain pine beetle pheromone-biosynthetic tissues and functional analysis of CYP6DE3. BMC Genom. 18, 311. https://doi.org/10.1186/s12864-017-3696-4.

Powell, D., Große-Wilde, E., Krokene, P., Roy, A., Chakraborty, A., Löfstedt, C., Vogel, H., Andersson, M.N., Schlyter, F., 2020. A highly contiguous genome assembly of a major forest pest, the Eurasian spruce bark beetle Ips typographus. bioRXiv. https://doi.org/10.1101/2020.11.28.401976.

Ramakrishnan, R., Roy, A., Kai, M., Svatoš, A., Jirošová, A. Metabolome and Transcriptome Related Dataset for Pheromone Biosynthesis in European Spruce Bark Beetle- *Ips typographus*. [Data in brief, in preparation].

Reid, M.L., Purcell, J.R.C., 2011. Condition-dependent tolerance of monoterpenes in an insect herbivore. Arthropod. Plant Interact. 5, 331–337. https://doi.org/10.1007/s11829-011-9137-4.

Renwick, J.A.A., Hughes, P.R., Krull, I.S., 1976. Selective production of *cis*- and *trans*-verbenol from (-)- and (+)-alpha-pinene by a bark beetle. Science 191, 199–201. https://doi.org/10.1126/science.1246609.

Roy, A., George, S., Palli, S.R., 2017. Multiple functions of CREB-binding protein during postembryonic development: identification of target genes. BMC Genom. 18, 996. https://doi.org/10.1186/s12864-017-4373-3.

Roy, A., Palli, S.R., 2018. Epigenetic modifications acetylation and deacetylation play important roles in juvenile hormone action. BMC Genom. 19, 934. https://doi.org/10.1186/s12864-018-5323-4.

Sarabia, L.E., López, M.F., Obregón-Molina, G., Cano-Ramírez, C., Sánchez-Martínez, G., Zúñiga, G., 2019. The differential expression of mevalonate pathway genes in the gut of the bark beetle *Dendroctonus Rhizophagus* (Curculionidae: Scolytinae) is unrelated to the de novo synthesis of terpenoid pheromones. Int. J. Mol. Sci. 20 https://doi.org/10.3390/ijms20164011.

Schlyter, F., Birgersson, G., Byers, J.A., Löfqvist, J., Bergström, G., 1987. Field response of spruce bark beetle, *Ips typographus* to aggregation pheromone candidates. J. Chem. Ecol. 13, 701–716. https://doi.org/10.1007/BF01020153.

Schlyter, F., Cederholm, I., 1981. Separation of the sexes of living spruce bark beetles, *Ips typographus* (L), (Coleoptera, Scolytidae). Z. Angew. Entomol. J. Appl. Entomol. 92, 42–47. https://doi.org/10.1111/j.1439-0418.1981.tb01650.x.

Seybold, S.J., Tittiger, C., 2003. Biochemistry and molecular biology of *de novo* isoprenoid pheromone production in the Scolytidae. Annu. Rev. Entomol. 48, 425–453. https://doi.org/10.1146/annurev.ento.48.091801.112645.

Smith, C.A., Want, E.J., O'Maille, G., Abagyan, R., Siuzdak, G., 2006. XCMS: processing mass spectrometry data for metabolite profiling using Nonlinear peak alignment, matching, and identification. Anal. Chem. 78, 779–787. https://doi.org/10.1021/ac051437y.

Song, M.M., Kim, A.C., Gorzalski, A.J., MacLean, M., Young, S., Ginzel, M.D., Blomquist, G.J., Tittiger, C., 2013. Functional characterization of myrcene hydroxylases from two geographically distinct Ips pini populations. Insect Biochem. Mol. Biol. 43, 336–343. https://doi.org/10.1016/j.ibmb.2013.01.003.

Tautenhahn, R., Böttcher, C., Neumann, S., 2008. Highly sensitive feature detection for high resolution LC/MS. BMC Bioinf. 9, 504. https://doi.org/10.1186/1471-2105-9-504.

Thom, D., Seidl, R., 2016. Natural disturbance impacts on ecosystem services and biodiversity in temperate and boreal forests. Biol. Rev. Camb. Phil. Soc. 91, 760–781. https://doi.org/10.1111/brv.12193.

Tillman, J.A., Holbrook, G.L., Dallara, P.L., Schal, C., Wood, D.L., Blomquist, G.J., Seybold, S.J., 1998. Endocrine regulation of de novo aggregation pheromone biosynthesis in the pine engraver, *Ips pini* (Say) (Coleoptera: Scolytidae). Insect Biochem. Mol. Biol. 28, 705–715. https://doi.org/10.1016/S0965-1748(97)00117-3.

Tillman, J.A., Lu, F., Goddard, L.M., Donaldson, Z.R., Dwinell, S.C., Tittiger, C., Hall, G. M., Storer, A.J., Blomquist, G.J., Seybold, S.J., 2004. Juvenile hormone regulates de novo isoprenoid aggregation pheromone biosynthesis in pine bark beetles, *Ips* spp., through transcriptional control of HMG-CoA reductase. J. Chem. Ecol. 30, 2459–2494. https://doi.org/10.1007/s10886-004-7945-z.

Wang, M., Carver, J., Phelan, V., et al., 2016. Sharing and community curation of mass spectrometry data with global natural products Social molecular networking. Nat. Biotechnol. 34, 828–837. https://doi.org/10.1038/nbt.3597.

Xu, L.T., Lu, M., Xu, D.D., Chen, L., Sun, J.H., 2016. Sexual variation of bacterial microbiota of Dendroctonus valens guts and frass in relation to verbenone production. J. Insect Physiol. 95, 110–117. https://doi.org/10.1016/j.jinsphys.2016.09.014.

Zhang, W.N., Ma, L., Xiao, H.J., Liu, C., Chen, L., Wu, S.L., Liang, G.M., 2017. Identification and characterization of genes involving the early step of Juvenile Hormone pathway in Helicoverpa armigera. Sci. Rep. 7, 16542. https://doi.org/10.1038/s41598-017-16319-z.

Supplementary material for

Metabolomics and transcriptomics of pheromone biosynthesis in an aggressive forest pest *Ips typographus*

Rajarajan Ramakrishnan[1] Jaromír Hradecký[1], Amit Roy[1], Blanka Kalinová[1], Rya C. Mendezes[2], Jiri Synek[1], Jaromír Bláha[1], Aleš Svatoš[2,3], Anna Jirošová[1*]

[1] *Faculty of Forestry and Wood Sciences, Czech University of Life Sciences Prague, Czech Republic*
[2] *Max Planck Institute for Chemical Ecology, Jena, Germany*
[3] *Institute of Organic Chemistry and Biochemistry, the Czech Academy of Sciences, Prague, Czech Republic*

Corresponding author
Anna Jirošová
jirosovaa@fld.czu.cz
Faculty of Forestry and Wood Sciences, Czech University of Life Sciences Prague, Czech Republic[1]

Postal address:
Faculty of Forestry and Wood Sciences,
Czech University of Life Sciences Prague
Kamýcká 129, 165 2.1 Praha 6 – Suchdol

Supplementary Table S1: Candidates chosen via local BLAST search from CyP450 gene and esterase gene families with reference to *I. typographus* genome database. Unipro UGENE – 2012

Gene labels and functions proposed:	Contig numbers	e- value	BLAST Score	% identity	Reference sequences from other bark beetles. (NCBI database).
Cytochrome P450					
Cis/trans-verbenol (CyP450 6A1 like/CyP6DE1) (Chiu et al. 2019)					
C1	**Ityp00496**	**3.34125e-15**	**92**	**63.89**	**XM_019898558.1**
C2	**Ityp03903**	**1.97311e-24**	**127**	**65.92**	**XM_019898558.1**
(CyP450 6a2 like/ CyP6DE3)					
C3	**Ityp03140**	**1 e-44**	**192**	**65**	**XM_019901630.1**
C4 (Nadeau et al. 2017)	**Ityp03230**	**9.32964e-16**	**94**	**63.85**	**XM_019898560.1**
Ipsdienol synthesis (CyP9T2) (Song et al. 2013)					
C5	**Ityp01834**	**1.80301e-12**	**81**	**69.59**	**DQ676820.1**
C6	**Ityp03146**	**9.97218e-16**	**93**	**69.26**	**DQ676820.1**
C7	**Ityp03153**	**0**	**991**	**96.21**	**DQ676820.1**
Hydrocarbon synthesis (CyP4G55/56) (MacLean et al. 2018)					
C8	**Ityp04140**	**2.01681e-17**	**100**	**65.11**	**JQ855659.1**
C9	**Ityp04142**	**3.41223e-27**	**136**	**65.81**	**JQ855659.1**
Esterase Proposed for pheromone storage (Bernier K., Sergerie R., Keeling CI. ESA 2020, unpublished)					
E1	**Ityp07084**	**0.110062**	**42**	**87.09**	**BT127766.1**
E2	**Ityp09460**	**3.36682e-08**	**66**	**71.2**	**BT127766.1**
E3	**Ityp11977**	**2.26854e-10**	**74**	**66.548**	**BT127766.1**

Supplementary Table S2: Primers designed for genes from the mevalonate pathway gene family. IDT primer quest designing tool was used with primer length of 18-25 bp Tm-55-65, GC-50-60%, Amplicon size:100-150 bp.

Contig numbers.	Gene names	Primer sequence	Length	Tm	GC %	Amplicon
ltyp09271	IPDS-F	CCCAGTTCTCTGTCCAAATC	20	60.033	50	
	IPDS-R	GCTCAATCTGTCCCATCAC	19	60.015	52.632	103
ltyp04875	IPPI/DMPPI-F	GAGGCCCTACTGAACGAAA	19	61.22	52.632	
	IPPI/DMPPI-R	ACTGAACGCCCTGTGTAG	18	61.13	55.556	126
ltyp09137	HMGS- F	CTGGTTGTTGCTGGAGAC	18	60.048	55.556	
	HMGS- R	GGCATTAGGGCCTACAATC	19	59.898	52.632	96
ltyp17150	HMGR- F	CAGAACCTGGAGCCAATG	18	59.907	55.556	
	HMGR-R	GCAGAGTGGTTGACCTATTG	20	60.304	50	141
ltyp06045	PMK- F	CTGCTCCTGTTAAGGATGTG	20	60.049	50	
	PMK- R	ACCCATCCTCTCCTCTTTC	19	60.189	52.632	139
ltyp09272	FPPS- F	GGGAACGGACATTCAAGAC	19	60.183	52.632	
	FPPS- R	GTTCTGACCTGCCGTAATG	19	60.199	52.632	110
ltyp14703	IDLDH -F	ATCCTCTCCTTGACCTATCC	20	59.8	50	
	IDLDH -R	ATCGGAGTGTCGCAGATA	18	59.862	50	92

Supplementary Table S3: Primers designed for the nine selected genes from the CyP450 gene family (C1-C9). IDT primer quest designing tool was used with primer length of 18-25 bp Tm-55-65, GC-50-60%, Amplicon size:100-150 bp.

Label	Gene names	Primer sequence	Length	Tm	GC %	Amplicon
C1	qCYP00496-F	GTGTTACAGCGGCATGAT	18	60.043	50	
	qCYP00496-R	CTGACGGGATTGGAGGATA	19	60.234	52.632	103
C2	qCYP03903-F	GTATTCGCCTGCTCATTCC	19	60.355	52.632	
	qCYP03903-R	CCGGTCTACTGGATCTGTT	19	60.392	52.632	114
C3	2qCYP03140-F	GGTGCCTGACTTTCTACAG	19	59.571	52.632	
	2qCYP03140-R	GTAGCCGATGTCTCAAACC	19	59.916	52.632	132
C4	qcyp_3230-F	CCAATCGTCACTGTTCTACC	20	59.954	50	
	qcyp_3230-R	TCGTCTGGGTTGTCGTAA	18	60.241	50	143
C5	qcyp_1834-F	CCTTTCCTTGATCGACTCTG	20	59.722	50	
	qcyp_1834-R	CCCTGTGGAACGGATAAAC	19	59.951	52.632	121
C6	qcyp_3146-F	GAAAGTGGCCTCCTGTTG	18	60.111	55.556	
	qcyp_3146-R	CATGTCGCCCACGTTAAG	18	60.393	55.556	107
C7	qcyp_3153-F	GTGAGCGTTGGAAGGAAA	18	59.858	50	
	qcyp_3153-R	CACTTCTGTTGGTCCGTTAG	20	60.152	50	140
C8	qcyp_4140-F	CTGAAGTGCCCGAAGAAC	18	60.047	55.556	
	qcyp_4140-R	CATCAACATCCAGGTCATCC	20	60.179	50	123
C9	qcyp_4142-F	AACCGCAATGGGTGTAAG	18	59.999	50	
	qcyp_4142-R	GAGGATGTCTGGATAGAGGTAG	22	60.322	50	127

4

Supplementary Table S4: Primers designed for the three genes (E1-E3) from the esterase gene family. IDT primer quest designing tool was used with primer length of 18-25 bp Tm-55-65, GC-50-60%, Amplicon size:100-150 bp.

Label	Gene names	Primer sequence	Length	Tm	GC %	Amplicon
E1	q_est_7084-F	GGGATGTTCCGATGAATACG	20	60.152	50	
	q_est_7084-R	TGCCAGGACACTCTCTATC	19	60.119	52.632	122
E2	q_est_9460-F	CTAGTGGCGCAGTTGATTAG	20	60.315	50	
	q_est_9460-R	GGGCATACTTGGAAGATTGG	20	60.495	50	142
E3	q_est_11977-F	CTTCGTGGAGTTGAAGTGG	19	60.066	52.632	
	q_est_11977-F	CCTCTACATCGGGCTCTAA	19	59.88	52.632	121

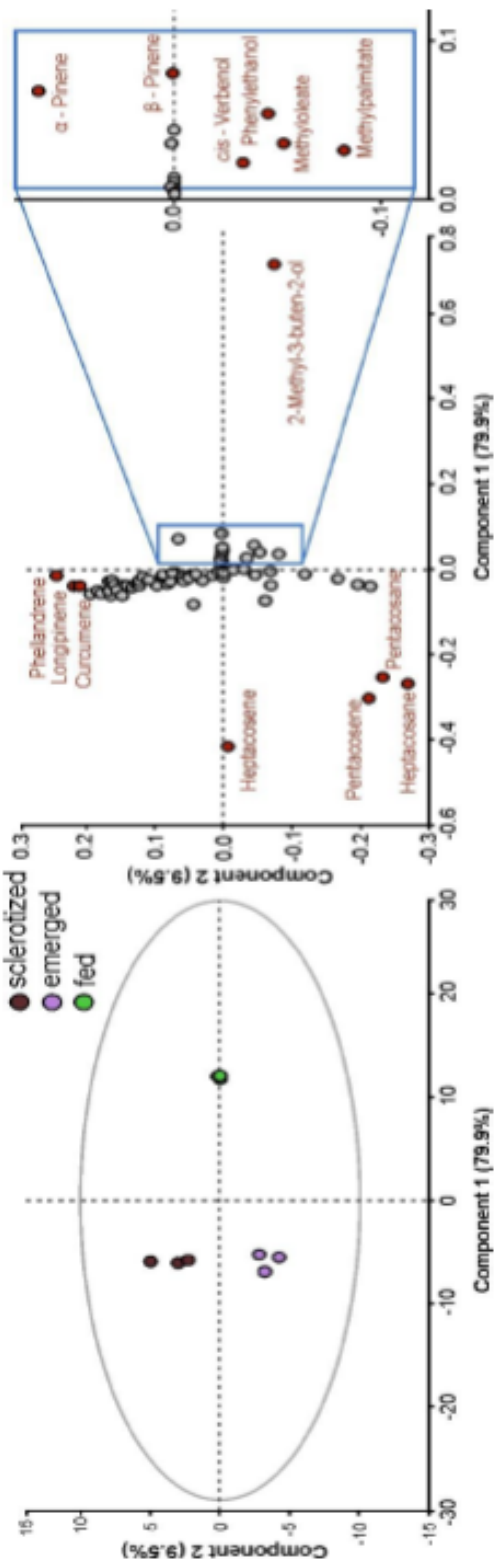

Supplementary Fig. S1 GC-MS metabolomics analysis of male beetle's gut extract. PCA plot from SIMCA software; separation of 3 life stages (immature, sclerotised, and fed). These stages were primarily involved in pheromone production.

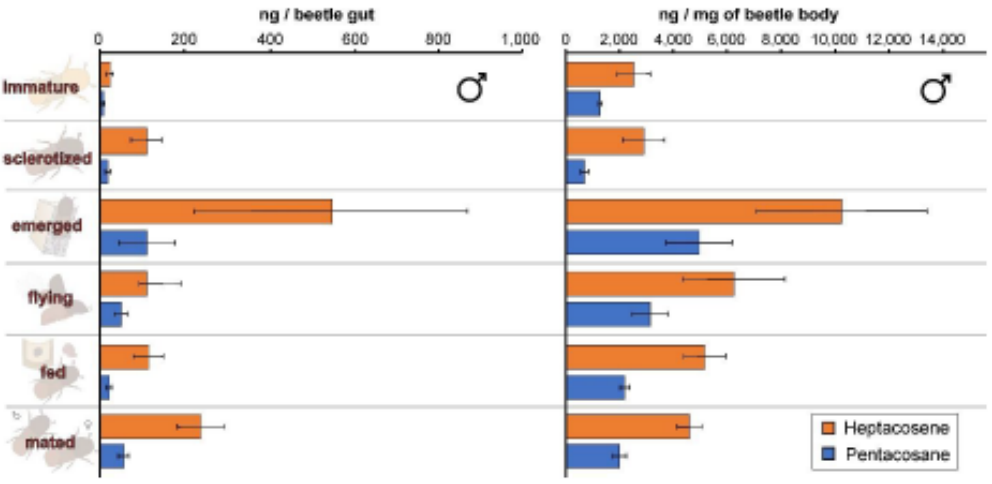

Figure S2. GC-MS quantification of two hydrocarbon representatives (unsaturated heptacosene and saturated pentacosane) from gut tissue and beetle body of *I. typographus* males at different life stages. x axis: mean ± SE

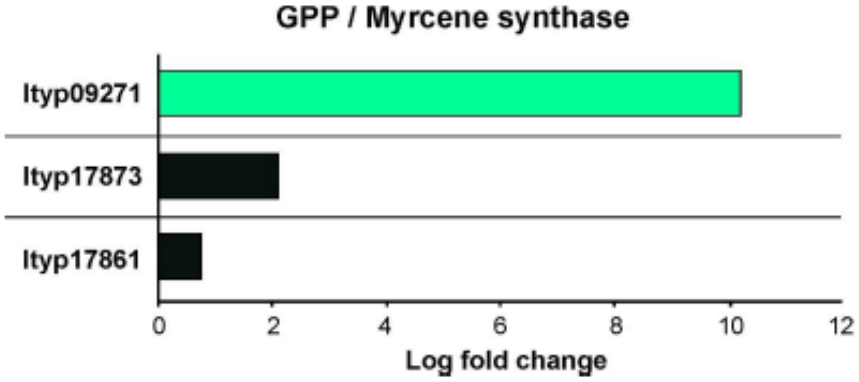

Supplementary Figure S3. Relative expression of GPP/myrcene synthase gene isomers from RNA-seq. data in fed male gut vs immature male gut. Green: Proposed IPDS candidate for 2-methyl-3-buten-2-ol synthesis. Black: isomers proposed for possible geranyl-di-phosphate synthase (GPPS) function towards myrcene synthesis.

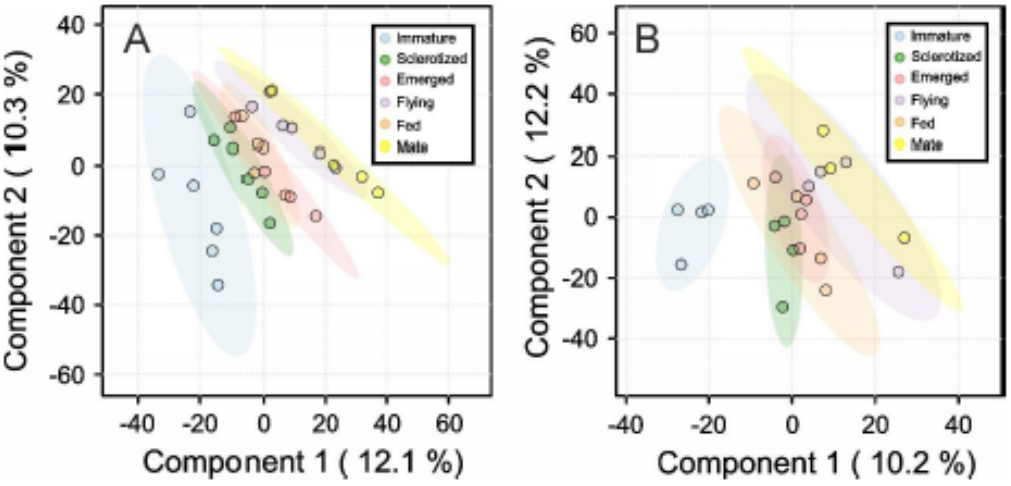

Supplementary Figure S4. Partial least squares-discriminant analysis (PLS-DA) of UHPLC-HR- MS/MS analysed metabolites from gut extracts of *I. typographus* male beetle - different life stages. PLS-DA was performed using MetaboAnalist 5.0 (Pang et al. 2021), an online tool for streamlined metabolomics data analysis. The coloured areas represent 95% of the confidence interval. A: positive ion mode. B: negative ion mode.

4.2 Publication 2:

Metabolome and transcriptome related dataset for pheromone biosynthesis in an aggressive forest pest *Ips typographus*

Citation: Ramakrishnan, R., Roy, A., Kai, M. R., Svatos, A. & Jirosova, A., 2022b. Metabolome and transcriptome related dataset for pheromone biosynthesis in an aggressive forest pest *Ips typographus*. Data in Brief, 41, 26. https://doi.org/10.1016/j.dib.2022.107912

Summary:

Publication 2 contains essential information apart from publication 1, Ramakrishnan et al., 2022a. The analysis of metabolomic and transcriptomic data from gut tissue of important life stages of *I. typographus* provided information on **various metabolites and relative gene families with other functions** along with pheromone biosynthetic functions. Primarily, metabolomic data from UHPLC –HR-MS/MS analysis has provided insight into metabolites in different measurement modes. The acquisition methods of this data (using bioinformatics software programs such as GNPS, and Sirus) are vital information for aiding similar analysis in the future and for developing bioinformatics tools for high-throughput metabolomics analysis. Expression patterns of a **multifunctional gene family** such as cytochrome P450, related to detoxification from the gut tissue of bark beetle life stages. Information on **standardized housekeeping genes** is vital for performing the quantitative real-time PCR analysis and filling the knowledge gap in the respective research field. This publication is valuable knowledge, allowing the researchers to make follow-up research questions evolved from the postulated hypothesis 1, which can support the identified multifunctional gene families.

Data in Brief 41 (2022) 107912

Contents lists available at ScienceDirect

Data in Brief

journal homepage: www.elsevier.com/locate/dib

Data Article

Metabolome and transcriptome related dataset for pheromone biosynthesis in an aggressive forest pest *Ips typographus*

Rajarajan Ramakrishnan[a], Amit Roy[a], Marco Kai[b], Aleš Svatoš[b], Anna Jirošová[a,*]

[a] EXTEMIT-K, Faculty of Forestry and Wood Sciences, Czech University of Life Sciences Prague, Czech Republic
[b] Max Planck Institute of Chemical Ecology, Jena, Germany

ARTICLE INFO

Article history:
Received 14 December 2021
Revised 17 January 2022
Accepted 1 February 2022
Available online 8 February 2022

Keywords:
Pheromone biosynthesis
Bark beetle
Spruce
Gut tissue
De-novo
Omics

ABSTRACT

Eurasian spruce bark beetle, *Ips typographus*, is an aggressive pest among spruce vegetation. *I. typographus* host trees colonization is mediated by aggregation pheromone, consisting of 2-methyl-3-buten-2-ol and *cis*-verbenol produced in the beetle gut. Other biologically active compounds such as ipsdienol and verbenone have also been detected. 2-Methyl-3-buten-2-ol and ipsdienol are produced *de-novo* in the mevalonate pathway and *cis*-verbenol is oxidized from α-pinene sequestrated from the host. The pheromone production is presumably connected with further changes in the primary and secondary metabolisms in the beetle. To evaluate such possibilities, we obtained qualitative metabolomic data from the analysis of beetle guts in different life stages. We used Ultra-high-performance liquid chromatography-electrospray ionization-high resolution tandem mass spectrometry (UHPLC-ESI-HRMS/MS). The data were dereplicated using metabolomic software (XCMS, Camera, and Bio-Conductor) and approximately 3000 features were extracted. The metabolite was identified using GNPS databases and *de-novo* annotation in Sirius program followed by manual curation.

DOI of original article: 10.1016/j.ibmb.2021.103680
* Corresponding author.
E-mail address: jirosovaa@fld.czu.cz (A. Jirošová).
Social media: @AJirosova (A. Jirošová)

https://doi.org/10.1016/j.dib.2022.107912

Further, we obtained differential gene expression (DGE) of RNA sequencing data for mevalonate pathway genes and CytochromeP450 (CyP450) genes from the gut tissue of the beetle to delineate their role on life stage-specific pheromone biosynthesis. CyP450 gene families were classified according to subclasses and given individual expression patterns as heat maps. Three mevalonate pathway genes and five CyP450 gene relative expressions were analyzed using quantitative real-time (qRT) PCR, from the gut tissue of different life stage male/female beetles, as extended knowledge of related research article (Ramakrishnan et al., 2022). This data provides essential information on pheromone biosynthesis at the molecular level and supports further research on pheromone biosynthesis and detoxification in conifer bark beetles.

Specifications Table

Subject	Omics: Metabolomics; Omics: Transcriptomics
Specific subject area	Molecular underpinning pheromone biosynthesis in *Ips typographus*.
Type of data	Table, Image, Chart.
How data were acquired	UHPLC-ESI-HR-MS/MS metabolomic analysis using MetaboAnalyst 5.0 RNA sequenced and analysed data using CLC workbench software Quantitative real-time PCR using the 2-ΔΔCt method
Data format	Analysed data.
Parameters for data collection	*Ips typographus* gut tissue, Different life stages.
Description of data collection	*Ips typographus* different life stages were collected from rearing and used for sample processing. Prepared samples were used for various downstream process such as RNA extraction for sequencing in the Illumina platform and ethylacetate extraction for metabolomic analysis.
Data source location	Institution: Czech university of Life sciences City: Prague Country: Czech Republic and Institution: Max-Planck Institute for Chemical Ecology City: Jena Country: Germany
Data accessibility	*Ips typographus* different tissue UHPLC–HRMS/MS data: Dryad DOI: doi_10.5061_dryad.f7m0cfxws__v1 https://datadryad.org/stash/share/fw11pHIRK2WagKbXczgVb4w0qd2-gpMAATSOWD5EEEs *Ips typographus* different tissue RNA seq. data. accession number: PRJNA679450 https://www.ncbi.nlm.nih.gov/bioproject/PRJNA679450
Related Research article	R. Ramakrishnan, J. Hradecký, A. Roy, B. Kalinová, C. R. Mendezes, J. Synek, J. Bláha, A. Svatoš, A. Jirošová, Metabolomics and transcriptomics of pheromone biosynthesis in an aggressive forest pest *Ips typographus*, Insect Biochem. Mol. Biol. (2022)0965–1748. 10.1016/j.ibmb.2021.103680.

Value of the Data

- Provided dataset of various metabolites and relative gene families from the gut tissue of *Ips typographus* is valuable for researchers with interest in studying different life stages of the bark beetle.
- Metabolomic data from UHPLC–HR-MS/MS analysis has provided insight of metabolites in different measurement modes and shared in dryad link. The acquisition methods of this data (using bioinformatics software programs such as GNPS, Sirus) are vital information for aiding similar analysis in the future and to developing bioinformatics tools for high-throughput metabolomics analysis.
- RNA seq. data revealed expression patterns of key gene families from the gut tissue of bark beetle life stages. This is valuable insight knowledge, allowing the researchers to follow up the present study with further research questions aligning with identified gene families.
- Information of standardized housekeeping genes and the quantitative real-time (qRT)- PCR data covers the knowledge gap, not included in the related research article.
- Henceforth, listed data in this article will be of added value for researchers to understand pheromone biosynthesis and metabolism of the related compounds in *I. typographus* and other bark beetle species and thus help to interrupt the beetle aggregation over spruce vegetation.

1. Data Description

The dataset we provided here is subjected to gut tissue of different life stages of the bark beetle, *I. typographus*. Ultra-high-performance liquid chromatography-electrospray ionization-high resolution tandem mass spectrometry (UHPLC-ESI-HR-MS/MS) data identified various metabolite compounds from the gut extracts using positive and negative ion mode and the results were shared in Table 1. Multivariate analysis of UHPLC–HR-MS/MS is shown in both positive and negative mode (Fig. 1a and b). Identified compounds clustering based on Partial least squares-discriminant analysis (PLS-DA) for different life stages of the beetle was given with different colours in Fig. 1a and b. Specific compounds masses responsible for the separation of life stages were listed with respective *m/z* ratio and retention time (RT) in Fig. 1a, B-G for positive mode, and in Fig. 1b, B-H for negative mode analysis. Fatty acids (C16 and C18) quantitative data over life stages are shown in Fig. 2. Proportions of identified metabolite classes from Table 1 are shown as Venn diagrams for both positive and negative ion mode in Fig. 3. Insight of di-glycosylated monoterpene alcohols was measured in both modes and masses were shared as peaks and CID spectra (Fig. 4). Mevalonate pathway compounds such as isopentyl-di-phosphate (IPP)/ dimethylallyl pyrophosphate (DMAPP) were visible in negative mode analysis with the help of synthetic standards and provided as peaks and CID spectra (Fig. 5).

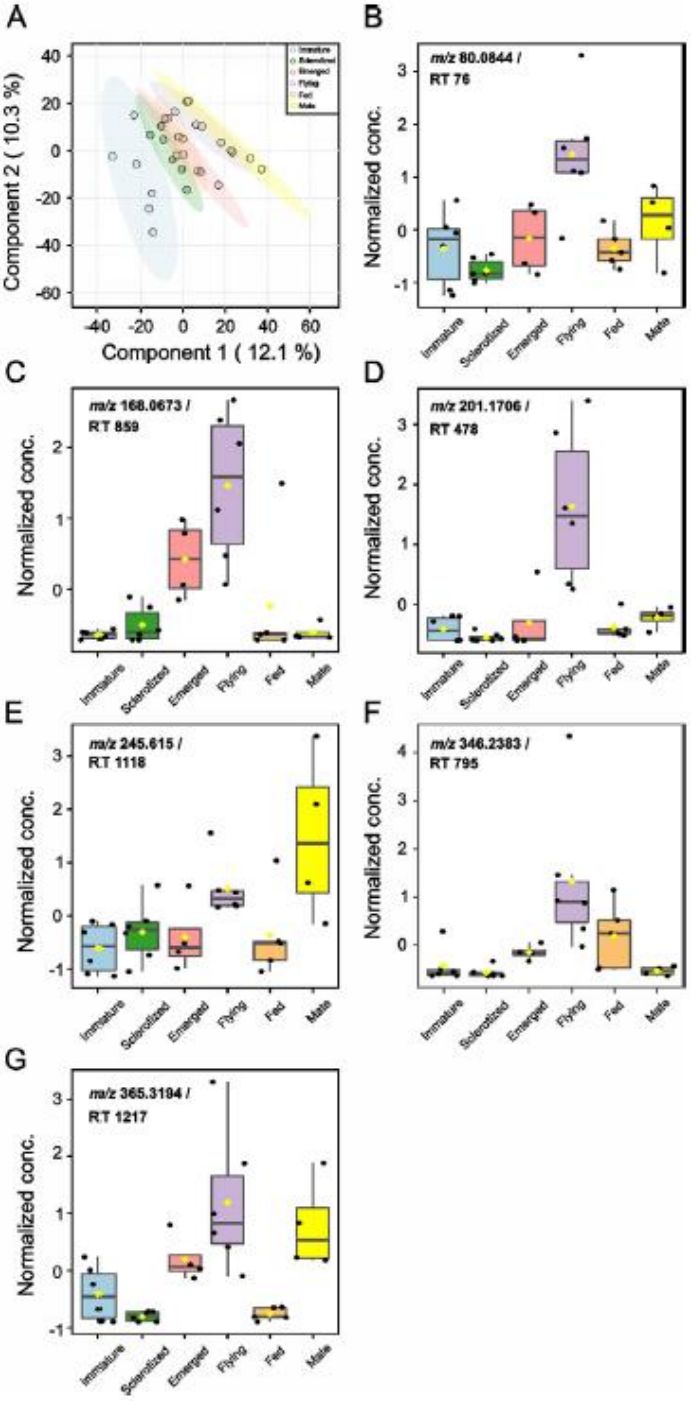

Fig. 1a. Uni- and multivariate analysis of UHPLC-ESI-HR-MS/MS analyzed metabolites extracted from different life stages of male *I. typographus*. (A) Partial least squares-discriminant analysis (PLS-DA) of *positive ion mode acquired data*. The colored areas represent 95% of the confidence interval between life stages of the beetle. (B–G) Correlation analysis of positive ion mode acquired mass features: (B) *m/z* 80.0844 at retention time (RT) 76 s, (C) *m/z* 168.0673 at RT 859 s, (D) *m/z* 201.1706 at RT 478 s, (E) *m/z* 245.615 at RT 1118 s, (F) *m/z* 346.2383 at RT 795 s, (G) *m/z* 365.3194 at RT 1217 s. PLS-DA and correlation analysis were performed using MetaboAnalyst 5.0 [8], an online tool for streamlined metabolomics data analysis.

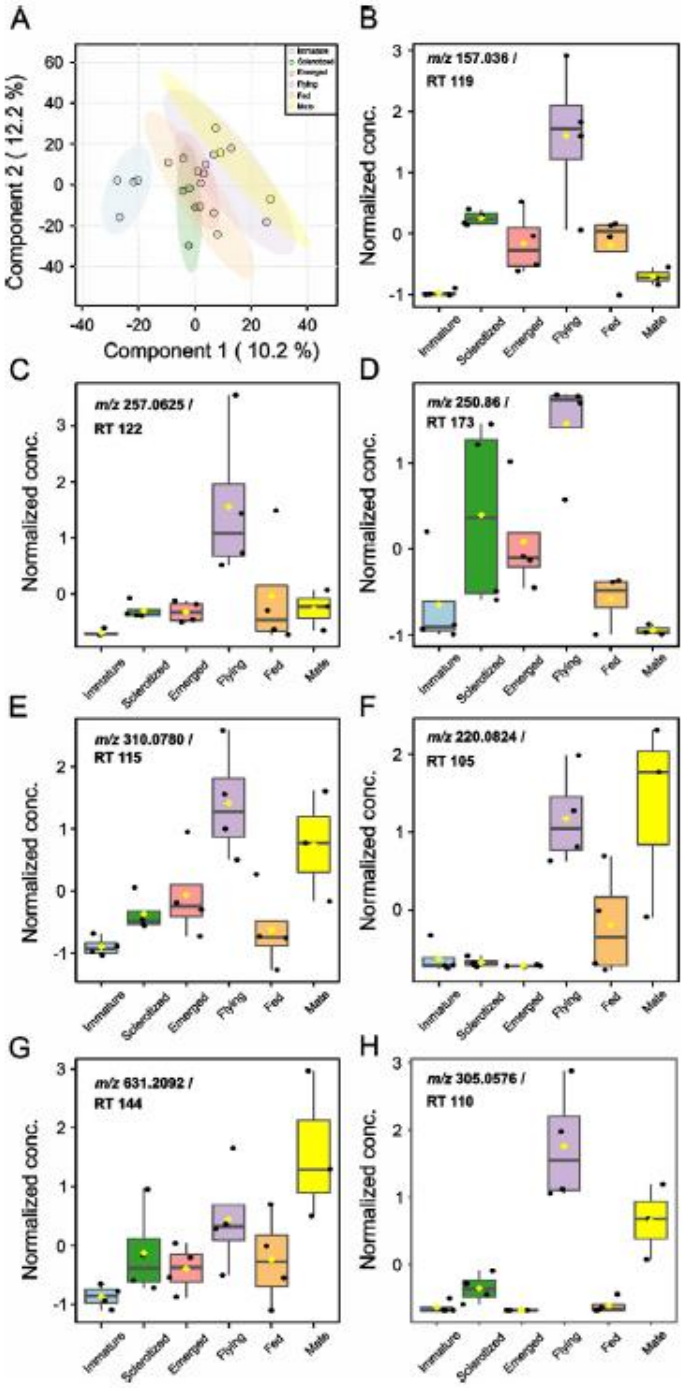

Fig. 1b. Uni- and multivariate analysis of UHPLC-ESI-HR-MS/MS analyzed metabolites extracted from different life stages of male *I. typographus*. (A) Partial least squares-discriminant analysis (PLS-DA) of *negative ion mode acquired data*. The coloured areas represent 95% of the confidence interval between life stages of the beetle (B–H). Correlation analysis of negative ion mode acquired mass features: (B) *m/z* 157.036 at retention time (RT) 119 s, (C) *m/z* 257.0625 at RT 122 s tentatively identified as 3-Dehydro-D-glucose 6-phosphate, (D) *m/z* 250.86 at RT 173 s, (E) *m/z* 310.0780 at RT 115 s tentatively identified as carboxy-neuraminic acid, (F) *m/z* 220.0824 at RT 105 s tentatively identified as N-Acetyl-D-Glucosamine, (G) *m/z* 631.2092 at RT 144 s, (H) *m/z* 305.0576 at RT 110 s. PLS-DA and correlation analysis were performed using MetaboAnalyst 5.0 [8], an online tool for streamlined metabolomics data analysis.

Table 1
List of all identified metabolites from UHPLC-HR-MS/MS measurement in both positive and negative ion mode using data dereplication in GNPS and manually edited with the help of Sirius data annotations. Only possible precursor masses are listed in the table.

Positive ion mode Precursor *m/z*	**ID GNPS pos**
159.113	Gly-Leu-Lys
177.164	dihydro-b-ionone 2-Butanone, 4-(2,6,6-trimethyl-2-cyclohexen-1-yl)- in S5,8,11, in MeOH S4, 6, 7,8,9,10 no in GCMS
179.129	Ile-Pro-Lys
180.132	Val-Ile-Lys
182.081	Tyrosine
187.143	Ile-Ile-Lys
189.11	Azelaic acid
189.134	N.epsilon.-Acetyl-L-lysine
189.125	Gly-Ile
192.061	L-Methionine, N-acetyl-
193.068	S-(5'-Adenosyl)-L-homocysteine
194.142	Val-Ile-Arg
194.636	Leu-Gln-Lys
195.123	Leu-Glu-Lys
197.125	Val-Phe-Lys
198.076	3,4-Dihydroxy-L-phenylalanine
203.15	N,N-DIMETHYLARGININE
204.087	N-Acetyl-D-glucosamine
204.131	Acetyl-DL-carnitine
204.131	Phe-Leu-Lys
209.092	L-kynurenine
209.19	2,4,7,9-Tetramethyl-5-decyne-4,7-diol
215.139	Pro-Val
217.128	N-.alpha.-Acetyl-L-arginine
219.134	Ser-Ile
219.174	Curcumol
220.117	Pantothenic acid
222.097	N-Acetyl-D-glucosamine
229.086	Resveratrol
229.159	Ile-Pro
231.17	Val-Ile
233.149	Thr-Ile
237.221	cis-9-Hexadecenoic acid
239.102	Gly-Tyr
241.031	CYSTINE

(continued on next page)

Table 1 (*continued*)

243.21	9(10)-EpOME
244.165	Lys-Pro
245.085	Piceatannol
245.129	Phe-Pro
245.186	Ile-Leu
245.233	N1-ACETYLSPERMINE
246.181	Lys-Val
247.129	Asp-Leu
251.046	**Diphenylphosphate**
253.118	Ser-Phe
256.263	Palmitamide
259.096	Rhapontigenin
259.129	L-Saccharopine gene ltyp17086 -2.747645682 -1.458195976 1.06606E-05 7.05172E-05 saccharopine dehydrogenase-like oxidoreductase
260.197	Ile-Lys
261.144	Ile-Glu
265.118	Phenylacetylglutamine
265.252	9-Octadecenamide, (Z)-
267.134	Thr-Phe
267.172	**Tributyl phosphate**
269.161	His-Ile
272.163	Pro-Arg
274.187	Val-Arg
275.2	9-OxoOTrE
277.103	L-.gamma.-Glutamyl-L-glutamic Acid
277.118	PyroGlu-Phe
277.216	13S-Hydroxy-9Z,11E,15Z-octadecatrienoic acid
279.17	Leu-Phe
281.113	.alpha.-L-Asp-L-Phe
282.279	9-Octadecenamide, (Z)-
284.294	Octadecanamide
285.083	Xanthosine
288.203	Ile-Arg
290.134	Ophthalmic acid (tripeptide), stress, gluthione analog
291.086	(+)-Catechin
293.113	PyroGlu-Tyr
293.247	13(S)-HODE methyl ester
294.147	Phe-Gln
295.165	Ile-Tyr
295.226	9-Oxo-10E,12Z-octadecadienoic acid
295.226	13-Keto-9Z,11E-octadecadienoic acid
297.127	Met-Phe
298.097	METHYLTHIOADENOSINE

(*continued on next page*)

Table 1 (*continued*)

302.206	Ile-Gly-Ile
302.305	D-erythro-Sphinganine
303.05	Quercetin
305.065	Taxifolin
307.083	Glutathione, oxidized
307.262	9Z,11E,13E-Octadecatrienoic acid ethyl ester
311.123	.alpha.-L-Glu-L-Tyr
311.258	Monopalmitolein (9c) -H2O
313.155	Phe-Phe
314.196	Heliotrine ??
315.195	1,4a-dimethyl-9-oxo-7-propan-2-yl-3,4,10,10a-tetrahydro-2H-phenanthrene-1-carboxylic acid
318.181	Leu-Trp
322.273	.alpha.-Linolenoyl ethanolamide
324.289	Linoleoyl ethanolamide
325.113	D-(+)-Cellobiose
329.149	Tyr-Phe
329.268	Monopalmitolein (9c)-H2O
332.218	Thr-Val-Leu
332.561	.beta.-Nicotinamide adenine dinucleotide
335.258	Monolinolenin (9c,12c,15c)-H2O
338.341	(Z)-13-Docosenamide
339.069	5-Aminoimidazole-4-carboxamide ribonucleotide
339.281	Monoelaidin-H2O
342.239	Ile-Pro-Ile
345.144	Tyr-Tyr
360.149	D-(+)-Trehalose
369.351	Cholestan-3-one, (5.alpha.)-
370.052	ADENOSINE-MONOPHOSPHATE
371.102	**Cyclopentasiloxane, decamethyl-**
371.23	PyroGlu-Ile-Lys
371.315	Hexanedioic acid, bis(2-ethylhexyl) ester
377.145	(-)-Riboflavin
384.114	Succinoadenosine
399.139	S-ADENOSYLMETHIONINE
399.235	PyroGlu-Ile-Arg
399.25	**Tris(2-butoxyethyl) phosphate**
400.342	Palmitoylcarnitine
428.036	Adenosine 5'-diphosphate
430.161	Serratiochelin Seratia bacteria siderofor
435.128	Naringenine-7-rhamnosidoglucoside (-H2O)
454.292	1-Palmitoyl-2-hydroxy-sn-glycero-3-phosphoethanolamine
457.111	Flavine mononucleotide

(*continued on next page*)

Table 1 (*continued*)

464.081	Adenylosuccinic acid
465.102	Isoquercitin
466.264	Rosiridoside B glycosilated OH-geranyl more likely glyc myrtanol NH4+ adduct C19H38O9N 466.2637 delta 049 mu in S6 and S7 two cycles!! Present in S7 GCMS
466.329	TOP19 Psoriasis feature - Unknown FeatureID=3668
468.308	1-Myristoyl-sn-glycero-3-phosphocholine
471.105	4-(3,4-dihydroxyphenyl)-7-hydroxy-5-((2S,3R,4S,5S,6R)-3,4,5-trihydroxy-6-(hydroxymethyl)oxan-2-yl)oxychromen-2-one
478.292	(5-((4-(5-(acetyl(hydroxy)amino)pentylamino)-4-oxobutanoyl)-hydroxyamino)pentylamino)-4-oxobutanoic acid ***siderophore***
480.243	(3,4,5-trihydroxy-6-((3,4,5-trihydroxyoxan-2-yl)oxymethyl)oxan-2-yl) 2,6,6-trimethylcyclohexene-1-carboxylate 480.2495 C21 H38 O11 N delta 1.04 mu
480.308	1-(9Z-Octadecenoyl)-sn-glycero-3-phosphoethanolamine
480.344	1-(1Z-Hexadecenyl)-sn-glycero-3-phosphocholine
482.323	1-Stearoyl-2-hydroxy-sn-glycero-3-phosphoethanolamine
482.36	1-Hexadecyl-sn-glycero-3-phosphocholine
489.114	Cytidin-5'-diphosphocholin
496.339	Lyso-PC(16:0)
510.355	1-Heptadecanoyl-sn-glycero-3-phosphocholine
522.355	1-(9Z-Octadecenoyl)-sn-glycero-3-phosphocholine
536.165	**Contaminants septum vial Thermo C4000-53 and C4000-54 serie**
608.088	URIDINE 5'-DIPHOSPHO-N-ACETYLGALACTOSAMINE
610.184	**Contaminants septum vial Thermo C4000-53 and C4000-54 serie**
628.194	**Contaminant vial septum ThermoFisher C5000-44B**
664.116	NAD
675.676	(Z)-13-Docosenamide (2M+H)+
686.182	**Contaminant vial septum ThermoFisher C5000-44B**
702.213	**Contaminant vial septum ThermoFisher C5000-44B**
744.553	1-Stearoyl-2-linoleoyl-sn-glycero-3-phosphoethanolamine
758.221	**Contaminants septum vial Thermo C4000-53 and C4000-54 serie**
759.222	Azadirachtin
776.232	**Contaminant vial septum ThermoFisher C5000-44B**

Negative ion mode	ID GNPS neg
Precursor *m/z*	
174.041	N-ACETYLASPARTATE
179.056	D-FRUCTOSE
187.098	Nonanedioate
188.056	N-ACETYLGLUTAMATE

(*continued on next page*)

Table 1 (*continued*)

191.035	Citric acid
191.019	ISOCITRIC ACID
193.035	GLUCURONATE
203.083	TRYPTOPHAN
203.083	L-Tryptophan
207.078	Kynurenine
209.03	MUCIC ACID
219.078	5-HYDROXYTRYPTOPHAN
221.082	Diethyl phthalate (NF)
243.062	URIDINE
245.093	N-acetyltryptophan
259.022	GLUCOSE 6-PHOSPHATE
267.073	INOSINE
271.061	Naringenin
275.017	6-PHOSPHOGLUCONATE
277.145	MoNA:932219 DBP
285.04	Tetrahydroxy-Flavone
287.056	(2S,3S)-3,5,7-trihydroxy-2-(4-hydroxyphenyl)-2,3-dihydrochromen-4-one
297.152	4-(decan-4-yl)benzenesulfonic acid
301.035	Quercetin
303.051	Taxifolin
306.077	GLUTATHIONE REDUCED
311.15	Pyrenophorol ??
313.239	12,13-DiHOME
321.049	THYMIDINE-MONOPHOSPHATE
322.044	CMP
323.029	URIDINE MONOPHOSPHATE
325.192	linoleic acid (formic acid adduct)
341.109	TREHALOSE
341.108	Isomaltulose
346.055	2'-DEOXYGUANOSINE 5'-MONOPHOSPHATE
347.04	INOSINE MONOPHOSPHATE
361.166	2,3-bis((4-hydroxy-3-methoxyphenyl)methyl)butane-1,4-diol
373.129	Nortrachelogenin
375.131	RIBOFLAVIN
402.995	URIDINE 5'-DIPHOSPHATE
426.022	ADENOSINE 5'-DIPHOSPHATE
431.098	Kaempferol-3-Rhamnoside
431.156	osmanthuside H in S6 S7
445.053	CDP-ETHANOLAMINE
445.208	2-((3,4-dihydroxy-4-(hydroxymethyl)oxolan-2-yl)oxymethyl)-6-((6,6-dimethyl-4-bicyclo(3.1.1)hept-3-enyl)methoxy)oxane-3,4,5-triol
447.089	Quercitrin

(*continued on next page*)

Table 1 (*continued*)

452.278	1-Palmitoyl-2-hydroxy-sn-glycero-3-phosphoethanolamine
463.088	Spiraeoside
478.294	1-(9Z-Octadecenoyl)-sn-glycero-3-phosphoethanolamine
480.31	1-Stearoyl-2-hydroxy-sn-glycero-3-phosphoethanolamine
503.162	Maltotriose
556.318	1-(9Z-Octadecenoyl)-sn-glycero-3-phosphocholine
558.064	ADENOSINE DIPHOSPHATE RIBOSE
565.047	Uridine-5'-diphospho-glucose disodium salt
571.294	1-Hexadecanoyl-sn-glycero-3-phospho-(1'-myo-inositol)
579.026	Uridine-diphosphate-glucuronic acid
588.074	Guanosine-5'-diphospho-beta-L-fucose
606.074	URIDINE 5'-DIPHOSPHO-N-ACETYLGALACTOSAMINE
609.146	Rutin
625.141	5,7-dihydroxy-2-(3-hydroxy-4-((2S,3R,4S,5S,6R)-3,4,5-trihydroxy-6-(hydroxymethyl)oxan-2-yl)oxyphenyl)-3-((2S,3R,4S,5S,6R)-3,4,5-trihydroxy-6-(hydroxymethyl)oxan-2-yl)oxychromen-4-one
662.101	beta-Nicotinamide adenine dinucleotide
784.15	FAD

Color code

aa nad short peptide
acid, FA amide or ester
nucleotide/nucleoside
Phenylpropanoide
Lipid
Sugar
stres induced phenylpropanoid
pheromone related
Terpene
Oxylipin
Co-factor
Siderophore
not confident ID
Contamination

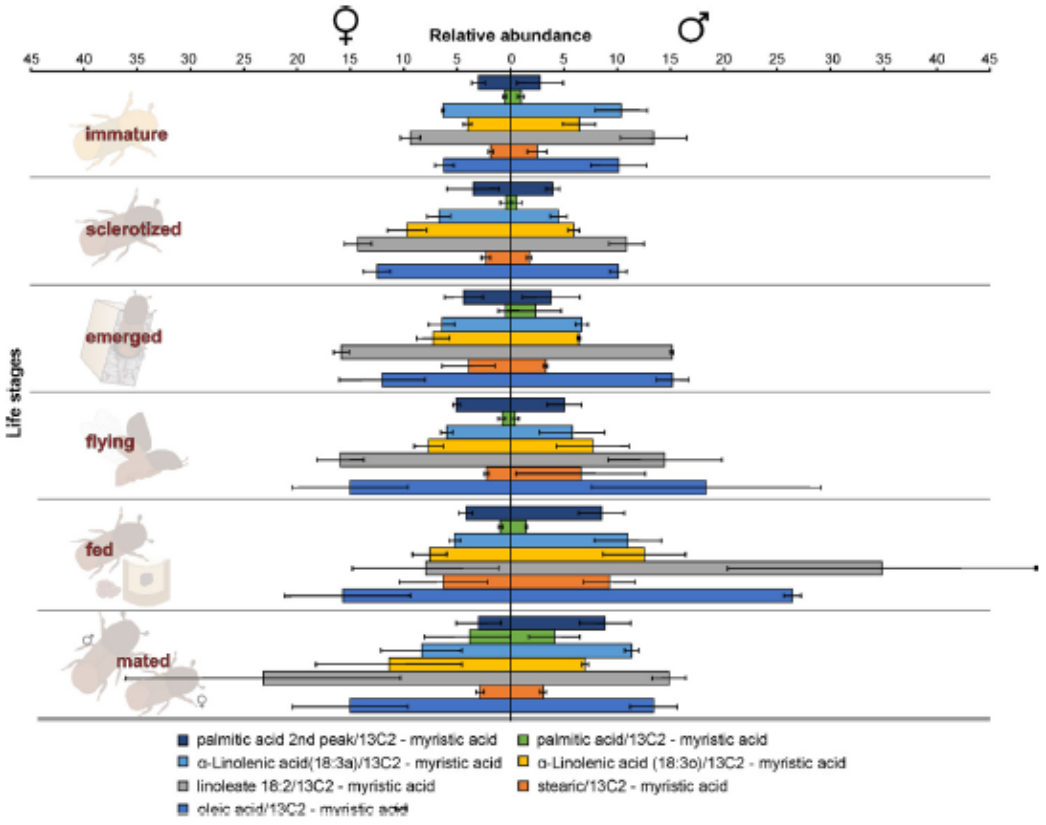

Fig. 2. Intensities of five essential fatty acids normalized to $^{13}C_2$-myristic internal standard signal intensities plotted over life stages of *I. typographus*. Guts extracts were analyzed on UHPLC-ESI-HR-MS/MS instrument in negative ion mode with TOP 5 scanning with one precursor ion scan and 5 MS/MS scans. Bars represent the standard error of the mean, $N = 3$.

Furtherly, RNA sequencing data is shown as heatmaps for the expression pattern of the interested gene families between the life stages of the beetle. Primarily, insight of gene families such as the mevalonate pathway genes as heat map expression (Fig. 7) and further sesquiterpene compound producing genes from the pathway was described using the quantitative real-time (qRT)- PCR (Fig. 8). Identified 56 Cytochrome P450 genes (CyP450) and their overall expression given as a heat map (Fig. 9), with specific subclusters based on names acquired from Gene Ontology (GO) web reference using sequence similarity approach (Table 2). The expression pattern of the CyP450 gene seven subclusters was provided separately as heat map expression pattern in Figs. 10A, 10B, 10C and 10D which belongs to CyP450 6 like, CyP450 9e2 like, CyP450 9a1 like, CyP450 4 like and unknown CyP450 respectively. Furthermore, we studied qRT- PCR data of functionally known CyP450 gene known with sequence similarity from other bark beetle species and provided their expression level between mated male gut tissue and mated female gut tissues of *I. typographus* in Fig. 11. Added information of the housekeeping gene list with thirteen genes was ranked and provided after standardization (Fig. 6), which supports the related research article [5] for future gene study in mentioned tissue of the beetle.

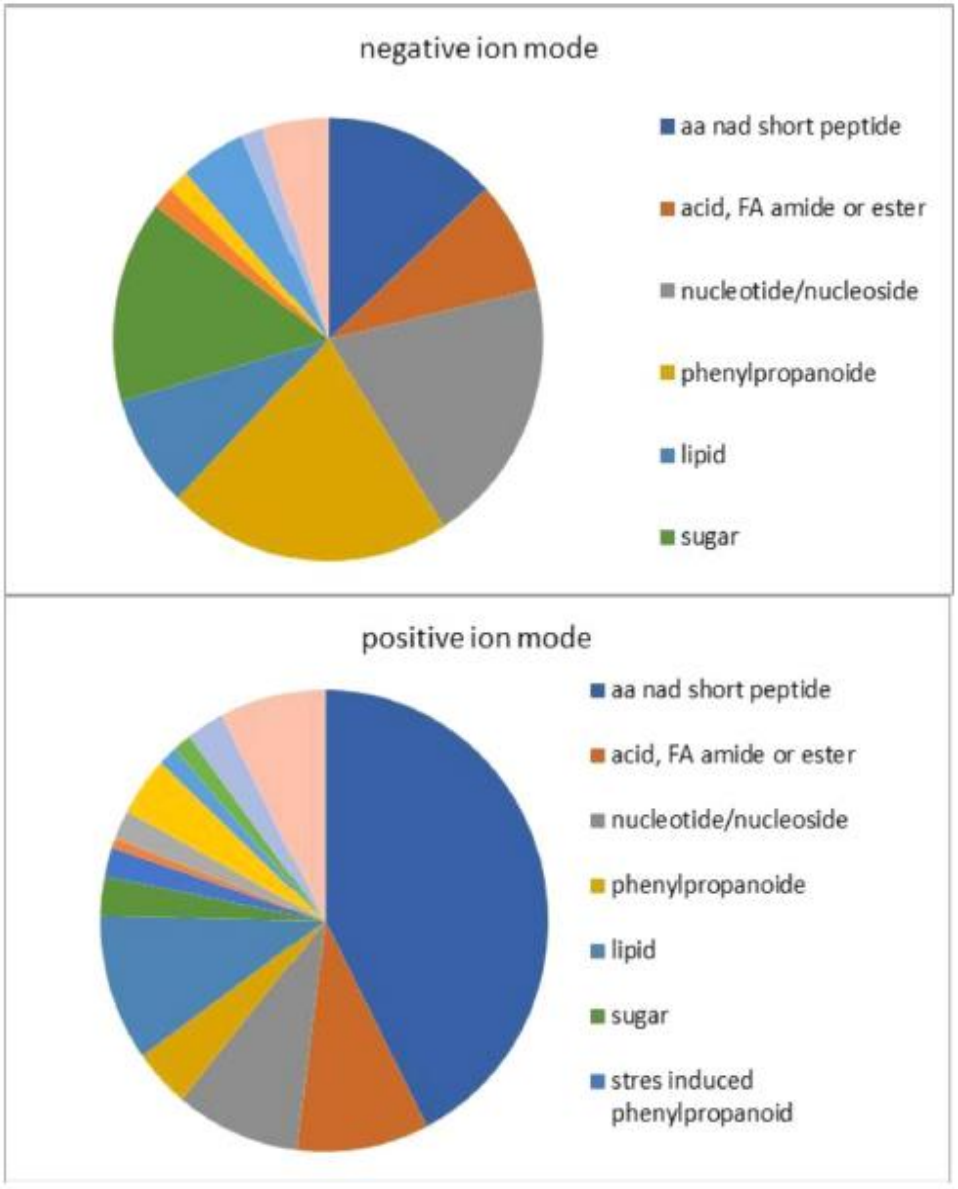

Fig. 3. Venn diagram of metabolite classes from UHPLC-ESI-HR-MS/MS measurement in both positive and negative ion mode using data dereplication in GNPS and manually edited with help of Sirius data annotations. Complete annotation is available in Table 1.

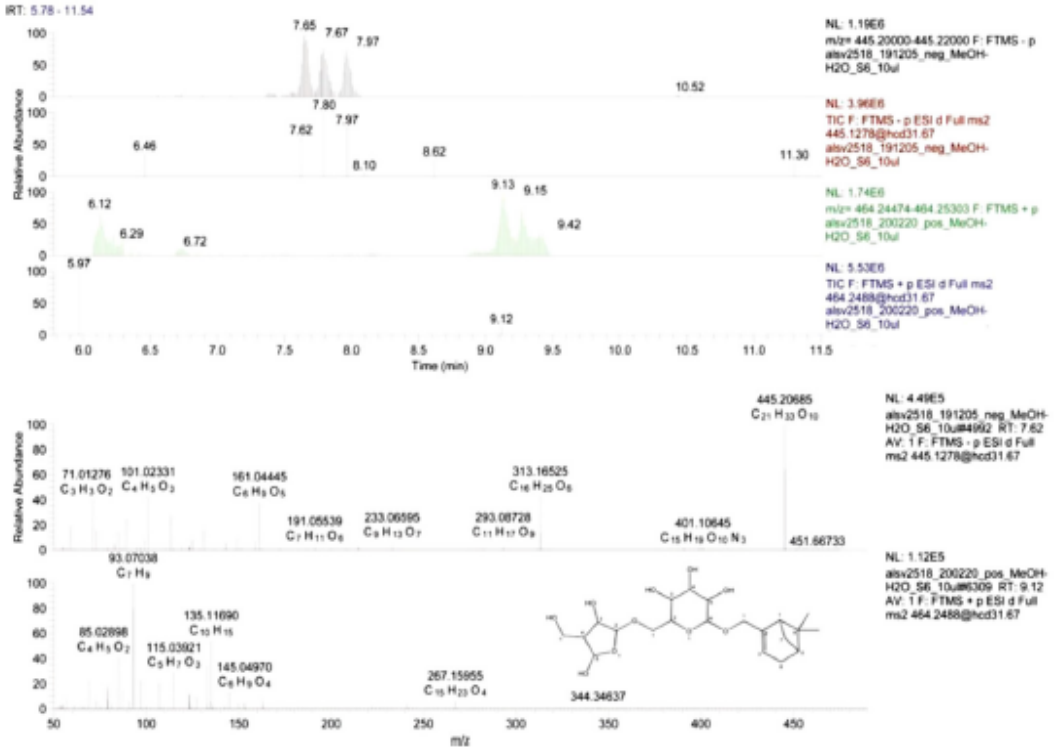

Fig. 4. *A sections of UHPLC-ESI-HR-MS/MS traces plotted at specific mass ranges (upper panel)*: From top: negative ion mode, MS trace @ *m/z* 445.20–445.22 corresponding to $[M\text{-}H]^-$ and MS/MS trace @ 445.127; positive ion mode MS trace @ *m/z* 464.24–464.25 corresponding to $[M+NH_4]^+$ and MS/MS trace @ 464.2488. Tree isobaric peaks are visible in both ion modes with similar intensities. The retention shift was due to a technical problem in one of the measurements. *CID spectra from isolated fixed precursor ion scans (lower panel)*: In negative ion mode, the intensive molecular peak is visible @ *m/z* 445.20685 with molecular composition $C_{21}H_{33}O_{10}$. Ion @ *m/z* 161.0445 with molecular composition $C_6H_5O_5$ is a deprotonated hexose. Two fragment ions $C_{16}H_{25}O_6$ and $C_{11}H_{17}O_9$ resulted from a loss of dehydro-pentose or monoterpene neutrals, respectively. In positive ion mode, molecular adduct peak is not visible, but low mass carbocation fragments (like $C_{10}H_{15}$ and C_7H_9) indicate monoterpene aglycone. The proposed structure of carbocation is given in the last CID spectra.

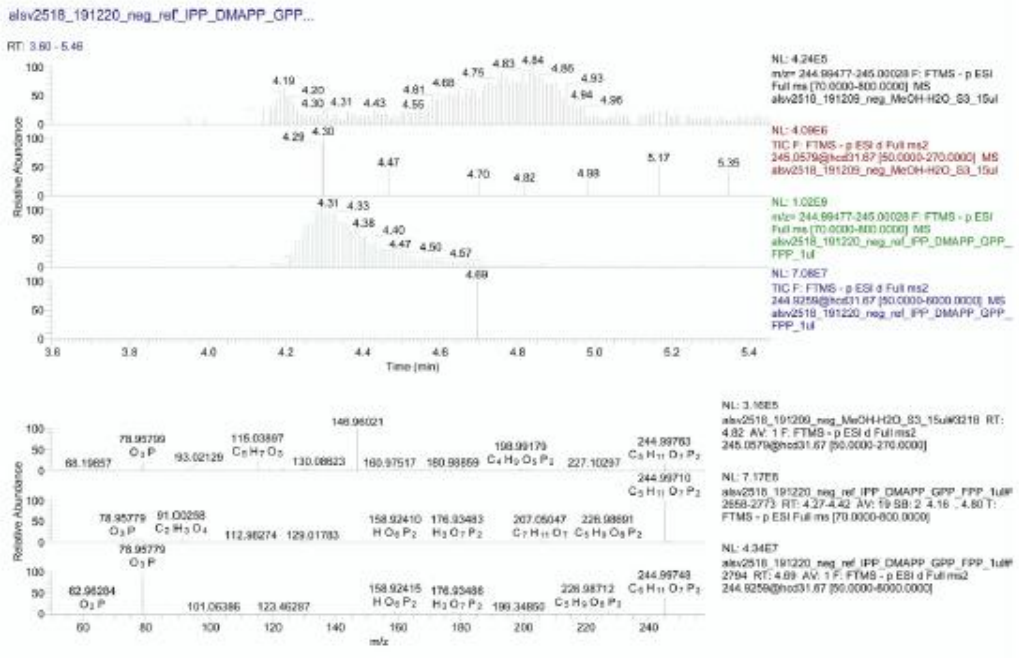

Fig. 5. *A sections of UHPLC-ESI-HR-MS/MS traces plotted at specific mass ranges (upper panel)*: Comparison of the gut extract with a mixture of IPP and DMAPP synthetic standards measured under identical conditions. From top: negative ion mode, MS trace @ *m/z* 244.99–245.00 corresponding to $[M-H]^-$ and MS/MS trace @ 245.06; mixture of standards, negative ion mode MS trace @ *m/z* 244.99–245.00 corresponding to $[M-H]^-$ and MS/MS trace @ 244.93. Several peaks are visible in the expected retention window. Full scan MS spectra were collected from Rt 4.27–4.42 min, retention window. *CID spectra from isolated fixed precursor ion scans (lower panel)*: From top: acquired spectra at Rt 4.82 min showing *m/z* 244.99763 deprotonated molecular ion $[M-H]^-$ and intense PO_3^- ion at *m/z* 78.95799. The second plot is MS trace from Rt 4.27–4.42 min, showing intense deprotonated molecular ion $[M-H]^-$ @ *m/z* 244.99710 with expected molecular composition. The plot below shows CID spectra of standards from isolated fixed precursor ion scans *m/z* 244.9259 showing a similar pattern as in the first plot from the gut extract.

Table 2
Identified 56 genes from CytochromeP450 gene family RNA seq data were clustered as shown in the table. Seven sub-cluster based on Multiple sequence alignment – Unipro UGENE v33.0 maximum likelihood is given as the table with the color difference. Sub-cluster 5, 6, and 7 were shown in similar colours since they were closely related. Cytochrome name replaced as Cy from RNA seq. data and the names were given based upon GO web reference using CLC workbench software. Tissue compared: fed male gut and immature male gut.

Contigs	CyP names	Contigs	CyP names
	Cluster 1		**Cluster 4**
Ityp04042	CyP450	Ityp16927	CyP450 307a1-like
Ityp04209	CyP450 CYP6CR2	Ityp03219	CyP450 CYP410a1
Ityp03230	CyP450	Ityp03221	CyP450 CYP410a1
Ityp03231	CyP450	Ityp03218	CyP450 CYP410a1
Ityp03902	CyP450	Ityp09555	CyP450 CYP410a1
Ityp03903	CyP450	Ityp05831	CyP450 4c21-like
Ityp02766	CyP450 CYP6BW2	Ityp05829	CyP450
Ityp03904	CyP450	Ityp05826	CyP450 4V2-like
Ityp00496	CyP450	Ityp05834	CyP450 4c21-like
Ityp10157	CyP450 CYP6BS2	Ityp05836	CyP450 4C1-like
Ityp03140	CyP450 CYP6DJ1v1	Ityp22414	CyP450 4c21-like
Ityp08010	CyP450 CYP6DG1v1	Ityp06189	CyP450 4c21-like
Ityp03872	CyP450 6A1-like	Ityp22415	CyP450 4g15-like
	Cluster 2	Ityp06190	CyP450 4g15-like
Ityp06081	CyP450 9e2-like	Ityp22416	CyP450 4c3-like isoform X1
Ityp03146	CyP450 9e2	Ityp06191	CyP450 4c3-like isoform X1
Ityp03153	midgut-specific cy P450	Ityp17996	NADPH-dependent CyP450 reductase
Ityp01834	CyP450 9e2-like	Ityp11675	NADPH-dependent CyP450 reductase
	Cluster 3	Ityp04142	CYP450 CYP4G55v3
Ityp14212	probable cy P450 301a1,	Ityp12866	CyP450 4d2-like
Ityp11191	CyP450 315a1,	Ityp09310	CyP450 CYP4CV1
Ityp09248	CyP450 CYP49a1	Ityp04137	CyP450 4d2-like isoform X1
Ityp18289	CyP450	Ityp00542	CyP450 4c3-like isoform X2
Ityp03031	CyP450	Ityp14975	CyP450 4C1-like
Ityp08528	CyP450	Ityp05150	CyP450 4C1-like
		Ityp07474	CyP450 18a1-like
	Cluster 5		**Cluster 6**
Ityp08942	probable CyP450 28a5	Ityp07311	CyP450 6k1-like isoform X1
Ityp10238	probable CyP450 6a17	Ityp04213	CyP450 6k1-like
	Cluster 7	Ityp10797	CyP450
Ityp01602	CyP450	Ityp01836	CyP450 9e2-like

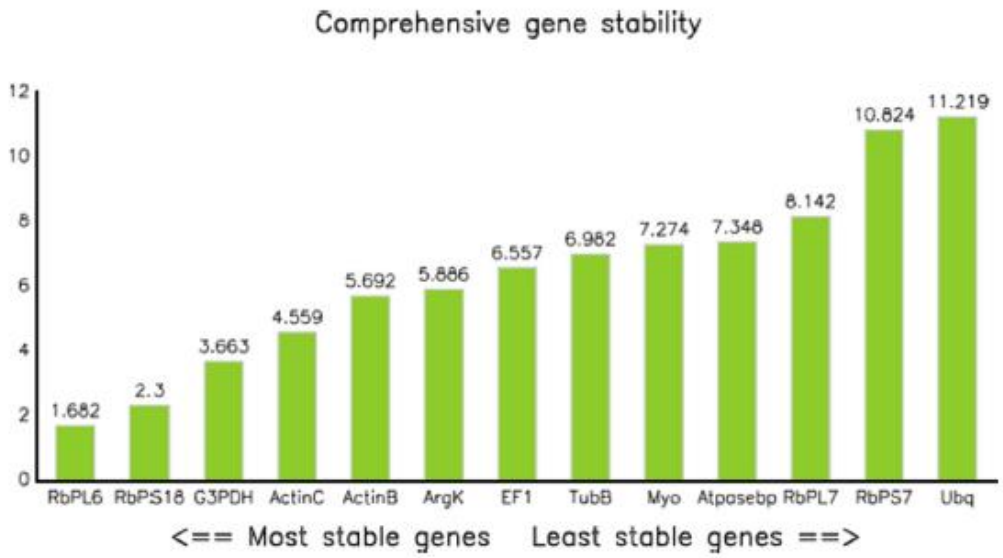

Fig. 6. Validation of 13 housekeeping genes from *I. typographus* gut tissue using methods including bestkeeper, deltact, Genorm, and Normfinder. RbPL6- Ribosomal protein L6; RbPS18- Ribosomal protein S18; G3PDH-Glyceraldehydes 3-phosphate dehydrogenase; ActinC- actin-5C; ActinB- Actin; ArgK- Arginine Kinase; EF1- Elongation factor 1-alpha; TubB-tubulin beta chain; Myo- myosin heavy chain, non-muscle isoform X2; Atpasebp- V-type proton ATPase catalytic subunit A; RbPL7- Ribosomal protein L7; RbPS7- ribosomal protein S7; Ubq- ubiquitin-conjugating enzyme E2 J2. Most stable Ribosomal proteinL6 (RbPL6) and RibosomalproteinS18 (RbPS18) (The first two from left) were chosen for qRT -PCR data analysis. The values over the bar represent the normalization factor.

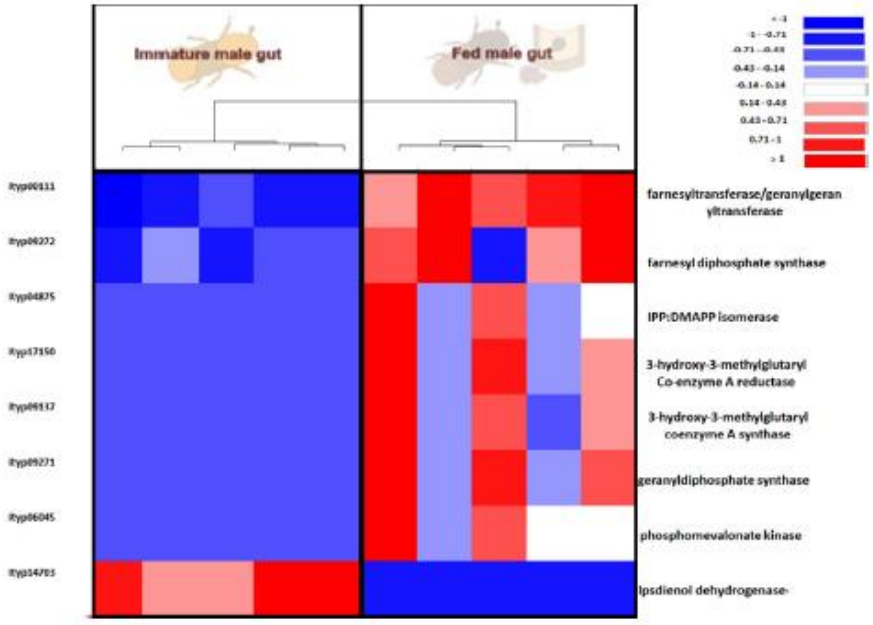

Fig. 7. Heat maps representing eight mevalonate pathway gene expressions from RNA seq. data comparison. Tissue compared: fed male beetle gut vs immature beetle male gut. The tree cluster shows the tissue difference with 5 biological replicates. Red: high expression; Blue: low expression. Software used: CLC workbench and XLSTAT-Student 2020 Licensed version. Y-axis Left side was given with contig number of transcripts annotated with *I. typographus* genome. Y-axis Right side was labeled with possible gene name from Gene Ontology (GO) reference.

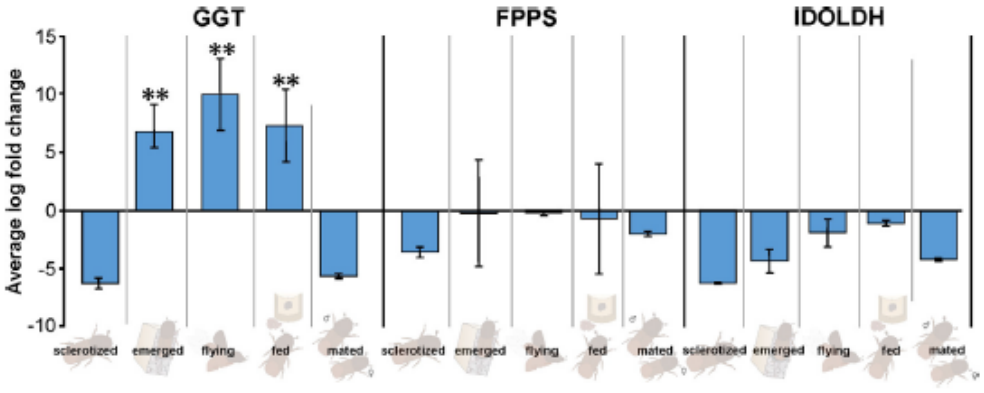

Fig. 8. qRT-PCR data- different life stage male gut tissue analyzed for expression of three genes from mevalonate pathway: GGT- geranylgeranyl transferase, FPPS-Farnesyl diphosphate synthase, and IDOLDH- Ipsdienol dehydrogenase. These genes were chosen due to the least expressed in RNA-seq. data and involved in further sesquiterpene synthesis in the mevalonate pathway.

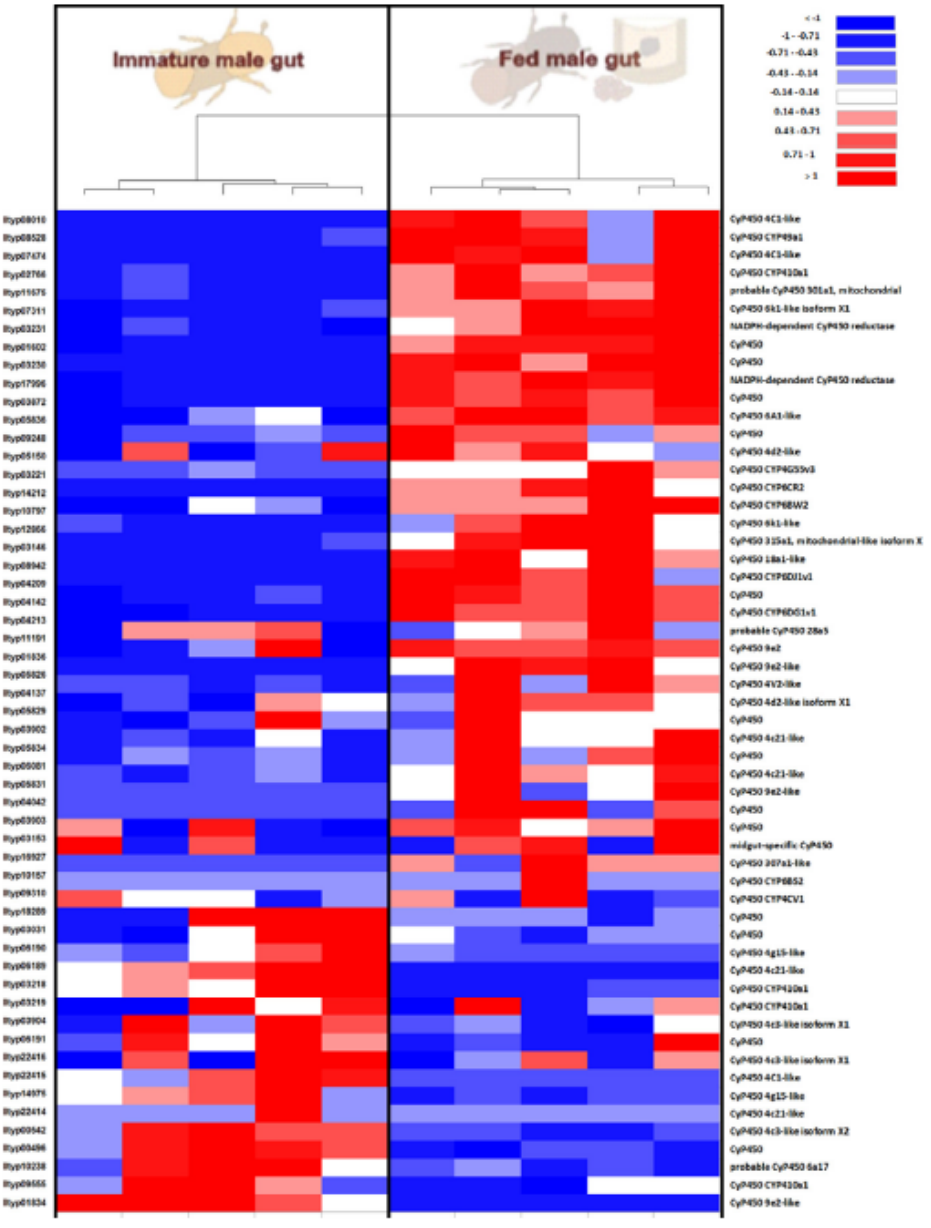

Fig. 9. Heat map showing expression of identified Cytochrome P450 gene family with 56 genes from RNA seq. data. Tissue compared: fed male gut vs immature male gut. The tree clustered the tissue difference with 5 biological replicates. Red: high expression; Blue: low expression. Software used: CLC workbench and XLSTAT-Student 2020 Licensed version. Y-axis Left side was given with contig number of transcripts annotated with *I. typographus* genome. Y-axis Right side was labeled with a possible gene name from GO reference.

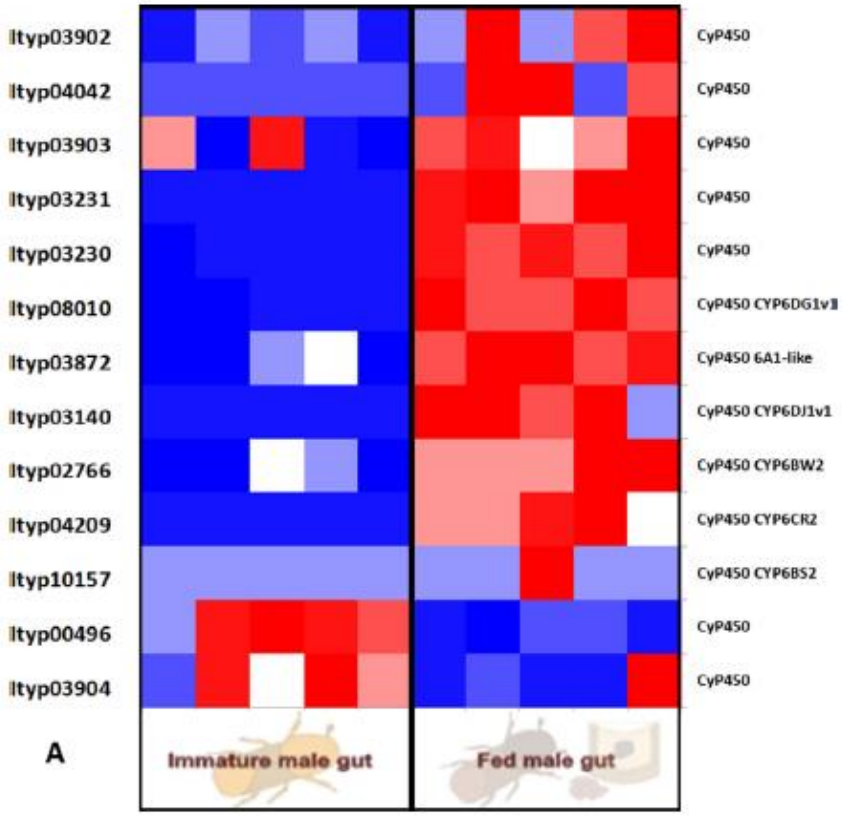

Fig. 10A. Heat map from RNA seq. data analysis showing the expression pattern of CyP450 gene_ sub-cluster 1 with possible 6 like gene family. Tissue compared: fed male gut vs immature male gut with 5 biological replicates. Red: high expression; Blue: low expression. Software used: CLC workbench and XLSTAT-Student 2020 Licensed version. Y-axis Left side was given with contig number of transcripts annotated with *I. typographus* genome. Y-axis Right side was labeled with a possible gene name from GO reference.

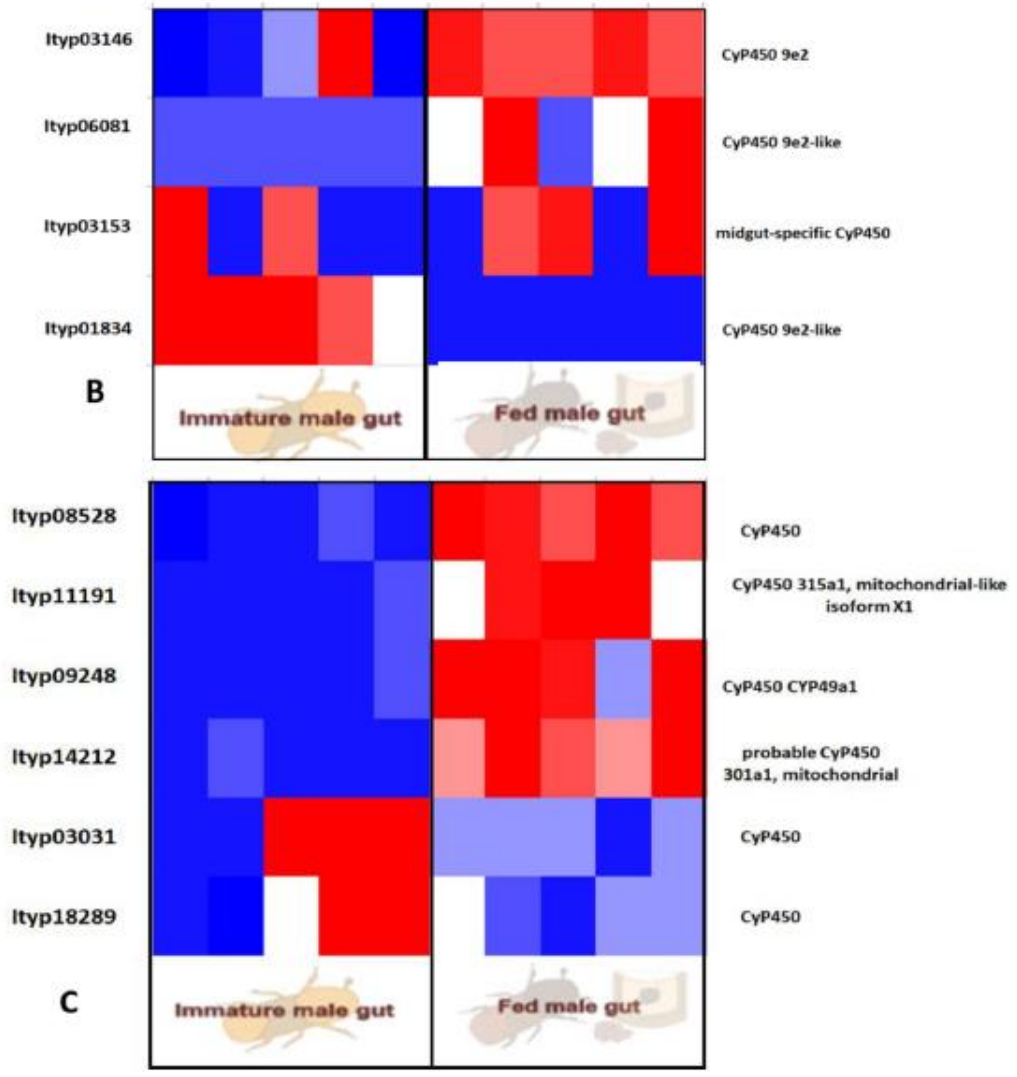

Fig. 10B. Heat map from RNA seq. data showing the expression pattern of CyP450 genes_ sub-cluster 2 with possible 9e2 like gene family. Fig. 10C: Heat map of TPM values showing CyP450 gene_ sub-cluster 3 with **possible 9a1** like gene family. Tissue compared: fed male gut vs immature male gut with 5 biological replicates. Red: high expression; Blue: low expression. Software used: CLC workbench and XLSTAT-Student 2020 Licensed version. Y-axis Left side was given with contig number of transcripts annotated with *I. typographus* genome. Y-axis Right side was labeled with the possible gene names from GO reference.

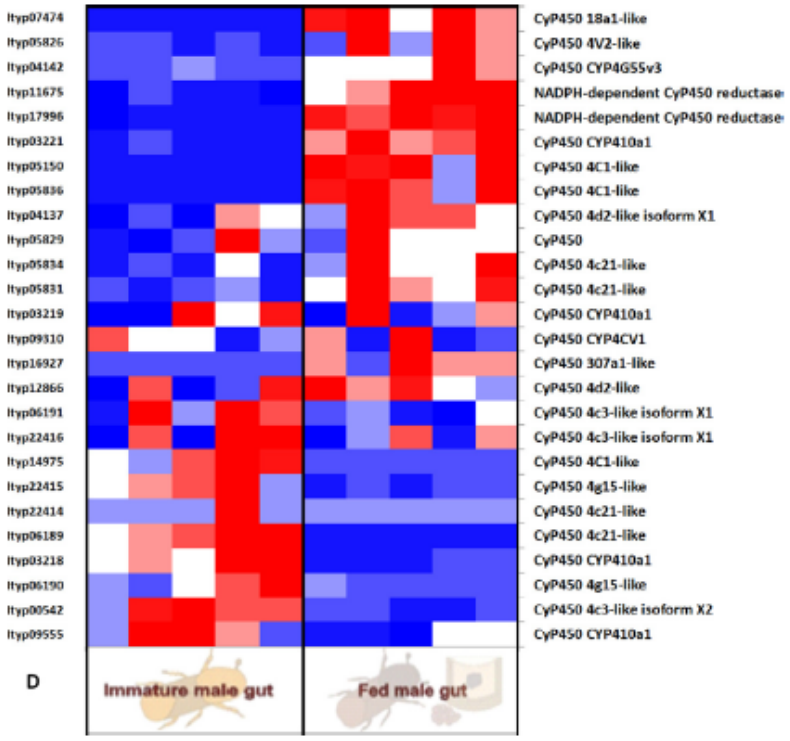

Fig. 10C. Heat map representing the expression pattern of *CyP450 gene_ sub-cluster 4* with 4 like gene family. Tissue compared: fed male gut vs immature male gut with 5 biological replicates. Red: high expression; Blue: low expression. Software used: CLC workbench and XLSTAT-Student 2020 Licensed version. Y-axis Left side was given with contig number of transcripts annotated with *I. typographus* genome. Y-axis Right side was labeled with the possible gene names from GO reference.

Fig. 10D. Heat map of TPM values representing *CyP450 gene_ sub-cluster 5, 6, and 7 with unknown CyP450* gene family. Tissue compared: fed male gut vs immature male gut with 5 biological replicates. Red: high expression; Blue: low expression. Software used: CLC workbench and XLSTAT-Student 2020 Licensed version. Y-axis Left side was given with contig number of transcripts annotated with *I. typographus* genome. Y-axis Right side was labeled with the possible gene names from GO reference.

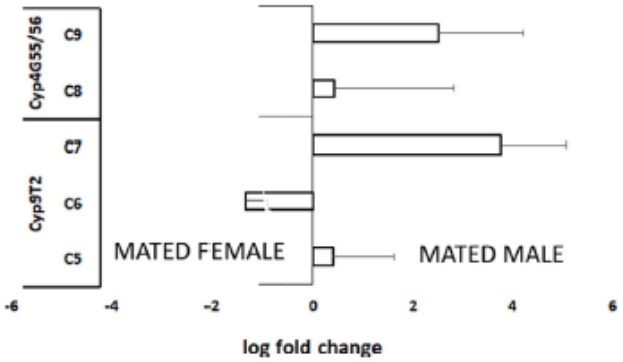

Fig. 11. *qRT PCR data*: Relative expression of Cyp450 genes C5-C9 in the mated male gut compared to mated female gut. C5-C7 are CyP450 gene candidates possibly involved in ipsdienol synthesis. C8-C9 are CyP450 gene candidates possibly involved in hydrocarbon synthesis. The number of biological replicates $N = 4$.

2. Experimental Design, Materials and Methods

Beetle rearing conditions and gut dissections were mentioned in relevant research article [5]. Before analysis, the guts were dissected from beetles of different life stages for further analysis.

2.1. Ultra-high-performance liquid chromatography- electrospray ionization -high resolution tandem mass spectrometry (UHPLC-ESI-HRMS/MS) analysis

Gut tissue was dissected (5 guts /sample) and collected in ethyl acetate (5 µl/gut) for storage at −80 °C before analysis. Gut extracts (solvent without gut) were removed for the nonpolar fraction. For polar extraction, rest of the solvent was removed by a gentle stream of nitrogen, and the remaining tissue was extracted (7 ml/gut) with MeOH/water/acetic acid (70/30/0.5 v/v) mixture containing $^{13}C_2$-myristic acid (1 µg/ml) standard. After sonication on ice (5 min) the tissue was disrupted with a pre-chilled Eppendorf tip and sonicated for an additional 5 min. The samples were then centrifuged at 4000 RPM for 3 min and the supernatant was collected in a new vial with 100 µl glass insert. Gut extracts with nonpolar and polar fractions were used for UHPLC−HRMS/MS analysis [5].

UHPLC-ESI-HRMS/MS was performed at Ultimate 3000 series RSLC (Dionex) coupled with Q-Exactive HF-X mass spectrometer (Thermo Fisher Scientific, Waltham, USA). Water (solvent A) and acetonitrile (solvent B, LiChrosolv hyper grade for LC-MS; Merck, Darmstadt, Germany), both with 0.1% (v/v) formic acid (Eluent for LC-MS, Sigma Aldrich, Steinheim, Germany), were used for the binary solvent system. After injection of 10 µl extract, chromatographic separation was performed with a constant flow rate of 300 µl/min using an Acclaim C18 column (150 × 2.1 mm, 2.2 µm; Dionex, Borgenteich, Germany). Solvent gradients (B 0.5–100% v/v for 15 min; 100% B for 5 min; 100–0.5% v/v for 0.1 min; 0.5% for 5 min) were used. Ionization in HESI ion source was achieved by 4.2 kV cone voltage, 35 V capillary voltage, and 300 °C capillary temperature in the transfer tube in positive ion mode and 3.3 kV cone voltage, 35 V capillary voltage, and 320 °C capillary temperature in negative mode. Mass spectra were recorded in the positive and negative ion mode at *m/z* 80–800 mass range in duplicate. Date-dependent acquisition using TOP5 routine was used with one survey scan mass resolution 60,000 (HWFM), and 5 CID scans with 7500 resolution in ca 0.3 s. Colision-induced dissociation (hcd) of quadrupole selected precursor (0.8 Da mass window) was done in a collision cell at typically normalised fragmentation energy 30 eV. For identification pairs of the accurate mass of ions and their collision-induced ionization fragments with the retention time values were interpreted using software XCALIBUR (Thermo Fisher Scientific, Waltham, USA).

To identify metabolites, samples were compared and statistically evaluated using the software MetaboAnalyst 5.0 [3,8], and determined masses were compared with the database. The high-resolution LC-MS raw spectra were first centroided by converting them to mzXML format using the MS Convert feature of ProteoWizard 3.0.18324. Data processing was subsequently carried out with R Studio v1.1.463 using the Bioconductor XCMS package v 3.4.2 [1,9,10], which contains algorithms for peak detection, peak deconvolution, peak alignment, and gap filling. The resulting peak list was uploaded into MetaboAnalyst 5.0 [3,8], a web-based tool for metabolomics data processing, statistical analysis, and functional interpretation where statistical analysis and modeling were performed. Missing values were replaced using a (K-nearest neighbor) KNN missing value estimation. Data filtering was implemented by detecting and removing non-informative variables characterized by near-constant values throughout the experimental conditions by comparing their robust estimate interquartile ranges (IQR). Data was auto-scaled out of the 3020 mass features originally detected, using the Principal Least Square Discriminant Analysis PLS-DA [4].

To identify candidate metabolites, the individual mass features that contributed to the separation between the different classes were further characterized by applying a range of univariate and multivariate statistical tests to determine their importance including the PLS-DA importance variables, *t*-test, and Random Forest. This information, along with retention time, accurate mass, and MS/MS spectra were used to probe into existing literature and databases. MS/MS spectra files were also centroided and imported into GNPS [11] for spectral matches and classical molecular networking. The obtained database hits were manually evaluated. First, we looked for the quality of mass spectral peak matching, and later, we considered only reasonable hits. The hits related to contaminations were determined at this stage and are labeled in black. Obtained hits were collected in Table 1 and colored depending on the biosynthetic class of described compounds.

2.2. Differential gene expression (DGE) analysis

2.2.1. RNA sequencing (RNA seq.) analysis

Dissected gut tissues were put in RNA*later* solution (10 µl/gut) and 10 guts per biological sample were used. RNA extraction was performed using the pre-optimized protocol [6,5]. The quality and quantity of the extracted RNA were evaluated using agarose gel and Qubit, respectively. Integrity was determined using the 2100 Bioanalyzer system (Agilent Technologies, Inc). Better quality RNA samples (RIN $>$ 7) were sent for sequencing (150 bp paired-end reads, minimum 30 mil. reads per sample) to Novo-gene sequencing company, China [5].

Quantification of gene expression from the RNA sequence data was performed using CLC workbench was used to standardize by pre-optimized setting for mapping exon regions exclusively with genome reference. The biases in the sequences datasets and different transcript sizes were corrected using the TPM algorithm to obtain correct estimates for relative expression levels. Finally, Empirical analysis of differential Gene expression (DGE) was performed using the recommended parameters [6,7]. For DGE, FDR corrected p-value cut off $<$ 0.05 and fold change cut off of $\pm$ 4 -fold as a threshold value for being significant. Differentially expressed genes were functionally annotated using the "cloud blast" feature within the "Blasto2GO plugin" in CLC Genomic Workbench. Nucleotide blast was done against the arthropod database with an E-value cut off 1.0E-10. Both, annex and GO slim was used to improve the GO term identification further by crossing the three GO categories (biological process, molecular function, and cellular component) to search for name similarities, GO term, and enzyme relationships within KEGG (Kyoto Encyclopedia of Genes and Genomes) pathway database [5].

2.2.2. Quantitative real-time-PCR (qRT-PCR) analysis

qRT-PCR was used to validate the list of selected genes. Primers were designed using IDT's primer design software as given in Tables 3 and 4. cDNA for RT-qPCR was synthesized using RNA from respective gut tissue samples. cDNA was synthesized using an M-MLV reverse transcriptase

Table 3
Primers designed for mevalonate pathway gene family in IDT primer quest designing tool with primer length of 18–25 bp Tm-55–65, GC-50–60%, Amplicon size:100–150 bp. Modified from Table S2 of relative research article [5].

S.no.	Contig numbers.	Gene names	Primer sequence	Length	Tm	GC%	Amplicon
1	Itryp00111	GGT-F	GGAACACCCAGTTGTCTCTA	20	60.932	50	
		GGT-R	GACTGGCTGCTGTCTTTG	18	60.369	55.556	128
2	Itryp09272	FPPS- F	GGGAACGGACATTCAAGAC	19	60.183	52.632	
		FPPS- R	GTTCTGACCTGCCGTAATG	19	60.199	52.632	110
3	Itryp14703	IDLDH -F	ATCCTCTCCTTGACCTATCC	20	59.8	50	
		IDLDH -R	ATCGGAGTGTCGCAGATA	18	59.862	50	92

Table 4
Primers designed for selected nine CyP450 gene families (C1-C9). IDT primer quest designing tool was used with primer length of 18–25 bp Tm-55–65, GC-50–60%, Amplicon size:100–150 bp. Modified from Table S3 from relative research article [5].

Label	Primer names with contig numbers.	Primer sequence	Length	Tm	GC%	Amplicon
C5	qcyp_1834-F	CCTTTCCTTGATCGACTCTG	20	59.722	50	
	qcyp_1834-R	CCCTGTGGAACGGATAAAC	19	59.951	52.632	121
C6	qcyp_3146-F	GAAAGTGGCCTCCTGTTG	18	60.111	55.556	
	qcyp_3146-R	CATGTCGCCCACGTTAAG	18	60.393	55.556	107
C7	qcyp_3153-F	GTGAGCGTTGGAAGGAAA	18	59.858	50	
	qcyp_3153-R	CACTTCTGTTGGTCCGTTAG	20	60.152	50	140
C8	qcyp_4140-F	CTGAAGTGCCCGAAGAAC	18	60.047	55.556	
	qcyp_4140-R	CATCAACATCCAGGTCATCC	20	60.179	50	123
C9	qcyp_4142-F	AACCGCAATGGGTGTAAG	18	59.999	50	
	qcyp_4142-R	GAGGATGTCTGGATAGAGGTAG	22	60.322	50	127

kit following the manufacturer protocol. Resulted in cDNA samples were diluted up to 1:4 with nuclease-free water, and qRT-PCR was performed using SYBR™ Green PCR master mix (Applied Biosystems, USA) under the following parameters: 95 °C for 3 min, 40 cycles of 95 °C for 3 s, 60 °C for 34 s [2,7,5]. Melt curves were generated to ensure single product amplification. The expression levels of the target genes were calculated using the 2-ΔΔCt method with optimized two housekeeping genes as a reference for normalization with four biological replications.

Ethics Statement

We have performed all beetle experiments comply with the ARRIVE guidelines and are being carried out in accordance with the U.K. Animals (Scientific Procedures) Act, 1986 and associated guidelines, EU Directive 2010/63/EU for animal experiments, or the National Institutes of Health guide for the care and use of laboratory animals (NIH Publications No. 8023, revised 1978).

Declaration of Competing Interest

None.

CRediT Author Statement

Rajarajan Ramakrishnan: Formal analysis, Writing – original draft; **Amit Roy:** Formal analysis, Writing – review & editing; **Marco Kai:** Formal analysis; **Aleš Svatoš:** Formal analysis, Writing – review & editing; **Anna Jirošová:** Formal analysis, Supervision, Writing – review & editing.

Acknowledgments

The project is funded by the Ministry of Education, Youth and Sport, Operational Programme Research, Development and Education "EXTEMIT-K," No. CZ.02.1.01/0.0/0.0/15_003/0000433 and Internal Grant commission (IGA A_20_02, RAJARAJAN RAMAKRISHNAN) at the Faculty of Forestry and Wood Sciences, Czech University of Life sciences, Prague, Czech Republic.

References

[1] H.P. Benton, E.J. Want, T.M.D. Ebbels, Correction of mass calibration gaps in liquid chromatography-mass spectrometry metabolomics data, Bioinformatics 26 (2010) 2488–2489, doi:10.1093/bioinformatics/btq441.
[2] C.H. Cheng, J.D. Wickham, L. Chen, D.D. Xu, M. Lu, J.H. Sun, Bacterial microbiota protect an invasive bark beetle from a pine defensive compound, Microbiome 6 (2018) 132, doi:10.1186/s40168-018-0518-0.
[3] J. Chong, O. Soufan, C. Li, I. Caraus, S.Z. Li, G. Bourque, D.S. Wishart, J.G. Xia, MetaboAnalyst 4.0: towards more transparent and integrative metabolomics analysis, Nucleic Acids Res. 46 (2018) W486–W494, doi:10.1093/nar/gky310.
[4] R.C. Menezes, B. Piechulla, D. Warber, A. Svatoš, M. Kai, Metabolic profiling of rhizobacteria serratia plymuthica and bacillus subtilis revealed intra- and interspecific differences and elicitation of plipastatins and short peptides due to co-cultivation, Front. Microbiol. 12 (2021) 685224, doi:10.3389/fmicb.2021.685224.
[5] R. Ramakrishnan, J. Hradecký, A. Roy, B. Kalinová, C.R. Mendezes, J. Synek, J. Bláha, A. Svatoš, A. Jirošová, Metabolomics and transcriptomics of pheromone biosynthesis in an aggressive forest pest *Ips typographus*, Insect Biochem. Mol. Biol. (2022) 0965–1748, doi:10.1016/j.ibmb.2021.103680.
[6] A. Roy, S. George, S.R. Palli, Multiple functions of CREB-binding protein during postembryonic development: identification of target genes, BMC Genom. 18 (2017) 996, doi:10.1186/s12864-017-4373-3.
[7] A. Roy, S.R. Palli, Epigenetic modifications acetylation and deacetylation play important roles in juvenile hormone action, BMC Genom. 19 (2018) 934, doi:10.1186/s12864-018-5323-4.
[8] Z. Pang, J. Chong, G. Zhou, D. Morais, L. Chang, M. Barrette, C. Gauthier, P.E. Jacques, S. Li, J. Xia, MetaboAnalyst 5.0: narrowing the gap between raw spectra and functional insights, Nucleic Acids Res. 49 (2021) W388–W396, doi:10.1093/nar/gkab382.
[9] C.A. Smith, E.J. Want, G. O'Maille, R. Abagyan, G. Siuzdak, XCMS: processing mass spectrometry data for metabolite profiling using nonlinear peak alignment, matching, and identification, Anal. Chem. 78 (2006) 779–787, doi:10.1021/ac051437y.
[10] R. Tautenhahn, C. Böttcher, S. Neumann, Highly sensitive feature detection for high resolution LC/MS, BMC Bioinform. 9 (2008) 504, doi:10.1186/1471-2105-9-504.
[11] M. Wang, J. Carver, V. Phelan, et al., Sharing and community curation of mass spectrometry data with global natural products social molecular networking, Nat. Biotechnol. 34 (2016) 828–837, doi:10.1038/nbt.3597.

4.3 Publication 3:

Juvenile hormone III induction reveals key genes in general metabolism, pheromone biosynthesis, and detoxification in Eurasian spruce bark beetle.

Citation: Ramakrishnan R, Roy A, Hradecký J, Kai M, Harant K, Svatoš A and Jirošová A (2024) Juvenile hormone III induction reveals key genes in general metabolism, pheromone biosynthesis, and detoxification in Eurasian spruce bark beetle. Front. For. Glob. Change. 6:1215813. http://doi.org/10.3389/ffgc.2023.1215813

Summary:

In publication 3, we checked hypothesis 2 by **screening the changes in genetic-level, protein level, and metabolite level by application of Juvenile hormone III on the beetle, *Ips typographus***. With the multi-omic approach, the focus was on the induced changes that correlate with the requirements of adult beetles to aggregate pheromone biosynthesis. These changes are expected to occur in a sex-specific fashion. Further comparison analysis from this study revealed certain metabolic induction in specific sexes of the beetles with reconfirmation of the key candidates from gene families, such as key gene from the mevalonate pathway, **isoprenoid-di-phosphate synthase (IPDS)**, and the **Cytochrome P450** gene candidates for justifying the first and second objectives of the hypothesis 2. The third gene family of **esterase** genes and the additional candidates from the gene family of **glycosyl hydrolases** supported the verbenyl conjugates story. Later mentioned pheromone conjugates concept in *I. typographus* is a novel finding for the *Ips* species, which was tested as the third objective.

frontiers | Frontiers in Forests and Global Change

TYPE Original Research
PUBLISHED 11 January 2024
DOI 10.3389/ffgc.2023.1215813

OPEN ACCESS

EDITED BY
Frank Chidawanyika,
International Centre of Insect Physiology and Ecology (ICIPE), Kenya

REVIEWED BY
Inusa Jacob Ajene,
International Centre of Insect Physiology and Ecology (ICIPE), Kenya
Casper Nyamukondiwa,
Botswana International University of Science and Technology, Botswana

*CORRESPONDENCE
Anna Jirošová
jirosovaa@fld.czu.cz

†These authors have contributed equally to this work

RECEIVED 02 May 2023
ACCEPTED 19 December 2023
PUBLISHED 11 January 2024

CITATION
Ramakrishnan R, Roy A, Hradecký J, Kai M, Harant K, Svatoš A and Jirošová A (2024) Juvenile hormone III induction reveals key genes in general metabolism, pheromone biosynthesis, and detoxification in Eurasian spruce bark beetle.
Front. For. Glob. Change 6:1215813.
doi: 10.3389/ffgc.2023.1215813

Juvenile hormone III induction reveals key genes in general metabolism, pheromone biosynthesis, and detoxification in Eurasian spruce bark beetle

Rajarajan Ramakrishnan[1†], Amit Roy[1], Jaromír Hradecký[1], Marco Kai[2], Karel Harant[3], Aleš Svatoš[2,4] and Anna Jirošová[1*†]

[1]Faculty of Forestry and Wood Sciences, Czech University of Life Sciences Prague, Prague, Czechia, [2]Max Planck Institute for Chemical Ecology, Jena, Germany, [3]Laboratory of Mass Spectrometry, BIOCEV, Faculty of Science Charles University in Prague, Prague, Czechia, [4]Institute of Organic Chemistry and Biochemistry, Czech Academy of Sciences, Prague, Czechia

Introduction: In recent years, bark beetle *Ips typographus*, has caused extensive damage to European Norway spruce forests through widespread outbreaks. This pest employs pheromone-assisted aggregation to overcome tree defense, resulting in mass attacks on host spruce. Many morphological and behavioral processes in *I. typographus* are under the regulation of juvenile hormone III (JH III), including the biosynthesis of aggregation pheromones and associated detoxification monoterpene conjugates.

Objectives and Methods: In this study, we topically applied juvenile hormone III (JH III) and performed metabolomics, transcriptomics, and proteomics in *I. typographus* both sexes, with focused aims; 1. Highlight the JH III-regulated metabolic processes; 2. Identify pheromone biosynthesis-linked genes; and 3. Investigate JH III's impact on detoxification conjugates linked to pheromonal components.

Results: Numerous gene families were enriched after JH III treatment, including genes associated with catalytic and oxidoreductase activity, esterases, phosphatases, and membrane transporters. Sex-specific enrichments for reproduction-related and detoxification genes in females and metabolic regulation genes in males were observed. On the protein level were enriched metal ion binding and transferase enzymes in male beetles. After JHIII treatment, mevalonate pathway genes, including terminal isoprenyl diphosphate synthase (IPDS), were exclusively 35- folds upregulated in males, providing evidence of *de novo* biosynthesis of pheromone components 2-methyl-3-buten-2-ol and ipsdienol. In addition, cytochrome P450 genes likely involved in the biosynthesis of *cis/trans*-verbenol, detoxification, and formation of ipsdienol, were 3-fold upregulated in the male gut. The increase in gene expression correlated with the heightened production of the respective metabolites. Detoxification conjugates, verbenyl oleate in the beetle fat body and verbenyl diglycosides in the gut, were induced by JHIII application, which confirms the hormone regulation of their formation. The JH III induction also increased the gene contigs esterase and glycosyl hydrolase up to proteins from male gut tissue. The esterase was proposed to release pheromone *cis*-verbenol in adult males by breaking down verbenyl oleate. The correlating analyses confirmed a reduction in the abundance of verbenyl oleate in the induced male beetle.

Conclusion: The data provide evidence of JH III's regulatory role in the expression of genes and enzymes related to fundamental beetle metabolism, pheromone biosynthesis, and detoxification in *Ips typographus*.

KEYWORDS

Ips typographus, juvenile hormone III, hormonal regulation, mevalonate pathway, CyP450, esterase, monoterpenyl diglycosides, isoprenyl di phosphate synthase

1 Introduction

The Eurasian Spruce Bark Beetle (*Ips typographus*, Coleoptera: Curculionidae) is a pest that severely affects Norway spruce (*Picea abies*) survival across Eurasia (Ward et al., 2022). In recent years, changing climate patterns resulting in extended periods of drought, along with human-induced factors such as establishing monoculture spruce tree plantations, have played a role in exacerbating its outbreaks (Hlasny et al., 2021). In the Czech Republic, from 2018 till 2022, over 50 million m^3 of spruce forest have been recorded with bark beetle-infested wood (Knizek et al., 2023). In Europe as a whole, *I. typographus* has killed twice as many trees in the past decade, approximately 70.1 million m^3 of timber, nearly all of it Norway spruce (Patacca et al., 2023).

In the class Insecta, many morphological and behavioral changes, such as body development, reproduction, parental care, mating behavior, molt and growth, diapause, and many other functions are hormonally regulated (Jindra et al., 2013; Smykal et al., 2014). The two most important classes of insect hormones are ecdysteroids and juvenile hormones (Pandey and Bloch, 2015). In Coleoptera pheromone biosynthesis concepts, juvenile hormone III (JH III) is the most studied (Keeling et al., 2016). The primary function of these hormones is to maintain juvenile characteristics and prevent premature metamorphosis (Goodman and Cusson, 2012). JH III is synthesized in the exocrine gland corpus allatum and transported through the hemolymph by binding proteins to its target receptors (Jindra and Bittova, 2020). JH III has been extensively used to study many gene families involved in insect growth and metamorphosis, along with social behavior (Riddiford et al., 2010; Trumbo, 2018).

First instar insect larvae initially contain a high titer of JH III, which is subsequently reduced as, the larvae undergo metamorphosis into pupae (Treiblmayr et al., 2006). In the pre-metamorphic stages, JH III has been studied for its influence on the development of larval muscles and the prothoracic glands producing ecdysteroids, as well as its role in restructuring gut development, fat body, and epidermis in various insect species (Riddiford et al., 2001; Riddiford, 2012; Jindra et al., 2013). In the adult insects, JH III influences various aspects, including pheromone production (Tillman et al., 2004) and social behavior (Trumbo, 2018), caste determination (Cristino et al., 2006); aggression and display (Emlen et al., 2006), migration (Zhu et al., 2009), and neuronal remodeling (Leinwand and Scott, 2021).

In bark beetles, JH III effects have primarily been studied in relation to pheromone biosynthesis induction. When the beetles bore into the host tree, JH III is released from the endocrine gland, initiating a series of hormonal signaling processes that lead to the production of aggregation pheromone components in male beetles (Bakke et al., 1977; Schlyter et al., 1987). In nature, this potent blend attracts conspecifics, both males and females, to mass attack to help overcome tree defense. In controlled laboratory conditions, pheromone biosynthesis induction can be achieved by topically applying JH III on the beetle abdomen (Byers and Birgersson, 1990; Ivarsson et al., 1993; Seybold et al., 1995; Tillman et al., 1998). This method triggers the *de novo* synthesis of pheromone compounds while avoiding potential interference with the metabolic pathways involved in the digestion of ingested phloem tissues. Pheromone induction using JH III has been demonstrated in bark beetles such as *Ips pini*, *Dendroctonus ponderosae*, and *Ips typographus* (Nardi et al., 2002; Tillman et al., 2004; Zhang et al., 2017; Fang et al., 2021a,b; Ramakrishnan et al., 2022a). However, certain *Ips* species such as *I. confusus* and *Ips grandicollis*, have been reported to be unresponsive to JH III-induced pheromone induction (Tillman et al., 2004; Bearfield et al., 2009).

The molecular-level effects of JH III on pheromone biosynthesis have been subsequently investigated in various species, including *Ips paraconfusus* (Ivarsson and Birgersson, 1995), *Ips pini* (Tillman et al., 1998; Blomquist et al., 2010), and *Dendroctonus ponderosae* (Keeling et al., 2016). JH III induction has been found to activate multiple gene families responsible for pheromone biosynthesis, especially in the mevalonate pathway (Sarabia et al., 2019).

In *I. typographus*, male pioneer beetles produce aggregation pheromone blends made up of several terpenoid compounds 2-methyl-3-buten-2-ol, *cis*-verbenol and minor amount of ipsdienol, after successfully boring into the tree bark. Both 2-methyl-3-buten-2-ol and ipsdienol are synthesized in beetle guts through the mevalonate pathway (Figure 1; Ramakrishnan et al., 2022a). In the context of bark beetle pheromone biosynthesis, previous studies have identified key enzymes in the pathway (Tillman et al., 1998). The pathway involves the condensation of acetoacetyl-CoA with acetyl-CoA catalyzed by *3-hydroxy-3-methyl glutaryl coenzyme-A synthase* (HMG-S), followed by a reduction of hydroxymethyl glutaryl-CoA to mevalonate, catalyzed by *3-hydroxy-3-methyl glutaryl coenzyme-A reductase* (HMG-R). Later, the mevalonate is phosphorylated by *phosphomevalonate kinase* (PMK), followed by several steps of modification to form the isoprenoid biosynthetic units, isopentenyl diphosphate and dimethyl allyl diphosphate (Buhaescu and Izzedine, 2007). Condensation of two isoprenoid units catalyzed by *geranyl diphosphate synthase* (GPPS) synthesizes geranyl diphosphate, the precursor of bark beetle monoterpenoid pheromones, such as myrcene and ipsdienol (Gilg et al., 2005; Keeling et al., 2006; Bearfield et al., 2009; Ramakrishnan et al., 2022a). In *I. typographus*, a gene was recently reported that likely encodes an *isoprenyl-diphosphate synthase* (IPDS) responsible for converting dimethylallyl diphosphate into 2-methyl-3-buten-2-ol, a transformation unique in insects (Ramakrishnan et al., 2022a). Ipsdienol biosynthesis also involves the oxidation of myrcene catalyzed by the cytochrome P450 enzyme CyP450T1/T2 (Sandstrom et al., 2006).

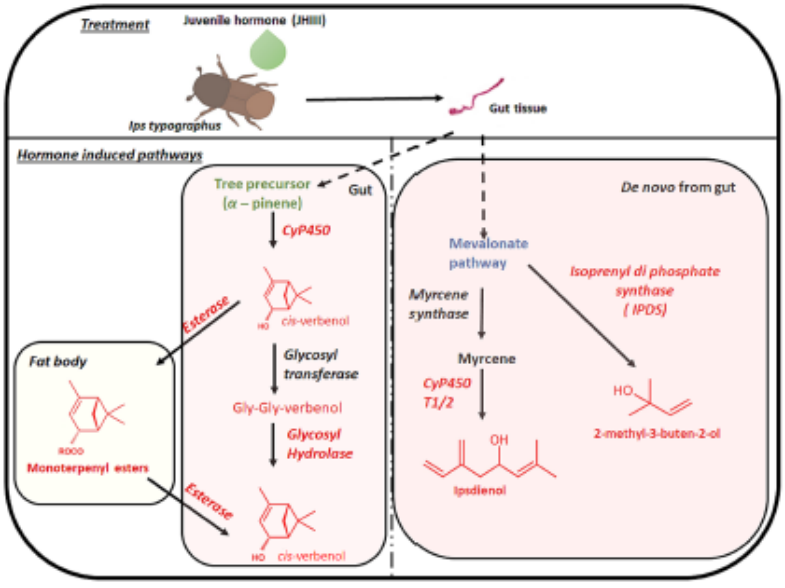

FIGURE 1
Proposed pheromone biosynthesis pathway with relative gene families from gut tissue and fat body of *Ips typographus* after topical application of JHIII. Red colour font highlights the pheromone compounds and relative gene families that are explained in this research article.

The third pheromonal component in *I. typographus*, *cis*-verbenol, is not synthesized *de novo* but is instead produced through the CyP450 catalyzed oxidation of (−)-α-pinene that adult beetles sequester from the tree (Renwick et al., 1976; Chiu et al., 2019). Additionally, a substantial amount of *cis*-verbenol has been detected in the gut of immature beetles that develop inside the bark, which is believed to be a result of detoxification of toxic α-pinene by these juvenile beetles (Ramakrishnan et al., 2022a). As part of this detoxification process, *cis*-verbenol (along with myrtenol as another detox product) is deposited in the form of monoterpenyl fatty acid esters in the fat body (Chiu et al., 2018; Ramakrishnan et al., 2022a). These conjugates can be hydrolyzed to provide free *cis*-verbenol in adult males when a supply of this pheromonal component is needed. In *I. typographus*, a candidate gene encoding a carboxylesterase (fatty acyl transferase) for the formation of verbenyl oleate (a fatty acid ester) in juvenile beetles was proposed and another carboxylesterase with ester bond cleaving function was suggested to be present in adult males (Ramakrishnan et al., 2022a,b). Another *cis*-verbenol conjugates, created through diglycosylation, has recently been discovered in the gut tissues of *I. typographus* (Ramakrishnan et al., 2022a). Detoxification via glycosylation is a common feature in insects (Hilliou et al., 2021), with UDP-*glycosyltransferases* being commonly studied as detoxification enzymes (Dai et al., 2021; Powell et al., 2021). In *I. typographus*, *cis*-verbenyl diglycosylate has been proposed as a potential parallel reservoir for the pheromone *cis*-verbenol released by adult males, a hypothesis that aligns with early hypotheses in *D. ponderosae* (Hughes, 1974; White et al., 1980). The effect of JH III on the formation of these detoxification conjugates or cleavage into pheromone-precursors has not been studied yet.

To learn more about the effect of JH III on bark beetle metabolism, we topically applied JH III to *I. typographus* and analyzed changes at the levels of gene transcripts, proteins, and metabolites in both sexes. The primary tissue studied was the gut, the site of pheromone biosynthesis and detoxification.

We hypothesize that JH III will induce correlated changes in genes, proteins and metabolites that reflect the requirements of adult beetles to aggregate and overcome the defense of their host trees by feeding on the phloem and reproduce. These changes are expected to occur in a sex-specific fashion. We also hypothesize that JH III will induce pheromone biosynthesis and the detoxification of spruce defense metabolites, especially those involved in the formation of aggregation pheromones.

By checking the above-mentioned hypothesis, genetic-level research of the bark beetle, *I. typographus* can lead to practical implications using RNA *interference* silencing of targeted genes and influence the pheromone metabolism. The RNAi technique for Coleopteran (wood-boring) insects has proven for highly susceptible and demonstrated recently on insects such as Emerald ash borer, Asian longhorn beetles, Chinese White pine beetle and Mountain pine beetle (Rodrigues et al., 2017; Dhandapani et al., 2020; Kyre et al., 2020).

2 Materials and methods

2.1 Beetle rearing

Spruce logs (*Picea abies*) naturally infested with *I. typographus* were collected from the Czech University of Life Sciences, Forest

Enterprise in Kostelec and Černými lesy, Czech Republic. The infested logs were stored in a cold chamber (4°C) until further use. The fresh spruce logs (approximately 50 cm) were infested with F0 generation beetles (150 beetles per log) and maintained under laboratory conditions (70% humidity, 24°C, 16:8 h day/night period, and ventilated plastic containers of 56 × 39 × 28 cm/45 L volume) for incubation to establish the F1 generation. After 4 weeks of incubation, F1-generation beetles were collected and sorted for male and female beetles. Subsequently, the beetles were treated with 0.5 µL of acetone (control) or 0.5 µL of a solution of 20 µg/µl JH III in acetone (10 µg of JH III) topically on the abdomen of the beetles. After application, the beetles were kept under laboratory conditions for 8 h. Beetles were frozen in liquid nitrogen and stored at −80°C until further use. Before analysis, the guts were dissected from stored frozen beetles for further downstream analysis. In this study, the beetle body refers to the tissue with fat remaining after removing the gut, elytra, and wings (Ramakrishnan et al., 2022a,b).

2.2 Metabolome

2.2.1 Gas chromatographic-mass spectrometry analysis

The frozen beetles were dissected to extract their guts, which were then placed in 2 mL analytical vials containing 100 µL of cold pentane (10 guts per vial). The beetle bodies were placed in separate vials containing 1 mL of chloroform (10 beetle bodies per vial). The extracts are obtained after overnight incubation at 4°C and tissue free solvents were separated using a short centrifuge (4,000 rpm,30s) and used for injection.

A Pegasus 4D GC × GC–MS system (LECO, St. Joseph, MI, USA) employing an Agilent 7,890 B and a consumable-free modulator was used to analyze the samples. One microliter of the extract was injected into a cold PTV injector (20C) in split mode at a ratio of 1:3. After injection, the inlet was heated to 275°C at a rate of 8°C/s. Separation was conducted on an HP-5MS UI capillary column (30 m, 0.25 mm i.d., 0.25 µm film thickness, Agilent) coupled to BPX-50 (1.2 m, 0.1 mm i.d., 0.1 µm film thickness, SGE). The GC oven temperature program was as follows: 40°C for 2 min; then ramped at a rate of 10°C min^{-1} to 200°C; then at 5°C min^{-1} to 320°C and held for 15 min. The second-dimension oven modulator had offsets of 5°C and 15°C, respectively. The modulation period was 5 s. The total GC runtime was 57 min. Ions (ionization energy of 70 eV) were collected in the mass range of 35–500 Da at a frequency of 100 Hz.

Automated spectral deconvolution and peak-finding algorithms were applied using ChromaTOF software (LECO, St. Joseph, MI, USA). For identification of the compounds, the mass spectra and retention indexes from the National Institute of Standards and Technology (NIST, 2017) mass spectral customized library were used. In the case of fatty acid ester (oleate) was identified using a targeted search using mass spectra and retention indexes obtained from synthetic standards (Chiu et al., 2018) measured under same conditions as in our previous studies (Ramakrishnan et al., 2022a). Relative abundances were defined as the percentage of the peak area of the targeted metabolite in relation to the sum of peak areas of all peaks in the chromatogram.

2.2.2 Ultra-high-performance liquid chromatography-electrospray ionization -high-resolution tandem mass spectrometry analysis

The polar fraction of guts was extracted by adding methanol, water, and acetic acid in a ratio of 70/30/0.5 (v/v) at a volume of 7 mL per gut. The mixture contained ^{13}C2-myristic acid (1 µg/mL) as an internal standard. The gut tissue was sonicated on ice for 5 min and disrupted using a pre-chilled Eppendorf tip. The samples were then centrifuged at 4000 RPM for 3 min, and the supernatant collected in a new vial with a 100 µL glass insert. The polar fractions of gut extracts were subjected to UHPLC-HRMS/MS analysis.

UHPLC-ESI-HRMS/MS was performed using an Ultimate 3,000 series RSLC system (Dionex) coupled to a Q-Exactive HF-X mass spectrometer (Thermo Fisher Scientific). Solvents A-water and B-acetonitrile (LiChrosolv hyper grade for LC–MS; Merck, Darmstadt, Germany), both with 0.1% v/v formic acid (eluent for LC–MS, Sigma Aldrich, Steinheim, Germany), were used for the binary solvent system. 10 µL of the extract was injected, and chromatographic separation was performed with a constant flow rate of 300 µL/min using an Acclaim C18 column (150 × 2.1 mm, 2.2 µm; Dionex, Borgenteich, Germany). Solvent gradients (B 0.5–100% v/v for 15 min; 100% B for 5 min; 100–0.5% v/v for 0.1 min; 0.5% for 5 min) were used. Ionization in the HESI ion source was achieved by 4.2 kV cone voltage, 35 V capillary voltage, and 300°C capillary temperature in the transfer tube in positive ion mode and 3.3 kV cone voltage, 35 V capillary voltage, and 320°C capillary temperature in negative mode. Mass spectra were recorded in both modes at a mass range of m/z 80–800 in duplicate. The obtained fragments with retention time values were interpreted using XCALIBUR software (Thermo Fisher Scientific, Waltham, United States; Ramakrishnan et al., 2022a,b). Metabolite samples were compared and statistically evaluated using MetaboAnalyst 4.0, and the determined masses were compared with the database (Chong et al., 2018). The amounts of three diglycosides of oxygenated monoterpenes (verbenol) were determined with mass spectra obtained from our previous work (Ramakrishnan et al., 2022b).

2.3 Transcriptome

2.3.1 Sample preparation

The beetle guts were dissected in RNAlater. Four biological replicate included three technical replicates each containing 10 pooled guts was used. Total RNA was extracted from male gut tissue samples using a pre-optimized protocol (Sellamuthu et al., 2022) and sent for sequencing with a NOVAseq6000 (PE150, 30 million raw reads) after quality determination using an agarose gel and a bioanalyzer. RNA (1 µg) was used for cDNA synthesis using the M-MLV reverse transcriptase kit following the manufacturer's protocol and stored at −80°C for downstream analysis.

2.3.2 Differential gene expression analysis

RNA-seq. Data were analyzed using CLC workbench 21.0.5 (QIAGEN Aarhus, Denmark) with a pre-optimized setting for mapping exon regions with genome reference (Naseer et al., 2023). Furthermore, sequence datasets and relative transcript expression levels were obtained using TPM values. Finally, an empirical DGE analysis was performed using the optimum parameters

(Ramakrishnan et al., 2022a). Genes with a false discovery rate (FDR)-corrected value of p cut-off of <0.05 and a fold change cut-off of ± four-fold as a threshold value for being significant. Differentially expressed genes were functionally searched in a cloud BLAST using the CLC Genomic Workbench. Gene Ontology term identification was performed using three categories (biological processes, molecular functions, and cellular components), and similar names were identified from the Kyoto Encyclopedia of Genes and Genomes pathway database (Kanehisa, 2002; Kanehisa et al., 2017).

2.3.3 Quantitative-real time PCR analysis

To validate the RNA seq. Data, genes were selected for qRT-PCR based on their varied expression levels. Primers were designed using IDT primer design software (Supplementary Table 4). A synthesized cDNA template was used for qRT-PCR validation using SYBR™ Green PCR master mix (Applied Biosystems, United States) under the following parameters: 95°C for 3 min, 40 cycles of 95°C for 3 s, and 60°C for 34 s. A melting curve was generated to ensure single-product amplification and eliminate the possibility of primer dimers and nonspecific amplicons. The relative expression levels of the target genes were calculated using the $2^{-\Delta\Delta Ct}$ method with two housekeeping genes (Sellamuthu et al., 2022) as a reference for normalization with four biological replications.

2.4 Proteome

2.4.1 Sample preparation

Frozen beetles were dissected under on dry ice, and four biological replicates of each treatment were used for protein extraction and analysis. Each biological replicate contained tissue of three individual guts. Protein extraction was lysed in cold buffer containing 50 mm Tris–HCl, pH 7.5, 1 mM EDTA, 150 mM NaCl, 1% N-octylglycoside, and 0.1% sodium deoxycholate. Gut tissue in the buffer with protease inhibitor mixture (Roche) was incubated for 15 min on ice. Lysates were cleared by centrifugation, and after precipitation with chloroform/methanol, proteins were resuspended in 6 m urea, 2 m thiourea, 10 mm HEPES, pH 8.0 and proceeded for digestion (Cox et al., 2014).

2.4.2 Protein digestion

The samples were homogenized and lysed by boiling at 95°C for 10 min in 100 mM TEAB (triethylammonium bicarbonate) containing 2% SDC (sodium deoxycholate), 40 mM chloroacetamide, and 10 mM Tris (2-carboxyethyl) phosphine, and further sonicated (Bandelin Sonoplus Mini 20, MS 1.5). The protein concentration was determined using a standard protein assay kit (Thermo Fisher Scientific). About 30 µg of protein per sample was used for MS sample preparation.

SP3 beads were used for sample processing. Five µl of SP3 beads were mixed with 30 µg protein in a lysis buffer and made up to 50 µL with TEAB (100 mM). Protein binding was induced by adding ethanol to a final concentration of 60% (vol/vol). The samples were thoroughly mixed and incubated at 24°C for 5 min. After SP3 was bound to the proteins, the tubes were placed on a magnetic rack, and the remaining unbound supernatant was discarded. Using 180 µL of 80% ethanol, beads were washed twice. After washing, samples were digested with trypsin (trypsin/protein ratio 1/30) and reconstituted in 100 mM TEAB at 37°C overnight. Digested samples were acidified with trifluoro acetic acid (TFA) to a final concentration of 1%. Finally, peptides were desalted using in-house stage tips packed with C18 disks (Empore; Rappsilber et al., 2007).

2.4.3 Nanoliquid chromatography-MS/MS analysis

nLC–MS/MS analysis was performed with nano-reversed-phase columns (EASY-Spray column, 50 cm × 75 µm ID, PepMap C18, 2 µm particles, 100 µm pore size). In this analysis, mobile phase buffer A (0.1% formic acid in water) and mobile phase buffer B (acetonitrile and 0.1% formic acid) were used. Samples were loaded in a trap column of C18 PepMap100, 5 µm particle size, 300 µm x 5 mm from Thermo Scientific. About 4 min at 18 µL/min loading buffer with water, 2% acetonitrile, and 0.1% trifluoroacetic acid were used for loading. Peptides were eluted with a mobile phase B gradient of 4–35% over 120 min. The eluted peptide cations were converted into gas-phase ions by electrospray ionization. A Thermo Orbitrap Fusion (Q-OT-qIT, Thermo Scientific) was used for the analysis. Survey scans of peptide precursors from 350 to 1,400 m/z were performed using an Orbitrap at 120 K resolution (200 m/z) with a 5×10^5 ion count target. Tandem MS was isolated at 1,5 Th using a quadrupole, HCD fragmentation with a normalized collision energy of 30, and rapid scan analysis in the ion trap. The second mass spectral ion count target was set to 10^4, and the maximum injection time was 35 ms. Precursors with charge state 2–6 were strictly sampled. The dynamic exclusion duration was set to 30 s with a 10 ppm tolerance around the selected precursor and its isotopes. Monoisotopic precursor selection was then performed. The instrument was run in top-speed mode with 2 s cycles (Hebert et al., 2014).

All data were analyzed and quantified using MaxQuant software (version 2.0.2.0; Cox and Mann, 2008). The FDR was limited to 1% for both full proteins and small peptides. The peptide lengths of the seven amino acids are specified. An MS/MS spectral search was performed using the Andromeda search engine against the *I. typographus* genome database. The C-termini of Arg and Lys were set for enzyme specificity, allowing the cleavage of proline bonds with a maximum of two missed cleavages. Cysteine dithiomethylation was selected as the fixed modification. Various modifications were considered with N-N-terminal protein acetylation and methionine oxidation. Matches between the run features from MaxQuant were used to transfer the identified peaks to other LC–MS/MS systems. Runs based on masses and retention times (with a maximum deviation of 0.7 min) were also considered for quantification. A label-free MaxQuant algorithm was used for quantification (Cox et al., 2014). Data analysis was performed using Perseus 1.6.15.0 (Tyanova et al., 2016).

2.5 Statistics

LC–MS data analysis was performed using MetaboAnalyst 4.0. GCxGC-TOF-MS data were cleaned for residua of analysis, normalized (constant raw sum), and evaluated using principal component analysis (PCA) in the SIMCA 17 software (Sartorius Stedim Data Analytics AB, Malmö, Sweden). T-test with 95% confidence interval was used to compare the abundance of control and treatment groups in TIBCO Statistics (United States, 2021). The data from transcriptome and proteome was normalized using CLC workbench 21.0.5 (QIAGEN Aarhus, Denmark) and MaxQuant software (version 2.0.2.0) respectively, and significant data ($p < 0.05$) were extracted for further

analysis. qRT-data was analyzed with one-way ANOVA, Fisher LSD test in TIBCO Statistics (United States, 2021).

3 Results

3.1 Total gene enrichment analysis from guts of males and females after JH III topical treatment

The functional aspects of JH III influenced gene families from adult males and females were gained by a gene enrichment analysis. The data gained from differential gene expression (DGE) with significance (FDR-corrected value of $p < 0.05$).

In males, the analysis revealed that a significant number of enriched genes were involved in metabolic processes. Additionally, functions such as catalytic activity, ester hydrolase, phosphatase activity, transporter and glycosyltransferase activities were also determined to be over-represented after JH III treatment by enrichment analysis. Gene functions related to lyase activity, small-molecule metabolic processes, carbohydrate metabolic processes, and lipid biosynthesis were also over-represented. Most importantly, we found that gene groups involved in pheromone biosynthesis functions, including isoprenoid biosynthesis, metabolic processes, and dephosphorylation were enriched. Gene functions related to oxidoreductase and alkaline phosphatase activity had the least coverage in terms of gene sequences (Figure 2A).

In female gut tissue, the GEA showed enrichment of membrane-related and membrane transporter activity-related genes rather than metabolic synthesis genes as in males. Several gene groups with functions related to detoxification, such as carboxylic acid transmembrane transporter, organic acid membrane transporter, amino acid transporter, alkaline phosphate activity, phosphatase activity, and protein dephosphorylation were identified as enriched. Genes responsible for oxidoreductase and catalytic activities, phosphoric ester hydrolase activity, phosphatase, and lipid metabolism process had higher sequence coverage in females than males. Furthermore, metal ion binding genes such as zinc ion binding and, carbohydrate metabolic process gene families were identified exclusively in female gut tissue. The gene groups for lyase activity and hydrolase activity were enriched in females as in males and many unknown genes were clustered under the "others" category "(Figure 2B). Taken together,

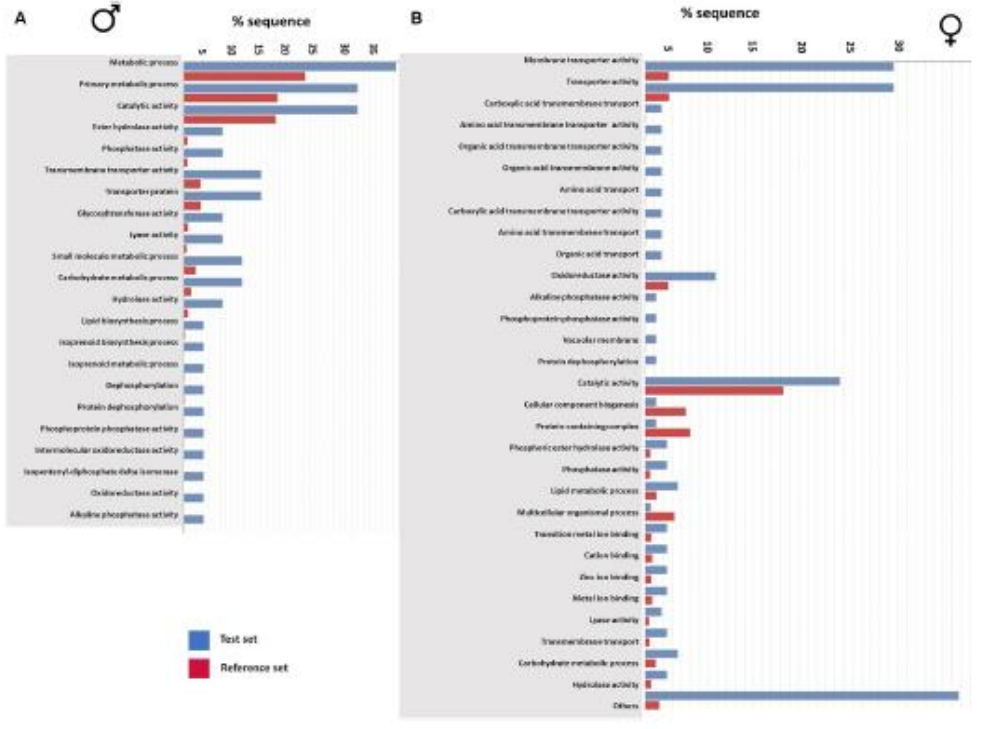

FIGURE 2
Gene enrichment analysis of transcripts from male gut tissue (A) and female gut tissue (B) after JHIII treatment. The data set were given as a test set (blue) to reference set (red) gene families known from reference websites as Gene Ontology. The possible functions of the genes were listed against the percentage of sequence coverage.

the gene enrichment analysis provided valuable insights into the over-representation of genes in males and females after JH III treatment.

3.2 Total protein enrichment analysis from guts of males and females after JH III topical treatment

The list of detected proteins was organized based on functional relevance. In the male gut tissue after JH III treatment, the identified proteins clustered into 456 known functions, while in the treated female gut formed 489 functional groups. Of these, 347 groups were common to both male-treated and female-treated gut samples. Similar to gene enrichment analysis, both sexes exhibited the highest numbers of plasma membrane-associated proteins (Supplementary Table 5).

The functional groups identified in male and female guts after JH III treatment were largely similar. Proteins related to the nucleus and nucleolus, ATP and RNA binding proteins were enriched in both sexes. However, in males, the number of proteins with functions related to metal ion binding and transferase activity was higher compared to females (Figure 3A). Whereas, in the female gut, the reproduction-related embryo development proteins were higher protein numbers (Figure 3B; Supplementary Table 5). Nevertheless, the differences between male and female guts after JH III treatment were minor in terms of gene transcripts and protein enrichments.

3.3 Metabolome

3.3.1 GC–MS analysis of extracts from guts and bodies of males and females after JH III topical treatment

Extracts of the guts and bodies of male and female *I. typographus* beetles subjected to JHIII treatment, were compared to their respective control groups, using comprehensive two-dimensional gas chromatography.

The initial Principal Component Analysis (PCA) revealed a distinct separation of JH III treated male gut samples from control samples treated with acetone. The first two components of the PCA plot accounted for 46.5% of the variance in the data (see Figure 4A). The primary compound responsible for this separation was identified as the main *I. typographus* aggregation pheromone component, 2-methyl-3-buten-2-ol. Additionally, compounds such as *cis*-verbenol and phenylethanol (male-specific compound) also contributed to this separation. In contrast, control male guts contained only phenylethanol and trace amounts of *cis*-verbenol, along with traces of other compounds such as verbenone, ipsdienol, and myrtenol (refer to Supplementary Figure 1).

The relative abundance of the pheromone precursor verbenyl oleate was determined in extracts from both the guts and the bodies (including the fat body) of beetles following JH III treatment and compared to a control (see Figure 4B). In both male and female beetle body extracts, JH III topical treatment led to a significant increase (1.5x in males, 15x in females) in the levels of verbenyl oleate compared to the control group.

This trend was also observed in extracts from female guts (15x increase). However, in the gut extracts of male beetles, JH III treatment resulted in a significant decrease (1.8x decrease) in the relative abundance of verbenyl oleate compared to the control group. This decrease is likely attributable cleavage of these monoterpene conjugates to give the free pheromone *cis*-verbenol (refer to Figure 4B). The absolute amount of verbenyl oleate in different beetle life stadia was 250 ng/mg of beetle body weight, as previously quantified (Ramakrishnan et al., 2022a) The content of free *cis*-verbenol in the guts of freshly emerged beetle was 5 ng/gut, which can be compared with control beetles in this study.

3.3.2 UHPLC-ESI-HRMS/MS analysis of guts extracts of males and females JH III topical treatment

Metabolic profiling of non-volatile and polar compounds in the gut tissues of JH III-treated males and females was conducted using a

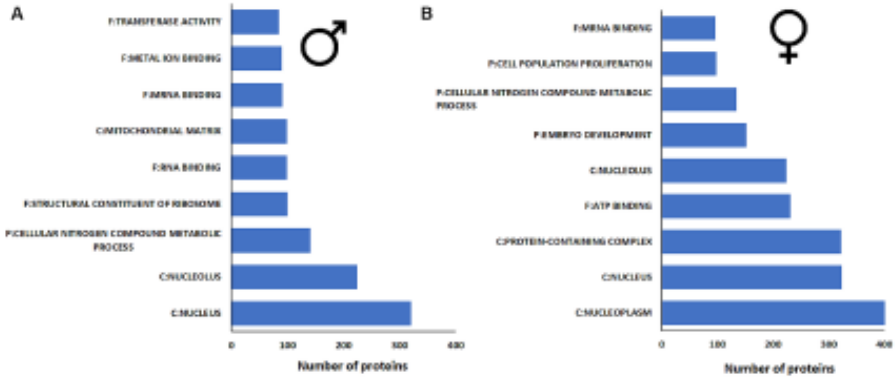

FIGURE 3
Protein enrichment analysis of proteins from (**A**) male gut tissue and (**B**) female gut tissue after JHIII treatment. The possible protein functions with significance $p < 0.05$ and functions containing more than 100 protein numbers are listed in this figure. A list of remaining functions with lower protein numbers are given in supplementary table 5.

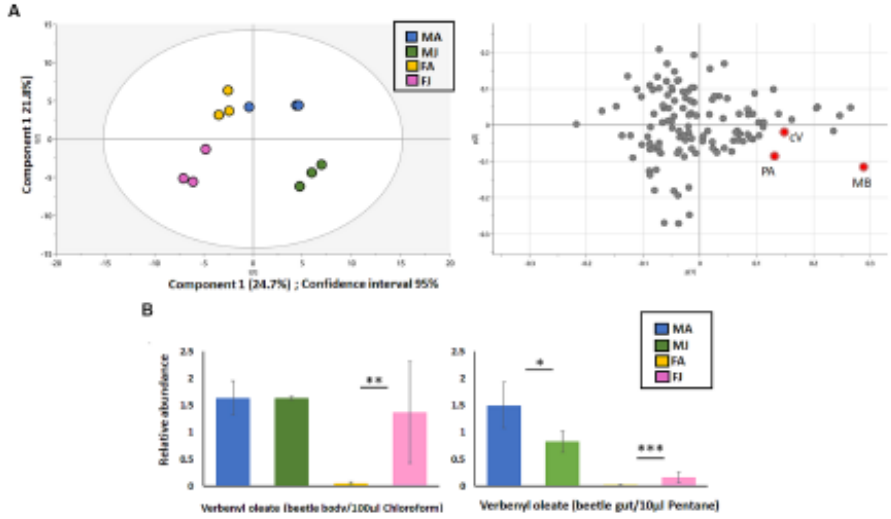

FIGURE 4
(A) Principal component analysis (PCA)of compounds identified by GCxGC-MS from *I. typographus* gut samples after JHIII induction in both sexes. The key component responsible for separation are highlighted in red color- PA- Phenylalthyl alcohol, MB- 2-methyl-3-buten-2-ol, cV-cis-verbenol. (B) Relative abundance of Verbenyl ester in *I. typographus* beetle body (left) and gut tissue (right) after JHIII induction compared to the control. MA, Males topically treated with acetone – control; MJ, Males topically treated with JHIII – treatment, FA, Females topically treated with acetone – control, FJ, Females topically treated with JHIII – treatment. Statistics: T test with paired independent parameters. *** represents $p < 0.001$, ** represents $p < 0.01$, * represents $p < 0.05$. $N = 3$.

non-targeted analysis via UHPLC/HRMS in both positive and negative ion modes. An unsupervised multivariate PCA was employed to assess differences among the sample groups.

In both ion modes measurements, JH III-treated males and females clustered distinct from the control group. In the negative ion mode, the PC analysis explained 55 and 61.2% of the total variance in males and females, respectively, (see Figure 5A, left). In the positive ion mode, the PC explained 60 and 50% of the total variance in males and females, respectively, (see Figure 5A, right). The determination of the total abundance of verbenyl diglycosides was calculated as the sum of the peak areas from the three individual verbenyl diglycoside peaks. After treatment with JH III in beetles, the total abundance of diglycosides content significantly increased in the guts of both sexes compared to the acetone-treated controls. There was no significant difference in the induction of these compounds by JH III between males and females (see Figure 5B). The actual amount of these compounds per beetle gut could not be determined due to the lack of standards.

3.4 Regulation of genes and proteins after JH III treatment in transcriptome and proteome of adult males and female beetles

3.4.1 Transcriptome-differential gene expression analysis

Overall, DGE analysis using the CLC workbench from the RNA sequence data obtained from beetle guts provided a clear distinction between gene sets in JH III-treated versus control beetles and males versus females, with samples from each group clustered together in principal component analysis (Supplementary Figure 2A). After JH III treatment, approximately 710 transcripts were upregulated, and 545 were downregulated in male gut tissue only, as depicted in a Venn diagram (Figure 6A). On the other hand, in female gut tissue only a total of 518 transcripts were upregulated, and 456 transcripts were downregulated. However, approximately 5,155 transcripts were upregulated, and 4,595 transcripts were downregulated in both male and female gut tissues. Notably, the total number of genes upregulated after treatment in the male beetle gut was higher (10,385 transcripts) than that in the female beetles (9,682 transcripts; Figure 6A; Supplementary Table 1).

3.4.2 Proteome-differential protein expression analysis

The results of the DPE analysis of JH III-treated beetle gut tissue yielded a comprehensive list of identified proteins exhibiting a significant fold change in their expression following treatment. Samples from each treatment (JH III vs. control) were clustered in principal component analysis (Supplementary Figure 2B). It is noteworthy that although JH III treatment is conventionally associated with pheromone production in adult male beetles, the female beetle gut tissue exhibited a higher number of identified proteins after treatment, 449 versus 229 in males. Among the total number of upregulated proteins, 79 were male-specific, 302 were female specific and 145 were detected in both male and female guts. Among the total number of downregulated proteins, 68 proteins male specific, 69 were

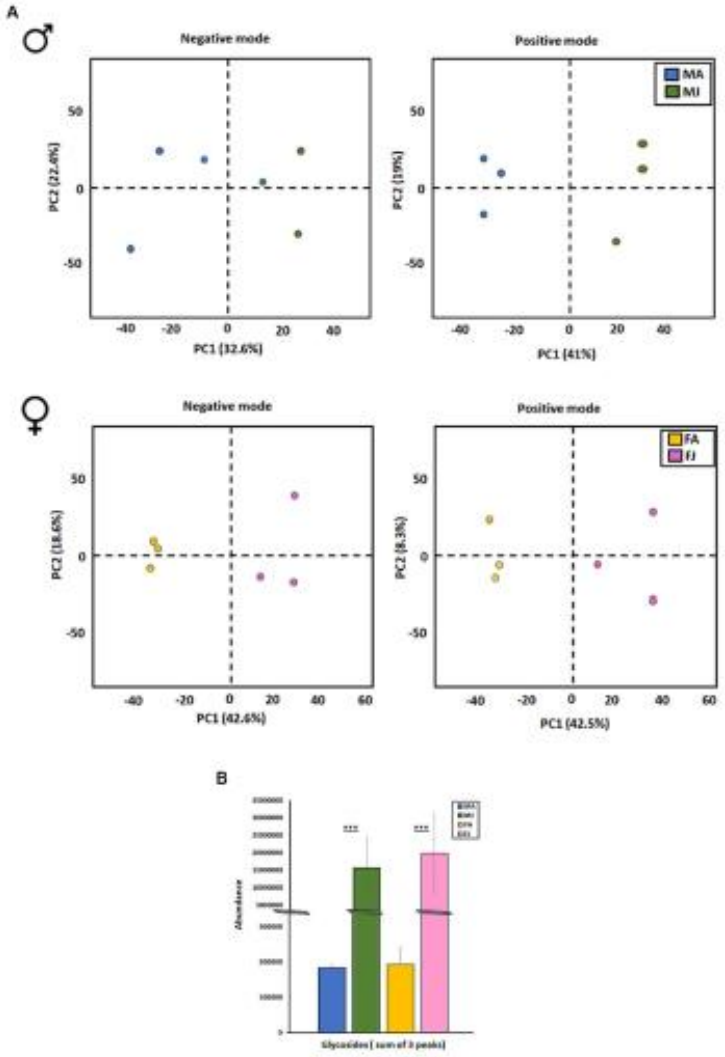

FIGURE 5
(A) Principal component analysis (PCA) of compounds identified by UHPLC-ESI-HRMS/MS analysis measured in negative (left) and positive mode (right). The data shows the overall separation of *I. typographus* gut samples after JHIII treatment in male (up) and female (down). (B) Abundance of Verbenyl di glycosides in *I. typographus* gut tissue after JHIII induction. MA, Males topically treated with acetone – control; MJ, Males topically treated with JHIII – treatment, FA, Females topically treated with acetone – control, FJ, Females topically treated with JHIII – treatment. T test with paired independent parameters. *** represents $p < 0.001$.

female specific and 27 were detected in both male and female guts (Figure 6B; Supplementary Table 2).

3.4.3 Comparison of transcriptome and proteome

To narrow down the upregulated genes from male gut tissue with possible functional significance, we compared the contig lists from the DGE and DPE analyses (Figure 6C). Although the number of identified proteins was 100-fold lower than the number of transcripts from the DGE analysis, the results of the comparison helped identify a unique set of gene contigs for further evaluation. The male gut tissue had 129 contigs from transcript and protein analysis, names are provided in Supplementary Table 3A. The key mevalonate pathway gene Ityp09271, isoprenyl-diphosphate synthase (IPDS) gene (functionally proposed for 2-methyl-3-buten-2-ol synthesis), was among the highly upregulated gene contigs. Other mevalonate pathway genes such as Ityp06045 phosphomevalonate kinase (PMK), Ityp09137,

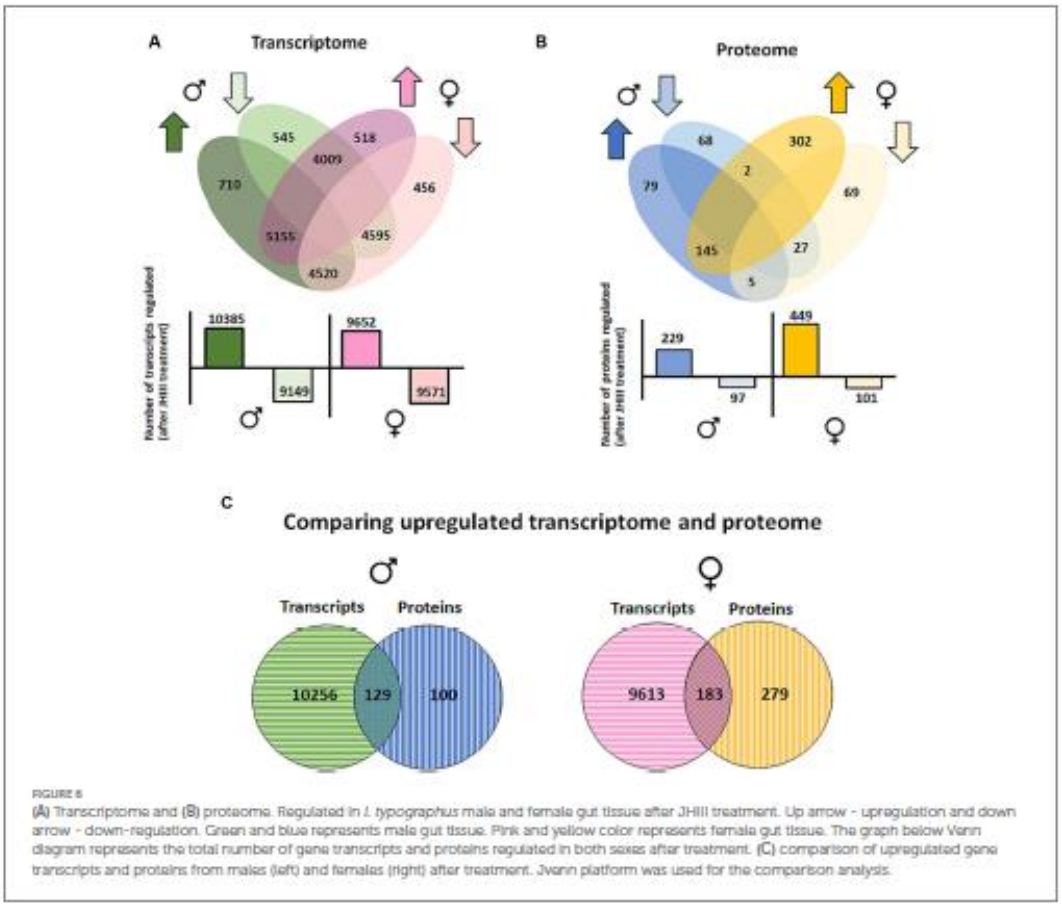

FIGURE 6
(A) Transcriptome and (B) proteome. Regulated in *I. typographus* male and female gut tissue after JHIII treatment. Up arrow - upregulation and down arrow - down-regulation. Green and blue represents male gut tissue. Pink and yellow color represents female gut tissue. The graph below Venn diagram represents the total number of gene transcripts and proteins regulated in both sexes after treatment. (C) comparison of upregulated gene transcripts and proteins from males (left) and females (right) after treatment. Jvenn platform was used for the comparison analysis.

3-hydroxy-3methyl glutaryl Co-A synthase (HMG-S), and Ityp04875, isopentenyl-di-phosphate isomerase (IPPI) were also upregulated at the gene transcript level. A similar pattern was seen for the contigs involved in hydrolase function (listed in the table as myrosinase), which are known to have a functional role for glycosyl hydrolase activity, acting on glycosyl bonds (GO:0016798), and transferase contigs, such as acetyltransferase and UDP-glucuronosyltransferase (highlighted in Supplementary Table 3A). Many ribosomal and membrane transporter contigs, such as V-type ATPases, were also upregulated, while several genes that have an unknown function were identified among the male-specific upregulated gene contigs (Supplementary Table 3A).

The female gut tissue had approximately 183 contigs from transcripts and protein analysis (Figure 6C; Supplementary Table 3B). Although the number identified in females was higher than that in males, mevalonate pathway genes were not predominant in the list of identified contigs in females. However, another geranyl-diphosphate synthase (Ityp17861) was upregulated. Furthermore, gene families, such as glycine dehydrogenase, ubiquitin carboxyl-terminal hydrolase, and vitellogenin-like, with functions likely in detoxification and oocyte formation, were found to be upregulated (Supplementary Table 3B). Similar to males, many genes related to mitochondria-related ribosomal proteins, elongation factors, binding proteins, and many functionally unknown genes and proteins were also found to be upregulated (Supplementary Table 3B).

3.4.4 Regulation of the mevalonate pathway after JH III treatment (involved in *de novo* pheromone biosynthesis)

Combining gene and protein expression with qRT-PCR allowed a more comprehensive overview of the effect of JHIII treatment and sex on the steps of the mevalonate pathway, which makes the *I. typographus* aggregation pheromones and pheromone precursors *de novo*. Information was obtained for the upregulation of the following genes by RNA-Seq and qRT-PCR: PMK (Ityp06045), HMG-S (Ityp09137), HMG-R (Ityp17150), IPPI (Ityp04875), and IPDS (Ityp09271; Figure 7A). Not all of these steps were identified at the protein level, but analysis revealed the upregulation of HMG-S, IPPI, and IPDS. Notably, we found that the IPDS gene was upregulated by up to 35-fold in male gut tissue compared with that in female gut tissue after JH III treatment (Figure 7B). Besides the IPDS gene,

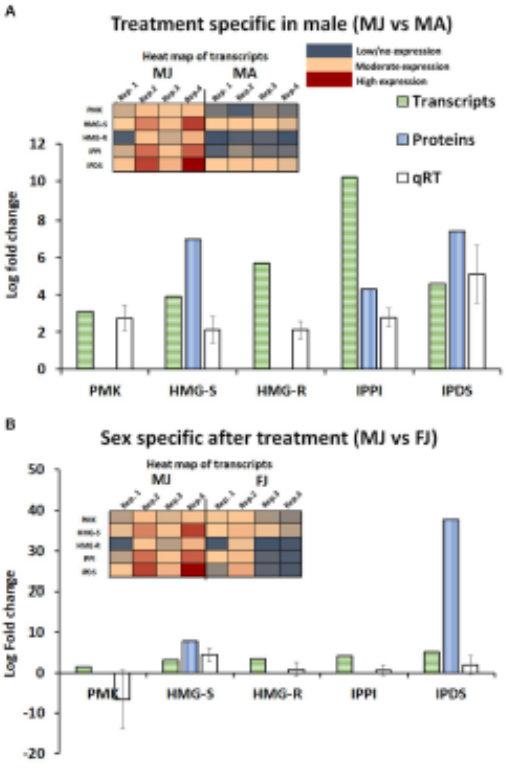

FIGURE 7
Mevalonate pathway key gene contigs expression pattern in transcriptome and proteome and qRT-PCR analysis of male gut tissue. (A) Treatment specific in male (JHIII vs. acetone). (B) Sex-specific after treatment (male vs. female). Phosphomevalonate kinase (PMK), 3-hydroxy-3-methyl glutaryl coenzyme-A synthase (HMG-S), 3-hydroxy-3-methyl glutaryl coenzyme-A reductase (HMG-R), Isopentyl-di-phosphate isomerase (IPPI), and Isoprenyl-di-phospate synthase (IPDS). MA, Males topically treated with acetone – control; MJ, Males topically treated with JHIII – treatment, FA, Females topically treated with acetone – control, FJ, Females topically treated with JHIII – treatment. $N = 4$. The error bar indicates standard error. The expression patterns of the gene transcripts are given in a heat map along with log fold change graph.

HMG-S was also significantly upregulated in JH III treated male gut tissue compared with that in treated females (Figure 7B). Additionally, we also found that IPPI was exclusively abundant in proteins from female gut tissue after treatment (Supplementary Figure 3).

3.4.5 Regulation of the cytochromeP450 (CyP450) gene family after JH III treatment (involved in pheromone biosynthesis and pheromone formation from host tree precursors)

A similar combined approach was taken to explore the regulation of CyP450 genes that are involved in pheromone biosynthesis by RNA-Seq and qRT-PCR; no proteins of this family were detected in our proteomic investigation. CyP450 contigs showing expression patterns above a 2-fold change with a significant value of p ($p < 0.05$) were confirmed by qRT-PCR analysis. Among the contigs previously proposed to be involved in pheromone biosynthesis (Ramakrishnan et al., 2022a), contigs Ityp3903 and Ityp0496 (proposed for verbenol synthesis), contigs Ityp3140 (proposed for detoxification), and Ityp3153 (proposed for ipsdienol) were all found to be upregulated genes in the JH III-treated male gut and are among the most highly upregulated genes measured in this study (Figure 8).

3.4.6 Regulation of esterase gene family after JH III treatment (involved in formation and cleavage of verbenyl fatty acid ester conjugates-possible pheromone precursors)

Among the esterase genes proposed for converting the stored verbenyl ester to *cis*-verbenol, Ityp11977 (which occurred in the early life stage) was not significantly influenced by JH III treatment in males according to transcriptome and proteome analysis. However, another esterase contig, Ityp09460, was found to be upregulated in the protein analysis and qRT-PCR but downregulated in the RNA-Seq. transcriptome (Figure 9A). In female gut tissue, none of these contigs were detected, except for Ityp11977 in qRT-PCR (Figure 9B).

3.4.7 Regulation of Glycosyl hydrolase gene family after JH III treatment (involved in formation and cleavage of verbenyl diglycoside conjugates possible pheromone precursor)

When comparing DGE and DPE analyses in male gut tissue, a set of gene families known for glycosyl-hydrolase function (GO:0016798) was significantly upregulated after JHIII treatment at both the transcript and protein levels with male specificity. This gene family nearly as abundant as the genes of the mevalonate pathway, may cleave stored verbenyl glucoside conjugates to give the free pheromone. Twelve gene contigs were detected from the family, four of which were also detected and significantly upregulated at the protein level, Ityp11770, Ityp00535, Ityp00943, and Ityp04256. These were also upregulated by qRT-PCR except for contig Ityp11770 (Figure 10A). All three contigs were more upregulated in males than in females (Figure 10B); for females, DGE, DPE, and qRT-PCR did not show consistent upregulation after JHIII treatment (Figure 10B; Supplementary Figure 4).

4 Discussion

4.1 Changes in gene expression, proteins, and metabolites after JHIII application to *I. Typographus*, highlighting overall metabolic regulation

The topical application of JH III to adult beetles has been studied in many bark beetle species (Keeling et al., 2016; Tian et al., 2020). In *I. typographus*, we have identified numerous metabolic pathways affected by this hormone by changes in their genes, proteins, and metabolites. JH III treatment has been demonstrated to induce pheromone biosynthesis in male *I. typographus* exclusively and the formation of monoterpene detoxification conjugates in both sexes. These findings correlate with the earlier reported impact of JH III on other bark beetles such as *D. ponderosa* (Chiu et al., 2018).

JH III treatment led to the notable upregulation of metabolic processes and relevant membrane transporters, consistent with observations on other Ips species (Keeling et al., 2006). In addition, there were strong differences in gene expression patterns between males and females of *I. typographus* encompassing functions such as catalytic activity, oxidoreductase activity, esterases, and phosphatases.

In male beetles, the treatment primarily influenced metabolic regulation, whereas, in females, it led to the induction of numerous reproduction-related genes such as vitellogenins (involved in oocyte biosynthesis). This observation can fit the well-documented influence of JH III on parenting behaviors in social insects (Trumbo, 2018). In addition to many membrane transporter activity genes in female guts, genes regulating detoxification processes, such as carboxylases and ubiquitin-carboxyl hydrolases were upregulated (Supplementary Table 3B).

A complementary protein enrichment analysis in this study also found sex-specific differences after JH III treatment. The male gut was enriched with proteins involved in metabolic processes and transferase activity-related proteins. These steps are key in the pheromone biosynthesis of *I. typographus* pioneer males. In the female gut after treatment, the embryo development-related proteins were among those upregulated (over 100 protein candidates), which correlated with the finding of vitellogenin upregulation at the gene level. Both sexes demonstrated upregulation of proteins involved in nuclear and detoxification processes. Unexpectedly, detoxification products of the host tree monoterpene-pinene, verbenyl fatty acid esters, were induced in the guts of both sexes by JHIII. This finding supports the recently proposed hypothesis that detoxification conjugates are produced in both sexes of bark beetles and later diverted to pheromone biosynthesis to the greatest extent in the pioneer sex in host finding-the males in *I. typographus* (Chiu et al., 2018; Ramakrishnan et al., 2022a). Nevertheless, the pathways involved in detoxification and pheromone biosynthesis need more study to understand the linkages between them.

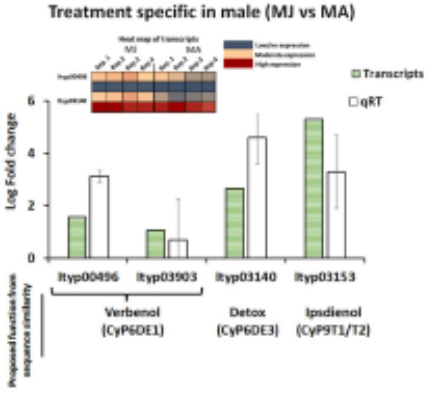

FIGURE 8
Cytochrome P450 gene contigs expression pattern in transcriptome and qRT-PCR expression analysis from *I. typographus* male gut tissue after JHIII treatment. The error bar indicates standard error. MA, Males topically treated with acetone – control; MJ, Males topically treated with JHIII – treatment. $N = 4$. The expression pattern of the transcripts is given in a heat map along with log fold change graph.

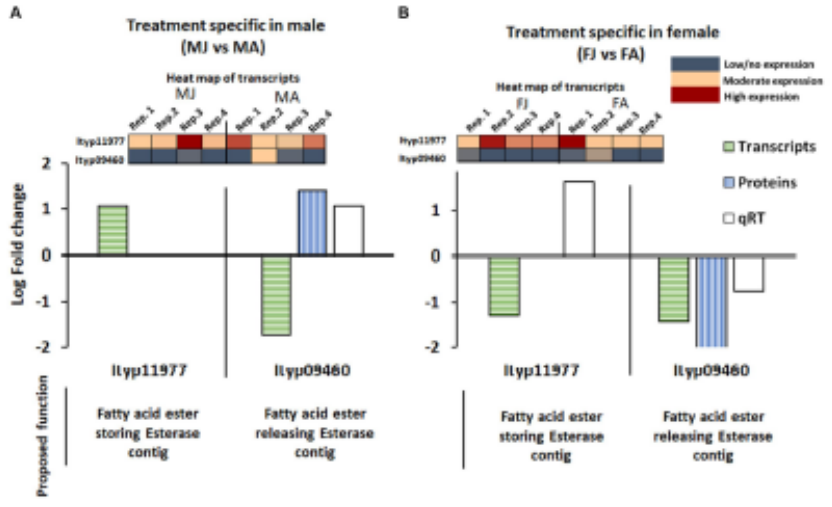

FIGURE 9
Esterase gene contigs expression pattern in the transcriptome, proteome, and qRT-PCR analysis from *I. typographus* male (**A**) and female (**B**) gut tissue after JHIII treatment. MA, Males topically treated with acetone – control; MJ, Males topically treated with JHIII – treatment; FA, Females topically treated with acetone – control; FJ, Females topically treated with JHIII – treatment. $N = 4$. The expression patterns of the gene transcripts are given in a heat map along with fold change graph.

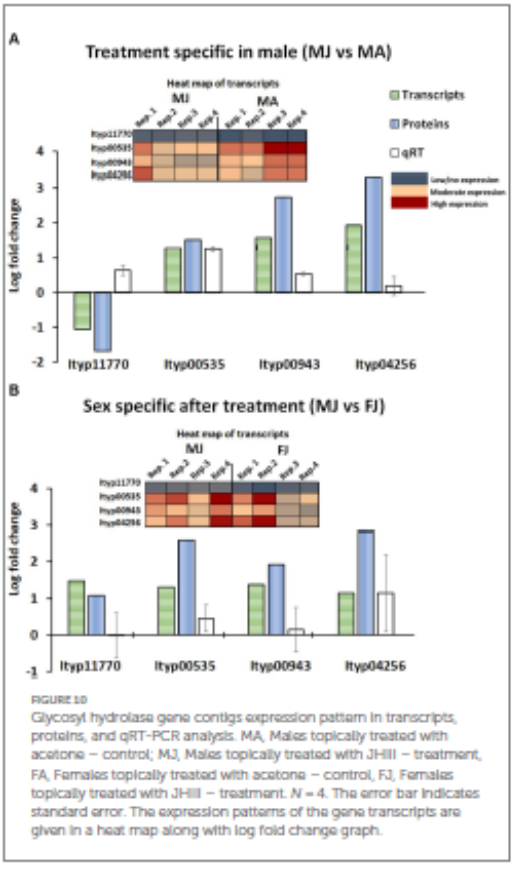

FIGURE 10
Glycosyl hydrolase gene contigs expression pattern in transcripts, proteins, and qRT-PCR analysis. MA, Males topically treated with acetone – control; MJ, Males topically treated with JHIII – treatment; FA, Females topically treated with acetone – control; FJ, Females topically treated with JHIII – treatment. $N = 4$. The error bar indicates standard error. The expression patterns of the gene transcripts are given in a heat map along with log fold change graph.

4.2 Identification of key genes responsible for pheromone biosynthesis

Two of the major male aggregation pheromone components of *I. typographus* are isoprenoids produced *de novo* by the mevalonate pathway were identified (Figure 7). The genes for this pathway have been annotated in the *I. typographus* genome (Powell et al., 2021; Naseer et al., 2023), and many of them are shown here to be upregulated exclusively in males. After JH III treatment, these genes have also been implicated in pheromone formation in other *Ips* species (Keeling et al., 2004).

In male *I. typographus*, topical treatment with JH III led to the overexpression of certain, upstream genes of the mevalonate pathway, including PMK (Ityp06045), HMG-S (Ityp09137), HMG-R (Ityp17150), and IPPI (Ityp04875). were relatively overexpressed in the gut. In addition, the upregulation of IPDS (Ityp09271) was observed at both the transcript and protein levels. This gene is a candidate for encoding the biosynthesis of the hemiterpene 2-methyl-3-buten-2-ol, which has not yet been functionally demonstrated. The upregulation of Ityp09271 aligns with the significant increase in 2-methyl-3-buten-2-ol content observed in the male gut after the treatment and corresponds with the biosynthetic pathway proposed in our previous study (Ramakrishnan et al., 2022a). In females, there was also reported upregulation of another IPDS, an ortholog of geranyl diphosphate synthase (Ityp17861; Ivarsson et al., 1993).

In addition to the observed increase in the levels of 2-methyl-3-buten-2-ol induced by JH III, two other pheromone components were also upregulated: ipsdienol (presumably produced *de novo*) and *cis*-verbenol (likely synthesized from α-pinene) and sequestered as a fatty acid ester (Ramakrishnan et al., 2022a). GC–MS measurements of gut tissue following the induction further revealed a significant increase in *I. typographus* male-specific compounds, such as myrtenol and phenyl ethanol (Supplementary Figure 1). Although behavioral activity for these compounds has not been reported in *I. typographus*, they also produced by the pheromone-producing sex of related bark species, *D. ponderosae* and *I. pini*, where their upregulation after the treatment has also been documented (Keeling et al., 2006, 2016). This suggests that the effect of JH III on pheromone biosynthesis is not limited solely to known behaviorally active compounds.

The effect of JH III- treatment on CyP450 enzymes was also studied, but this was only feasible at the gene transcript level as CyP450 proteins could not be identified in our proteomics work. In the transcriptome analysis, we searched for gene candidates with sequence similarities to functionally known genes from other bark beetle studies, including those involved in *cis*-verbenol biosynthesis (Chiu et al., 2019; Ramakrishnan et al., 2022a), detoxification mechanisms (CyP6DE3), and ipsdienol biosynthesis (CyP9T1/T2; Song et al., 2013; Nadeau et al., 2017).

Interestingly, CyP450s genes in all three functional classes were upregulated after JH III treatment with CyP6DE1, known in another bark beetle species for its role in *trans*-verbenol biosynthesis (Chiu et al., 2019). The contigs from *I. typographus* male gut exhibited lower expression levels compared to the gene contigs suggested for detoxification (CyP6DE3) and ipsdienol biosynthesis (CyP9T1/T2; Sandstrom et al., 2006). The effect of topically applied JH III on pheromone biosynthesis appears to be broader than just the induction of *de novo* synthesized compounds. In addition to regulating isoprenoid biosynthesis, this hormone affects the production of pheromonal components by influencing a variety of other biosynthetic mechanisms such as the hydroxylation of host tree monoterpenes.

4.3 Effects of JH III on the formation and cleavage of detoxification conjugates related to pheromonal components

In this study, topically applied JH III also influenced the production of verbenyl-fatty acid ester and verbenyl-diglycosides, which are conjugates of the pheromone *cis*-verbenol. Since *cis*-verbenol may also be regarded as a detoxification product of α-pinene, its esters, and glycosides may help to alleviate toxicity by stabilizing the initial detoxification product. However, our main objective was to test the hypothesis that these esters and glycosides are precursors of *cis*-verbenol in adult males when they need to release large quantities of these pheromones during the attack on the host tree.

Furthermore, the compound, verbenyl-oleate production after JH III treatment has significantly induced in the fat bodies of both sexes of adult beetles. The induction rate was 10 times higher in females than in males. We previously established from the production curve of this compound at different life stages (Ramakrishnan et al., 2022a) that verbenyl oleate

abundance is male-specific during adult beetle stages. However, in this study, we report that treatment can also induce its production in female adult beetles. This finding suggests a strong regulatory role for JH III in the formation of these compounds in the beetle.

The content of verbenyl oleate in the gut is 100 times lower than in the fat body of *I. typographus* (Ramakrishnan et al., 2022a). Despite the gut being the site for biosynthesis of this compound during the juvenile stages and later in adult males free *cis*-verbenol release occurs. Also, JH III induced an increase in verbenyl oleate abundance in female guts similar to that in the fat body and reduced its content in male guts. These findings support the existing hypothesis that the cleavage of verbenyl fatty acyl esters is specific to adult males and that verbenyl esters serve as precursors for the active pheromonal *cis*-verbenol in pioneer male *I. typographus* (Ramakrishnan et al., 2022a). Both the formation and cleavage steps of verbenyl fatty acid esters are regulated by JH III, indicating that the responsible enzymes (esterase, also known as carboxylesterases or fatty acid transferases) are likely regulated at the gene or protein level.

The esterase contig Ityp11977, which was previously reported in earlier life stages of *I. typographus* for verbenyl fatty acyl ester formation (Ramakrishnan et al., 2022a), was also identified in the guts of beetles after treatment. This observation aligns with the finding that the candidate Ityp11977 was exclusively expressed (as shown in qRT-PCR analysis) in the female gut after treatment (see Figure 9). We also identified another contig from esterase - Ityp09460, expressed in the male gut following the treatment, coinciding with a reduction in verbenyl ester levels. This observation leads us to propose the involvement of this esterase candidate in the release of *cis*-verbenol through the cleavage of ester bonds in the male gut, a novel finding in *I. typographus*. It is worth noting that this esterase is known for several detoxification functions in other insects (Blomquist et al., 2021).

In our previous study, other *cis*-verbenyl conjugates in the guts of beetles were identified as three verbenyl-diglycosides differing structurally by glycosidic parts (Ramakrishnan et al., 2022a,b). Glycosylated alcohols are known to serve as detoxification products, and they may have relevance to bark beetle pheromone biosynthesis in other species (Blomquist et al., 2021). In this study, we observed a significant 100-fold increase in the content of these compounds in the guts following the treatment, and this induction showed similar rates in both sexes of adult beetles. This demonstrates the JH III regulation over the formation of these compounds.

Furthermore, to test the hypothesis that these compounds could serve as alternative pheromonal *cis*-verbenol precursors, we searched and identified for possible genes within specific glycosyl hydrolase gene families. Later, the gene for potential male-specific release to free *cis*-verbenol. Notably, we identified four contigs from the glycosyl hydrolase gene family that were overexpressed exclusively in the male gut after treatment. However, the uncertainty in the abundance of male-specific verbenyl diglycosides (not similar to verbenyl ester), together with low quantity in the gut and absence in the fat body (unpublished data) we presume that these compounds are more likely a detoxification product rather than a pheromone precursor. Thus, we have observed a strong induction of JH III on the formation of both verbenyl conjugates discussed. Originally, these compounds serve as binding agents for the detoxification product of α-pinene, specifically *cis*-verbenol in our case, but additionally, our findings proved that verbenyl fatty acyl esters are possessed by adult males as an alternative pheromone precursor (Chiu et al., 2018; Ramakrishnan et al., 2022a).

Hence, obtaining the specific gene candidates directs us to practical application by targeting the genes of pheromone biosynthesis for silencing in *I. typographus*. Targeting the species-specific non-lethal genes of the beetle along with characterizing them aims to address the pest's aggregation behavior with minimum ecological damage. A similar approach was demonstrated in a moth, Helicoverpa armigera when reproduction was modified by silencing genes responsible for sex pheromones production (Dong et al., 2017).

The main objective of RNAi-based Forest pest management is to reduce the forest pest population level below the epidemic level (Hlasny et al., 2021). Similarly, genes involved in pheromone production in bark beetles can be targeted via RNAi to disrupt communication, such as aggregation of pheromone signal for a mass attack in *I. typographus*. However, selecting an appropriate delivery method for specific insect orders is challenging. In wood-feeding insects, the aspect of dsRNA delivery can be achieved by spraying over the tree trunk (Li et al., 2015) or by injecting it into the tree's sap stream (Hunter et al., 2012). The delivery of dsRNA by these methods will be used for effective silencing of the pheromone biosynthetic genes in the beetle upon phloem-feeding. However, appropriate method should be considered while choosing the for effective outcome (Joga et al., 2021). This approach is familiar with existing forest pest management practices (i.e., silvicultural, biological), and can aid a multi-faceted management approach that keeps the tree-killing forest pest populations in the endemic stage while conserving the beneficial species.

In conclusion, these findings establish a foundation for understanding the genetic mechanisms underlying pheromone biosynthesis in *I. typographus* following JH III treatment. However, a logical next step would be to conduct functional validation of the identified gene candidates involved in pheromone biosynthesis. This approach could lead to effective pest management strategies, such as RNA interference, aimed at manipulating the mass attack behavior of this aggressive pest (Joga et al., 2021).

Data availability statement

All the data and resources generated for this study are included in the article and the supplemental materials. The RNA sequences have been submitted in NIH under the accession PRJNA934749. The Proteome data have been submitted in Proteome Xchange under the identifier PXD039243. We are willing to share all the data and resources in this study with the public.

Ethics statement

Ethical approval was not required for the study involving animals in accordance with the local legislation and institutional requirements because We have performed all beetle experiments that comply with the ARRIVE guidelines and were carried out in accordance with (Scientific Procedures) Act, 1986 and associated guidelines, EU Directive 2010/63/EU for animal experiments.

Author contributions

RR: conceptualization, methodology, formal analysis, resources, and writing – original draft. AR: RNA-seq, data curation, molecular

work support, and writing – review and editing. JH: GC-metabolomic data analysis and method writing. MK: UHPLC/HRMS-MS data analysis. KH: proteomics data analysis and method writing. AS: UHPLC/HRMS-MS data analysis and reviewing. AJ: conceptualization, methodology, formal analysis, writing – review and editing, and supervision. All authors contributed to the article and approved the submitted version.

Funding

RR, AR, JH, AS, and AJ are supported by Czech Science Foundation "GACR," no. 23-07916S; RR was supported by IGA A_20_22 RAJARAJAN RAMAKRISHNAN at the Faculty of Forestry and Wood Sciences, Czech University of Life sciences, Prague, CR; AR is supported by Excellent team grant 202 3–24, Faculty of Forestry and Wood Sciences, Czech University of Life Sciences, Prague, CR; AR, JH, and AJ were supported by Ministry of Education, Youth and Sport, Operational Program Research, Development and Education "EXTEMIT-K," no. CZ.02.1.01/0.0/0.0/15_003/0000433.

Acknowledgments

We acknowledge the editing and valuable comments of Jonathan Gershenzon on the final manuscript version and the constructive comments of Fredrik Schlyter, Hynek Burda and Ewald Grosse-Wilde on the earlier version of the manuscript.

Conflict of interest

The authors declare that the research was conducted in the absence of any commercial or financial relationships that could be construed as a potential conflict of interest.

Publisher's note

Supplementary material

The Supplementary material for this article can be found online at: https://www.frontiersin.org/articles/10.3389/ffgc.2023.1215813/full#supplementary-material

References

Bakke, A., Froyen, P., and Skattebol, L. (1977). Field response to a new pheromonal compound isolated from *Ips-typographus*. *Naturwissenschaften* 64, 98–99. doi: 10.1007/bf00437364

Bearfield, J. C., Henry, A. G., Tittiger, C., Blomquist, G. J., and Ginzel, M. D. (2009). Two regulatory mechanisms of Monoterpenoid pheromone production in *Ips* spp. of bark beetles. *J. Chem. Ecol.* 35, 689–697. doi: 10.1007/s10886-009-9652-2

Blomquist, G. J., Figueroa-Teran, R., Aw, M., Song, M. M., Gorzalski, A., Abbott, N. L., et al. (2010). Pheromone production in bark beetles. *Insect Biochem. Mol. Biol.* 40, 699–712. doi: 10.1016/j.ibmb.2010.07.013

Blomquist, G. J., Tittiger, C., MacLean, M., and Keeling, C. I. (2021). Cytochromes P450: terpene detoxification and pheromone production in bark beetles. *Current Opinion in Insect Sci.* 43, 97–102. doi: 10.1016/j.cois.2020.11.010

Buhaescu, I., and Izzedine, H. (2007). Mevalonate pathway: a review of clinical and therapeutical implications. *Clin. Biochem.* 40, 575–584. doi: 10.1016/j.clinbiochem.2007.03.016

Byers, J. A., and Birgersson, G. (1990). Pheromone production in a bark beetle independent of myrcene precursor in host pine species. *Naturwissenschaften* 77, 385–387. doi: 10.1007/bf01135739

Chiu, C. C., Keeling, C. I., and Bohlmann, J. (2018). Monoterpenyl esters in juvenile mountain pine beetle and sex-specific release of the aggregation pheromone *trans*-verbenol. *Proc. Natl. Acad. Sci. U. S. A.* 115, 3652–3657. doi: 10.1073/pnas.1722380115

Chiu, C. C., Keeling, C. I., and Bohlmann, J. (2019). The cytochrome P450 CYP6DE1 catalyzes the conversion of α-pinene into the mountain pine beetle aggregation pheromone *trans*-verbenol. *Sci. Rep.* 9:1477. doi: 10.1038/s41598-018-38047-8

Chong, J., Soufan, O., Li, C., Caraus, I., Li, S. Z., Bourque, G., et al. (2018). MetaboAnalyst 4.0: towards more transparent and integrative metabolomics analysis. *Nucleic Acids Res.* 46, W486–W494. doi: 10.1093/nar/gky310

Cox, J., Hein, M. Y., Luber, C. A., Paron, I., Nagaraj, N., and Mann, M. (2014). Accurate proteome-wide label-free quantification by delayed normalization and maximal peptide ratio extraction, Termed MaxLFQ. *Molecular & Cellular Proteomics* 13, 2513–2526. doi: 10.1074/mcp.M113.031591

Cox, J., and Mann, M. (2008). MaxQuant enables high peptide identification rates, individualized p.p.b.-range mass accuracies and proteome-wide protein quantification. *Nat. Biotechnol.* 26, 1367–1372. doi: 10.1038/nbt.1511

Cristino, A. S., Nunes, F. M., Lobo, C. H., Bitondi, M. M., Simões, Z. L., da Fontoura Costa, L., et al. (2006). Caste development and reproduction: a genome-wide analysis of hallmarks of insect eusociality. *Insect Mol. Biol.* 15, 703–714. doi: 10.1111/j.1365-2583.2006.00696.x

Dai, L. L., Gao, H. M., and Chen, H. (2021). Expression levels of detoxification enzyme genes from *Dendroctonus armandi* (Coleoptera: Curculionidae) fed on a solid diet containing pine phloem and Terpenoids. *Insects* 12:15. doi: 10.3390/insects12100926

Dhandapani, R. K., Gurusamy, D., Duan, J. J., and Palli, S. R. (2020). RNAi for management of Asian long-horned beetle, Anoplophora glabripennis: identification of target genes. *J Pest Sci* 93, 823–832. doi: 10.1007/s10340-020-01197-8

Dong, K., Sun, L., Liu, J. T., Gu, S. H., Zhou, J-J., Yang, R-N., et al. (2017). RNAi-Induced Electrophysiological and Behavioral Changes Reveal Two Pheromone Binding Proteins of Helicoverpa armigera Involved in the Perception of the Main Sex Pheromone Component Z11-16:Ald. *J. Chem. Ecol.* 43, 207–214. doi: 10.1007/s10886-016-0816-6

Emlen, D., Szafran, Q., Corley, L., and Dworkin, I. (2006). Insulin signaling and limb-patterning: candidate pathways for the origin and evolutionary diversification of beetle 'horns'. *Heredity* 97, 179–191. doi: 10.1038/sj.hdy.6800868

Fang, J. X., Zhang, S. F., Liu, F., Cheng, B., Zhang, Z., Zhang, Q. H., et al. (2021a). Functional investigation of monoterpenes for improved understanding of the relationship between hosts and bark beetles. *J. Appl. Entomol.* 145, 303–311. doi: 10.1111/jen.12850

Fang, J. X., Du, H. C., Shi, X., Zhang, S. F., Liu, F., Zhang, Z., et al. (2021b). Monoterpenoid signals and their transcriptional responses to feeding and juvenile hormone regulation in bark beetle *Ips hauseri*. *J. Exp. Biol.* 224:9. doi: 10.1242/jeb.238030

Gilg, A. B., Bearfield, J. C., Tittiger, C., Welch, W. H., and Blomquist, G. J. (2005). Isolation and functional expression of an animal geranyl diphosphate synthase and its role in bark beetle pheromone biosynthesis. *Proc. Natl. Acad. Sci. U. S. A.* 102, 9760–9765. doi: 10.1073/pnas.0503277102

Goodman, W. G., and Cusson, M. (2012). The juvenile hormones. *Insect Endocrinol.* 8, 310–365. doi: 10.1016/B978-0-12-384749-2.10008-1

Hebert, A. S., Richards, A. L., Bailey, D. J., Ulbrich, A., Coughlin, E. E., Westphall, M. S., et al. (2014). The one hour yeast proteome. *Mol. Cell. Proteomics* 13, 339–347. doi: 10.1074/mcp.M113.034769

Hilliou, F., Chertemps, T., Maibeche, M., and Le Goff, G. (2021). Resistance in the genus Spodoptera: key insect detoxification genes. *Insects* 12:27. doi: 10.3390/insects12060544

Hlasny, T., Konig, L., Krokene, P., Lindner, M., Montagne-Huck, C., Muller, J., et al. (2021). Bark beetle outbreaks in Europe: state of knowledge and ways forward for management. *Current Forestry Reports* 7, 138–165. doi: 10.1007/s40725-021-00142-x

Hughes, P. R. (1974). Myrcene - precursor of pheromones in *Ips* beetles. *J. Insect Physiol.* 20, 1271–1275. doi: 10.1016/0022-1910(74)90232-7

Hunter, W. B., Glick, E., Paldi, N., and Bextine, B. R. (2012). Advances in RNA interference: dsRNA Treatment in Trees and Grapevines for Insect Pest Suppression. *Southwest. Entomol.* 37, 85–87. doi: 10.3958/059.037.0110

Ivarsson, P., and Birgersson, G. (1995). Regulation and biosynthesis of pheromone components in the double spined bark beetle *Ips duplicatus* (coleoptera, scolytidae). *J. Insect Physiol.* 41, 843–849. doi: 10.1016/0022-1910(95)00052-v

Ivarsson, P., Schlyter, F., and Birgersson, G. (1993). Demonstration of *de-novo* pheromone biosynthesis in *Ips-duplicatus* (coleoptera, scolytidae) - inhibition of ipsdienol and e-myrcenol production by compactin. *Insect Biochem. Mol. Biol.* 23, 655–662. doi: 10.1016/0965-1748(93)90039-u

Jindra, M., and Bittova, L. (2020). The juvenile hormone receptor as a target of juvenoid "insect growth regulators". *Arch. Insect Biochem. Physiol.* 103:e21615. doi: 10.1002/arch.21615

Jindra, M., Palli, S. R., and Riddiford, L. M. (2013). "The juvenile hormone signaling pathway in insect development" in *Annual review of entomology*. ed. M. R. Berenbaum, vol. 58, 181–204. doi: 10.1146/annurev-ento-120811-153700

Joga, M. R., Mogilicherla, K., Smagghe, G., and Roy, A. (2021). RNA interference-based forest protection products (FPPs) against wood-boring coleopterans: Hope or hype? *Front. Plant Sci.* 12:733608. doi: 10.3389/fpls.2021.733608

Kanehisa, M. (2002). The KEGG database. *Silico Simulation of Biolog. Processes* 247, 91–103. doi: 10.1002/0470857897.ch8

Kanehisa, M., Furumichi, M., Tanabe, M., Sato, Y., and Morishima, K. (2017). KEGG: new perspectives on genomes, pathways, diseases and drugs. *Nucleic Acids Res.* 45, D353–D361. doi: 10.1093/nar/gkw1092

Keeling, C. I., Bearfield, J. C., Young, S., Blomquist, G. J., and Tittiger, C. (2006). Effects of juvenile hormone on gene expression in the pheromone-producing midgut of the pine engraver beetle, *Ips pini*. *Insect Mol. Biol.* 15, 207–216. doi: 10.1111/j.1365-2583.2006.00629.x

Keeling, C. I., Blomquist, G. J., and Tittiger, C. (2004). Coordinated gene expression for pheromone biosynthesis in the pine engraver beetle, *Ips pini* (Coleoptera: Scolytidae). *Naturwissenschaften* 91, 324–328. doi: 10.1007/s00114-004-0523-y

Keeling, C. I., Li, M., Sandhu, H. K., Henderson, H., Saint Yuen, M. M., and Bohlmann, J. (2016). Quantitative metabolome, proteome and transcriptome analysis of midgut and fat body tissues in the mountain pine beetle, *Dendroctonus ponderosae* Hopkins, and insights into pheromone biosynthesis. *Insect Biochem. Mol. Biol.* 70, 170–183. doi: 10.1016/j.ibmb.2016.01.002

Knízek, M., Zahradník, P., and Liška, J. (2023). Sborník referátů z celostátního semináře s mezinárodní účastí Připravky na ochranu lesa – realita a budoucnost. *Zpravodaj ochrany lesa, Škodliví činitelé v lesích Česka. Svazek.* 26, 2022/23.

Kyre, B. R., Bentz, B. J., and Rieske, L. K. (2020). Susceptibility of mountain pine beetle (Dendroctonus ponderosae Hopkins) to gene silencing through RNAi provides potential as a novel management tool. *For. Ecol. Manag.* 73, 0378–1127. doi: 10.1016/j.foreco.2020.118322

Leinwand, S. G., and Scott, K. (2021). Juvenile hormone drives the maturation of spontaneous mushroom body neural activity and learned behavior. *Neuron* 109, 1836–1847.e5. doi: 10.1016/j.neuron.2021.04.006

Li, H., Guan, R., Guo, H., and Miao, X. (2015). New insights into an RNAi approach for plant defence against piercing-sucking and stem-borer insect pests. *Plant Cell Environ.* 38:2277–2285. doi: 10.1111/pce.12546

Nadeau, J. A., Peterell, J., Tillett, R. L., Jung, K., Foroohi, M., MacLean, M., et al. (2017). Comparative transcriptomics of mountain pine beetle pheromone-biosynthetic tissues and functional analysis of CYP9DE3. *BMC Genomics* 18:311. doi: 10.1186/s12864-017-3696-4

Nardi, J. B., Young, A. G., Ujhelyi, E., Tittiger, C., Lehane, M. J., and Blomquist, G. J. (2002). Specialization of midgut cells for synthesis of male isoprenoid pheromone components in two scolytid beetles, *Dendroctonus jeffreyi* and *Ips pini*. *Tissue Cell* 34, 221–231. doi: 10.1016/s0040-8166(02)00004-6

Naseer, A., Mogilicherla, K., Sellamuthu, G., and Roy, A. (2023). Age matters life-stage, tissue, and sex-specific gene expression dynamics in *Ips typographus* (Coleoptera: Curculionidae: Scolytinae). *Front. for. glob.* 6:1124754. doi: 10.3389/ffgc.2023.1124754

NIST (2017).Inorganic Crystal Structure Database. *NIST Standard Reference Database Number 3*, Gaithersburg MD: National Institute of Standards and Technology. 20899. doi: 10.18434/M32147

Pandey, A., and Bloch, G. (2015). Juvenile hormone and ecdysteroids as major regulators of brain and behavior in bees. *Current Opinion in Insect Sci.* 12, 26–37. doi: 10.1016/j.cois.2015.09.006

Palacca, M., Lindner, M., Lucas-Borja, M. E., Cordonnier, T., Fidej, G., Gardiner, B., et al. (2023). Significant increase in natural disturbance impacts on European forests since 1950. *Glob. Change Biol.* 29, 1359–1376. doi: 10.1111/gcb.16531

Powell, D., Grosse-Wilde, E., Krokene, P., Roy, A., Chakraborty, A., Lofstedt, C., et al. (2021). A highly-contiguous genome assembly of the Eurasian spruce bark beetle, *Ips typographus*, provides insight into a major forest pest. *Commun. Biol.* 4:1059. doi: 10.1038/s42003-021-02602-3

Ramakrishnan, R., Hradecky, J., Roy, A., Kalinova, B., Mendezes, R. C., Synek, J., et al. (2022a). Metabolomics and transcriptomics of pheromone biosynthesis in an aggressive forest pest *Ips typographus*. *Insect Biochem. Mol. Biol.* 140:103680. doi: 10.1016/j.ibmb.2021.103680

Ramakrishnan, R., Roy, A., Kai, M. R., Swins, A., and Jirosova, A. (2022b). Metabolome and transcriptome related dataset for pheromone biosynthesis in an aggressive forest pest *Ips typographus*. *Data Brief* 41:107912. doi: 10.1016/j.dib.2022.107912

Rappsilber, J., Mann, M., and Ishihama, Y. (2007). Protocol for micro-purification, enrichment, pre-fractionation and storage of peptides for proteomics using StageTips. *Nat. Protoc.* 2, 1896–1906. doi: 10.1038/nprot.2007.261

Renwick, J. A. A., Hughes, P. R., and Krull, I. S. (1976). Selective production of cis-verbenol and trans-verbenol from (−)- and (+)-α-pinene by a bark beetle. *Science* 191, 199–201. doi: 10.1126/science.1246609

Riddiford, L. M. (2012). How does juvenile hormone control insect metamorphosis and reproduction? *Gen. Comp. Endocrinol.* 179, 477–484. doi: 10.1016/j.ygcen.2012.06.001

Riddiford, L. M., Cherbas, P., and Truman, J. W. (2001). Ecdysone receptors and their biological actions. *Vitamins and Hormones - Advan. Res. App.* 60, 1–73. doi: 10.1016/s0083-6729(00)60016-x

Riddiford, L. M., Truman, J. W., Mirth, C. K., and Shen, Y. C. (2010). A role for juvenile hormone in the prepupal development of *Drosophila melanogaster*. *Development* 137, 1117–1126. doi: 10.1242/dev.037218

Rodrigues, T. B., Dhandapani, R., Duan, J., and Palli, S. R. (2017). RNA interference in the Asian Longhorned Beetle: Identification of Key RNAi Genes and Reference Genes for RT-qPCR. *Scientific Reports.* 7:8913. doi: 10.1038/s41598-017-08813-1

Sandstrom, P., Welch, W. H., Blomquist, G. J., and Tittiger, C. (2006). Functional expression of a bark beetle cytochrome P450 that hydroxylates myrcene to ipsdienol. *Insect Biochem. Mol. Biol.* 36, 835–845. doi: 10.1016/j.ibmb.2006.08.004

Sarabia, L. E., Lopez, M. F., Obregon-Molina, G., Cano-Ramirez, C., Sanchez-Martinez, G., and Zuniga, G. (2019). The differential expression of mevalonate pathway genes in the gut of the bark beetle *Dendroctonus rhizophagus* (Curculionidae: Scolytinae) is unrelated to the de novo synthesis of terpenoid pheromones. *Int. J. Mol. Sci.* 20:20. doi: 10.3390/ijms20164011

Schlyter, F., Birgersson, G., Byers, J. A., Lofqvist, J., and Bergstrom, G. (1987). Field response of spruce bark beetle, Ips typographus to aggregation pheromone candidates. *J. Chem. Ecol.* 13, 701–716. doi: 10.1007/BF01020153

Sellamuthu, G., Bily, J., Joga, M. R., Synek, J., and Roy, A. (2022). Identifying optimal reference genes for gene expression studies in Eurasian spruce bark beetle, *Ips typographus* (Coleoptera: Curculionidae: Scolytinae). *Sci. Rep.* 12:4671. doi: 10.1038/s41598-022-08434-3

Seybold, S. J., Quilici, D. R., Tillman, J. A., Vanderwel, D., Wood, D. L., and Blomquist, G. J. (1995). De-novo biosynthesis of the aggregation pheromone components Ipsenol and Ipsdienol by the pine bark beetles *Ips paraconfusus* lanier and *Ips pini* (say) (coleoptera-scolytidae). *Proc. Natl. Acad. Sci. U. S. A.* 92, 8393–8397. doi: 10.1073/pnas.92.18.8393

Smykal, V., Daimon, T., Kayukawa, T., Takaki, K., Shinoda, T., and Jindra, M. (2014). Importance of juvenile hormone signaling arises with competence of insect larvae to metamorphose. *Dev. Biol.* 390, 221–230. doi: 10.1016/j.ydbio.2014.03.006

Song, M. M., Kim, A. C., Gorzalski, A. J., MacLean, M., Young, S., Ginzel, M. D., et al. (2013). Functional characterization of myrcene hydroxylases from two geographically distinct *Ips pini* populations. *Insect Biochem. Mol. Biol.* 43, 336–343. doi: 10.1016/j.ibmb.2013.01.003

Tian, C. B., Li, Y. Y., Huang, J., Chu, W. Q., Wang, Z. Y., and Liu, H. (2020). Comparative transcriptome and proteome analysis of heat acclimation in predatory mite *Neoseiulus barkeri*. *Front. Physiol.* 11:16. doi: 10.3389/fphys.2020.00426

Tillman, J. A., Holbrook, G. L., Dallara, P. L., Schal, C., Wood, D. L., Blomquist, G. J., et al. (1998). Endocrine regulation of de novo aggregation pheromone biosynthesis in the pine engraver, *Ips pini* (say) (Coleoptera: Scolytidae). *Insect Biochem. Mol. Biol.* 28, 705–715. doi: 10.1016/s0965-1748(97)00117-3

Tillman, J. A., Lu, F., Goddard, L. M., Donaldson, Z. R., Dwinell, S. C., Tittiger, C., et al. (2004). Juvenile hormone regulates *de novo* isoprenoid aggregation pheromone biosynthesis in pine bark beetles, *Ips* spp., through transcriptional control of HMG-CoA reductase. *J. Chem. Ecol.* 30, 2459–2494. doi: 10.1007/s10886-004-7945-z

Treiblmayr, K., Pascual, N., Pulachs, M.-D., Keller, T., and Belles, X. (2006). Juvenile hormone titer versus juvenile hormone synthesis in female nymphs and adults of the German cockroach, *Blattella germanica*. *J. Insect Sci.* 6, 1–7. doi: 10.1673/031.006.4301

Trumbo, S. T. (2018). Juvenile hormone and parental care in subsocial insects: Implications for the role of juvenile hormone in the evolution of sociality. *Current Opinion in Insect Sci.* 28, 13–18. doi: 10.1016/j.cois.2018.04.001

Tyanova, S., Temu, T., Sinitcyn, P., Carlson, A., Hein, M. Y., Geiger, T., et al. (2016). The Perseus computational platform for comprehensive analysis of (prote)omics data. *Nat. Methods* 13, 731–740. doi: 10.1038/nmeth.3901

Ward, S. F., Brockerhoff, E. G., Turner, R. M., Yamanaka, T., Marini, L., Fei, S. L., et al. (2022). Prevalence and drivers of a tree-killing bark beetle, *Ips typographus* (Coleoptera, Scolytinae), in international invasion pathways into the USA. *J. Pest. Sci.* 96, 845–856. doi: 10.1007/s10340-022-01559-4

White, R. A., Agosin, M., Franklin, R. T., and Webb, J. W. (1980). Bark beetle pheromones - evidence for physiological synthesis mechanisms and their ecological implications. *Zeitschrift Fur Angewandte Entomologie-J. Applied Entomol.* 90, 255–274. doi: 10.1111/j.1439-0418.1980.tb03526.x

Zhang, W. N., Ma, L., Xiao, H. J., Liu, C., Chen, L., Wu, S. L., et al. (2017). Identification and characterization of genes involving the early step of juvenile hormone pathway in *Helicoverpa armigera*. *Sci. Rep.* 7:16542. doi: 10.1038/s41598-017-16319-z

Zhu, H., Gegear, R. J., Casselman, A., Kanginakudiru, S., and Reppert, S. M. (2009). Defining behavioral and molecular differences between summer and migratory monarch butterflies. *BMC Biol.* 7:14. doi: 10.1186/1741-7007-7-14

Juvenile Hormone Induction Unveils Key Genes Involved in Pheromone Biosynthesis and Detoxification in the Eurasian Spruce Bark Beetle

Rajarajan Ramakrishnan[1], Amit Roy[1], Jaromír Hradecký[1], Marco Kai[2], Karel Harant[4], Ales Svatoš[2,3], Anna Jirošová[1*].

Supplementary data:

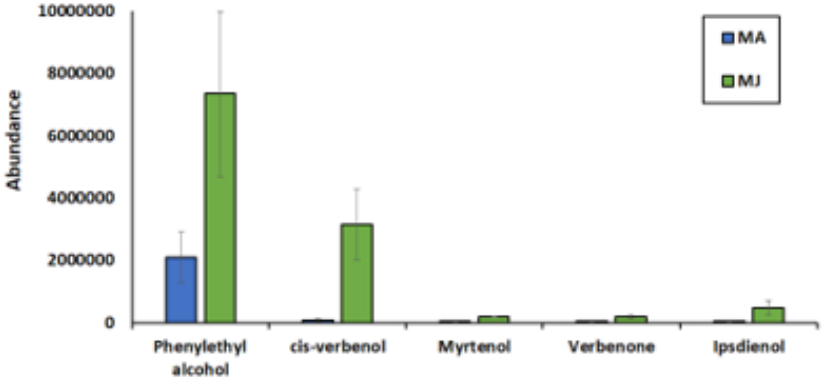

Supplementary Figure 1:GCXGC-MS data- Quantification of Pheromone compounds from *I. typographus* male gut tissue after JHIII induction. MA- Males topically treated with acetone – control; MJ- Males topically treated with JHIII – treatment The error bar indicates standard error. N=3.

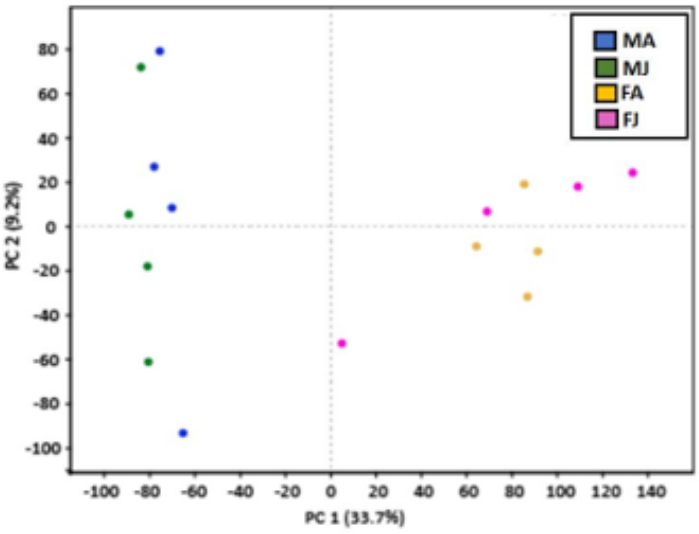

Supplementary Figure 2A: PCA of transcriptome data (RNA- sequencening) analysis from *I. typographus* gut tissue after JHIII induction in both sex . MA- Males topically treated with acetone – control; MJ- Males topically treated with JHIII – treatment, FA- Females topically treated with acetone – control, FJ-Females topically treated with JHIII – treatment. N=4.

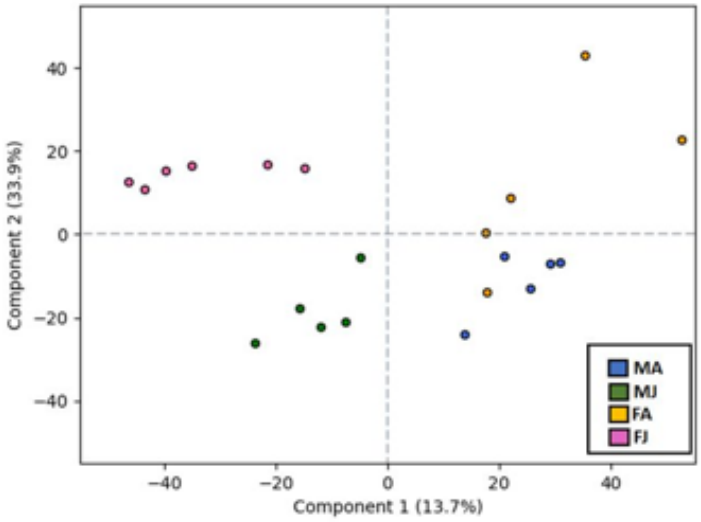

Supplementary Figure 2B: PCA of proteome data from *I. typographus* gut tissue after JHIII induction in both sex . MA- Males topically treated with acetone – control; MJ- Males topically treated with JHIII – treatment, FA- Females topically treated with acetone – control, FJ-Females topically treated with JHIII – treatment. N=4

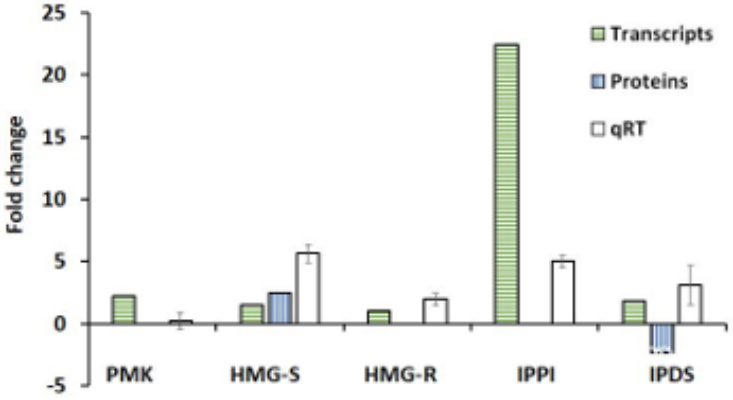

Supplementary Figure 3: Mevalonate pathway gene contigs relative expression in *I. typographus* **female gut tissue** after JHIII treatment. phosphomevalonate kinase (PMK),3-hydroxy-3-methyl glutaryl coenzyme-A synthase (HMG-S), 3-hydroxy-3-methyl glutaryl coenzyme-A reductase (HMG-R), isopentyl-di-phosphate isomerase (IPPI), and *isoprenyl-di-phospate synthase (IPDS)*. The error bar indicates standard error. MA- Males topically treated with acetone – control; MJ- Males topically treated with JHIII – treatment, FA- Females topically treated with acetone – control, FJ-Females topically treated with JHIII – treatment. N=4.

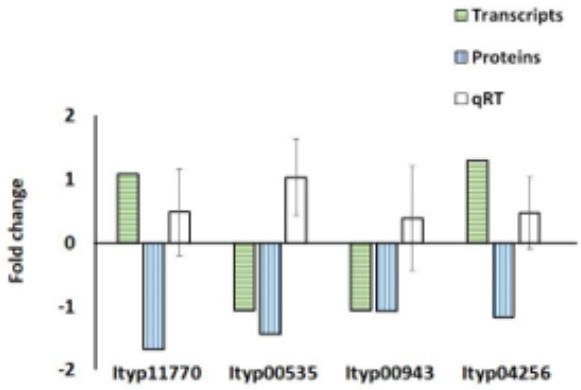

Supplementary Figure 4: **Glycosyl hydrolase** gene contigs relative expression of in female gut tissue after JHIII treatment. The error bar indicates standard error. MA- Males topically treated with acetone – control; MJ- Males topically treated with JHIII – treatment, FA- Females topically treated with acetone – control, FJ-Females topically treated with JHIII – treatment. N=4.

5. DISCUSSION:

This study provided comprehensive insights into the pheromone biosynthesis in *Ips typographus*, which aligns with past research and provides many key in-depth findings up to gene level information that supports the research field strongly with evidence (Birgersson et al., 1984; Ramakrishnan et al., 2022a, 2022b). Another interesting phenomenon of inducing pheromone biosynthesis in bark beetles using juvenile hormone (JH III). To our knowledge, this research study is conducted for the first ever in *I. typographus* of different life stages and JH III treatment (induced hormone regulation), demonstrating pheromone biosynthesis aimed to test hypotheses 1 (Key life stages of the beetle) and Hypothesis 2 (JH III treated beetle). The *I. typographus* males, as the pioneer sex of the beetle in finding hosts have been focused on this study for aggregation pheromone biosynthesis.

Ips typographus aggregation pheromone blend consists of 2-methyl-3-buten-2-ol and *cis*-verbenol. These components were highly produced by male colonizing beetles, which was again proved to be abundant in the respective male gut in this study. Surprisingly, the life stage research revealed that the aggregation pheromone *cis*-verbenol started appearing in the juvenile beetles and disappeared during beetle maturation. Later, *cis*-verbenol reappeared as soon as they emerged from the host. *cis*-verbenol, the compound particularly known for being derived from a tree precursor (*α*-pinene), is also linked to monoterpene detoxification among early life stages of both sexes, such as larvae, pupae, and immature beetles. Other components from the beetle such as verbenone follow a similar pattern as in *cis*-verbenol (precursor of verbenone synthesis) among the various life stages. Ipsdienol, a compound known exclusively for *Ips* species was identified only in males from the mating chamber. Many compounds with unknown biological activity, such as *trans*-verbenol, myrtenol, phenyl ethanol, and myrcene, were also identified and quantified in gut tissues of *I. typographus* developed stages with specific sex (male), supporting the previous knowledge on these compounds and justifies the hypothesis 1 (Birgersson et al., 1984, Ramakrishnan et al., 2022a, 2022b).

Followed by, hypothesis 2 was tested by the hormone induction using Juvenile hormone (JH III) for targeted pheromone biosynthesis research, which is available for many bark beetle species (Tillman et al., 2004; Bearfield et al., 2009; Chiu et al., 2018; Fang et al., 2021). However, not all *Ips sp.* follow the same regulation pattern after hormone treatment, and *Ips typographus* was not addressed in this platform (Tillman et al., 2004). Here, we have attempted aggregation pheromone quantification from the *I. typographus sp.* gut after JH III treatment with a focus on *de novo* synthesis of the aggregation pheromones such as 2-methyl-3-buten-2-ol and the results were similar as in *I. pini*, where JH III treatment influences *de novo* pheromone synthesis (Seybold and Tittiger, 2003). Added to that, *cis*-verbenol and verbenone were also upregulated, thus a precursor-mediated biosynthesis was postulated for the pheromone cleaving mechanism from respective conjugates after JH III treatment. GC-MS measurements of gut tissue following the induction further revealed a significant increase in *I. typographus* male-specific compounds, such as myrtenol and phenyl ethanol. This suggests that the effect of JH III on pheromone biosynthesis is not limited solely to known behaviourally active compounds and to an extent the JH III also activates many detoxification and reproductive gene families on the beetle and is highly dependent on the sex of the beetle (Ramakrishnan et al., 2024).

2-methyl-3-buten-2-ol biosynthesis concept (*de novo* from the beetle):

Aiming the first objective from the hypotheses, the pheromone precursors were measured in detail using metabolomics of UHPLC-HR-MS/MS, which revealed the presence of many compounds in positive and negative modes, especially mevalonate-5-phosphate. at all life stages. The evident presence of mevalonate-5-phosphate in the flying male beetles, followed by a reduction during the fed male stage and reappeared during the mated males, provided the compound's possibility as substrate in pheromone biosynthesis. Hypothetically, mevalonate-5-phosphate could be an active upstream substrate for 2-methyl-3-buten-2-ol synthesis. The higher amount of mevalonate-5-phosphate during the flying stage also supports previous data on flight muscle activation driving certain *de novo* pheromone biosynthesis in other *Ips* sp., (Ivarsson et al., 1998).

Thus, the mevalonate pathway study involving a variety of isoprenoid genes from the pathway with intermediate components was targeted in both sexes for respective functions.

A further intent to verify the primary objective, with relevant approaches to highlight the gene family involved in the biosynthesis of 2-methyl-3-buten-2-ol has provided clarified knowledge of our bark beetle species. The DGE analysis of the gut tissues with *I. typographus* genome annotation revealed distinct expression patterns of certain gene families as in other research of many Insects with similar interests (Blomquist et al., 2010; Jirosová et al., 2017). In our study, genes involving pheromone synthesis and detoxification genes were upregulated after feeding in the beetle. By co-relating on a previous finding from *Ips* sp., (Lanne et al., 1989) and our metabolomic data on mevalonate-5-phosphate intermediate, we narrowed down the analysis on mevalonate pathway gene family members, including PMK (Ityp06045), HMG-S (Ityp09137), HMG-R (Ityp17150), IPPI (Ityp04875) and IPDS (Ityp09271). These genes were shown to influence pheromone production in *Ips* sp., especially HMG-R, which when inhibited, completely blocks pheromone production pathways (Ivarsson et al., 1993; Tillman et al., 2004). In particular, the isoprenoid gene family member isoprenoid-di-phosphate synthase (IPDS) - Ityp09271, was identified in the fed male gut of *I. typographus*, along with 2-methyl-3-buten-2-ol (Ramakrishnan et al., 2022a). Since the mevalonate pathway supplies the five-carbon and the up-regulation of the entire mevalonate pathway in fed adult male beetles, we proposed that IPDS could play the role of a novel hemiterpenoid prenyl transferase in 2-methyl-3-buten-2-ol *de novo* synthesis. Though IPDS is known to be involved in pheromone synthesis in other insects (Lancaster et al., 2018) such as the bark beetle *D. ponderosae* (frontalin pheromone) (Keeling et al., 2013), we are proposing a function for IPDS in hemiterpene synthesis in the animal family for the first time. The actual known function of IPDS is also known as GPPS, in the extension of myrcene synthesis (Gilg et al., 2005; Gilg et al., 2009). Based on the involvement of GPPS in myrcene synthesis, we identified other paralog genes of IPDS/GPPS— Ityp17873 and Ityp17861— from reported different life stage RNA-seq data. The expression of these

isomers was not as high as the proposed candidate Ityp09271 in the fed male gut. Thus, the low expression of the GPPS gene isomers co-relates with the low ipsdienol (myrcene derivative) presence during the fed stage. Even though studies showing the involvement of the mevalonate pathway in other bark beetles (Bearfield et al., 2009; Sarabia et al., 2019) and insects have been published, our study is the first reported detailed molecular analysis of the gene family in *Ips typographus sp.,* as per our knowledge.

Similarly, after topical treatment with JH III, male *I. typographus* overexpressed certain upstream genes of the mevalonate pathway, including PMK (Ityp06045), HMG-S (Ityp09137), HMG-R (Ityp17150), and IPPI (Ityp04875) in the gut. In addition, the upregulation of IPDS (Ityp09271) was observed as well as protein levels after treatment. Hence, this gene is a primary candidate for encoding the biosynthesis of the hemiterpene 2-methyl-3-buten-2-ol, which has not yet been functionally demonstrated. The upregulation of Ityp09271 aligns with the significant increase in 2-methyl-3-buten-2-ol content observed in the male gut after the treatment and corresponds with the biosynthetic pathway proposed in our previous study (Ramakrishnan et al., 2022a). In females, there was also reported upregulation of another IPDS, an ortholog of geranyl-di-phosphate synthase (Ityp17861) (Ivarsson et al., 1993; Ramakrishnan et al., 2022a, 2022b, 2024).

***cis*-Verbenol biosynthesis concept:**

cis-Verbenol biosynthesis focused on the second objective of the hypotheses, which involves the oxidation of (-) *α*-pinene that adult beetles sequester from the tree (Renwick et al., 1976; Chiu et al., 2019). It is already known that the CYP450 gene is involved in verbenol synthesis in bark beetle sp., (Nadeau et al., 2017). Here, we found 56 CYP450 genes expressed in the gut tissue of *I. typographus* (Ramakrishnan et al., 2022b), accounting for 66.6% of the total number of CYP450 genes (84) in the beetle genome (Powell et al., 2020). CyP450- C1 (Ityp3903) and C2 (Ityp0496) showed high sequence similarity with CYP450 (A1 like- CYP6DE1) from *D. ponderosae* involved in *trans*-verbenol production (Chiu et al. 2019). In addition, we also identified candidate CYP450- C3 (Ityp3140) and CYP450- C4 (Ityp3230), showing sequence similarity with the

CyP450 gene family (A2-like) -CYP6DE3, known to be involved in the detoxification in other bark beetles (Nadeau et al., 2017). Though we selected candidates involved in two different functions, these four CYP450 genes were all expressed in the fed and immature life stages. As reported by Chiu et al. (2019) the gene involved in *trans*-verbenol production is also involved to some extent in the *cis*-verbenol synthesis and detoxification mechanism of *α*-pinene (Renwick et al., 1976; Reid and Purcell, 2011). We propose four identified candidates (C1-C4) as possible *cis/trans*-verbenol synthesizing from *α*-pinene in the bark beetle. Functional validation of the gene candidate is required before naming the gene for the proposed function. Furthermore, CYP450 genes, Ityp4140 and Ityp4142, similar to CYP4Gs involved in converting lengthy aldehydes and alcohols into hydrocarbons, were identified with the help of a known sequence from recent studies (MacLean et al., 2018). Also, CYP450 (Ityp1834 and Ityp3153), similar to CYP9T1/T2, known for myrcene hydrolase, was proposed (Song et al., 2013). Though there is recent research on CYP6 involvement in aggregation pheromone production in other *Ips* sp. (Fang et al., 2021), the corresponding CYP450 gene from the 6-like family needs to be identified for further functional clarification in *I. typographus.*

The effect of JH III- treatment on CYP450 enzymes was also studied, but this was only feasible at the gene transcript level as CYP450 proteins could not be identified in our proteomics work. In the transcriptome analysis, we searched for gene candidates with sequence similarities to functionally known genes from other bark beetle studies, including those involved in *cis*-verbenol biosynthesis (Chiu et al., 2019; Ramakrishnan et al., 2022a), detoxification mechanisms (CYP6DE3), and ipsdienol biosynthesis (CYP9T1/T2) (Song et al., 2013; Nadeau et al., 2017; Ramakrishnan et al., 2022a and 2022 b).

Interestingly, CYP450 genes in all three functional classes were upregulated after JH III treatment with CYP6DE1, known in another bark beetle species for its role in *trans*-verbenol biosynthesis (Chiu et al., 2019). The contigs from *I. typographus* male gut exhibited lower expression levels compared to the gene contigs suggested for detoxification (CYP6DE3) and ipsdienol biosynthesis (CYP9T1/T2) (Sandstrom et al.,

2006). The effect of topically applied JH III on pheromone biosynthesis appears to be broader than just the induction of *de novo* synthesized compounds. In addition to regulating isoprenoid biosynthesis, this hormone affects the production of pheromonal components by influencing a variety of other biosynthetic mechanisms such as the hydroxylation of host tree monoterpenes (Ramakrishnan et al., 2024).

Pheromone storage concept:

Testing the final objective of the hypotheses, *I. typographus* life stages and JH III treatment influence trace amounts of *cis*-verbenol and verbenone, which proves that precursor-mediated biosynthesis, was also found induced after JH III treatment. Thus, *cis*-verbenol may be synthesized after JH III treatment from the gut, as postulated in our hypothesis of verbenol release from the stored verbenyl oleate. This release could involve certain esterase, hydrolase, and fatty acyl transferase gene families expressed in the gut tissue after the treatment (Chiu et al., 2018).

Since *cis*-verbenol biosynthesis patterns were seen among the different life stages of the beetle gut, we showed that verbenyl oleates were found to be initially in the immature beetle of both sexes. Later, only verbenyl oleate synthesis continued with male specificity in the mature beetles. Similar to a study in *D. ponderosae* by Chiu et al. (2018) we analyzed extracts from the beetle body (focused on the fat body without the gut) and quantified the possible detoxification products (verbenyl oleate and myrtenyl oleate) from the beetle's body. Verbenyl oleate is a putative pheromone storage fatty acid ester for the pheromone, *cis*-verbenol. The relative abundance of *cis*-verbenol, verbenyl-oleate, and methyl oleate showed an interesting pattern between life stages. Moreover, the co-relation of the verbenyl oleate reduction and methyl oleate increasing with pheromonal *cis*-verbenol can be seen in fed and mated stages. At the immature stage, the abundance of verbenyl oleate was high, whereas the abundance of methyl oleate was low. From this finding, we propose that *α*-pinene from the host source undergo detoxification into oxygenated monoterpenes *cis*-verbenol and myrtenol, which further bind to lipid molecules, such as methyl oleate, to form verbenyl oleate and myrtenyl oleate and are stored in the fat body of *I. typographus* during the early life

stages. Later, when feeding males tend to produce *cis*-verbenol as an aggregation pheromone compound, where *α*-pinene is a limited resource, the stored esters can be broken down into the required pheromones and residues of lengthy fatty acids. A similar concept was also proposed and studied in *D. ponderosae* (Chiu et al., 2018). Our hypothesis of methyl oleate and *cis*-verbenol oleate synthesis from the monoterpenyl esters is a novel concept proposed yet in the beetle pheromone storage mechanism. Added to that, other detoxification products, such as verbenyl and myrtenyl diglycosides were identified via UHPLC-HR-MS/MS for possible pheromone storage. *cis*-Verbenol was also synthesized after JH III treatment from the gut, as mentioned hypothesis of verbenol release from the stored verbenyl oleate (Ramakrishnan et al., 2022a, 2022b).

The esterase gene (Esterase FE4-like and venom carboxylesterase – 6 like) identified in this work shows high similarity with the esterase gene BT127766.1 from *D. ponderosa*, which is involved in a possible pheromone storage function (Bernier et al., 2020). Respective candidates were selected from the RNA seq. data based upon sequence similarity. To verify the proposed functional correlation, the involvement of the esterase gene family identified in this study in *cis*-verbenol storage as a fatty acid ester in the immature stage was evaluated. Further validation of the mentioned sequences in the life stages of *I. typographus* showed that esterase Ityp11977 (E3) occurs in the immature stage. Since *cis*-verbenol occurs in the immature stage and verbenyl oleate in the immature body, the proposed candidate can be considered a valid gene for functional study, also investigated in other bark beetles (Chiu et al., 2018). Further, we also hypothesize another two-step conversion of verbenyl oleate to *cis*-verbenol and fatty acids. The first step would be the hydrolysis of the oleate catalyzed by another esterase, and consequently, the released fatty acid would be methylated by a putative methyltransferase.

Added to that, we also identified four contigs from the glycosyl hydrolase gene family that were overexpressed exclusively in the male gut after treatment. However, the uncertainty in the abundance of male-specific verbenyl diglycosides (not similar to verbenyl ester), together with low quantity in the gut and absence in the fat body

(unpublished data), we presume that these compounds are more likely a detoxification product rather than a pheromone precursor. Thus, we have observed a strong induction of JH III on the formation of both verbenyl conjugates discussed. Originally, these compounds served as binding agents for the detoxification product of *α*-pinene, specifically *cis*-verbenol in our case, but additionally, our findings proved that verbenyl fatty acyl esters are possessed by adult males as an alternative pheromone precursor (Chiu et al., 2018; Ramakrishnan et al., 2022a). We would like to highlight that, the fatty acid esters and glycosides concept from this study exceed the existing knowledge from the literature in the bark beetle study (Ramakrishnan et al., 2024).

6. CONCLUSION:

In conclusion, the findings from this research establish a foundation for understanding the genetic mechanisms behind pheromone biosynthesis in different life stages of *I. typographus*. Followed by, the method of Juvenile Hormone III treatment on the beetle has ensured the occurrence of the relative gene families from the *I. typographus* gut tissue.

The primary conclusion confirmed the first objective from hypotheses 1 and 2, by proving the involvement of mevalonate gene families in the male *I. typographus* gut at the fed life stage (attacking stage)and JH III treated beetle, towards the key aggregation pheromone, 2-methyl-3-buten-2-ol. Initially, the compound mevalonate-5-phosphate as an intermediate from the pathway was identified, which supports the past findings of labeled mevalonate in the 2-methyl-3-buten-2-ol. Followed by, the genes PMK (Ityp06045), HMG-S (Ityp09137), HMG-R (Ityp17150), IPPI (Ityp04875), and an IPDS (Ityp09271) were identified and quantified from the pathway of feeding male beetle guts. Furthermore, hypothesis 2 was justified by confirming the pathway key candidates also in protein level after inducing the pheromone using JHIII on the beetle ensures the key gene, IPDS to target for reducing the 2-methyl-3-buten-2-ol biosynthesis.

The secondary conclusion confirms the second objective in the hypotheses, which is the concept of *cis*-verbenol biosynthesis in the beetle. Enough evidence persists for the conversion of tree precursor (*α*-pinene) into verbenol by a key Cytochrome P450 (CYP6DE1). Using sequence similarity to the functionally validated gene, Ityp03903, and Ity0496 are the key gene candidates from *I. typographus* gut tissue of certain life stages and JHIII treated beetle. Among a total of identified 52 CYP450 genes, the proposed candidates can potentially target to reduce the *cis*-verbenol biosynthesis.

The third conclusion is to highlight the final objective of the hypotheses, the storage concept of the verbenol components. As the beetles could not access the tree precursors all their lifetime, storage of the component during the resource availability is certain for many insects. Key genes such as Esterase EF4, Ityp11977, and Ityp09460 are

the potential candidates that are proposed for storing and releasing these verbenol form esters, verbenyl oleate. Furthermore, an additional concept of verbenyl-di-glucoside derivatives (a by-product from detoxification) from the beetle has been proposed for similar storage and sex-specific release using a glycosyl hydrolase, Ityp11770, Ityp00943, Ityp00535, and Ityp04256. Nevertheless, later-mentioned gene families fail to meet the criteria of sex-specific importance. Along with the respective pheromonal components the other male-specific functionally unknown components such as myrtenol, myrtanol, or phenylethanol were identified and quantified. On the gene level, biosynthetic gene families were reported in the data set of the mentioned research publications.

Taken together, this study approach and findings could lead to engineering effective pest management strategies, such as RNA *interference*, aimed at manipulating the mass attack behavior of this aggressive pest (Joga et al., 2021). Hence, this study leads to a deeper, more molecular understanding of the pheromone biosynthesis of *Ips typographus*.

7. RECOMMENDATIONS FOR FUTURE DEVELOPMENT OF THE RESEARCH FIELD:

Though many aspects of pheromone biosynthesis from the beetle, *Ips typographus* have been covered in this study, the research also involves certain limitations. Many potential gene candidates were identified based on relative abundance for co-relation study with analytical results. However, further functional validation of the reported genes is required to support the claims. Hence, a logical next step is to conduct research on the functional expression of the identified gene candidates for *in vivo* and *in vitro* model systems. The *in vitro* assay can be performed to express the targeted genes, by cloning the desired gene length into bacterial expression vectors such as pDEST15, generating an N-terminal his-tag fusion in *Escherichia coli* bacterial cells. The expression can also be performed in insect (*Spodoptera frugiperda* -sf9) cell lines using specific vectors such as pFastBac and pENTR4 vectors for gene families of Cytochrome P450 and esterases. This approach will lead to describing the gene/enzyme function by performing substrate-specific enzyme assays to detect the targeted end products. For enzyme assay, substrates with radioactive labeling can also be utilized for monoterpenes enantiomers such as +/- *α*-pinene, +/- *β*-pinene, and +/- limonene with variations as required and derive novel findings with the help of established analytical methods. Furthermore, the approach of this research lays the background for performing similar research on more bark beetle species.

8. PRACTICAL APPLICATION OF THIS RESEARCH FINDINGS:

Modern techniques like gene editing using CRISPR and silencing by RNA *interference* for the targeted potential genes can facilitate this study's findings. The latter-mentioned RNA-*i* can be efficiently incorporated by synthesizing a double-stranded RNA (*ds*RNA) from a species-specific target gene with an appropriate delivery mechanism. Although the use of RNA*i* in integrated pest management is a newly considered methodology, its potential has so far been successfully demonstrated for several groups of insects with species speficicty. Thus, our study contributes not only to a general knowledge of the biosynthesis of unique pheromones in this species, can also enable to the identification of targets for future eco-friendly management.

9. REFERENCES:

1. Adams, A.S., Boone, C.K., Bohlmann, J., Raffa, K.F., 2011. Responses of Bark Beetle-Associated Bacteria to Host Monoterpenes and Their Relationship to Insect Life Histories. J chem Ecol 37, 808–817.
2. Andrle, M., 2017. Conifers are more at home here than previously thought. Charles University Arch. 2017 1–4
3. Aw, T., Schlauch, K., Keeling, C.I., Young, S., Bearfield, J.C., Blomquist, G.J., Tittiger, C., 2010. Functional genomics of mountain pine beetle *(Dendroctonus ponderosae*) midguts and fat bodies. BMC Genomics 11, 215.
4. Bakke, A., Froyen, P. & Skattebol, L. 1977. Field response to a new pheromonal compound isolated from *Ips typographus*. Naturwissenschaften, 64(2), 98-99.
5. Bakke, A. 1976. Spruce Bark Beetle, *Ips typographus* " Pheromone Production and Field Response. Naturwissenschaften 63.
6. Bearfield, J.C., Henry, A.G., Tittiger, C., Blomquist, G.J., Ginzel, M.D., 2009. Two Regulatory Mechanisms of Monoterpenoid Pheromone Production in *Ips* sp. Of Bark Beetles. J chem Ecol 689–697.
7. Benton, H.P., Want, E.J., Ebbels, T.M.D., 2010. Correction of mass calibration gaps in liquid chromatography-mass spectrometry metabolomics data. Bioinformatics. 26 2488–2489.
8. Bentz, B.J., Rgnire, J., Fettig, C.J., Hansen, E.M., Hayes, J.L., Hicke, J.A., Kelsey, R.G., Negron, J.F., Seybold, S.J., 2010. Climate change and bark beetles of the western United States and Canada: Direct and indirect effects. Bioscience 60, 602–613
9. Bernier, K., Sergerie, R., Keeling, C.I.E.S.A., 2020. Functional Characterization of a *Dendroctonus ponderosae* Esterase. Entomology Society of America -ESA conferencevposter, Universit´e Laval Quebec, Canada- unpublished).
10. Biedermann, P.H.W., Müller, J., Grégoire, J.C., Gruppe, A., Hagge, J., Hammerbacher, A., Hofstetter, R.W., Kandasamy, D., Kolarik, M., Kostovcik, M., Krokene, P., Sallé, A., Six, D.L., Turrini, T., Vanderpool, D., Wingfield, M.J., Bässler, C., 2019. Bark Beetle Population Dynamics in the Anthropocene: Challenges and Solutions. Trends Ecol. Evol. 34, 914–924.
11. Birgersson, G., 1984. Quantitative variation of Pheromone components in the spruce bark beetle *Ips Typographus* from different attack phases. J. Chem. Ecol. 10.
12. Birgersson G., 1989. Volatiles released from individual spruce bark beetle entrance holes Quantitative variations during the first week of attack. J Chem Ecol.;15(10):2465-83.
13. Blomquist, G.J., Figueroa-Teran, R., Aw, M., Song, M.M., Gorzalski, A., Abbott, N.L., Chang, E., Tittiger, C., 2010. Pheromone production in bark beetles. Insect Biochem. Mol. Biol. 40, 699–712
14. Blomquist, G. J., Tittiger, C., MacLean, M. & Keeling, C. I., 2021. Cytochromes P450: terpene detoxification and pheromone production in bark beetles. Current Opinion in Insect Science, 43, 97-102.
15. Bohlmann, J., Gershenzon, J., 2009. Old substrates for new enzymes of terpenoid biosynthesis. Proc. Natl. Acad. Sci. U. S. A. 106, 10402–10403.

16. Brand, J.M., Bracke, J.W., Britton, L.N., Markovetz, A.J., Barras, S.J., 1976. Bark beetle pheromones: productionof verbenone by a mycangial fungus of *Dendroctonus frontalis*. J. Chem. Ecol. 2, 195-199.
17. Byers, J.A., 1989. Chemical ecology of bark beetles. Experiencia. Experientia 45.
18. Byers, J.A., Birgersson, G., 1990. Pheromone production in a bark beetle independent of myrcene precursor in host pine species. Naturwissenschaften 77, 385-387
19. Chakraborty, A., Modlinger, R., Ashraf, M. Z., Synek, J., Schlyter, F., and Roy, A. 2020. Core mycobiome and their ecological relevance in the gut of five *Ips* bark beetles (Coleoptera: Curculionidae: Scolytinae). Front. Microbiol. 11:568853. doi: 10.3389/fmicb.2020.568853
20. Cheng, C.H., Wickham, J.D., Chen, L., Xu, D.D., Lu, M., Sun, J.H., Bacterial microbiota protect an invasive bark beetle from a pine defensive compound. Microbiome. 6, 132 (2018).
21. Chiu, C.C., Keeling, C. I., Bohlmann J., 2017. Toxicity of pine monoterpenes to mountain pine beetle. Sci Rep 7:8858.
22. Chiu, C.C., Keeling, C.I., Bohlmann, J., 2019. The cytochrome P450 CYP6DE1 catalyzes the conversion of α -pinene into the mountain pine beetle aggregation pheromone trans -verbenol. Sci. Rep. 2–11.
23. Chiu, C.C., Keeling, C.I., Bohlmann, J., 2018. Monoterpenyl esters in juvenile mountain pine beetle and sex-specific release of the aggregation pheromone *trans*-verbenol. PNAS 2–7.
24. Chong, J., Soufan, O., Li, C., Caraus, I., Li, S.Z., Bourque, G., Wishart, D.S., Xia, J.G., 2018. MetaboAnalyst 4.0: towards more transparent and integrative metabolomics analysis. Nucleic Acids Res. 46, W486–W494.
25. Cloonan, N. et al. 2008 Stem cell transcriptome profiling via massive-scale mRNA sequencing. Nat. Methods 5, 613–619.
26. Cox, J. & Mann, M., 2008. MaxQuant enables high peptide identification rates, individualized p.p.b.-range mass accuracies and proteome-wide protein quantification. Nature Biotechnology, 26(12), 1367-1372.
27. Cox, J., Hein, M. Y., Luber, C. A., Paron, I., Nagaraj, N. & Mann, M., 2014. Accurate Proteome-wide Label-free Quantification by Delayed Normalization and Maximal Peptide Ratio Extraction, Termed MaxLFQ. Molecular & Cellular Proteomics, 13(9), 2513-2526.
28. Cristino, A. S., Nunes, F. M., Lobo, C. H., Bitondi, M. M., Simões, Z. L., da Fontoura Costa, L., Lattorff, H. M., Moritz, R. F., Evans, J. D., & Hartfelder, K., 2006. Caste development and reproduction: a genome-wide analysis of hallmarks of insect eusociality. Insect molecular biology, 15(5), 703–714.
29. Dong K., Sun L., Liu J. T., Gu S. H., et al., 2017. RNAi-Induced Electrophysiological and Behavioral Changes Reveal Two Pheromone Binding Proteins of Helicoverpa armigera Involved in the Perception of the Main Sex Pheromone Component Z11-16:Ald. Journal of Chemical Ecology, 43(2):207-214.

30. EEA 2014. European forest ecosystems—state and trends. EEA Report 5, European Environment Agency, pp. 128.
31. Emlen, D., Szafran, Q., Corley, L. & Dworkin, I., 2006. Insulin signaling and limb-patterning: candidate pathways for the origin and evolutionary diversification of beetle 'horns. Heredity 97, 179–191.
32. Ernst, U.R., Votavová, A., Hanus, R., Valterová, I., Jedlicka, P., 2016. Gene Expression Dynamics in Major Endocrine Regulatory Pathways along the Transition from Solitary to Social Life in a Bumblebee, Bombus terrestris. Front. Physiol. 7, 1–20.
33. Fang, J. X., Du, H. C., Shi, X., Zhang, S. F., Liu, F., Zhang, Z., Zu, P. J. & Kong, X. B., 2021. Monoterpenoid signals and their transcriptional responses to feeding and juvenile hormone regulation in bark beetle *Ips hauseri*. Journal of Experimental Biology, 224(9), 9.
34. Figueroa-Teran, R., Welch, W.H., Blomquist, G.J., Tittiger, C., 2012. Ipsdienol dehydrogenase (IDOLDH): a novel oxidoreductase important for *Ips pini* pheromone production. Insect Biochem. Mol. Biol. 42, 81–90.
35. Frick, S., Nagel, R., Schmidt, A., Bodemann, R.R., Rahfeld, P., Pauls, G., Brandt, W., Gershenzon, J., Boland, W., Burse, A., 2013. Metal ions control product specificity of isoprenyl diphosphate synthases in the insect terpenoid pathway. Proceedings of the National Academy of Sciences of the United States of America 110, 4194–4199
36. Galko, J., Nikolov, C., Kunca, A., Vakula, J., Gubka, A., Zúbrik, M., Rell, S., Konôpka, B., 2016. Effectiveness of pheromone traps for the European spruce bark beetle: A comparative study of four commercial products and two new models. For. J. 62, 207–215.
37. Gilg, A. B., Bearfield, J. C., Tittiger, C., Welch, W. H. & Blomquist, G. J., 2005. Isolation and functional expression of an animal geranyl diphosphate synthase and its role in bark beetle pheromone biosynthesis. Proceedings of the National Academy of Sciences of the United States of America, 102(28), 9760-9765.
38. Gilg, A. B., Tittiger, C., Blomquist, G. J., 2009. Unique animal prenyltransferase with monoterpene synthase activity. Naturwissenschaften 96, 731–735. Gordon, K. H., and Waterhouse, P. M., 2007. RNAi for insect-proof plants. Nat. Biotechnol. 25, 1231–1232.
39. Goodman, W.G. & Cusson, M., 2012. The Juvenile Hormones. Insect Endocrinology, 8, 310-365.
40. Gries, 1990. Conversion of phenylalanine to toluene and 2-phenylethanol by the pine engraver, *Ips pini* (Say) (Coleoptera, Scolytidae). Birkhfiuser Verlag 46, 329–331.
41. Hartmann, H., Bastos, A., Das, A.J., Esquivel-muelbert, A., Hammond, W.M., Martínez-vilalta, J., Mcdowell, N.G., Powers, J.S., Pugh, T.A.M., Ruthrof, K.X., Allen, C.D., 2022. Climate change risks to global forest health: emergence of unexpected events of elevated tree mortality worldwide. Annu. Rev. Plant Biol. 73, 673–702.
42. Hartmann, H., Moura, C.F., Anderegg, W.R., Ruehr, N.K., Salmon, Y., Allen, C.D., &..., O'Brien, M., 2018. Research frontiers for improving our understanding of drought-induced tree and forest mortality. New Phytol. 15–28.
43. Hall, G.M., Tittiger, C., Andrews, G.L., Mastick, G.S., Kuenzli, M., Luo, X., Seybold, S.J., Blomquist, G.J., 2002. Midgut tissue of male pine engraver, *Ips pini*,

synthesizes monoterpenoid pheromone component ipsdienol de novo. Naturwissenschaften 89, 79–83.
44. Hebert, A. S., Richards, A. L., Bailey, D. J., Ulbrich, A., Coughlin, E. E., Westphall, M. S. & Coon, J. J., 2014. The One Hour Yeast Proteome. Molecular & Cellular Proteomics, 13(1), 339-347.
45. Hlásny T, Krokene P, Liebhold A, Montagné-Huck C, Müller J, Qin H, Raffa K, Schelhaas MJ, Seidl R, Svoboda M, Viiri H. 2019. Living with bark beetles: impacts, outlook and management options, From Science to Policy 8. 1-52.
46. Hlásny, T., Konig, L., Krokene, P., Lindner, M., Montagné-Huck, C., Muller, J., Qin, H., Raffa, K. F., Schelhaas, M. J., Svoboda, M., Viiri, H. & Seidl, R., 2021. Bark Beetle Outbreaks in Europe: State of Knowledge and Ways Forward for Management. Current Forestry Reports, 7(3), 138-165.
47. Hlásny, T.; Barka, I.; Merganičová, K.; Křístek, Š.; Modlinger, R.; Turčáni, M.; Marušák, R. A New Framework for Prognosing Forest Resources under Intensified Disturbance Impacts: Case of the Czech Republic. For. Ecol. Manag. 2022, 523, 120483.
48. Hughes, P. R. (1974) Myrcene - Precursor of pheromones in *Ips* beetles. Journal of Insect Physiology, 20(7), 1271-1275.
49. Hunt, D.W.A., Borden, J.H., Pierce Jr., H.D., Slessor, K.N., King, G.G.S., Czyzewska, E.K., 1986. Sex-specific production of ipsdienol and myrcenol by *Dendroctonus ponderosae* (Coleoptera: Scolytidae) exposed to myrcene vapors. J. Chem. Ecol. 12, 1579-1586.
50. Hunter W.B., Glick E., Paldi N., Bextine B. R. 2012. Advances in RNA *interference*: *ds*RNA Treatment in Trees and Grapevines for Insect Pest Suppression. Southwestern Entomologist, 37(1):85-87.
51. Ivarsson, P. & Birgersson, G. 1995. Regulation and biosynthesis of pheromone components in the double-spined bark beetle *Ips duplicatus* (Coleoptera, Scolytidae). Journal of Insect Physiology, 41(10), 843-849.
52. Ivarsson, P., Schlyter, F., Birgersson, G., 1993. Demonstration of de novo pheromone biosynthesis in *Ips duplicatus* (Coleoptera: Scolytidae): inhibition ofipsdienol and E-myrcenol production by compactin. Insect Biochem. Mol. Biol. 23, 655-662
53. Jansen, S., Konrad, H. & Geburek, T. The extent of historic translocation of Norway spruce forest reproductive material in Europe. Annals of Forest Science 74, 56 (2017).
54. Jirosov´a, A., Janˇcaˇrík, A., Menezes, R.C., Bazalov´a, O., Dolejˇsov´a, K., Vogel, H., Jedliˇcka, P., Buˇcek, A., Brabcov´a, J., Majer, P., Hanus, R., Svatoˇs, A., 2017. Co-option of the sphingolipid metabolism for the production of nitroalkene defensive chemicals in termite soldiers. Insect Biochem. Mol. Biol. 82, 52–61.
55. Jindra, M., Palli, S. R. & Riddiford, L. M. 2013. The Juvenile Hormone Signaling Pathway in Insect Development. In: Berenbaum, M. R. (ed.) Annual Review of Entomology, Vol 58. 181-204.

56. Jindra, M. & Bittova, L. 2020. The juvenile hormone receptor as a target of juvenoid "insect growth regulators". Archives of Insect Biochemistry and Physiology, 103(3), 7.
57. Jindra, M., Palli, S. R. & Riddiford, L. M. 2013. The Juvenile Hormone Signaling Pathway in Insect Development. In: Berenbaum, M. R. (ed.) Annual Review of Entomology, Vol 58. 181-204. 10.1146/annurev-ento-120811-153700.
58. Jönsson, A.M., Appelberg, G., Harding, S., Bärring, L. 2009. Spatio-temporal impact of climate change on the activity and voltinism of the spruce bark beetle, *Ips typographus*. Glob. Chang. Biol. 15, 486–499.
59. Joga MR, Zotti MJ, Smagghe G and Christiaens O. 2016. RNA*i* Efficiency, Systemic Properties, and Novel Delivery Methods for Pest Insect Control: What We Know So Far. Front. Physiol. 7:553.
60. Joga, M. R., Moglicherla K., Smagghe G and Roy A. 2021 RNA *interference*-based forest protection products (FPPs) against wood-boring coleopterans: Hope or hype? Frontiers in Plant Science 12: 733608.
61. Katherine E. Fisher, Richard L. Tillett, Misha Fotoohi, Cody Caldwell, Juli Petereit, Karen Schlauch, Claus Tittiger, Gary J. Blomquist, Marina MacLean. 2021. RNA-Seq used to identify ipsdienone reductase (IDONER): A novel monoterpene carbon-carbon double bond reductase central to *Ips confusus* pheromone production, Insect Biochemistry and Molecular Biology, 129, 0965-1748.
62. Kautz, M.; Schopf, R.; Ohser, J. The “Sun-Effect”: Microclimatic Alterations Predispose Forest Edges to Bark Beetle Infestations. Eur. J. For. Res. 2013, 132, 453–465.
63. Keeling, C.I., Li, M., Sandhu, H.K., Henderson, H., Man, M., Yuen, S., 2016. Quantitative metabolome, proteome and transcriptome analysis of midgut and fat body tissues in the mountain pine beetle, *Dendroctonus ponderosae* Hopkins, and insights into pheromone biosynthesis. Insect Biochem. Mol. Biol. 70, 170–183.
64. Keeling, C.I., Blomquist, G.J., Tittiger, C., 2004. Coordinated gene expression for pheromone biosynthesis in the pine engraver beetle, *Ips pini* (Coleoptera: Scolytidae). Naturwissenschaften 91, 324–328.
65. Knížek, M., 2020. Historie a současnost kůrovcových kalamit ve střední Evropě. Zpravodaj ochrany lesa. Škodliví činitelé v lesích Česka.
66. Knížek, M., 2019. Historie a současnost kůrovcových kalamit ve střední Evropě. Zpravodaj ochrany lesa.Škodliví činitelé v lesích Česka.
67. Kogan, M., 1998. Integrated pest management: Historical perspectives and contemporary developments. Annu. Rev. Entomol. 43, 243–270.
68. Lancaster, et al., 2018. *De novo* formation of an aggregation pheromone precursor by an isoprenyl diphosphate synthase-related terpene synthase in the harlequin bug. PNAS 115, E8634–E8641.
69. Lanne, B.S., Ivarsson, P., Johnson, P., Bergstrom, G., Wassgren, A.B., 1989. Biosynthesis of 2-methyl-3-buten-2-ol, a pheromone component of *Ips typographus* (Coleoptera: Scolytidae). Insect Biochem. 19, 163-168.

70. Lehmanski, L. M., Kandasamy, D., Andersson, M. N., Netherer, S., Alves, E. G., Huang, J., et al. 2023. Addressing a century old hypothesis–do pioneer beetles of *Ips typographus* use volatile cues to find suitable host trees?. New Phytol. 238, 1762–1770.
71. Leinwand, S. G., & Scott, K., 2021. Juvenile hormone drives the maturation of spontaneous mushroom body neural activity and learned behavior. Neuron, 109(11), 1836–1847. 10.1016/j.neuron.2021.04.006
72. Leufvi, A., Bergström, G., 1984. Interconversion of Verbenols and bark beetle *Ips typographus*. J. Chem. Ecol. 10, 1349–1361.
73. Li H., Guan R., Guo H., Miao X. 2015. New insights into an RNAi approach for plant defence against piercing-sucking and stem-borer insect pests. Plant Cell and Environment, 38(11), 2277-2285.
74. Lorenc F., Knížek M., Liška J., Lubojacký J., Zahradník P., Zahradníková M., Šrámek V., Novotný R. 2018. Výskyt lesních škodlivých faktorů v Česku v roce 2017. Lesnická práce 97 (6): 12 – 16.
75. Lorio P. L., Mason G. N., Autry G. L., 1982. Stand Risk Rating for the Southern Pine Beetle: Integrating Pest Management with Forest Management, Journal of Forestry, Volume 80, 4, 212–214.
76. Lubojácký, J., Lorenc, F., Véle, A., Knížek, M., 2023. Výskyt lesních škodlivých faktorů v Česku v roce 2022. Zprav. Ochr. lesa. Lesn. práce 6, 49–53.
77. Marini L., Okland B., Jönsson AM., Bentz B., Carroll A., Forster B., Grégoire J-C., Hurling R., Nageleisen LM., Netherer S., Ravn HP., Weed A., Schroeder M., 2017. Climate drivers of bark beetle outbreak dynamics in Norway spruce forests. Ecography 40: 1426-1435.
78. Miyakawa H., Watanabe M., Araki M., Ogino Y., Miyagawa S., Iguchi T. 2018. Juvenile hormone-independent function of Krüppel homolog 1 in early development of water flea Daphnia pulex, Insect Biochemistry and Molecular Biology, Volume 93, 12-18.
79. Nadeau, J.A., Petereit, J., Tillett, R.L., Jung, K., Fotoohi, M., MacLean, M., Young, S., Schlauch, K., Blomquist, G.J., Tittiger, C., 2017. Comparative transcriptomics of mountain pine beetle pheromone-biosynthetic tissues and functional analysis of CYP6DE3. BMC Genom. 18, 311.
80. Nakamura, C.E., Abeles, R.H., 1985. Mode of interaction of b-hydroxy-b-methyl-glutaryl coenzyme A reductase with strong binding inhibitors: compactin and related compounds. Biochemistry 24, 1364-1376
81. Nardi, J. B., Young, A. G., Ujhelyi, E., Tittiger, C., Lehane, M. J. & Blomquist, G. J., 2002 Specialization of midgut cells for synthesis of male isoprenoid pheromone components in two scolytid beetles, *Dendroctonus jeffreyi* and *Ips pini*. Tissue & Cell, 34(4), 221-231.
82. Naseer, A., Mogilicherla, K., Sellamuthu, G. & Roy, A., 2023. Age matters Life-stage, tissue, and sex-specific gene expression dynamics in *Ips typographus* (Coleoptera: Curculionidae: Scolytinae). Frontiers in Forests and Global Change, 6.
83. Netherer, S., Kandasamy, D., Jirosová, A. et al. 2021. Interactions among Norway spruce, the bark beetle *Ips typographus* and its fungal symbionts in times of drought. J Pest Sci 94, 591–614.

84. Peltonen M., 1999. Windthrow and dead-standing trees as bark beetle breeding material at forest-clearcut edge Scand. J. For. Res., 14, pp. 505-511
85. Plesa, I., Dan, C., Truța, A., Holonec, l., Sestras, A.F., Boscaiu, M., Sestras, R.E., 2017. Spruce Trees Growth and Forest Landscape Depending on Microstational Factors and Ecological Conditions. Not. Sci. Biol. 9, 582–588.
86. Powell, D., Grosse-Wilde, E., Krokene, P., Roy, A., Chakraborty, A., Lofstedt, C., Vogel, H., Andersson, M. N. & Schlyter, F., 2021. A highly contiguous genome assembly of the Eurasian spruce bark beetle, *Ips typographus*, provides insight into a major forest pest. Communications Biology, 4(1), 9.
87. Przepióra, F., Loch, J., Ciach, M., 2020. Bark beetle infestation spots as biodiversity hotspots: Canopy gaps resulting from insect outbreaks enhance the species richness, diversity and abundance of birds breeding in coniferous forests. For. Ecol. Manage. 473.
88. Pureswaran DS., Gries R., Borden JH., Pierce JHD. 2000. Dynamics of pheromone production and communication in the mountain pine beetle, *Dendroctonus ponderosae* Hopkins, and the pine engraver, *Ips pini* (Say) (Coleoptera: Scolytidae). Chemoecology, 10:153-168
89. Raffa, K. F., Andersson, M.N., Schlyter, F., 2016. Host Selection by Bark Beetles: Playing the Odds in a High-Stakes Game, 1st ed, Advances in Insect Physiology. Elsevier Ltd.
90. Raffa, K., 1983. The Role of Host Plant Resistance in the Colonization Behavior and Ecology of Bark Beetles (Coleoptera: Scolytidae). Ecol. Monogr. 53, 27–49.
91. Ramakrishnan, R., Hradecký, J., Roy, A., Kalinová, B., Mendezes C. R., Synek, J., Bláha, J., Svatoš, A., Jirošová, A., 2022a Metabolomics and transcriptomics of pheromone biosynthesis in an aggressive forest pest *Ips typographus*. Insect Biochem. Mol. Biol 0965-1748.
92. Ramakrishnan, R., Roy, A., Kai, M. R., Svatos, A. & Jirosova, A., 2022b. Metabolome and transcriptome related dataset for pheromone biosynthesis in an aggressive forest pest *Ips typographus*. Data in Brief, 41, 26.
93. Ramakrishnan R, Roy A, Hradecký J, Kai M, Harant K, Svatoš A and Jirošová A. 2024. Juvenile hormone III induction reveals key genes in general metabolism, pheromone biosynthesis, and detoxification in Eurasian spruce bark beetle. Front. For. Glob. Change. 6:1215813
94. Rappsilber, J., Mann, M. & Ishihama, Y., 2007. Protocol for micro-purification, enrichment, pre-fractionation and storage of peptides for proteomics using StageTips. Nature Protocols, 2(8), 1896-1906.
95. Renwick, J. A. A., Hughes, P. R. & Krull, I. S., 1976. Selective production of *cis*-verbenol and trans-verbenol from (-)- and (+)-α-pinene by a bark beetle. Science, 191(4223), 199-201.
96. Riddiford, L. M., Cherbas, P. & Truman, J. W., 2001. Ecdysone receptors and their biological actions. Vitamins and Hormones - Advances in Research and Applications, Vol 60, 60, 1-73

97. Roy, A., Palli, S.R., 2018. Epigenetic modifications acetylation and deacetylation play important roles in juvenile hormone action. BMC Genomics. 19, 934.
98. Roy, A., George, S., Palli, S.R., 2017. Multiple functions of CREB-binding protein during postembryonic development: identification of target genes. BMC Genomics 1–14.
99. Sarabia, L. E., Lopez, M. F., Obregon-Molina, G., Cano-Ramirez, C., Sanchez-Martinez, G. & Zuniga, G., 2019. The Differential Expression of Mevalonate Pathway Genes in the gut of the bark beetle *Dendroctonus rhizophagus* (Curculionidae: Scolytinae) is unrelated to the de novo synthesis of terpenoid pheromones. International Journal of Molecular Sciences, 20(16), 20.
100. Seidl R., Müller J., Hothorn T., Bässler C., Heurich M., Kautz M., Kaplan I. Small beetle, large-scale drivers: 2016. How regional and landscape factors affect outbreaks of the European spruce bark beetle. J. Appl. Ecol., 53 (2), pp. 530-540,
101. Schlyter, F., and Cederholm, I. 1981. Separation of the sexes of living spruce bark beetles, *Ips typographus* (L.) (Coleoptera: Scolytidae). Z. Angew. Entomol. 92:42-47.
102. Schlyter, F., Birgersson, G., Byers, J.A., Lofqvist, J., Bergstrom, G., 1987. Field response of spruce bark beetle, *Ips typographus* to aggregation pheromone candidates. Journal of Chemical Ecology. 13,701-716.
103. Schlyter, F., Zhang, QH., Liu, GT. et al., 2001. A successful Case of Pheromone Mass Trapping of the Bark Beetle *Ips duplicatus* in a Forest Island, Analysed by 20-year Time-Series Data. Integrated Pest Management Reviews 6, 185–196.
104. Schmidt-Vogt H, 1977. Die Fichte (1), 1st edn. Paul Parey, Hamburg, Berlin.
105. Sellamuthu, G., Bily, J., Joga, M. R., Synek, J. & Roy, A., 2022. Identifying optimal reference genes for gene expression studies in Eurasian spruce bark beetle, *Ips typographus* (Coleoptera: Curculionidae: Scolytinae). Scientific Reports, 12(1), 17.
106. Schmitz RF., 1972. Behaviour of *Ips pini* during mating, oviposition and larval development. (Coleoptera: Scolytidae). Can Entomol 104:1723–1728
107. Seybold, S. J., Quilici, D. R., Tillman, J. A., Vanderwel, D., Wood, D. L. & Blomquist, G. J., 1995. *De-novo* biosynthesis of the aggregation pheromone components ipsenol and ipsdienol by the pine bark beetles *Ips paraconfusus* lanier and *Ips pini* (say) (coleoptera-scolytidae). Proceedings of the National Academy of Sciences of the United States of America, 92(18), 8393-8397.
108. Sickle V., GA., 1989. The status of mountain pine beetle in western Canada, 1988. Pp 6–8 in: Amman GD (ed) Proceedings-Symposium on the Management of Lodgepole Pine to Minimize Losses to the Mountain Pine Beetle. USDA, For. Serv. Gen. Tech. Rep.
INT–262.
109. Silverstein, R.M., Rodin, J.O., Wood, D.L., 1966. Sex attractants in frass produced by male *Ips confusus* in ponderosa pine. Science 154, 509-510
110. Smith, C.A., Want, E.J., O'Maille, G., Abagyan, R., Siuzdak, G., 2006. XCMS: processing mass spectrometry data for metabolite profiling using Nonlinear peak alignment, matching, and identification. Anal. Chem. 78, 779–787.

111. Smykal, V., Daimon, T., Kayukawa, T., Takaki, K., Shinoda, T. and Jindra, M., 2014. Importance of juvenile hormone signaling arises with competence of insect larvae to metamorphose. Developmental Biology, 390(2), 221-230.
112. Song, M. M., Kim, A. C., Gorzalski, A. J., MacLean, M., Young, S., Ginzel, M. D., Blomquist, G. J. & Tittiger, C. 2013. Functional characterization of myrcene hydroxylases from two geographically distinct *Ips pini* populations. Insect Biochemistry and Molecular Biology, 43(4), 336-343.
113. Sparks, M.E.; Rhoades, J.H.; Nelson, D.R.; Kuhar, D.; Lancaster, J.; Lehner, B.; Tholl, D.; Weber, D.C.; Gundersen-Rindal, D.E. 2017. A Transcriptome Survey Spanning Life Stages and Sexes of the Harlequin Bug, Murgantia histrionica. Insects, 8, 55.
114. Stark, R., Grzelak, M., Hadfield, J., 2019. RNA sequencing: the teenage years. Nat. Rev. Genet. 20, 631–656
115. Szabó, P., Kuneš, P., Svobodová-Svitavská, H., Švarcová, M.G., Křížová, L., Suchánková, S., Müllerová, J., Hédl, R., 2017. Using historical ecology to reassess the conservation status of coniferous forests in Central Europe. Conserv. Biol. 31, 150–160.
116. Tittiger, C., Blomquist, G.J., 2016. Pheromone Production in Pine Bark Beetles, 1st ed, Advances in Insect Physiology. Elsevier Ltd.
117. Tautenhahn, R., Böttcher, C., Neumann, S., 2008. Highly sensitive feature detection for high resolution LC/MS. BMC Bioinformatics. 9, 504.
118. Tillman, J. A., Holbrook, G. L., Dallara, P. L., Schal, C., Wood, D. L., Blomquist, G. J. & Seybold, S. J., 1998. Endocrine regulation of de novo aggregation pheromone biosynthesis in the pine engraver, *Ips pini* (Say) (Coleoptera: Scolytidae). Insect Biochemistry and Molecular Biology, 28(9), 705-715.
119. Tillman, J. A., Lu, F., Goddard, L. M., Donaldson, Z. R., Dwinell, S. C., Tittiger, C., Hall, G. M., Storer, A. J., Blomquist, G. J. & Seybold, S. J., 2004. Juvenile hormone regulates de novo isoprenoid aggregation pheromone biosynthesis in pine bark beetles, *Ips* spp., through transcriptional control of HMG-CoA reductase. Journal of Chemical Ecology, 30(12), 2459-2494.
120. Tillman, J. A., Lu, F., Goddard, L. M., Donaldson, Z. R., Dwinell, S. C., Tittiger, C., Hall, G. M., Storer, A. J., Blomquist, G. J. & Seybold, S. J., 2004. Juvenile hormone regulates de novo isoprenoid aggregation pheromone biosynthesis in pine bark beetles, *Ips* spp., through transcriptional control of HMG-CoA reductase. Journal of Chemical Ecology, 30(12), 2459-2494.
121. Trumbo, S. T., 2018. Juvenile hormone and parental care in subsocial insects: implications for the role of juvenile hormone in the evolution of sociality. Current Opinion in Insect Science, 28, 13-18.
122. Treiblmayr, K., Pascual, N., Piulachs, M-D., Keller, T., Belles, X., 2006. Juvenile hormone titer versus juvenile hormone synthesis in female nymphs and adults of the German cockroach, Blattella germanica. J. Insect Sci. 6:1–7.
123. Tyanova, S., Temu, T., Sinitcyn, P., Carlson, A., Hein, M. Y., Geiger, T., Mann, M. & Cox, J., 2016. The Perseus computational platform for comprehensive analysis of (prote)omics data. Nature Methods, 13(9), 731-740.
124. Wang, Z., Gerstein, M., Snyder, M., 2009. RNA-Seq: a revolutionary tool for transcriptomics in Western Equatoria State. Nat. Rev. Genet. 10, 57.

125. Wang, M., Carver, J., Phelan, V., et al. 2016. Sharing and community curation of mass spectrometry data with Global Natural Products Social Molecular Networking. Nature Biotechnology 34, 828-837.
126. Wermelinger, B. 2019. Pheromone production in bark beetles. Insect Biochem. Mol. Biol. 40, 0–2.
127. Wermelinger B. 2004. Ecology and management of the spruce bark beetle *Ips typographus* - A review of recent research. For. Ecol. Manag. 202, 67–82.
128. White, R. A., Agosin, M., Franklin, R. T. & Webb, J. W., 1980. Bark beetle pheromones evidence for physiological synthesis mechanisms and their ecological implications. Zeitschrift Fur Angewandte Entomologie-Journal of Applied Entomology, 90(3), 255-274.
129. Vanderwel, D., 1994. Factors affecting pheromone production in beetles. Arch. Insect Biochem. Physiol. 25, 347-362.
130. Vanderwel, D., Gries, G., Singh, S.M., Borden, J.H., Oehlschlager, A.C., 1992. (E)- and (Z)-6-nonen-2-one: biosynthetic precursors of endo- and exo-brevicomin in two bark beetles (Coleoptera: Scolytidae). J. Chem. Ecol. 18, 1389-1404.
131. Zhu, H., Gegear, R. J., Casselman, A., Kanginakudru, S., & Reppert, S. M., 2009. Defining behavioral and molecular differences between summer and migratory monarch butterflies. BMC biology, 7, 14.